Downloaded from orbit.dtu.dk on: Apr 25, 2024

DTU Library

Market-Based Methods For The Coordinated Use Of Distributed Energy Resources - TSO-DSO coordination in liberalized power systems

Hermann, Alexander Niels August

Publication date:
2019

Document Version
Publisher's PDF, also known as Version of record

Link back to DTU Orbit

Citation (APA):
Hermann, A. N. A. (2019). *Market-Based Methods For The Coordinated Use Of Distributed Energy Resources - TSO-DSO coordination in liberalized power systems*. Technical University of Denmark.

General rights
Copyright and moral rights for the publications made accessible in the public portal are retained by the authors and/or other copyright owners and it is a condition of accessing publications that users recognise and abide by the legal requirements associated with these rights.

- Users may download and print one copy of any publication from the public portal for the purpose of private study or research.
- You may not further distribute the material or use it for any profit-making activity or commercial gain
- You may freely distribute the URL identifying the publication in the public portal

If you believe that this document breaches copyright please contact us providing details, and we will remove access to the work immediately and investigate your claim.

Ph.D. Thesis
Doctor of Philosophy

DTU Electrical Engineering
Department of Electrical Engineering

Market-Based Methods For The Coordinated Use Of Distributed Energy Resources

TSO-DSO coordination in liberalized power systems

Alexander Niels August Hermann

Kongens Lyngby 2019

DTU Electrical Engineering
Department of Electrical Engineering
Technical University of Denmark

Elektrovej
Building 325
2800 Kongens Lyngby, Denmark
Phone +45 4525 3500
elektro@elektro.dtu.dk
www.elektro.dtu.dk

DANMARKS TEKNISKE UNIVERSITET
Center for Electric Power and Energy (CEE)
DTU Electrical Engineering

Market-Based Methods For The Coordinated Use Of Distributed Energy Resources

TSO-DSO coordination in liberalized power systems

Dissertation, by Alexander Niels August Hermann

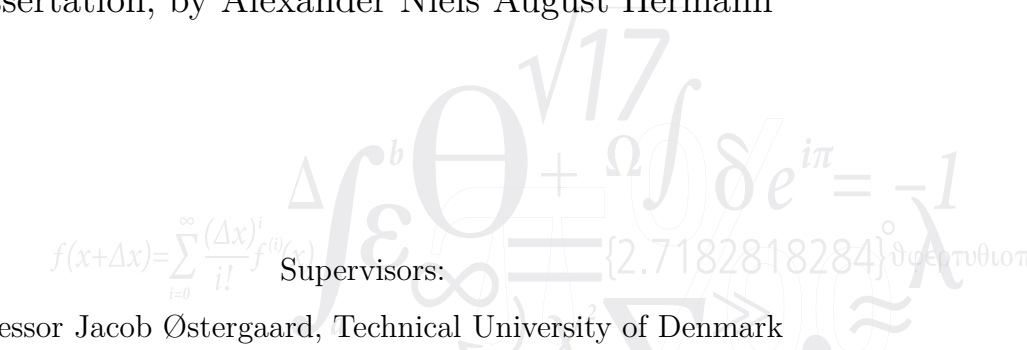

Supervisors:

Professor Jacob Østergaard, Technical University of Denmark

Associate Professor Jalal Kazempour, Technical University of Denmark

Assistant Professor Shaojun Huang, University of Southern Denmark

DTU - Technical University of Denmark, Kongens Lyngby - July 2019

Market-Based Methods For The Coordinated Use Of Distributed Energy Resources, TSO-DSO coordination in liberalized power systems

This thesis was prepared by:
Alexander Niels August Hermann

Supervisors:
Professor Jacob Østergaard, Technical University of Denmark
Associate Professor Jalal Kazempour, Technical University of Denmark
Assistant Professor Shaojun Huang, University of Southern Denmark

Dissertation Examination Committee:
Professor Pierre Pinson (Chairman)
Department of Electrical Engineering, Technical University of Denmark, Denmark

Professor Doctor Christoph Weber
Faculty of Business Administration and Economics, University of Duisburg-Essen, Germany

Doctor Florin Capitanescu
Luxembourg Institute of Science and Technology, Luxembourg

Center for Electric Power and Energy (CEE)
DTU Electrical Engineering
Elektrovej, Building 325
DK-2800 Kgs. Lyngby
Denmark

Tel: (+45) 4525 3500
Fax: (+45) 4588 6111
E-mail: elektro@elektro.dtu.dk

Release date: 25. March 2019

Edition: 1.0

Class: Internal

Field: Electrical Engineering

Remarks: The dissertation is presented to the Department of Electrical Engineering of the Technical University of Denmark in partial fulfillment of the requirements for the degree of Doctor of Philosophy.

Copyrights: ©Alexander Niels August Hermann, 2014– 2019

ISBN: 000-00-00000-00-0

Education is the most powerful weapon which you can use to change the world.

— Nelson Mandela

To my parents

Preface

This Ph.D. thesis was prepared at the department of electrical engineering at the Technical University of Denmark in fulfillment of the requirements for acquiring a Ph.D. degree in electrical engineering.

The work done for this thesis has been carried out over a period of 4 years from 2015 to 2019 with some intermissions totaling 1 year. The work comprises 2 papers that are currently under review by the IEEE Transactions on Power Systems and the most recent manuscripts are attached in the back of this thesis.

Kongens Lyngby, March 24, 2019

Alexander Niels August Hermann

Acknowledgements

First of all I would like to thank my supervisor Professor Jacob Østergaard for his always helpful attitude and open door policy. He was instrumental in shaping my PhD work and his great emphasis on structure and dissemination work has left a great impression on me. Without his support this PhD project could not have happened.

A very special thank you to my co-supervisor Associate Professor Jalal Kazempour who through his great experience has guided me through for the last few years. His very meticulous approach to research work was an amazing inspiration and his skills in structuring and disseminating research have taught me much. He is one of the most ambitious scholars I have had the pleasure of working with in my time at DTU.

I would also like to extend my thanks to my co-supervisor Assistant Professor Shaojun Huang who is with the University of Southern Denmark. His insights into the world of distribution system optimization has helped me very much and I particularly enjoyed our discussions.

Working together with Postdoc Tue Jensen from the ESOM group at Risø was a great pleasure, and I would like to thank him very much for his always helpful attitude and great insights. Tue has an amazing positive approach to sharing his knowledge and is always keen on new projects and collaboration, and he has always been a great inspiration. Furthermore, I would like to thank Tue for his comments on the manuscript.

A special thanks also to the many colleagues at CEE, I very much enjoyed having the company of all of you. A special thank you to Tiago Sousa for his comments on the manuscript.

Also I must thank my family for their unwavering support and understanding. Especially I would like to mention Anne and thank her; she has had such a great patience and understanding for all the weekend work and late nights that I had to be at the office. I could not have done it without her support.

Contents

Abstract

The penetration of Distributed Energy Resources (DERs) in distribution networks is expected to rise significantly due to the electrification of the transport sector, solar photo-voltaic installations and growth in small scale storage and generation. Also, several existing loads can be converted into Demand Response (DR) units and the total share of DR as a subset of DERs is projected to be large; especially flexibility from Thermostatically Controlled Loads (TCLs) is cast to provide a substantial part of the total DR-based flexibility in distribution networks. The increased participation of DERs in power system operations can pose an array of challenges to the Distribution System Operator (DSO), but may also be perceived as an opportunity to leverage the embedded flexibility to meet network constraints. This requires new operational methods as the distribution networks are currently passive, and with little possibility of active control which is mostly limited to voltage control based on historical data and crude forecasts. Optimizing low-voltage distribution feeders is complex due to the non-convex nature of power flows and leads to optimality and pricing issues in market-based settings. This is addressed through the use of convex relaxation techniques in this thesis.

The power transfer through distribution networks will see drastic increases due to non-controllable Renewable Energy Source (RES) power in-feed (mostly Photo-Voltaic (PV) in urban distribution systems) and increased energy demand caused by Electric Vehicle (EV) charging loads and electrification of building heating and cooling. In order for the DSO to use TCL-based DR units to mitigate congestion issues caused by this increased energy transfer, the complex physical properties and limitations of these TCL-based DR units have to be incorporated into a market compatible framework. This thesis proposes a novel setting of using asymmetric block offers to embed the limitations of TCL-based DR into market compatible structures. This proposal coupled with the modeling of the network through convex conic programming leads to an efficient and cost-effective framework to use DR units and other DERs to mitigate congestion, and thus can decrease the cost of energy delivery and operation of the distribution network.

One of the issues requiring higher amounts of available flexibility in the power system is the increasing penetration of renewable energy sources such as wind- and solar-based generation and the accompanying stochastic generation profiles. The very nature of renewable energy sources requires a large amount of flexibility due to forecast errors and intermittent generation. Organizing the flexibility properly in the

day-ahead stage can help the steady and economic supply of energy. The growing need for flexibility has lead to the proposal of market designs that enable aggregated DERs to provide ancillary services to the Transmission System Operator (TSO), however this may pose a series of challenges to the DSO. At the same time proposals for market-based approaches to be employed by the DSO are receiving growing support and recognition. Coordinating the various proposed local markets with wholesale energy and TSO-level flexibility markets is a daunting task, as the size of the problem is immense and coordination requirements are complex. In the future there may be different market platforms available for DERs which they can use to increase their profits and the inherent economic incentives will aid their proliferation. In order to be efficient, those market-based methods have to be developed such that they provide a clear and transparent stimulus to all involved agents. Creating these market-based methods is also difficult due to the conflicting objectives of agents, and thus the complexity of sharing resources needs to be addressed by clearly defined hierarchical or distributed system organization. Taking on a hierarchical setup, this thesis proposes a construct to include coordination between local markets and wholesale in the scheduling stage.

Another challenge that needs to be addressed by future market platforms and their coordination is that electricity markets are designed to be operated deterministically, i.e. they do not take into account the growing share of uncertain generation in the scheduling stages. This can lead to high costs in the balancing stage when the intermittent production of renewable energy sources becomes apparent. The incorporation of uncertainties in market-based settings may in the future lead to improved dispatch, however the ideal stochastic dispatch is not implemented in wholesale markets for several reasons. For example, it violates several market desirable properties such as revenue adequacy and cost recovery of agents. In order to improve the uncertainty aware dispatch in the scheduling stage, this thesis proposes a design that defines interface variables between the forward trading wholesale and DSO-level markets. This is shown to approximate the ideal stochastic dispatch. By finding optimal exchange characteristics of local DSO-level markets with wholesale energy markets the TSO-DSO coordination of DER flexibility is enabled in the scheduling stage and thus decreases the expected cost of operating the power system. For given values of these “coordination variables” the DSO-level markets are independently imposing caps on the quantity bids of DERs in the wholesale markets. The potential benefit of this pre-qualification on the social welfare of the overall system is quantified and compared to other coordination schemes. By coordinating local markets the uncertainty awareness of the day-ahead dispatch is increased, while maintaining the current sequential dispatch of scheduling and balancing, thus preserving the market desirable properties of deterministic markets. A further advantage of this optimal coordination scheme is the non-iterative solution strategy, i.e. the market operators do not need to exchange multiple messages.

Resumé

Andelen af distribuerede energikilder i distributionsnettet forventes at stige betydeligt som følge af elektrificering af transportsektoren, solcelle installationer og vækst i små energilager og små generatorer. Flere eksisterende strømforbrugere kan konverteres til "Demand Response" (DR) enheder, og den samlede andel af DR enheder (som er en delmængde af distribuerede energikilder) forventes at være stor; særlig fleksibilitet fra termostat kontrollerede strømforbrugere kommer til at udgøre en væsentlig del af den samlede DR baserede fleksibilitet i distributionsnettet. Den øgede deltagelse af distribuerede energikilder i el systemet kan føre til en række udfordringer for el distributions netværks operatøren, men kan også ses som en mulighed for at udnytte den medfølgende fleksibilitet til at overholde netværksbegrænsninger. Dette kræver nye driftsmetoder, da distributionsnetværket i øjeblikket er passivt, med få muligheder for aktive målinger og kontrol. De er begrænset til spændingskontrol baseret på historiske data og prognoser af forbrugsmønstre. De få aktive kontrolmetoder er ikke optimeret med hensyn til tab eller omkostninger og forbedrer derfor ikke systemets sociale velfærd. Hvis det nuværende paradigme for driften af distributionssystemer opretholdes, vil det i sidste ende føre til store investeringer i sjældent anvendt infrastruktur. Dette skyldes, høje spids-belastningsstrømme som følge af den høje andel af distribuerede energikilder. Der findes flere forslag til at anvende informations- og kommunikationsteknologier for at forbedre den koordinerede brug af distribuerede energikilder på distributions netværks niveau. Selv om dette kan være teknisk muligt, er den optimale anvendelse af disse distribuerede energikilder besværligt og kræver avanceret modellerings teknikker. For tiden er der meget debat omkring hvilke paradigmer der skal bruges for at øge tilgængeligheden af fleksibilitet af små distribuerede energikilder. En af de udfordringer der kræver store mængder af fleksibilitet i el systemet, er den stigende andel af vedvarende energikilder som vind- og solbaseret strøm produktion og de medfølgende stokastiske produktions profiler. De vedvarende energikilders opførsel kræver stor fleksibilitet på grund af begrænset præcision af produktionsudsigterne og sporadisk produktion. Planlægning af fleksibilitet med avanceret metoder kan sikre den stabile og økonomiske bæredygtige forsyning af energi.

For at distributions netværks operatøren skal kunne anvende termostat baserede DR enheder til at øge den mulige tilslutnings mængde af distribuerede energikilder i nuværende netværk, skal de komplekse fysiske egenskaber og begrænsninger indarbejdes i et markedskompatibelt program. Denne afhandling præsenterer en ny metode

ved brug af asymmetriske blok tilbud for at medregne begrænsningerne af termostat baseret DR enheder. Samlet kan disse nye asymmetriske blok tilbud være kompatible med markeds clearing metoder. Denne kombination med modelleringen af netværket fører til en omkostningseffektiv ramme for anvendelse af DR enheder og andre distribuerede energikilder. Dette kan reducere omkostningerne ved energiforsyningen og drift af distributionsnetværket og øge mængden af mulig tilslutnings kapacitet.

Det voksende behov for fleksibilitet i nettet har ført til forslag af nye markedsdesigns, der gør det muligt at aggregere distribuerede energikilder for at tilbyde services til transmissionssystemoperatøren. Dog kan dette føre en række udfordringer for distributions netværks operatøren. Samtidigt er der mange forslag til at implementere markedsbaserede tiltag for at yde services på distributions niveau. Koordinering af disse foreslåede lokale markeder med eksisterende energi markeder og transmissions niveau fleksibilitetsmarkeder er en svær opgave, da størrelsen af problemet er enormt og koordineringsbehovene er komplekse. I fremtiden kan der være forskellige markedsplatforme til rådighed for distribuerede energikilder, som de kan bruge for at øge deres profit, og de tilhørende økonomiske incitamenter kan føre til vækst af denne teknologi. For at være effektive skal disse markeds baserede metoder udvikles således, at de giver en klar og gennemsigtig stimulans til alle involverede deltagere. Oprettelse af disse markedsbaserede metoder er også vanskelig på grund af de komplekse fysiske egenskaber af el-netværk der skal modelleres og af spil mellem deltagere. Derfor skal delingen af ressourcer behandles mellem forskellige markeder defineres gennem en hierarkisk eller distribueret systemorganisation. Ved at bruge en hierarkisk opsætning foreslår denne afhandling en konstruktion til at koordinere mellem lokale markeder og energi markeder i planlægningsfasen.

En anden udfordring, der skal løses af fremtidige markedsplatforme og koordineringen af disse, er at el markederne er beregnet til at operere deterministisk, dvs. de tager ikke højde for den stigende andel af usikker generation pga. vind og sol energi i planlægningsfasen. Dette kan medføre høje omkostninger i real tids balanceringen, når den tilfældige produktion af vedvarende energikilder bliver tydelig. Inkorporering af usikkerheder i markedsbaserede metoder kan i fremtiden føre til forbedret planlægning. Men den ideelle stokastiske model implementeres ikke i energi markeder af flere grunde. Eksempelvis bryder det flere vigtige egenskaber, såsom at summen af alle handler dækker omsætningerne og omkostningsgenvinding af deltagere. For at forbedre den usikkerhedsbevidste planlægning i markederne foreslår denne afhandling et design, der definerer grænseflade variabler mellem grossistmarkederne og markeder på DSO-niveau. Dette kan tilnærme den ideelle stokastiske planlægning. Ved at finde optimale interaktions karakteristika af lokale DSO markeder med engrosenergimarkeder er TSO-DSO-koordinationen gjort muligt og reducerer dermed de forventede omkostninger ved driften af el-systemet. For givne værdier af disse " koordinerings variabler " sætter DSO niveau markederne selvs en begrænsning på mængden af energi som distribuerede energikilder må handle på engrosmarkederne. Den potentielle fordel ved denne præ-kvalifikation bliver kvantificeret og sammenlignet med andre koordineringsordninger. Ved at koordinere lokale markeder øges usikkerhedsbevidstheden af den daglige planlægning, samtidig med at den nuværende

sekventielle opdeling af markeder opretholdes. Derved bevares de nødvendige egenskaber markederne. En yderligere fordel ved denne optimale koordination er den ikke-iterative løsningsstrategi, dvs. markedsoperatørerne behøver ikke at udveksle meddelelser eller information om priser flere gange.

Acronyms

ATC Available Transfer Capacity

ADNM Active Distribution Network Management

BFM Branch Flow Model

BIM Bus Injection Model

BRP Balance Responsible Party

DA Day-Ahead

DER Distributed Energy Resource

DR Demand Response

DSO Distribution System Operator

EV Electric Vehicle

FLECH Flexibility Clearing House

GNE Generalized Nash Equilibrium

ICT Information and Communications Technology

KKT Karush Kuhn Tucker

LMP Locational Marginal Pricing

MILP Mixed-integer Linear Program

MPEC Mathematical Program with Equilibrium Constraints

OPF Optimal Power Flow

PCC Point of Common Coupling

PSD Positive Semi-Definite

PV Photo-Voltaic

QCP Quadratically Constrained Program

RES Renewable Energy Source

RT Real-Time

SDP Semi-Definite Program

SOCP Second-Order Cone Program

TCL Thermostatically Controlled Load

TSO Transmission System Operator

List of Figures

List of Tables

Nomenclature

Symbols used in Chapter 4 for the asymmetric block offers

Sets and indices

C	Set of demand response units c
D	Set of offers d of each demand response unit
I	Set of distribution-level conventional generators i
L_n	Set of all facilities located at node n
$n, m \in \mathcal{N}$	Set of nodes n and m
$l \in \mathcal{L}$	Set of lines $l = (n, m) \in N \times N$, cartesian product of nodes
PCC	Point of common coupling, i.e., the node connecting the distribution and transmission levels
$t, \tau \in T$	Set of time steps t and τ
Φ_n	Set of all nodes connected to node n

Free Variables

p_{nt}/q_{nt}	Net active/reactive power injection at node n and time step t (positive for power injection) [kW/kVAr]
p_{lt}/q_{lt}	Active/reactive power flow from node n to m at time step t [kW/kVAr]

Non-negative Variables

$p_t^{\mathrm{up/dn,S}}$	Active power up/down-regulation provided by the transmission grid at time step t [kW]
$p_{it}^{\mathrm{up/dn}}$	Active power up/down-regulation provided by generator i at time step t [kW]
$q_t^{\mathrm{up/dn,S}}$	Reactive power up/down-regulation provided by the transmission grid at time step t [kVAr]
$q_{it}^{\mathrm{up/dn}}$	Reactive power up/down-regulation by generator i at time step t [kVAr]
$r_{dct}^{\mathrm{up/dn}}$	Active power up/down-regulation provided by demand response offer d of unit c at time step t [kW]

s_{tn}^{up}	Load curtailment at node n and time step t [kW]
v_{nt}	Squared voltage magnitude at node n and time step t [p.u.]
φ_{lt}	Squared current magnitude in line l connecting node n to m [p.u.]

Binary Variables

o_{dct}	Activation of block d of demand response unit c at time step t

Parameters

A_{dc}	Orientation of offer d of demand response unit c. Equal to 1 if begins with up-regulation, equal to 0 otherwise
B_l	Shunt susceptance of line connecting node n to m [p.u.]
$C_t^{\text{p/q},\uparrow/\downarrow\text{S}}$	Active/reactive up/down-regulation price provided from transmission level at the PCC at time step t [¢/kWh or ¢/kVArh]
$C_{dct}^{\text{DR}\uparrow/\downarrow}$	Active power up/down-regulation offer price of demand response unit c, offer d, time t [¢/kWh]
C^{Shed}	Cost of load shedding [¢/kWh]
$C_{it}^{\text{p/q},\uparrow/\downarrow}$	Active/reactive up/down-regulation offer price of conventional generator i at time step t [¢/kWh or ¢/kVArh]
D_{nt}^{disp}	Scheduled active power consumption of all inflexible loads at node n and time step t from the day-ahead market [kW]
DR_{ct}^{disp}	Scheduled active power consumption of demand response unit c at time step t from the day-ahead market [kW]
G_l	Shunt conductance of line connecting node n to m [p.u.]
$\overline{F}_{nj}$	Capacity of line connecting node n to j [kVA]
$\overline{P}_i^{\text{up/dn}}$	Maximum active power up/down-regulation capability of generator i [kW]
$\overline{P}^{\text{up/dn,S}}$	Maximum active power up/down-regulation that can be provided by transmission level [kW]
$P_{dc}^{\text{rsp/rb}}$	Response/rebound power of offer d of demand response unit c [kW]
P_{it}^{disp}	Dispatched active power production of generator i at time step t from the day-ahead market [kW]
P_{ct}^{cap}	Maximum active power consumption of demand response unit c at time step t [kW]
P_i^{cap}	Active power capacity of generator i [kW]
$\overline{Q}^{\text{up/dn,S}}$	Maximum reactive power up/down-regulation that can be provided by transmission level [kVAr]
$\overline{Q}_i^{\text{up/dn}}$	Maximum reactive power up/down-regulation capability of generator i [kVAr]

Q_{nt}	Total reactive power consumption at node n and time step t [kVAr]
R_l	Resistance of line l connecting node n to m [p.u.]
S_t^{disp}	Dispatched import/export of active power from the transmission system at time t from the day-ahead market [kW]
$T_{dc}^{\text{rsp/rb/rec}}$	Response/rebound/recovery duration of demand response offer d of unit c [time step]
$\overline{V}_n^{\text{sq}}$, $\underline{V}_n^{\text{sq}}$	Upper and lower limits for voltage magnitude squared at node n [p.u.]
X_l	Reactance of line l connecting node n to m [p.u.]

Symbols used in Chapter 5 for the PCC optimizer

Indices and sets:	
$d \in \mathcal{D}$	Index for flexible demands or DR units
$e \in \mathcal{E}$	Index for distribution feeders
$g \in \mathcal{G}$	Index for conventional generators
$n, m \in \mathcal{N}$	Indices for nodes in both DSO and TSO networks
$l \in \mathcal{L}$	Index for lines; $l = (n, m)$
$r \in R$	Index for renewable energy sources (RES)
$\omega \in \Omega$	Index for renewable power scenarios
Subsets and special labels:	
$\mathcal{D}_n, \mathcal{G}_n, R_n$	Set of assets located at node n
$\mathcal{D}_e^{\text{D}} \subset \mathcal{D}$	Set of demands connected to distribution feeder e
$\mathcal{D}^{\text{T}} \subset \mathcal{D}$	Set of demands connected to the transmission grid
$\mathcal{G}_e^{\text{D}} \subset \mathcal{G}$	Set of generators connected to distribution feeder e
$\mathcal{G}^{\text{T}} \subset \mathcal{G}$	Set of generators connected to the transmission grid
$\mathcal{L}_e^{\text{D}} \subset \mathcal{L}$	Set of lines in distribution feeder e
$\mathcal{L}^{\text{T}} \subset \mathcal{L}$	Set of lines in transmission grid
$\mathcal{N}_e^{\text{D}} \subset \mathcal{N}$	Set of nodes in distribution feeder e
$\mathcal{N}^{\text{T}} \subset \mathcal{N}$	Set of nodes in transmission grid
$\rightarrow n \subseteq \mathcal{L}$	Set of lines ending at node n
$n \rightarrow \subseteq \mathcal{L}$	Set of lines originating at node n
$n_e^{\text{HV}} \in \mathcal{N}^{\text{T}}$	Node at HV-side of the PCC of feeder e
$n_e^{\text{LV}} \in \mathcal{N}_e^{\text{D}}$	Node at LV-side of the PCC of feeder e
l_e	PCC of feeder e connecting HV- and LV-side nodes
$l' = (m, n)$	Line in the opposing direction of line l
Variables of the PCC optimizer:	
$\overline{f}_e / \underline{f}_e$	Upper/lower limit on import/export of apparent power at the PCC of feeder e [MVA]

$\pi_e^{\text{PCC,DA}}$	Day-ahead price at the PCC of feeder e [$/MWh]
$\pi_e^{\uparrow/\downarrow\text{PCC}}$	Regulating offer markup for up/down-regulation at the PCC of feeder e in real time [$/MWh]
Variables at the day-ahead stage:	
$\widetilde{p}_{g/d}^{DA}$	Active power dispatch of DSO-level generator g / demand d in the local DSO market. This value is treated as a cap on the quantity bid to the DA market [MW]
$\widehat{p}_{g/d}^{DA}$	Active power dispatch of generator g / demand d in the DA market [MW]
s^{DA}	Total active power load curtailed [MW]
w_r^{DA}	Active power dispatch of RES r [MW]
Variables at the real-time stage under scenario ω:	
$p_{g\omega}^{\uparrow/\downarrow}$	Active power up/down-regulation of generator g [MW]
$p_{d\omega}^{\uparrow/\downarrow}$	Active power up/down-regulation of demand d [MW]
$p_{g\omega}^{RT}/q_{g\omega}^{RT}$	Final active/reactive production of generator g, i.e, its dispatch in DA plus the regulation in RT [MW/MVAr]
$p_{l\omega}^{RT}/q_{l\omega}^{RT}$	Final active/reactive power flow across line l, i.e, the flow dispatched in DA plus the regulation in RT [MW/MVAr]
$s_{n\omega}^{RT}$	Total active power load curtailed at node n [MW]
$s_{n\omega}^{q,RT}$	Total reactive power load curtailed at node n [MVAr]
$\theta_{n\omega}^{RT}$	Voltage angle at TSO-level node n [rad]
$w_{r\omega}^{\uparrow/\downarrow}$	Active power up/down-regulation of RES r [MW]
$w_{r\omega}^{RT}$	Final active power production of RES r [MW]
$v_{n\omega}^{RT}$	Squared voltage magnitude at DSO-level node n [p.u.]
$\varphi_{l\omega}^{RT}$	Squared current magnitude flow in DSO-level line l [p.u.]
Parameters:	
$\overline{P}_{g/d}, \underline{P}_{g/d}$	Upper/lower active power limit for output of generator g and consumption of demand d [MW]
$\overline{Q}_{g/d}, \underline{Q}_{g/d}$	Upper/lower reactive power limit for output of generator g and consumption of demand d [MVAr]
$R_l/X_l/S_l$	Resistance/reactance/flow limit of line l [p.u.]/[MVA]
$\overline{V}_n, \underline{V}_n$	Upper/lower limit for voltage magnitude of node n [p.u.]
$VOLL$	Value of lost load [$/MWh]
W_r^{DA}	Power forecast of RES r in the DA stage [MW]
$W_{r\omega}^{RT}$	Power generation of RES r in RT under scenario ω[MW]
$\pi_{g/d}^{DA}$	Marginal offer/bid price of generator g / demand d in the DA stage [$/MWh]
π^{R}	Offer price of RES (assumed to be zero) [$/MWh]
$\pi_{g/d}^{\uparrow/\downarrow}$	Regulating offer markup in RT for up/down-regulation of generator g / demand d [$/MWh]
$\pi^{\uparrow/\downarrow R}$	Up/down-regulation offer of RES in RT [$/MWh]

CHAPTER 1

Introduction

1.1 Background

The future of power systems is highly challenged with the aim to change to a carbon-free and Renewable Energy Source (RES) based system. The move towards more RES and away from centralized power plants in the energy mix means that the dispatchability of generation decreases [1], [2]. This is caused by the fact that the generation output of RES is subject to external factors determined by the weather and therefore stochastic in nature. Consequently, it introduces variability and uncertainty in the planning process, both for short- and long-term decisions. Additionally, the electrification of other sectors such as transport and heating will increase the total demand for electric energy and further heighten variability and uncertainty of the real-time power balance. Ensuring the economic, safe and steady supply of energy is of utmost importance to the end-user, which contrasts with the stochastic nature of RES energy production. The ever increasing RES penetration is therefore challenging the economic and secure operation of the electric power system under the current operating paradigms. For example, in Denmark the total yearly energy output of wind power in the years 1990 to 2015 has increased from below 1TWh to 14TWh, while the yearly power consumption has remained almost constant between 30TWh to 35TWh in the same period [3].

The research to enable increased RES penetration to lower emissions in the electric power system has many facets. One theme that has increasingly found support is to leverage the flexibility[1] of DERs to offset the imbalance caused by stochastic RES production. The term "DER" encompasses a large variety of technologies, such as domestic heat pumps, rooftop solar Photo-Voltaics (PVs), battery storage, small-scale distributed generation which are all connected to distribution networks [6] and thus located close to end-users. The system operators can potentially use DERs to meet various needs such as balancing, congestion management or voltage profile corrections if their flexibility is made available.

The owners of DERs must have a clear motivation to cooperate with system operators and be aware of their investment opportunities in this technology in order to facilitate the meaningful deployment. The economic incentives through the liberal-

[1] The taxonomy of flexibility within power systems is not entirely unified. For a review of DER types and sources of flexibility see [4]. Also [5] provides an overview of how Distributed Energy Resources (DERs) can provide value in smart grids.

ization of electricity markets are an enabling factor to motivate the proliferation of DERs [7]. Entry barriers are being continuously reduced so that ever smaller units are able to participate in trading on existing market platforms and new emerging market designs [8]. Heightened participation in markets will increase competition which can ensure the affordable supply of electricity, assuming efficient and well designed markets. However, designing meaningful remuneration mechanisms to spur the investments in DERs is very challenging, due to the potentially vast number of participants and uncertainty of future policy of system operation. Furthermore, moving energy trading into the new domain of small-scale DERs requires new modeling techniques due to different physical properties of distribution networks [9].

Some of the major challenges that are appearing due to increasing RES and DER penetration and electrification of ever more systems, are the high variability of power production & consumpion, high peak loads and thus transfer of more energy through distribution networks if loads are uncontrolled, and bi-directional power-flows in radial feeders. Therefore, the operation of the distribution networks will have to undergo major changes to increase the hosting capacity of DERs in a cost-efficient way. The networks which have been previously safeguarded by over-sizing of components, may in the future need to be much more actively managed by exploiting flexibility of new technologies. It is recognized by the research community that the intelligent use of DERs can defer grid investments [10]–[12], and uncover hidden flexibility in the power system. In general, the passive operation of distribution grids may lead to expensive investment into rarely used infrastructure. This is mainly due to the peak loading situations that cannot be controlled or mitigated in passive distribution feeders and it is one of the issues that current research is addressing.

When integrating RESs in the power system and offsetting their variable production using DERs, several problems can be identified. Firstly, it requires a rethinking of the Distribution System Operators (DSOs) role in power systems which does not currently partake actively in scheduling energy or activation of flexibility. Secondly, the use of DERs to meet various grid constraints has to be combined with the liberalized energy markets which were designed in a time when RES penetration was lower and of less concern and are mainly targeted at large power plants and wholesale of energy. Thirdly, the conflicting objectives of different stakeholders is important to recognize and has to be addressed in future power systems, in order to resolve conflicts and guarantee efficient use of resources.

1.2 Research questions

The aim of this thesis is to propose novel ways of integrating DERs in power system operations to (i) increase the loadability of distribution systems and defer infrastructure investments, (ii) enhance the use of DERs to offset unpredictable production of RESs, and (iii) explore frameworks for different operators to simultaneously use DER flexibility through market compatible approaches. To achieve these goals, the research of this thesis is focused on *market-based solutions* built upon mathematical

tools and optimization techniques. Further, the focus of the conducted research is concerned with the short-term operational aspects of increasing RES and DER penetration. The long-term planning of infrastructure and expensive investment in RES and DERs is viewed as outside the scope, however it is important to note that the improved short-term operations of networks will also influence the economics of long-term investment plans. Especially the scheduling of the day-ahead markets and their outcomes up until the real-time stage where the actual delivery of energy takes place is the topic of the current research. The first part of the work takes the view of a DSO, that wishes to use market-based operational planning to mitigate congestion issues. This may be more economical for the operator than network upgrades. This part of the work takes the Day-Ahead (DA) market outcomes as given inputs which influence the operational tasks of the DSO. The second part of the work is directed at the use of DER flexibility in a coordinated manner. It assumes that the DSO and Transmission System Operator (TSO) both have an interest in using the same flexible resources to optimize their systems. The research objectives are grouped into the two following main questions.

I. How can complicated demand response technical properties be included by the DSO for congestion management in a precise and effective economic dispatch mechanism?

A large amount of the available DER penetration is expected to be in the form of demand response [7], [9], [13], [14], which can be classified into three groups depending on their operational capabilities [15], [16]; These are (i) curtailable loads, i.e. loads that are partially or entirely reducing consumption, (ii) deferrable loads, i.e. the loads can be shifted to other hours typically in the same day such as charging of electric vehicles, and (iii) Thermostatically Controlled Load (TCL), meaning the power consumption change is subject to an immediate reaction after the change in the opposite direction. The phenomenon in the last demand response type is termed the *rebound effect* (also referred to as *kick-back effect*) [17]–[19]. A large amount of the available loads that are possible to use as Demand Response (DR) are TCLs and thus subject to the rebound effect. For example, supermarket refrigeration [17], [20]–[22] or heat-pumps with thermal storage [23]–[26] are identified as possible sources of DR. If not considered properly in a dispatch of DRs, the rebound effect may cause unforeseen problems or lead to sub-optimality of market clearing algorithms.

Since DR units often will be connected to the distribution grid, the DSO may have an interest in using them in future market-based methods for congestion management. This requires the accurate modeling of the underlying distribution network with details such as voltage magnitudes, active and reactive power flows. These models should be sufficiently accurate, transparent, computationally efficient and achieve well defined results. The last issue pertains to the use of convex models, as this property leads to the provable convergence to globally optimal solutions. However, the nature of power flows is non-convex and therefore the used convex models must

sufficiently approximate this system to yield feasible and cost-efficient results. A number of works have used linear models [27]–[30] which are simple but efficient approximations for the power flow. Recently, the use of convex relaxation through conic programming is improving the power system modeling [31]–[36] which can improve the dispatch and control of DR resources in distribution networks. The choice of modeling frameworks will impact the use of demand response and other DERs. In light of the complicated nature of DR interactions with markets and network modeling of distribution network, this thesis seeks transparent models for decision making by the DSO while inherently taking into account the rebound effect.

II. How can the scheduling of DERs be coordinated in day-ahead between TSO and DSOs in a practical framework to counter uncertainty of intermittent RES generation?

The DERs connected to distribution grids may not only be used by DSOs to mitigate congestion or voltage issues. Demand response usually provides a cheaper alternative to classical means of providing balancing power [17], [37]. To decrease cost the TSO may in the future choose to use aggregated DERs for balancing, while DSOs and Balance Responsible Partys (BRPs) seek to use the same resources to meet other goals. Conflicts may therefore arise when DERs connected to distribution networks are providing services to the TSO if it causes operational issues to the DSO. Coordination of DSO and TSO actions are therefore pertinent and can be achieved at multiple temporal or organizational levels, i.e. either the scheduling or the activation of energy and reserves in system wide or local organizational structures.

In a holistic market view, a market clearing that includes DERs may be very intricate due to large number of offers and competing incentives of participants, market operators and system operators [38]–[41]. If on the other hand, the needs of the TSO and DSOs are completely separately handled, and coordination is not taken into account, it may result in counteracting control actions that lead to sub-optimal operation of the power system. It is an ongoing research question how the responsibilities should be distributed among TSO and DSOs and how their access to resources can be coordinated in liberated markets. The emphasis should be put on socially responsible models for coordinating the different system operators, such that the available DER flexibility can contribute to improve the social welfare of the system. Several research works have been published to show methods of coordinating the use of DER flexibility by the TSO and DSOs [38], [41]–[51]. These works have addressed coordination in the real-time activation of DER flexibility, or are not congruent with scheduling under current European sequential market clearing frameworks. In order to motivate the implementation of coordination schemes, this thesis seeks a framework that is scalable and adaptable to the energy trading floors in operation today while taking into account the forecasting uncertainty of intermittent RES production. Therefore, the conducted research investigates the optimality conditions in the scheduling stage by modeling the sequential and hierarchical structures of the different trading floors

and proposes novel methods to achieve optimal coordination.

1.3 Scientific contributions

Much recent research has been done in proposing frameworks for DERs to be scheduled such that voltage violations and congestion can be mitigated and thus aid the DSO in system operation. One way to schedule DERs for the DSO is to use price-based approaches, where the DER is offering its services in a market or mechanism as an individual profit maximizers [28], [29], [52]. Another possibility is for the DERs to be rewarded with incentives such as proposed in [29], [53], [54] if they are aiding the operator in avoiding contingencies. For a comprehensive overview of congestion management in distribution feeders see [55] or [56]. However, none of the previous works in congestion management have modeled the inherent rebound effect of TCL-based demand response units. The modeling of the rebound effect can be quite challenging due to the inter-temporal coupling of power injections that they create. One method is to use dynamic programming [57] in order to capture inter temporal coupling of power injections. Dynamic programming is however not a compatible method for market clearing. In [58] it was proposed to use *asymmetric block offers*, a novel type of market offer, to a-priori model rebound effect in the market clearing process. In [58] the TSO balancing market was considered, and no analysis of the power flow model was included.

A first contribution of this PhD thesis is therefore the development of a novel congestion management method which leverages the underlying flexibility of DR units with an inherent rebound effect. Demand response units that must rebound after activation, are units that can only provide up- or down-regulation power with the constraint that they need to rebound in the opposite direction in a following time period. This kind of behaviour is expected from TCL-based DR units, such as supermarket refrigeration or building temperature control. **[Paper A]** introduces a market mechanism, where aggregators can offer the flexibility of DR units with rebound effect to the DSO in the form of asymmetric block offers. The DR units offer their services in the form of these offers which consist of two parts, a response and a rebound. Each of these parts is either a load increase or decrease, and it is the responsibility of the DR unit or aggregator to make sure that they are physically feasible for the underlying load. The advantage of these asymmetric block offers is that the offer, and thereby the market clearing mechanism, is inherently taking into account the physical characteristics of the DR units and that they are transparent and easy to understand to the system operators. The relation of the power flows and congestion in distribution networks is complicated, as they can be caused by both voltage level violations and thermal line flow limits. The non-convexity of these relations further complicates modeling and thus market-based methods to mitigate them.

A second contribution of **[Paper A]** is to make a comparative analysis of different Optimal Power Flow (OPF) models in radial distribution networks and their impact on the dispatch of asymmetric blocks offers from the TCL-based DR units. Three

different models are implemented, each with increasing complexity and thus precision. Since any market-based mechanism needs to be able to be executed within a limited time-frame, computational burden and precision of the underlying physical model are generally counterbalancing each other and a trade-off needs to be made. Therefore, the most precise models may not necessarily be the right choice to be implemented practically. In recent years, a lot of contributions with convex relaxations of the non-convex AC power flow equations have been made [31], [32], [55], [59]. For radial distribution feeders, especially the convex branch flow formulation through Second-Order Cone Programs (SOCPs) is gaining more support [60]. The SOCP models can however be challenging to solve and therefore linear and sequential linear programming models are also considered. The results provided in **[Paper A]** provide an analysis of the re-dispatch outcomes when using these different power flow models, including convex relaxations, in connection with the asymmetric block offers.

The rapid increase of RES penetration leads to an increased need for balancing and other ancillary services due to intermittent of power injections. Since many research works suggest that aggregated DERs should be offered to system operators to provide these services [4], [9], [37], new models need to be developed to make this possible and at the same time be easily adaptable by system operators. DERs that are activated by the TSO as fast acting reserves may lead to congestion issues and voltage problems that the DSO cannot handle, if not managed properly. The connection of distributed generation can cause and array of issues to the DSOs [61], [62] and this may be magnified if they respond to unpredictable price signals from the TSO. The coordinated use of flexibility stemming from DERs is therefore pertinent, however there are a host of challenges relating to this. The low-voltage networks operated by DSOs are of massive size themselves, and the TSO does not take into account distribution grids when optimizing power flows. An integrated co-optimization of DSO and TSO networks is unlikely to be implemented in practice due to the sheer size of the problem [45], [46] and policy driven issues [63]. Therefore, a promising alternative is to optimize power flows in a decentralized fashion that respects operational regions of different system operators. Also, privacy concerns exist, which may dissuade the TSO and DSOs from sharing all information about their operating domains with each other. Much work has been done in proposing various ways of using DER flexibility in DSO-level markets to provide congestion management [29], [64]–[68]. However, it is not clear how DSO-level markets can provide access to the TSO to share these resources. DERs participating in balancing markets of the TSO, without any control or oversight may be an untenable position for any DSO. Further, the objectives of DSOs and TSOs when using the same resources may be contradictory and therefore any coordination must take into consideration the objectives the different agents. New market players called “aggregators” enable to pool DER into packages and thus lower the barrier for market participation of small DER units. This development may increase the DER quantity on markets and thus the need for coordination. Previous works on TSO-DSO coordination have focused on the activation of DERs close to real-time [41], [42], [44], [45], [49], [50]. However, the bulk of the energy is traded in day-ahead markets and premiums are usually applied by the providers of balancing

power when moving closer to real time. Therefore, the research conducted in [**Paper B**] has focused on building a framework for quantifying gains from coordination built on top of existing day-ahead markets, which may be realized via local flexibility markets. Further, the policy changes required by proposing decentralized market clearing may be too drastic changes for system operators that prefer smaller changes to the operational policies [45], [46]. The work conducted in [**Paper B**] is concerned with the issue of coordinated use of energy and flexibility from DERs by TSO and DSOs in the day-ahead stage, considering incremental changes to current market clearing procedures. The paper introduces a novel way of considering prices and flow limits at the interface between different system domains. In order to achieve an equilibrium between the different trading floors which will increase system social welfare, these "coordination variables" are then optimized respecting hierarchical system operation. An approach based on game theory is applied, in order to frame the interactions of different trading floors, both local and system wide markets. The resulting model is a leader-follower type game (Stackelberg game), that captures the hierarchical nature of the interactions of agents and temporally spaced (sequential) trading floors. This setup is making it possible to reveal the optimal prices for arbitrage trading between different system operators' domains with respect to the social welfare of the system. The setup is implemented as a bi-level optimization problem whit a stochastic scenario-based approach to capture uncertainty of RES production. This in effect uncovers the highest possible system-wide social-welfare increase that coordination may achieve if local markets are employed by DSOs.

The scientific contributions of both [**Paper A**] and [**Paper B**] are providing paths of integrating DERs into proposed and existing market platforms while taking into account the specifics of modeling power flows in low-voltage distribution networks. The modeling aspect is one part that makes this class of power system optimization particularly hard, since the non-convexities of AC power flows are usually more important to take into account than in high-voltage transmission networks.

1.4 Organization

The thesis consists of two main parts. Part I is a report that summarizes the work that was carried out for this thesis. It consists of Chapters 2 through 6. Chapters 2 and 3 present the theoretical background on TSO-DSO coordination methods and the modeling used in the applied research. Specifically, Chapter 2 is a review on current Nordic electricity markets, proposed market-based solutions for DSOs and frameworks for TSO-DSO coordination. Chapter 3 delivers the mathematical background and presents different optimization models, which can be used to model power flows and clear markets on DSO-level. Chapters 4 and 5 present the main findings developed in this thesis to enhance the DER participation in markets based on [**Paper A**] and [**Paper B**], respectively. Chapter 6 draws conclusions from the presented research and discusses its applicability to current and future power systems. Also, future

critical research directions are outlined to direct the reader towards unsolved aspects in the avenue of market-based methods for the coordinated use of DERs.

Part II consists of all the papers that were written and submitted for publication. The papers can be found in the annex of this thesis. The papers that were produced for this thesis are the following:

[Paper A] "**Congestion Management in Distribution Networks With Asymmetric Block Offers**" – This is a journal article submitted to the IEEE Transactions on Power Systems in August 2018 with reviews received in December 2018. It was resubmitted in January 2019 and is currently in the second round of reviews.

[Paper B] "**TSO-DSO Coordination via Optimizing Interface Capacity Limits**" – This is a journal article submitted to the IEEE Transactions on Power systems and currently undergoing review.

The following papers were written during this PhD but are not actively contributing towards the thesis and are not included in Part II:

[Paper C] "**Convex relaxation of Optimal Power Flow in Distribution Feeders with embedded solar power**" – Peer reviewed conference proceeding in *Energy Procedia*, 3rd International Conference on Power and Energy Systems Engineering, CPESE 2016, 8-10 September 2016, Kitakyushu, Japan Kitakyushu, Japan.

[Paper D] "**Topology optimisation of PMSM rotor for pump application**" – Peer reviewed conference publication, 2016 XXII International Conference on Electrical Machines (ICEM), Lausanne, Switzerland.

CHAPTER 2

TSO-DSO coordination of flexible resources

The liberalization of the electricity sector was started in Europe in the 90s with the splitting up of vertically integrated utilities [69], [70]. A major change was the introduction of forward trading markets for wholesale of electricity. Liberalized electricity markets are justified by the notion that free markets increase competition and thus work to reduce cost [71], [72]. In theory, this ultimately leads to end-user prices that more closely reflect the actual price of energy production, transmission and distribution. Electricity markets have been evolving ever since, and are under constant change as new innovations in market design are introduced as well as adapting to new technologies. Recently, through the increase in Renewable Energy Sources (RESs) penetration, the uncertainty of the real-time production in the system has increased, and is challenging the deterministic market approaches used to trade wholesale energy. In figure 2.1 the past and forecast yearly production from different energy sources in Denmark is shown. This graph illustrates the fast growth of especially wind power in Denmark, while at the same time conventional large power stations are reducing their output or are being outright shut down. This requires a rethinking of current deterministic market structures that can reap the benefit of enhanced interactions of RES and Distributed Energy Resources (DERs). However, this involves the changing of the operational aspects of several agents in the power systems.

In this chapter, the currently existing Nordic electricity markets are described, and proposed methods to include the Distribution System Operators (DSOs) in markets are summarized as well as TSO-DSO coordination schemes. Specifically, in Section 2.1 the challenges on market integration of DERs are summarized. Section 2.2 introduces the reader to current Nordic market designs and discusses future design challenges. In Section 2.3 the proposals for DSO-level market-based methods are reviewed briefly, and future issues that have not been addressed by current literature are discussed. Finally, in Section 2.4 the connection between TSO and DSOs is discussed, and proposals of TSO-DSO coordination are presented.

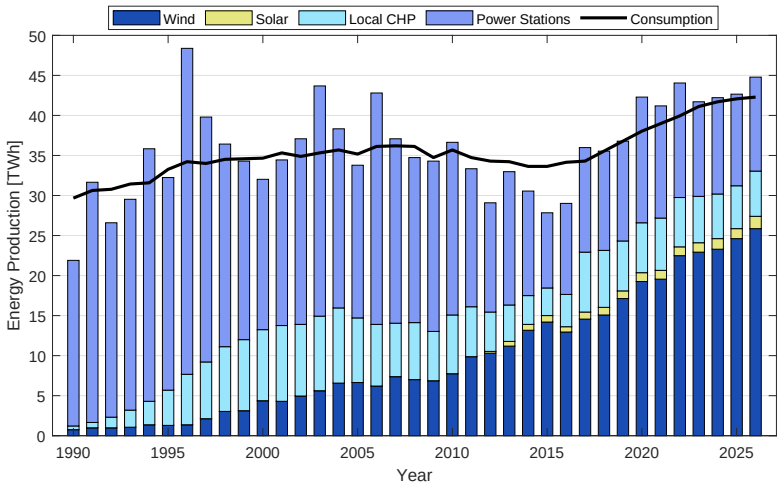

Figure 2.1: Energy production by source in Denmark, historical and forecast [3].

2.1 On the market integration of small flexible resources

The connection of ever more RESs (as evidenced in figure 2.1) to the power system poses a series of new challenges. One of the big issues of increasing RES penetration is the stochastic nature of the power injection and the resulting balancing needs to the Transmission System Operator (TSO). In the power system where it is of essence to maintain a stable frequency which is strongly correlated to the generated and consumed power [73], the balancing of intermittent RES generation becomes a problem [2]. For the DSO, the increasing DER penetration can lead to congestion problems due to limited hosting capacity of current distribution feeders [74] and many distribution feeders will not be able to handle reverse power flows due to limited capability of protection equipment and voltage regulators [75].

The annual addition of DER capacity expected to be connected in the United States is shown in figure 2.2. This historical and predicted deployment data brings to attention the acceleration of DER deployment. In addition to distributed generation, the increase of electric vehicle charging load and demand response will accelerate in the next years. Ultimately, it will lead to a higher average load, but particularly the peak loading will increase drastically if the power injections/load patterns are allowed to be uncontrolled. The increasing penetration of DERs provides an opportunity to use their inherent flexibility to balance out the stochastic RES production [12], [43], [58]. Therefore, an increasing number of DERs is expected to participate in ancillary

services markets on TSO level [12]. Also, the share of DERs in day-ahead and intra-day markets will increase as new market models develop and requirements for DERs to take part in economic dispatch are created. For example, demand response units can be used for balancing power provision [58] and distributed battery storage can be used for arbitrage trading to flatten out the fluctuating prices due to variable wind power in-feed [37], [76].

Different market opportunities lie on the DSO level. The DSOs may wish to use the flexibility of DERs such as demand response for congestion management and voltage control. Currently, there are no commercial DSO-level markets to use DER flexibility [43], but there have been some demonstration projects involving actual distribution grids. For example, the EcoGrid 2.0 project in Denmark has demonstrated a DSO mid-term market for demand response [78]. An issue at the moment is the lack of clear policies in most European countries to allow the DSO to procure flexibility from local DERs. However, there are already discussions on European level proposing paths to establish local flexibility markets [63], [79]. Another demonstration project is the SmartNet project, which has studied trans-European TSO-level markets and their coordination with DSO-level markets [80], [81].

In the past RES-based DERs, for example roof top Photo-Voltaic (PV) generation has been subject to advantageous policies. In many countries, distributed PVs are exempt from taking part in the economic dispatch and are being rewarded with highly incentivised feed-in tariffs [82], [83]. Similarly, RES sources connected directly to transmission grids have not been participating in balancing responsibilities either,

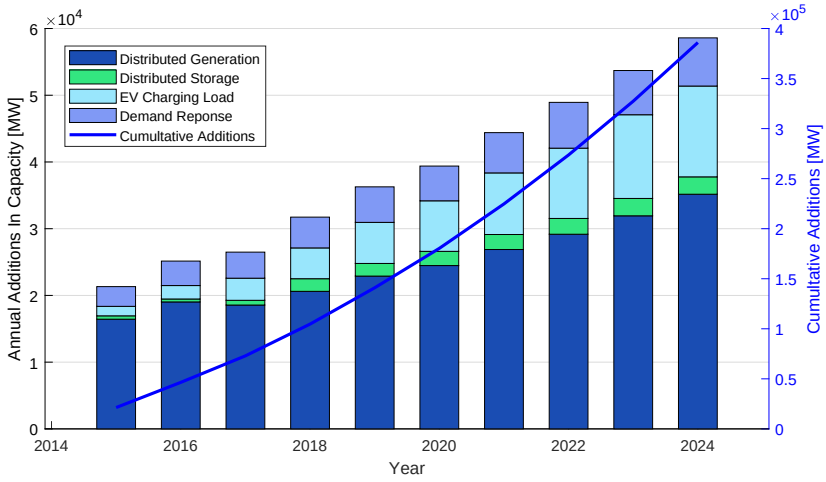

Figure 2.2: Annual additions in DER capacity to the distribution power systems in the United States [77].

which inflates their actual value to society [84], [85]. A phase-out of this incentive scheme is anticipated in the future forcing RES to some extent to participate in the dispatch on the same grounds as other loads and generators [86], [87]. In practice, DERs will be clustered in groups by new market players, the so-called load and/or generation *aggregators*. This construct has several advantages. Firstly, aggregated DERs will have larger volumes that will allow to pass market entry barriers. Secondly, it will decrease the market clearing complexity because clustered offers are decreasing the number of single offers/bids. Thirdly, single DER owners such as residential battery storage may not be willing to have an active market role and thereby they can delegate their market participation strategy. The clustering of small units has been designated under various terms in the literature, one recurring theme is the idea of "virtual power plants" (VPP) where the aggregators control a series of DERs and other resources in a coordinated manner to offer services similar to centralized power plants [2], [10], [88], [89]. Some other options for RES and DERs to respect dispatching and taking part in wholesale markets is to establish *local energy markets* [90], energy communities or peer-to-peer markets [91] that in a coordinated manner interact with wholesale markets on a higher level (national or even cross-boarder).

The increased participation of DERs in markets will have several remarkable effects on existing markets. In general, the participation of RES in the day-ahead markets decreases the spot price of electricity because RES have a very low marginal cost of production[1]. Distributed solar PV proliferation will further push this development, especially in countries that have good meteorological and geographical prerequisites for solar power. Also, the flexibility of DERs such as demand response and storage will shift the flexibility patterns in the power system. This means that ancillary services, such as real-time balancing of power can in the future be realized in a distributed manner reducing reliance on large centralized power plants [63]. Until now it is mainly large spinning reserves and reserve generation capacity in centralized power plants that is responsible for primary frequency control and real-time balancing of power[2].

For the DSO the development of increased DER dispatchability and controllability means that active management of DERs can be an attractive solution to mitigate congestion and voltage issues. However, the frameworks that allow such an active management of DERs are currently a topic of active research [56]. The liberalization of DSO-level operations is projected to provide tools to cope with the increased transfer of power through distribution networks and help the proliferation of DERs [14]. Local market models are not only a dynamic method for the DSO to manage

[1] Often they will offer their production at zero or evenat negative prices due to incentives [83] in order to be certain of being dispatched. The market clearing price will be determined by the highest accepted offer.

[2] The terminology on "balancing power" is not entirely streamlined in the literature, which is a major problem as there may be variations on terms that can pertain to the same function. In the Nordic countries the term "regulating power" is mostly preferred. Other types of balancing alike services are sometimes called "frequency restoration reserves" or "frequency containment reserves" ect. We do not discuss the function of inertia by rotating masses, which is aiding frequency and power balance in actual real-time.

its networks, but they are also incentivising the deployment and investments into smart grid technology. For example in [26] it is concluded that the current policies in German distribution systems are hardly able to give good returns on investments of domestic heat pumps with thermal storage. It is there argued that the policies should enable more dynamic real-time pricing that reflect the current operating conditions of the network in order to promote economic signals to invest in heat storage. In [92] the effect of local pricing measures on the behaviour of distributed heat pumps is modeled together with the power injections of distributed PV. Similarly, an analysis on the economic viability of battery storage in distribution grids is carried on in [76].

The discussion above highlights some of the benefits of DER integration in markets and the creation of new markets tailored for DSO and DER applications. However, several new problems arise in this avenue of research. For example, the competing objectives of DERs to maximize profit in energy wholesale markets, the TSOs objective to balance the grid and ensure safety and stability margins, and the DSOs objective to mitigate congestion can be hard to align properly. Consider this simple circular example: The use of DERs for grid balancing by the TSO can cause congestion issues to the DSO, who will then activate other DERs to mitigate this congestion which again causes imbalance to the TSO. This situation has already been reported by DSOs today, when the TSO is activating combined heat and power plants connected to distribution grids [93]. To resolve these issues many works are discussing the coordination of DSO and TSO use of DERs. This coordination can also be coupled with the wholesale of energy from DERs to increase social welfare to the end-user.

In the next section, a short review of existing Nordic electricity markets is presented in order to give some background on the underlying mechanisms that current research is trying to amend to accommodate DERs and increasing RES penetration in the energy mix.

2.2 Nordic electricity markets

The Nordic wholesale electricity markets are operated by an independent market operator, which is distinct from the TSO. The Nordic market operator is Nordpool which operates the day-ahead market, and the intra-day market. These are also known as the spot-market and the ELBAS market [94]. The majority of the energy is traded in the day-ahead market. Additionally, the Nordic TSOs operate a joint regulating energy market which is used to correct any imbalances that arise due to deviations from the day-ahead and intra-day schedules. In this section, mainly the Nordic market architecture will be presented so that the reader can better comprehend the coordination schemes that are presented in the subsequent sections; we will also touch upon differences to other European markets or United States markets so that the reader will be informed of particular design choices. However, we will not in depth describe these other market designs and architectures. For a more comprehensive description of the United States market architecture see [95].

2.2.1 Existing markets

The Nordic market clears the day-ahead market in a zonal fashion, where day-ahead prices are uniform across an entire zone. The zones can incorporate large geographical areas. For example, Denmark is split into two pricing zones DK-east and DK-west[3]. On the other hand, the US day-ahead markets adopt a Locational Marginal Pricing (LMP) method, where the prices can differ between neighbouring transmission nodes. The Nordic market regulations prohibit the use of LMPs [14]. Trading between zones is also possible but is limited by the TSOs before Balance Responsible Partys (BRPs) submit their bids to day-ahead markets [96]. A schematic of the different markets up to and after actual delivery of energy is given in figure 2.3. The day-ahead markets and intra-day markets are used to trade energy, where the intra-day market closes 60 minutes before the delivery hour. All market bids have to go through a BRP, which is responsible towards the TSO to maintain balance (i.e. balancing responsible). The BRP can also participate in the regulating market[4], which is run by the TSO. Activation of regulating power has to happen within a specified time-frame, usually no later than 15 minutes [88] before actual delivery. After the actual delivery of power, the TSO collects metering data and calculates the deviations of BRPs from their schedules and the activated up- and down regulation. This determines the real-time price, which is used to collect payments from BRPs that deviated from their schedules and then payments to the activated regulating offers are made. Every market participant has to provide their offers/bids through a BRP. The interaction of BRPs with their customer is beyond this thesis, however many large scale producers or aggregators register as BRPs themselves if they have enough capacity to act as such.

The Nordic market setup does not include any grid model in any of the above mentioned markets and therefore the actual nodal power flows are not taken into account when clearing the markets. It is solely the responsibility of the TSO that the voltage and line loading constraints are respected at real-time, which is done by activating different regulating offers. This may lead to sub-optimality with regards to cost but is a result of the current policies. Further the activation and reservation of reserves are split up, such that the outcome may be sub-optimal as well. In contrast, the US market design solves this by having an integrated day-ahead auction for both reserve reservation and energy with LMP pricing. This may however result in vastly different prices across small geographic areas and can be perceived as “unfair” by some market participants that reside in weak areas of the grid.

The current market design philosophy does not take into account the low-voltage networks of the DSO, neither in Europe nor in the US markets. This means that the DSOs main avenue is grid reinforcement by long-term planning. However, grid expansion is a costly undertaking especially in urban areas with underground cables. To a minor degree DSOs are able to pre-qualify the participation of larger distribution network connected dispatchable generators, such as combined heat and power plants,

[3]The TSO in Denmark (Energinet) labels them DK-1 and DK-2

[4]It may be called the ”balancing service provider” when referring to the regulating market.

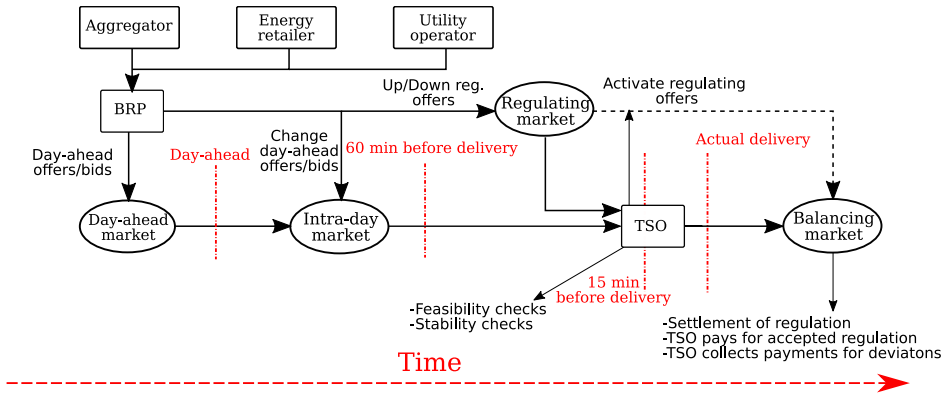

Figure 2.3: Schematic of the Nordic market design philosophy.

which participate in TSO balancing or ancillary services markets [80]. There are also instances of DSOs operating small scale distributed generation or battery storage [97], however this may in the future be against market regulations as the system operators are not supposed to own and operate generation that competes with market-based mechanisms [98]. It is often argued that the DSO should operate local flexibility markets instead of investing in its own hardware for flexibility provision [11], [63]. The DSO may only in exceptional instances operate its own storage facilities and may not participate in any outside markets in order gain a profit [76]. However it is clear that any DSO controlled storage units would be distorting any markets that provide similar services in a local area. Ropenus *et al.* [98] suggest that the DSO should be allowed to offer incentives to DERs to connect at high benefit locations [86]. In Section 2.3 some of the market-based proposals in the literature for DSO network support will be discussed.

Day-ahead market: The Day-Ahead (DA) market in the Nordic region is operated by NordPool which clears an integrated market for 13 European countries. The market is split into different pricing zones which are more or less static depending on the country. For example Denmark uses two static pricing zones, where in Norway zones can be reconfigured dynamically using market splitting [99]. The trading between pricing zones is limited by Available Transfer Capacitys (ATCs) which are determined before market participants submit their offers for generation and bids for consumption. If the ATCs between zones are achieved (i.e. at ATC capacity) the zones are split into different pricing zones. In the US the markets use a different pricing strategy termed LMP, where every node can have a different price based on congestion in single transmission lines. Further, US markets also clear a unit com-

mitment problem in the day-ahead market, which allows for reservation of capacities in the day-ahead stage. This co-optimizes energy and reserve capacities at the cost of introducing binary non-convexities.

Intra-day markets: The intra-day market is cleared by the market operator and changes the energy consumption schedule of the BRPs. The BRPs are here able to readjust their consumption or production profiles up to 60 minutes before the delivery hour. This may be necessary for the BRPs if the uncertainty of the forecast in the day-ahead stage was high and updated forecasts for consumption or RES generation are available. Compared to the day-ahead market and the regulating market only small amounts of energy are traded in the intra-day market in the Nordic region [88]. An example of an intra-day market with high trading volumes can be found in Spain [100], which can be attributed to specific regulations which incentivize trading closer to real-time. For example in Spain, the balance responsibility is given also to RES operators, where other countries have regulations that may exempt them from this. For an overview of intra-day market liquidity and market design see [101].

Ancillary services markets: The TSO or multiple TSOs in cooperation can operate ancillary services markets. These account for a large part of the transacted energy and include the regulating and balancing power market[5]. The TSO is directly responsible for real-time balancing of production and demand, and uses market-based methods for the procurement of balancing needs. In the regulating power market the generators and flexible demands can submit their bids for up- and down-regulations through their BRPs. The TSO can activate those bids to balance out any imbalances that may occur due to deviations from the day-ahead and intra-day market outcomes. For an overview of European balancing markets and different design choices see [103]. In 2018 five Nordic TSOs from Finland, Sweden, Norway, Åland and Denmark have agreed to implement a common balancing power market [104]. Generally, the regulating markets are trading energy (MWh) with a resolution of 15 min to 1 hour, but other design choices exist.

Capacity markets: Some TSOs implement reserve capacity markets, where reserves can be booked in the form of capacity bids (MW). Capacity markets can be long-term markets as proposed in the French capacity market [105], where monthly auctions are held to award reserve capacity contracts that have to be able to deliver within a very short time-frame. In US markets reserve capacity is usually cleared through co-optimization with energy, while in Europe the capacity markets are cleared independently from energy markets. The trend of RES reducing the clearing price in energy markets due to their low marginal costs, may cause large centralized power

[5] Here the Energinet Terminology is used, where the regulating market is the pre-delivery bidding market and the balancing market is the post-delivery settlement market. Other TSOs may reverse this terminology. Unification of terminology is expected in the future due to streamlining by the pan-European TSO network ENTSO-E [102]

plants to be unable to recover their investment costs by being uncompetetive. They may however be needed as reserve capacity units to be able to balance intermittent RES production. The problem of cost recovery may be exaggerated if there are price caps on ancillary services that should otherwise remunerate capacity availability through activation payments. This issue is termed the *missing money* problem which may affect investment decisions of generators [106]. Therefore, the capacity markets are being designed such that capacity can be rewarded, whether energy is delivered or not. Some works argue that capacity markets are the main solution to ensuring reserve capacity availability, e.g. [107]. Others argue that the opposite may be true and the answer is well designed energy and ancillary services markets, e.g. [106], [108].

2.2.2 Design challenges

Currently, Nordic and also European electricity market designs are missing specific features that limit the optimal use of RES generation and DERs. First, the clearing of the day-ahead market happens without taking into account the uncertainties of the renewable energy sources or varying demand. This means that the day-ahead stage is a purely deterministic problem that is myopic with regard to real-time outcomes. Second, the underlying grid structure of the power system is not taken into account when clearing the market. This means that trades which are physically impossible to fulfill can happen. Third, the optimization of power flows, which is done by the TSO does not take into account the network topology of any DSOs, which means that high DER dispatching by the TSO can create problems at DSO level.

In figure 2.4 some of the shortcomings of current markets are illustrated. Figure 2.4a shows how the DA market clearing process is handled, where different pricing zones can be utilized. Within the pricing zones, no network constraints are modeled for the DA market. The DA market agent clears the market with the bids and offers from loads and generators which can also be located at DSO network level. The capacity between two neighbouring zones is the ATC, which determines how much energy can be transacted between different pricing zones. If the ATC is reached in the day-ahead market clearing, the zones will be split up and the clearing price in the neighbouring zones will be different. When moving to the real-time operation of the grid, the TSO can operate ancillary services markets to optimize the power flows in the grid, but still not taking into account the DSO level networks. This is illustrated in figure 2.4b where the DSO networks are connected to the transmission system with dashed lines.

The day-ahead market does only take into account the real power injections at the Point of Common Coupling (PCC) of any DSOs, because reactive power flows are not considered at any market stage. This is illustrated in figure 2.4c, where the green lines represent the active power constraints that can be inferred from the loads and DERs at the distribution level. However, reactive power also plays an important role in distribution networks to regulating the voltage level. The reactive power injection

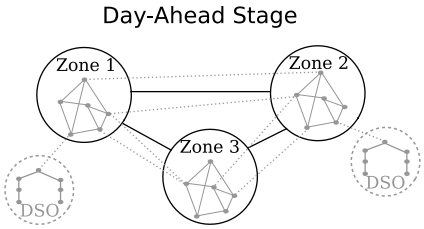

(a) The day-ahead market only takes into account flow between pricing zones, even if flow between zones exists over multiple links.

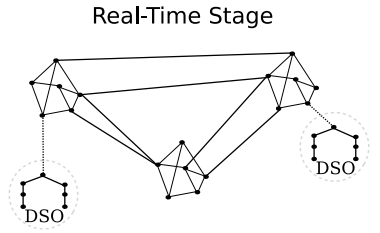

(b) Real-time OPF by TSO does not take into account the flow to the DSO.

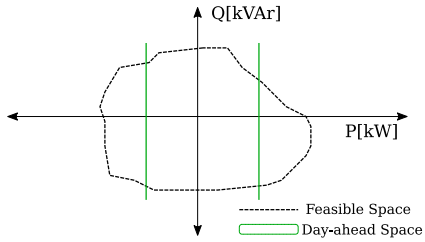

(c) Actual feasible space of power injections into DSO network and the assumed constraints in the DA-market where no reactive power constraints are set.

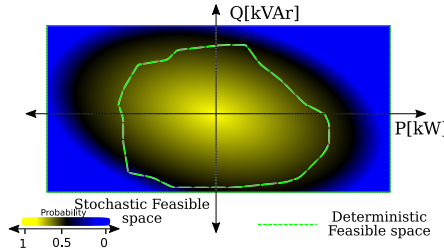

(d) The stochastic feasible space of a DSO in real-time. The stochastic production of PV in a distribution network is influencing the feasible injection region.

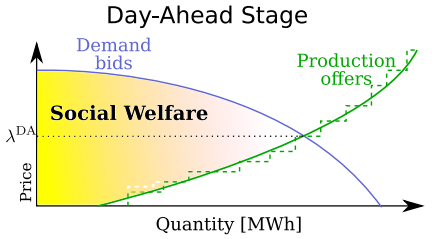

(e) The day-ahead market is deterministic and finds a single clearing price λ^{DA} at which all trades are paid.

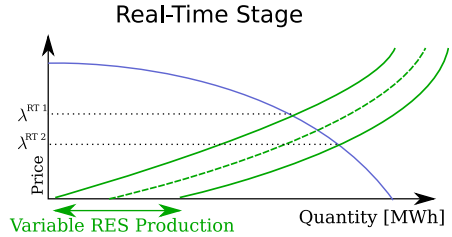

(f) Real-time OPF by TSO does not take into account the flow to the DSO (Source: adapted from [109]).

Figure 2.4: Depiction of Nordic electricity market design specifics. The day-ahead markets are myopic with respect to real-time outcomes and network power flows in real-time. Further the DSO networks are not included in the optimization problems of the TSO in real-time.

can also influence the feasible space of the active power injections, which is shown by the dashed line. When moving to the real-time operation, the feasible power injection

at the PCC can be seen to be influenced by fluctuating RES. This is depicted in figure 2.4d where the feasible space is connected with a probability of actually being feasible. Therefore, any active dispatch of DER should take into consideration the uncertainty that may arise from forecast errors.

The successively higher costs of generators is called the "merit order curve" which is the reason for the underlying stair shape of the offer curve as illustrated in figure 2.4e. Usually only linear cost offers are allowed, but generators can submit several *blocks* of offers in order to approximate their internal unit commitment constraints [110]. In contrast the US type markets allow for unit commitment constraints to be incorporated directly in the market clearing which however leads to binary non-convexities in the market clearing. The advantage of having a deterministic market with convex cost functions is that a single market clearing price λ^{DA} can be found and the merit order of offers will be respected. Furthermore, the deterministic markets fulfill the desirable qualities of *revenue adequacy* and *cost recovery*. Revenue adequacy means that the payments collected from the demands cover all the payments made to generators at the cleared quantity and clearing price. Under cost recovery it is established that all market participants will be paid at minimum at their marginal offer[6].

The variable RES production can cause imbalances at the real-time stage, which is not taken into account when clearing the day-ahead market because it is purely deterministic. There is a wide field of publications that describe uncertainty estimation methods to make decisions in electricity market to improve the day-ahead dispatch; an overview can be found in [111]. The ideal situation when clearing the day-ahead market would be to clear the market with a stochastic optimization problem which takes into account uncertainties of RES. Under this regime however, the cost recovery and revenue adequacy are only fulfilled in the *expectation* and not in the realization of specific scenarios in real-time [112]. This is one of the reasons that the Nordic market designs are deterministic, although this is a myopic choice. The resulting deviation of real-time prices is shown in figure 2.4f, where the fluctuating prices are caused by intermittent RES generation in real-time. In the future, a larger share of electric vehicles may also increase the uncertainty due to charging and the corresponding intermittent load profiles may cause price deviations in a similar manner.

2.3 Market-based solutions for a DSO

DSO-level market methods are an ongoing research topic due to the hastily changing nature of distribution networks and their merits for increasing the hosting capacity of DERs. Some countries and researchers have even adapted terminology for the changing role of the DSO; for example, in the United Kingdom, the term "Distribution Network Operator" is used to represent classic operators of passive distribution networks. The term "Distribution System Operator", is meant to highlight the more

[6] In fact only the marginal producer will be paid at the offer price.

active involvement of the system operator in controlling DERs, similar to a TSO. Other sources use the term "Active Distribution Network Management (ADNM)" to describe the growing active role of the DSO. In essence the creation of local markets or market-based methods is used to increase the DER hosting capacity in distribution networks, which can be very limited for passive networks [74], [75]. Common to most approaches is that they model the network and apply mathematical programming methods or other modeling techniques to optimize use of existing infrastructure through market-based operations or by offering incentive programs.

2.3.1 Current responsibilities of a DSO

DSOs are the system operators of medium- to low-voltage networks that distribute energy at customer level. In most cases the DSO is in effect a monopoly[7] with the objective to minimize the cost of energy delivery to the customer while ensuring adequate safety margins of the loading of components. In addition to operating the networks (cables, transformers etc.), the DSO is the operator of the customer side meters. In the case of small residential customers, the customer side meters are read manually in long intervals for yearly settlement purposes. For larger industrial customers hourly remote metering has been available in most European countries for some years now[8]. The roll-out of smart meters to all customers is expected to be finished in 2020 in Denmark [113], which will enable more effective monitoring, control and metering of flexible loads and DERs. Further, the integration of Information and Communications Technology (ICT) in the distribution network will improve access to information and can enable enhanced coordination of local resources with the system operators.

The specifics of metering and ICT technology that enable coordinated usage of DERs are outside the scope of this thesis. For the remainder of the thesis it is therefore assumed to be possible to control single DERs at low-voltage level at whichever time-resolution is necessary[9]. However, it is important to understand that smart meters and ICT technology are an important enabler and prerequisite for DSO smart grid functionality and the specifics of different technologies are an active area of research. This thesis is more concerned with modeling and optimization techniques that can be studied in a decoupled manner of the underlying technology that is applied.

There is a clear distinction between the duties that fall to the TSO and the duties that fall to the DSO. In current Nordic settings, the DSO is solely responsible for

[7] Monopoly is meant in the sense that there usually is only one distribution grid which transports energy to customers. In Denmark as well as other European countries, the state regulates the earnings of DSOs, as is the case with other state sanctioned monopolies. Often the DSO will be owned directly or indirectly by the state, municipalities or customers.

[8] customers with an annual consumption above 100,000 kWh must have smart meters for hourly settlements [88].

[9] The current generation of smart meters being deployed in Denmark are unsuited for live control of DERs and are designed for remote hourly settlement. It is expected that the next generation meters will start being deployed in the near future [114].

the safe operation of distribution hardware and the safe supply of energy to the customers. This means that line thermal loading and over- and under-voltages are the main concerns of the DSO. Therefore congestion management is a widely studied topic in DSO networks [29], [56]. In contrast the TSO is mainly focused on stability issues and contingency planning such as frequency stability, voltage stability, $N-1$ contingencies and angle stability [73], and congestion plays a smaller role than in DSO networks. Further it is the TSO which is responsible for the real-time balancing of the network and therefore has to have sufficient reserve capacity in order to balance any deviation of the power schedules from the BRPs.

2.3.2 Existing proposals for DSO-level market-based solutions

Proposed market designs for DSOs are similar to existing TSO-level ancillary services markets in many aspects, but differ in certain ways to meet the specific DSO requirements. As mentioned, the DSO is mainly concerned with equipment safeguarding such as thermal line ratings and voltage issues and therefore the markets or market-based methods have to reflect these requirements.

Since the equipment rating is an important cost factor in distribution networks, the power flows of the network have to be taken into account when operating a DSO market. The power flows in an electric network are governed by the physical properties described by Kirchhoff and Ohms law. Also, because virtually all distribution systems are alternating current (AC) networks, the physical particularities caused by alternating currents have to be taken into account. Therefore AC power flow is suitable, which is a set of non-linear equations taking into account the underlying physical properties of the network. A market clearing method can be cast as an optimization problem, thus the AC power flow model has to be incorporated into an optimization model if the market clearing is to take into account the full network properties. The resulting model is dubbed the AC optimal power flow (AC-OPF) model. The full AC-OPF model may often not be a very practical model due to non-convexities induced by the quadratic relations of currents, voltages and angles, and thus several simplifications and altercations (through *convex relaxation*) can be used with yielding very precise results as presented in the next chapter [31], [32].

DSO level markets can be formulated as optimization problems or more specifically as Optimal Power Flow (OPF) models and thus take into account the network properties of distribution grids. If current day-ahead markets are assumed, the DSO market-based methods need to take into account the outcomes of the wholesale day-ahead market. This can be done either ex-ante (before day-ahead market clearing) or ex-post (after day-ahead market clearing). Ex-ante methods are agnostic about day-ahead market outcomes but uncertainty modeling can be used to improve the expected gains of those methods.

One ex-ante market-based method is the dynamic tariff method [29] in which the DSO calculates in-feed tariffs at different network points with an OPF model and publishes them to the DER aggregators before day-ahead market clearing. The

dynamic tariff is based on the LMP strategy also used in US style markets. The dynamic tariff method is a price-based market-based method, because it prices the use of network capacity to the end-user. It does not require a separate market as the tariffs are added to the spot price of the day-ahead market. Regulations may limit the use of this method under European laws, due to non-discriminatory rules on geographic locations in the networks of market participants [115]. To circumvent these regulatory obstacles, the similar dynamic power tariff [116] has been prescribed which prices feed-in power. Instead of price-based methods similar incentive based methods [54], [117], [118] can be used that are compatible with European regulations.

The Flexibility Clearing House (FLECH) is another proposal where the DSO uses ex-ante methods [64], [119]. In the FLECH architecture, the DSO clears a day-ahead market for flexibility capacity or energy within its domain, which it then activates in real-time to mitigate congestion. The cleared flexible capacity can also be offered to the TSO to help real-time balancing if it is not used by the DSO and there are no grid constraints limiting the use.

A different DSO market structure is presented in [65] where the DSO operates its own retail market and buys power on the wholesale day-ahead market. This market design philosophy has the DSO take on the role of energy retailer towards the end-user, which is quite different from today's energy retailers. Currently energy retailers are buying energy through BRPs at the day-ahead spot market and are therefore separate actors not connected to the DSO. The market design in [65] is termed a *transactive market* due to the DSO transacting energy from wholesale markets to customers. The main idea of this approach is to decentralize retail markets into local distribution areas, where the DSO is interacting with wholesale markets on behalf of prosumers or energy retailers. The policy to implement this scheme is however not entirely clear, especially within European settings, as the DSO is not allowed to profit from trading energy under current regulation. Trading of energy and profiting from this is currently limited to the energy retailers that operate without geographic restrictions across entire trading zones, which would obviously be different for a DSO that engages in energy trading. For a bibliographical review of transactive methods see [120]. In [90] the effects of local energy markets on system prices are analyzed and framed as a transactive market concept.

2.3.3 Challenges of existing proposals for DSO-level market-based solutions

The above mentioned market-based mechanisms or market designs for DSO congestion management show some drawbacks to key aspects of modern power systems with high RES and DER penetration.

A large part of the flexibility that can be leveraged for congestion management is expected to be based on Demand Response (DR) [14], [56]. DR consists of flexible loads that can change their consumption behaviour with the aim to participate in markets [15]. The aggregated use of DR is expected to have a large enough impact

to compete with conventional generation in terms of quantity. The operation of DR is often very cheap due to its low marginal costs. Understanding the DR operational properties is relevant to achieve well dimensioned local DSO markets. For example, it is important to understand the underlying physics of the DR units so that the bidding format reflects the value that they bring to the market [37]. Additionally, understanding which factors motivate the deployment of DR technology can help proliferation. Participation and sufficient market liquidity is important in order for the system to be operated with good reliability [8], [11]. However, proliferation of residential DR is a topic with many facets and analyzing them may bring better understanding and helps rapid deployment [26]. For example, some works try to price end-user discomfort of residential DR units [89], [121]. This is sometimes described by disutility functions that quantify end-user discomfort when their appliances are not operating at the desired set-points due to DR participation [122], [123]. For example, this can be an air-conditioning unit in a residential building that changes the room temperature from the desired set-point by a few degrees in order to reduce consumption in a period. However, this is difficult to align with markets and settlement prices because quantifying user discomfort may not be straight forward. In [14] the regulatory issues of integrating demand response in a European setup are analyzed. Further [9] analyzes the techno-socio-economic barriers of DR deployment from a owner perspective and argues that uncertainty of cost-recovery is hindering investments. Understanding the motivation of residential DR and appropriate modeling techniques to understand DR behaviour and physical characteristics are also important as analyzed in [13]. Network modeling issues in connection with DR deployment are discussed in [124]. Therefore, the design of efficient and meaningful markets is an important aspect, both to the system operator and to the prosumer[10]. It can also be mentioned that non-technical social related barriers can hinder the participation in markets if they are opt-in for residential users [114].

Many DR units can be scheduled without any direct discomfort to the user, which could be the case for Thermostatically Controlled Loads (TCLs) with heat storage capacity [58]. Some examples for this are large refrigeration units in supermarkets, water heating systems with heat pumps and insulated storage [26], industrial cooling systems etc. Common to these TCL-based DR units is that they will have to increase their consumption after a decrease due to the need to return to their base-line temperature settings. This phenomenon in DR units is termed the *rebound* which can cause overload problems if not taken into account in DR scheduling [23]. In figure 2.5 an example load profile of a DR unit with rebound is depicted. Here the DR is activated at some time-stage to reduce its power consumption, which is followed by an increase in a subsequent time period. This is one of the internal DR characteristics that is important to understand in local markets with high penetration of DERs. If the DSO market method relies on DR units with non-negligible rebound, a congestion management mechanism may fail if it does not take into account the rebound. On

[10]Prosumer is a portmanteau that is used to highlight that distribution level consumers may also have small scale generation, and can therefore act as both producer and consumer.

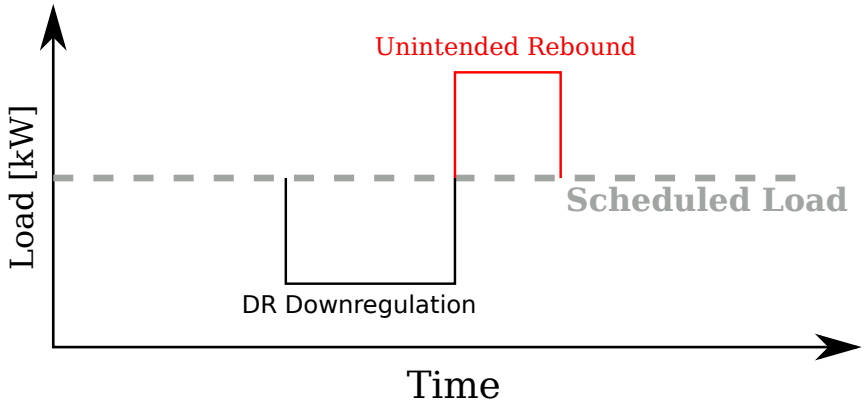

Figure 2.5: Unintended rebound effect of demand response unit.

the background of DR units with inherent rebound effect, we examine in [**Paper A**] how a market clearing mechanism for DSO use which inherently takes into account the rebound can be designed. We find this work that the a congestion management mechanism dispatches DR with rebound effect has high sensitivity to the used system constraints, and therefore the rebound effect is important to model precisely.

Another shortcoming of current proposals for DSO market-based methods is that they fail to quantify their impact on total system welfare if they operate uncoordinated with other markets, which is linked to the real-time usage of TSO level networks. In [41], [42] the impact of coordination between DSO markets and TSO markets in real-time is analyzed. Gaming behaviour in local markets is another issue, which in [38] is analyzed as the efficiency of local markets given coordination with global markets and whether it is in fact correct to model local markets as maximizing social welfare. Since most of the DSO market methods usually take up capacity of local DERs, they block capacity that may otherwise be used by TSOs or other DSOs, BRPs or aggregators. The total system social welfare is usually not accounted for by current design proposals for DSO-level markets and this should be kept in mind when designing coordination schemes. Also, the real-time operation of the network may be subject to uncertain behaviour of RES on either TSO or DSO side, which can be harder to mitigate if flexible capacity has been locked up in a DSO day-ahead schedule for congestion management.

2.4 Interactions of TSO and DSOs

This section discusses the interplay of DSO- and TSO-level markets for flexibility procurement from a system view-point. The entire power system can be viewed as a decentralized system, where the market operators, the TSO and the DSOs concur-

rently act to operate it according to their own performance metrics. As proposed by other works [11], [38], [48], [64], [119] the DSOs may operate independent flexibility markets in the day-ahead stage, in order to reserve capacity in DERs which it can later activate to mitigate congestion. The interactions of TSO and DSOs are an ongoing research subject when different markets and interests for use of DERs exist.

Specifically, we will shortly discuss the implications of decentralization pertaining to TSO-DSO coordination. Subsequently, a short summary of casting decentralized system coordination as hierarchical or distributed coordination will be discussed.

2.4.1 Decentralization of system operations

The current discussion at EU level about the future role of the DSO emphasizes a decentralized design philosophy in operating the power system [86]. In a decentralized power system the operational aspects happen in (local) markets or control structures, and outcomes of these local operations are only shared with the local and upstream agents. Decentralized system architectures have some favorable properties, such as scalability and information privacy and separation. These are valuable properties in power systems, as the integration of DERs complicates system operation and thus scalable operational paradigms are necessary to facilitate large scale deployment. However, decentralized systems have to embed some methods to share resources, which otherwise would inflate the possibility of single actors within each decentral market to employ market power if there is low market liquidity. Also internal balancing resources might be paid too much and over-utilized due to possible gains that are not realized when spatial smoothing of uncertain production can be taken into account [125].

There are separated duties between the different agents, which jointly work to operate the power system. In this case the wholesale market operator, the TSO and the DSOs form a distributed entity to operate the power system through different markets and control actions. The duties are separated by geographical and functional schemes among those three agents, which thereby determine the nature of their interplay. Depending on the future shaping of policies and implementation of local markets, the relation between the agents may lead them to compete for resources.

Hierarchical or distributed decentralization

In the avenue of decentralized systems, there are two ways of framing the relation between different agents, namely hierarchical organization or distributed organization[11]. In the first structure, the hierarchical, agents (for example TSO or DSO) perform their own operations independently and serially while the top of the hierarchy

[11] The taxonomy of distributed systems with regards to power systems is not very well established but an attempt to unify language usage is made in [126]; One take-away of [126] is that hierarchical and distributed decentralization are orthogonal concepts. This means that a decentralized system may be realized as a hierarchy that may or may not be distributed and, vice versa a distributed system may or may not be hierarchical.

is determining the initial set-points of lower level agents. In the field of hierarchical system structures, the interplay is most properly modeled by leader-follower type games, also named Stackelberg games [44], [127]–[129]. Current market structures with the day-ahead spot market and balancing markets in real-time can be viewed as an open-loop hierarchical optimization problems, thus constituting a sequential (time separated) hierarchical structure. Currently the day-ahead market and real-time balancing are sequential and hierarchical, meaning that the day-ahead stage is not taking into account the uncertainty of variables but simply using a point forecast. In the case where the leaders in hierarchical structures take into account the reaction of the followers by modeling their behaviour, the hierarchical structure becomes a closed loop problem, where the leaders optimize their own metric being aware of followers possible actions. For example, considering a day-ahead market with stochastic information about the real-time outcomes of uncertain variables could be framed as a hierarchical closed loop problem, with the day-ahead market as a leader. Another example can be the activation of distributed reserves, where the local DSO has the first pick rights and anticipates the actions of a TSO that also accesses those reserves [41]. Another prominent use of hierarchical optimization is to analyze the optimal coordination outcome when an idealized oversight authority can allocate exchange prices to different agents [96], [130].

In contrast, distributed optimization structures are horizontal where agents are not sorted by any hierarchy, such that their interactions more closely resemble peers that interact with each other without centralized controllers. Such a distributed structure can be used to describe agents that manage their domains simultaneously, such as neighbouring regional system operators [46], [125]. Distributed systems can converge to the same set-point or objective metric as their centralized counterparts, if the distributed agents share the same objective function or metric and their communication is complete and adequate. In the case of differing objectives, the distributed system operation may be subject to gaming strategies, which are difficult to mathematically analyze [131]. Distributed system designs are for example peer-to-peer energy networks where agents communicate with each other to trade energy [11], [132], [133]. When gaming strategies in distributed systems appear, the existence and uniqueness of equilibrium points are often hard to prove. The case of distributed operations within TSO-DSO coordination has been analyzed with a Generalized Nash Equilibrium (GNE) approach in [41], [44].

The solution strategy of both distributed and hierarchical systems can be implemented as GNE [44], [134]. While this may be over complex for simple interaction mechanisms it can capture complex interactions between competing objectives in distributed or hierarchical system structures. In the case of gaming behaviour, the use of GNE modeling, though computationally complex, can often shed light on complex behaviour of agents and thus help to implement policies that are useful to society.

2.4.2 Relation of decentralized operation to local DSO markets

In this thesis we study *hierarchical* markets, where the DSO may opt to reserve capacity from DERs before they can participate in the wholesale markets. In [**Paper A**], the hierarchy is an open-loop process, where the DSO is choosing an activation scheme of DR units after the wholesale market has been cleared. The concept of a DSO level market is expanded in [**Paper B**] to a closed-loop hierarchy, which is analyzed with an idealized oversight authority that is regulating the interplay between DSO and TSO to exchange flexibility capacity in the day-ahead stage. These flexible resources are then activated in a perfectly coordinated real-time stage. The results in [**Paper B**] show how local flexibility markets can approximate integrated central market settings, thus approximating *market completeness* in a global fashion.

Market completeness is the concept where all assets have a price for every possible outcome of uncertainties [135]. This means that constraints in the optimization problems should be valued at a single price available to all agents. No practical market is entirely complete, but most literature assumes market completeness as part of the social welfare maximization assumptions. In contrast, an *incomplete* market has price gaps that arise due to imperfect coordination between different markets, and therefore lead to sub-optimality in trading resources. The lack of arbitrage trading options is one source of market incompleteness [125], [135]. In practice, the degree of market completeness is often discussed when proposing new market designs.

Recently, with the proposals of ever more decentralized systems to schedule energy and capacity in power systems, the concept of allowing market incompleteness has emerged for TSO-DSO coordination [43] and also for peer to peer markets [91]. As we show in [**Paper B**], the hierarchical organization of markets can lead to optimal outcomes for the full system social welfare. However, this is an idealized situation which is meant as a guideline for future design and implementation of coordination policies. In general, for practical coordination schemes the question arises to which extent market incompleteness, and therefore sub-optimality should be accepted.

2.4.3 Existing proposals for coordination

The design philosophy of current markets has to a large extent been inspired by traditional central power plants that need to be planned and scheduled in the day-ahead stage with lead-times of 12 to 36 hours. Also the traditional vertical operation of power systems has influenced the market design. This has lead to the implementation of the day-ahead market as a forward trading spot market, where today the majority of energy is traded. Also, the majority of the flexibility has traditionally been provided by large centralized power plants in the form of excess generation capacity.

In contrast, the flexibility of future power systems is in large part expected to be located at the low-voltage level in the form of demand response and other DERs. Further, decentralized generation in distribution networks is expected to inject large amounts of energy, in the form of rooftop solar PV or residential battery storage

facilities etc. The DSO may therefore consider to use local flexibility, in order to avoid overloading the low-voltage distribution feeders [56].

Coordination between TSO and DSO can happen in the various time-stages of existing and proposed markets. The traffic light concept has been proposed in several independent works to coordinate the DSO with different markets [8], [63], [93], [136]–[138]. This concept has the DSO acting with oversight authority on DERs participating in different markets that schedule or activate reserves and/or energy and defines different operating conditions according to traffic light colours (i.e. a normal state without interference, an alert state where the DSO restricts certain trades or actively re-dispatches, and an emergency state where trading is suspended). For example, the day-ahead market which in Europe is cleared independently of system operators can be used for coordination, if the DSO regulates the participation in the market. The prime objective for the DSO is congestion management, while for the TSO it is balancing power and congestion management [8]. When flexible resources are used to respond to the uncertainty of RES, it is logical to expect that the coordination should happen as close to real-time as possible, when a large part of the uncertainty has been removed due to better short term forecasts [17]. However, the bulk of energy is traded in the day-ahead market, and some degree of coordination early on can decrease the expected costs of operating the power system [63]. This argument can be amended by the fact that moving closer to real-time the prices increase for energy and balancing capacity [96].

Below some recent coordination proposals are presented with explanations and comments. The terminology used here is not based on any consensus, rather it is used as a reference within this thesis. There exists little to no consensus on specific terminology related to TSO-DSO coordination. The closest to a consensus would be the presented schemes of the SmartNet project [80] of which some terminology is adapted here and has also been used in other publications. Rather than presenting new terminology or accept a consensus, it is here the main target to collect and explain some schemes to give the reader some background knowledge and to contrast the different proposed schemes. A comprehensive overview of different coordination mechanisms between TSOs and DSOs can be found in [63], where also the coordination methods are compared to methods of coordination between different TSOs. Coordination among several TSOs becomes important when access to balancing capacity and ancillary services connected to neighbouring TSOs and/or pricing zones is enabled. Many of the current TSO-TSO coordination schemes have been used as inspiration for new TSO-DSO coordination proposals.

- **Centralized common TSO-DSO market:** This coordination structure has been proposed by Caramanis et. al. [46], which requires an integrated clearing and activation of energy and reserves. Essentially it amounts to co-optimization when scheduling both transmission and distribution level networks, and therefore is a very complicated and large problem to solve. The main scientific contributions in [46] is (i) to include extra variables for the flow of reserve power when scheduling it, such that activation of it always becomes feasible and, (ii)

to decompose the problem into localized problems that communicate with each other in an iterative manner to achieve global optimality. This scheme can bring the total system social welfare close to the global optimum if the communication between the decentralized market agents is adequate. The decentralization methods that have been proposed are consensus based algorithms based on the alternating direction method of multipliers. These methods are in turn derived from Lagrangian relaxation techniques and the market agents need to exchange dual variables (prices) to update each other on the desired set-points. With modern consensus based algorithms the dual variable updates can happen asynchronously.

- **Decentralized common TSO-DSO market:** The DSO and TSO both operate their own flexibility markets, while there are cost functions at the interface to share flexibility. In the day-ahead stage, coordination could happen like in [48], which modelled a cooperative game through Shapley-value allocations when the DSO and TSO reserve flexibility. The coordination in real-time is more problematic, as the feasibility of power flows has to be ensured all the time. Therefore, the DSOs must calculate a feasible space for power flows at the interface with the TSO. The DSO has to do this before the clearing of the TSO balancing market and therefore the DSO is agnostic about realization of uncertain variables. One method is for the DSO to provide the market clearing agent a "residual supply function" with prices for different adjustments of the energy flow at the interface for real power as was done in [139]. The shared functions should be linearized around the operating point. The residual supply function can be extended by incorporating reactive power flow at the interface, which amounts to providing the TSO balancing market with a two-dimensional feasible space with different prices for flow adjustments [49]. An extension of this is to incorporate the probabilities of the underlying feasible injection region by stochastic optimization [50]. This will allow the injection region to be always feasible under different realizations of uncertain variables.

- **Trade permission system:** The main idea for coordinating here is to have a centralized market which collects bids and offers from both TSO and DSO connected units. Coordination is achieved by the DSO blocking any trade that is infeasible within its own network, which is achieved through forecasting by the DSO. This scheme is labeled "centralized ancillary services market" in the case of referring to real-time coordination under this scheme and is used within the SmartNet project. The scheme works for both the day-ahead market trading, where the DSO can block bids and offers that violate its network constraints, or for the balancing procurement in the ancillary services market of the TSOs. The DSO must ex-ante calculate the power flow in its system taking into account the uncertain nature of uncontrolled loads and PV generation, and then limit the offers and bids of flexible loads and generators to the global markets. This scheme is closely related to the notion of a traffic light concept.

- **Local flexibility market:** Under this scheme the DSO operates separate markets to provide services for itself from units either connected to its own domain while also having the option to contract offers from the TSO domain. There are different views on what responsibilities should be given to the DSO. For example, in some works it has been proposed that the DSO becomes responsible for balancing power such that it will operate an ancillary services market similar to the TSO. Other works are however more adherent to the current structure where the DSO markets are solely for congestion management and the TSO remains the balancing regulator. In the SmartNet project, this scheme is coined "local ancillary services market", which clears different markets at TSO and DSO level, depending the imbalance location. This scheme can be very difficult to control due to contradicting objectives and possibly gaming behaviour by the TSO and DSO. For example, DSO connected units participate in a TSO ancillary services market without coordination with the DSO, or vice-versa if the DSO procures services from TSO connected units. A series of papers have analyzed the gaming behaviour that may occur between TSO and DSO through non cooperative games cast as GNE problems [41], [42], [140].

  If the responsibility of the DSO is only congestion management, like it is the case today, the local DSO markets are merely used to reschedule flexible units such that line rating will not be violated. This can be done ex-ante market clearing, in order to reserve some flexibility for a re-dispatch after market clearing. The issue is then, how flexible units prioritize the participation in DSO or TSO markets. Local flexibility markets can have issues with coordination both at the day-ahead stage and the real-time stage.

- **Shared balancing responsibility:** The term stems from the SmartNet project and may also be understood as "local units for local markets". The scheme allows flexibility of DSO connected resources only to be available to the DSO and TSO connected resources only to be available to the TSO. This coordination scheme takes advantage of the fact that the only thing the DSO and TSO need to agree on is the power flow in the interface. Once the interface flows are fixed, each system operator needs to balance its own network with respect to its own network constraints. One option is to calculate the interface flows from the day-ahead market and then not allowing the interface flow to change in subsequent flexibility or ancillary services markets. Under this scheme the global system optimality is hard to achieve, if the day-ahead dispatches are not coordinated well. For example, using the outcomes of interface flows inferred from current forward markets (day-ahead and intra-day markets) where all units participate equally without restrictions, there will not be any coordination leading to global sub-optimality. The shared balancing responsibility is the only coordination scheme where the TSO has no access to DERs in the DSO networks. This may limit the usefulness of this approach, however it is very practical as there is a clear distinction between the areas of responsibility. Also, the DSO

becomes responsible for real-time balancing of its own network, and therefore has to mimic the TSO when operating its networks.

The above mentioned different coordination schemes have applications in different temporally spaced markets. The time-frame of coordinating the networks and thus the connected units is important, and therefore we here highlight the differences between real-time and day-ahead coordination. In figure 2.6 a schematic of possible coordination time stage is presented. The DSO can either coordinate in the day-ahead stage when the spot-market is cleared, or in real-time when the TSO is using flexibility to balance the production and consumption. As mentioned earlier, the spot market is not taking into account the uncertainty of any RES or loads, mainly due to pricing and regulation issues. Therefore the temporal coordination of day-ahead and real-time markets is not used for wholesale markets. However, the DSO is not limited by the same regulations and can therefore clear a day-ahead flexibility market with stochastic information and coordinate with the day-ahead wholesale markets or day-ahead scheduling of reserves. For example, the DSO can limit the day-ahead sale of energy by DERs in the wholesale market in order to leave ample capacity to react to real-time fluctuations in production and consumption. In real-time, the DSO can coordinate the activation of flexibility with the TSO according to the above mentioned schemes.

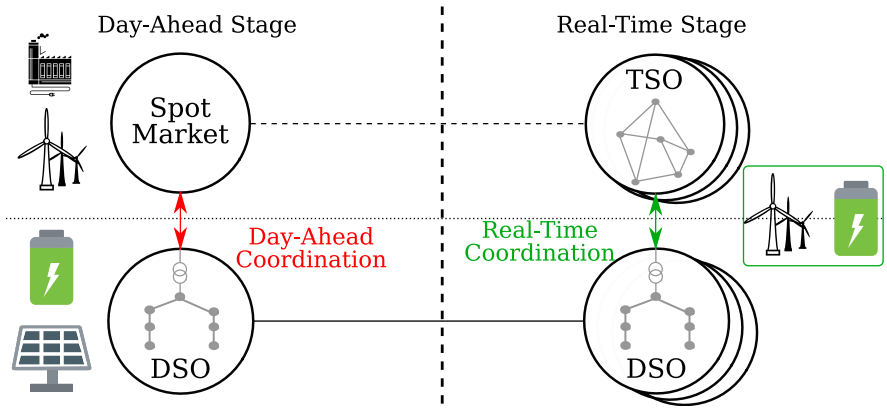

Figure 2.6: Time frame of coordination methods. The day-ahead spot market is myopic with respect to uncertainties in real-time. Therefore the line from Spot market to TSO is dashed. In contrast the DSO can use stochastic information to plan the day-ahead dispatch.

CHAPTER 3

DSO-level optimal power flow methods

The physical properties governing the power system can have implications to the market outcomes of electric energy markets. Currently energy wholesale markets are cleared with deterministic views on outcomes of uncertain variables, such as the intermittent Renewable Energy Source (RES) production, and without information regarding nodal power flows. The power flows are later optimized by the system operators if there is need for corrections. Therefore, the Optimal Power Flow (OPF) models have implications with relation to the activation of reserves and balancing offers close to the real-time stage for the Transmission System Operator (TSO). The Distribution System Operator (DSO) may also choose to use these models to optimize the power flows in its network, whether it is regarding capacity allocation or activation of flexible resources either in day-ahead or other time stages.

This chapter reviews the mathematical models used to model network properties, that will later be used in connection with market based methods to exploit potential flexibility of Distributed Energy Resource (DER).

3.1 Original optimal power flow models

The relation of currents, voltages and power in an AC power-system is described by a set of non-convex equations. This is due to the sinusoidal nature of the voltages and currents. The relation can be stated in the form of quadratic equations, and thus the full AC-OPF model is a non-convex Quadratically Constrained Program (QCP) model [141].

3.1.1 Short detour into graph theory and network representation

The power flow models can be stated in two equivalent ways, the Bus Injection Model (BIM) or the Branch Flow Model (BFM) depending on which variables are chosen to represent the model. As the name suggests, in BIM the main variables represent nodal power injections and nodal voltages. In contrast in BFM, the variables represent line

flows of apparent power and currents. Because the models represent the same systems, they are equivalent, however their difference in notation give them different qualities in analyzing power flows. For a comprehensive description of the two models and proof of equivalence between them we refer the reader to [142]. We will here give a short summary of the particularities of the two models .

Consider first the BIM. Let the network be represented by an undirected graph $\widetilde{\mathcal{G}} = (\mathcal{N}, \widetilde{\mathcal{L}})$, where $\mathcal{N}$ is the set of vertices (nodes) and $\widetilde{\mathcal{L}} \subseteq \mathcal{N} \otimes \mathcal{N}$ is the set of all edges (lines). Here $\otimes$ denotes the Cartesian product of the sets of all nodes $\mathcal{N}$. The graph is undirected which means $(n, m) \in \widetilde{\mathcal{L}}$ if and only if $(m, n) \in \widetilde{\mathcal{L}}$. For a line l that connects node n to m we write $l = (n, m) \in \mathcal{L}$. The notation $l \in n \sim m$ is used to denote the set of all lines from node n. We use $l = (n, m)$ and $l \in n \sim m$ interchangeably to denote a link. In BIM, all variables are indexed by $n \in \mathcal{N}$ while the weights (impedances in the case of power systems) belonging to edges $\widetilde{\mathcal{L}}$ are undirected, i.e. $Z_{nm} = Y_{nm}^{-1}$, being the impedance in line $l = (n, m)$ and $Z_{nm} = Z_{mn}$. We also write Z_l and Y_l for the line impedance and admittance respectively.

In contrast, the BFM adopts a representation that pertains to a directed multi-graph $\mathcal{G} = (\mathcal{N}, \mathcal{L})$ and all flow variables are directed. Specifically, $\mathcal{L} \subseteq \mathcal{N} \otimes \mathcal{N}$ and if $(n, m) \in \mathcal{L}$ then $(m, n) \notin \mathcal{L}$. We use (n, m) and $l \in n \rightarrow$ interchangeably, to denote a line from node n. The line ending in node n is $(m, n) = l \in\rightarrow n$. We will also use the notation $n \sim m$ in relation to BFM to denote either (n, m) or (m, n) as it is mostly unambiguous what is meant. Any variables that describe line-flow are not necessarily undirected, meaning that $p_l = p_{nm} \neq p_{mn} = p_{l'}$. In BFM the line flows are the main variables which are directed depending on which end of the line is assumed the sending end (i.e. sending end power is not equal to receiving end power because of losses).

3.1.2 Mathematical representation

The full non-convex QCP-OPF model can be written in set notation in quite compact form. The objective function $f(\Xi)$ is not explicitly defined here. We use Ξ to denote the variables in the optimization problem. These consist of active power variables, reactive power variables and voltages, $\Xi = \{p, q, v\}$. Many possible choices exist for the objective function including generation cost minimization, loss minimization, social welfare maximization etc. The generic OPF model is given in model (3.1) in complex set notation. Here we use the BIM model, which we augment with a variable for active and reactive power line flow p_l and q_l, thus using a hybrid BIM. This is possible as the two models are equivalent as shown in [142]. These "flow" variables can however easily be substituted away by combining equations (3.1b) with (3.1c)

and (3.1d), which yields a pure BIM.

$$\begin{aligned}
\min_{\Xi\in\mathcal{X}} \quad & f(\Xi) && && \text{(3.1a)}\\
\text{s.t.} \quad & s_l = v_n\,(v_n^* - v_m^*)\,Y_{nm}^*, && \forall l=(n,m)\in\mathcal{L}, && \text{(3.1b)}\\
& \sum_{l\in n\sim m} p_l = p_n, && \forall n\in\mathcal{N}, && \text{(3.1c)}\\
& \sum_{l\in n\sim m} q_l = q_n, && \forall n\in\mathcal{N}, && \text{(3.1d)}\\
& \underline{P_n} \le p_n \le \overline{P_n}, && \forall n\in\mathcal{N}, && \text{(3.1e)}\\
& \underline{Q_n} \le q_n \le \overline{Q_n}, && \forall n\in\mathcal{N}, && \text{(3.1f)}\\
& p_l^2 + q_l^2 \le \overline{F}_l^2, && \forall l\in\mathcal{L}, && \text{(3.1g)}\\
& \underline{V}_n \le |v_n| \le \overline{V}_n, && \forall n\in\mathcal{N}, && \text{(3.1h)}\\
& s_l = p_l + jq_l, && \forall l=(n,m)\in\mathcal{L}. && \text{(3.1i)}
\end{aligned}$$

Note here that OPF problem (3.1) does not have any notation for the current. The problem covers the power flows completely by modeling active, reactive power injections and complex voltages. Later we will convert to the BFM where modeling current is appropriate, as will be shown in section 3.3.1. Here v is a complex column vector with entries v_n which are variables for the voltage phasor at each node n. The line admittance is Y_{nm} for a line $l=(n,m)\in\mathcal{L}$.

Parameters with overlines and underlines denote upper and lower bounds, respectively. The nodal voltages are linked to line flows in (3.1b) through the line admittance, where v_n^* denotes complex conjugate voltage at node n. Nodal power injections and the line flow are related in (3.1c) and (3.1d) for active and reactive power respectively. The box constraints (3.1e) and (3.1f) limit active and reactive power injections. The apparent line flow limit is $\overline{F}_l$, which limits the active and reactive line flows in constraint (3.1g). The constraint in (3.1h) limits the voltage to upper and lower bounds, while (3.1i) is the apparent power flow in a line and $j=\sqrt{-1}$.

Lets denote the feasible set of optimization (3.1) as $\mathcal{X}$; this set is non-convex because of constraint (3.1a). This constraint is a quadratic constraint due to the multiplication of voltages on the right-hand side. The convex relaxation techniques that we use later in the form of conic optimization are finding lower bounds to problem (3.1) by optimizing over the convex hull of $\mathcal{X}$ [143].

The constraints (3.1b) through (3.1d) can be reformulated using the admittance matrix of a transmission or distribution network. The definition of the admittance matrix is:

$$\mathbf{Y}_{nm} = \begin{cases} -Y_{nm}, & \text{if } n\neq m \text{ and } n\sim m,\\ \sum_{m\sim n} Y_{nm}, & \text{if } n=m,\\ 0, & \text{otherwise.}\end{cases}$$

The voltage vector can then be related to the real and reactive power injections by the following equation:

$$p_n + jq_n = \mathrm{diag}_n(vv^*\mathbf{Y}^*), \quad \forall n \in \mathcal{N},$$

where $\mathrm{diag}_n(\cdot)$ is the nth diagonal entry of a matrix and $\mathbf{Y}^*$ denotes the hermitian (complex) transpose. Using the admittance matrix instead of (3.1b),(3.1c) and (3.1d) in (3.1) is fully equivalent. If this notation is used it will give the pure BIM instead of the hybrid model we present in (3.1).

The formulation in (3.1) is a steady state approximation of real power systems, as it omits things such as phase-imbalance, transformer tap-positions, harmonics, dynamics, load- and generator-models to name a few [141]. However, this model even due to its seemingly simplicity is NP-hard [144], [145]. This means there is no performance guarantee for any known algorithm to converge to a global optimal solution.

3.1.3 Voltage polar coordinate representation

The model in (3.1) is written in voltage-rectangular complex notation. This can be very beneficial for short-hand notation, however a more intuitive notation from the power-systems perspective, can be the voltage polar notation. In this way, a sense of voltage angles is maintained which can help understanding the nature of active-reactive power flows and their relation to sinusoidal voltages and currents of AC power transmission. This notation also removes the use of complex notation in favor of phase angles and magnitudes. The complex voltage is rewritten using $v = |v|e^{j\theta}$, where $|\cdot|$ denotes magnitude and θ is the phase angle of the voltage phasor. The voltage-polar coordinate system OPF is achieved by replacing constraint (3.1b) with the following two constraints:

$$p_l = G_l|v_n|^2 - |v_n||v_m|\left(G_l\cos\left(\theta_n - \theta_m\right) - B_l\sin\left(\theta_n - \theta_m\right)\right), \ \forall l \in \mathcal{L}, \tag{3.2a}$$

$$q_l = B_l|v_n|^2 - |v_n||v_m|\left(G_l\sin\left(\theta_n - \theta_m\right) + B_l\cos\left(\theta_n - \theta_m\right)\right), \ \forall l \in \mathcal{L}. \tag{3.2b}$$

Here, clearly the constraints in (3.2) are also non-convex due to sinusoidal relations of power flows and voltage angles.

3.2 Linear approximations

In the literature, the linear power flow approximation is generally denoted as the DC-OPF, however this is a bit of a misdemeanor, as DC power transmission still contain losses and voltages which are non-convex and omitted in the linear OPF. The linear OPF is achieved by setting all voltages in the system to one per-unit, and assuming that conductances G_l are negligible compared to the susceptances B_l. Furthermore it will be assumed that the angle differences $\theta_n - \theta_m$ are small, such

that $\sin(\theta_n - \theta_m) \approx \theta_n - \theta_m$. It will be assumed that the active power flows are large compared to reactive power flows, therefore all reactive power flow are removed.

The result is the following approximation:

$$\min_{\Xi} \quad f(\Xi) \tag{3.3a}$$

$$\text{s.t.} \quad \sum_n p_n = 0, \tag{3.3b}$$

$$p_l = B_l(\theta_n - \theta_m), \qquad \forall l = (n,m) \in \mathcal{L}, \tag{3.3c}$$

$$\sum_{l \in n \sim m} p_l = p_n, \qquad \forall n \in \mathcal{N}, \tag{3.3d}$$

$$\underline{P}_n \leq p_n \leq \overline{P}_n, \qquad \forall n \in \mathcal{N}, \tag{3.3e}$$

$$|p_l| \leq \overline{F}_l, \qquad \forall l \in \mathcal{L}. \tag{3.3f}$$

It can be noticed that the model ignores the losses in the system as (3.3b) forces the sum of all injections to equal to zero. The line flow in (3.3c) is a first order Taylor-series approximation of the sinusoidal term in (3.2a). Further, the model omits the reactive power flows and injections. This linear model has been shown to give a good approximation where active power losses and voltages are not too important, as is often the case in high-voltage transmission system. Because of its tractability it is often used by TSOs to optimize power flows.

A different method of representing the linear OPF can be achieved by applying power transmission distribution factors as first presented in [146]. This way, the angle variables θ_n disappear, and the injections are related to line flows through shift factors. Using the power transmission distribution factors may result in a model with slightly less computational burden due to the reduced number of variables.

3.2.1 Decoupled linear power flow

The decoupled power flow is the linear power flow approximation given in (3.3) with an additional linear approximation of the reactive power flow. It is called decoupled because the reactive power flow is not linked to the active power flow. The same assumptions as in the linear power flow are here made, except that only one of the multiplicative voltage magnitudes $|v_n|$ in equation (3.2) is set to one, instead of both.

Thus, the decoupled linear power flow is given as:

$$\min_{\Xi} \quad f(\Xi) \tag{3.4a}$$

$$\text{s.t.} \quad q_l = B_l \left(|v_n| - |v_m| \right), \qquad \forall l = (n,m) \in \mathcal{L}, \tag{3.4b}$$

$$\sum_{l \in n \sim m} q_l = q_n, \qquad \forall n \in \mathcal{N}, \tag{3.4c}$$

$$\underline{Q}_n \leq q_n \leq \overline{Q}_n, \qquad \forall n \in \mathcal{N}, \tag{3.4d}$$

$$\underline{V}_n \leq |v_n| \leq \overline{V}_n, \qquad \forall n \in \mathcal{N}, \tag{3.4e}$$

$$\text{Equations (3.3b) - (3.3f) (linear Power Flow).} \tag{3.4f}$$

The decoupled linear power flow equations now also maintains a sense of voltage magnitude, the voltage is only dependent on the line susceptance since it is assumed that lines are lossless. The voltage estimation can be improved for distribution networks, where it is the case that the reactance is smaller than the resistance (i.e. $X_l << R_l$) by including the resistance in the voltage estimation. The simple voltage approximation that links active and reactive line flow with voltage magnitude is from [147]:

$$|v_m|^2 = |v_n|^2 - 2(R_l p_l + X_l q_l), \quad \forall l \in \mathcal{L}. \tag{3.5}$$

It is important to notice that the expression in (3.5) uses squared voltage magnitude. Therefore, the process to linearize is to replace the squared voltage magnitude with another variable $u_n = |v_n|^2$. For radial systems the equations (3.4b) can be removed due radial power flows only having one possible flow path which will be discussed in the next section.

3.2.2 Network flow in radial systems

In the linear power flow approximation in (3.3) and (3.4), the line flow is governed by the line susceptance as the dominant factor to define the flow in each line as a function of nodal injections. This means that the power flow can not just take any arbitrary path from node n to m but is restricted by an approximation of Ohm's law and as such must flow along all possible paths with flow magnitudes according to the line weight (i.e. susceptance). This model is very useful when the network is *meshed*, because there will be several paths from one node to another. However, in radial networks there is only one possible path between any two arbitrary node sets. A network is called radial if the undirected graph $\mathcal{G}$ that describes its network is a tree [32], [33], [60]. Most distribution networks are typically radial due to safety reasons. Because radial (tree) networks are a simplification of general graphs, the line flow equations can be simplified. Equation (3.3c) and (3.4b) can therefore in the case of a radial system be simplified into (3.6). This simplification somewhat reduces computational burden as it removes the voltage angles from (3.3c) and the voltage

magnitude from (3.4b) and thus reduces the number of variables.

$$p_{l'} + p_l = 0, \quad \forall l \in \mathcal{L}, \tag{3.6a}$$
$$q_{l'} + q_l = 0, \quad \forall l \in \mathcal{L}. \tag{3.6b}$$

The notation $p_{l'}$ indicates the flow in the line when reversing sending and receiving end, i.e. $l = (n, m)$ and $l' = (m, n)$. The flow equations in (3.6) are also called the network-flow approximation, and have been inspired by the traveling salesman problem because the power can flow along any possible path between a node set n and m. If the network-flow model is used for meshed networks, it will result in a crude approximation of the power flows, however for radial networks it is equivalent to the linear OPF in (3.3).

To recap, here all the constraints in the radial distribution system linear decoupled OPF with voltage approximation are collected together.

$$\min_{\Xi} \quad f(\Xi) \tag{3.7a}$$
$$\text{s.t.} \quad \sum_n p_n = 0, \qquad \forall n \in \mathcal{N}, \tag{3.7b}$$
$$p_{l'} + p_l = 0, \qquad \forall l \in \mathcal{L}, \tag{3.7c}$$
$$q_{l'} + q_l = 0, \qquad \forall l \in \mathcal{L}, \tag{3.7d}$$
$$\sum_{l \in n \sim m} p_l = p_n, \qquad \forall n \in \mathcal{N}, \tag{3.7e}$$
$$\underline{P}_n \leq p_n \leq \overline{P}_n, \qquad \forall n \in \mathcal{N}, \tag{3.7f}$$
$$|p_l| \leq \overline{F}_l, \qquad \forall l \in \mathcal{L}, \tag{3.7g}$$
$$\sum_{l \in n \sim m} q_l = q_n, \qquad \forall n \in \mathcal{N}, \tag{3.7h}$$
$$\underline{Q}_n \leq q_n \leq \overline{Q}_n, \qquad \forall n \in \mathcal{N}, \tag{3.7i}$$
$$\underline{V}_n^2 \leq u_n \leq \overline{V}_n^2, \qquad \forall n \in \mathcal{N}, \tag{3.7j}$$
$$u_m = u_n - 2(R_l p_l + X_l q_l), \qquad \forall l \in \mathcal{L}. \tag{3.7k}$$

3.2.3 Linear loss approximation

In the previous section we have shown how to include an approximation for the voltage magnitude in the linear OPF approximation. An approximation of losses is slightly more complex, since losses approximately are quadratic to the flow in a line. Therefore, the approach taken in reference [148], [149] and presented here, incorporates a sequential linear programming method in which sequential linear cuts are applied to the optimization problem. This process is depicted also in Fig. 3.1 where three iterations ν_1 through ν_3 are shown. For every added cut the approximation becomes more precise and will usually converge after few iterations. For this procedure the

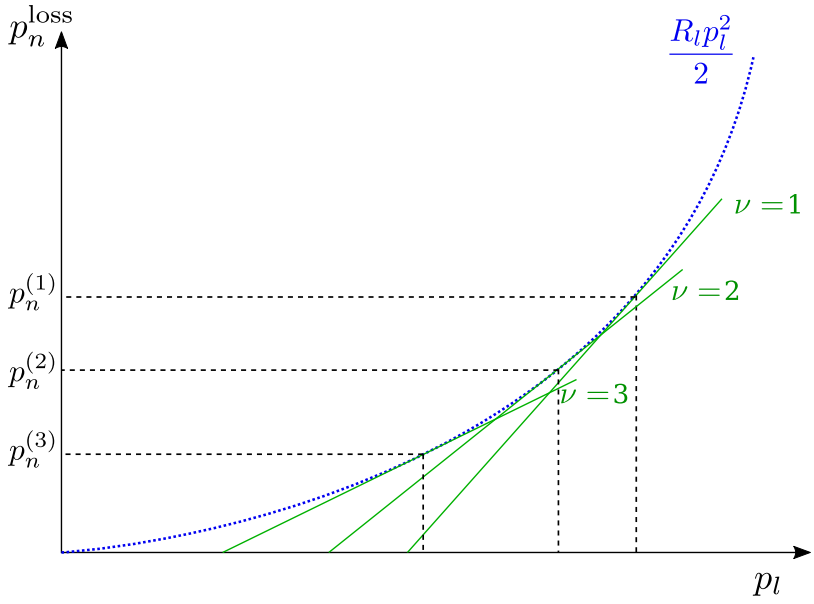

Figure 3.1: Loss-cut procedure in sequential linear programming to approximate losses. Linear loss-cuts are in green; they are added iteratively when solving the linear OPF model. The blue curve shows the quadratic relation between line-flows and losses.

whole OPF problem has to be solved iteratively, and for the first iteration there are no losses. Subsequent iterations then add increasing losses through new linear cuts.

The loss in a line assigned to the node it is connected to can be approximated as:

$$P_n^{\text{loss,fix}} = \sum_{l \in n \sim m} \left(\frac{R_l p_l^2}{2} \right) = \sum_{l \in n \sim m} R_l \left(\frac{\theta_n - \theta_m}{X_l} \right)^2 /2, \quad \forall n \in \mathcal{N}. \tag{3.8}$$

Here the losses are a quadratic function of the line flows. The procedure used in references [148]–[150] is then to add half of the losses to the consumption of every

node connected to the ends of the line. The loss-cut model is given in (3.9):

$$\min_{\Xi, y_n^{(\nu)} \geq 0} \quad f(\Xi)^{(\nu)} - \sum_n C^y y_n^{(\nu)} \tag{3.9a}$$

$$\text{s.t.} \quad \sum_n^N \left(p_n^{(\nu)} - p_n^{\text{loss}(\nu)} - y_n^{(\nu)} \right) = 0, \tag{3.9b}$$

$$p_n^{(\nu)} - p_n^{\text{loss}(\nu)} - y_n^{(\nu)} = \sum_{l \in L_n} p_l^{(\nu)}, \qquad \forall n \in \mathcal{N}, \tag{3.9c}$$

$$p_n^{\text{loss}(\nu)} - \sum_{l \in L_n} (R_l P_{lr}^{\text{fix}}) p_l^{(\nu)} \geq -P_{nr}^{\text{loss,fix}}, \qquad \forall n, r = \{1, \ldots, \nu - 1\}, \tag{3.9d}$$

$$p_n^{\text{loss}(\nu)} \geq 0 \qquad \forall n \in \mathcal{N}, \tag{3.9e}$$

$$\text{Equations (3.7c)-(3.7k) (decoupled linear flow)}, \tag{3.9f}$$

where r is the index of loss-cuts, and parameter $P_{nr}^{\text{loss,fix}}$ is the fixed loss obtained from the line flow of the previous iterations by solving (3.8). A slack variable $y_n^{(\nu)}$ is introduced in order to upper bound the losses of the optimization problem; it is added to the objective function, where it can add virtual losses at a small negligible profit, in order to avoid adding high artificial losses in the intermediate iterations before convergence, as detailed in [148]. Furthermore, parameter P_{lr}^{fix} is the flow in the line l connecting nodes n and m from the previous iterations. The problem (3.9) has to be solved iteratively, adding one cut per iteration in (4.9d). The convergence is reached at iteration ν once $\left| \sum_n P_{n,(r=\nu)}^{\text{loss,fix}} - \sum_n p_n^{\text{loss},(\nu)} \right| \leq \epsilon$, where ϵ is a small tolerance. Note that the optimal value of slack variable $y_n^{(\nu)}$ should be zero in the final iteration.

3.3 Convex relaxations of optimal power flows

The full QCP-OPF problem in (3.1) can be rewritten into a model using matrix notation by introducing the valid constraint $\mathbf{W} = vv^*$. Substituting, the QCP from (3.1) is rewritten as:

$$\min_{p,q,\mathbf{W}} \quad f(\Xi) \tag{3.10a}$$

$$\text{s.t.} \quad p_l + iq_l = (\text{diag}_n(\mathbf{W}) - \mathbf{W}_{nm}) y_{nm}^*, \qquad \forall l = (n,m) \in \mathcal{L}, \tag{3.10b}$$

$$\underline{V}_n^2 \leq \text{diag}_n(\mathbf{W}) \leq \overline{V}_n^2, \qquad \forall n \in \mathcal{N}, \tag{3.10c}$$

$$\mathbf{W} \succeq 0, \tag{3.10d}$$

$$\text{rank}(\mathbf{W}) = 1, \tag{3.10e}$$

$$\text{Equations (3.1c) to (3.1g)}. \tag{3.10f}$$

The model in (3.10) is equivalent to the full non-convex QCP problem and it is a non-convex Semi-Definite Program (SDP) model. Note here, that the notation $\text{diag}_n(\mathbf{W})$ indicates the nth entry of the diagonal of matrix $\mathbf{W}$. The notation $\succeq$ is used in the sense of eigenvalues, i.e. constraint (3.10d) consitutes that the matrix $\mathbf{W}$ shall only have non-negative eigenvalues. The eigenvalue constraint captures the definition of a Positive Semi-Definite (PSD) matrix. Therefore, the difference of (3.1) and (3.10) is that the voltage vector v is replaced with a semi-definite matrix $\mathbf{W}$ of rank one. The only non-convexity in this model is arising from equation (3.10e) – by dropping this constraint, it effectively becomes a SDP convex relaxation. Solving an OPF model as a convex SDP was first proposed in [151] and the exactness of the relaxation was discussed in [31]. This thesis does not use the SDP relaxation, but rather the Second-Order Cone Program (SOCP) relaxed power flow presented next. This is because it has been shown that SOCP models are in many circumstances exact relaxations of the QCP model in (3.1) if the network is radial, and balanced three-phase operation is considered. For meshed networks or unbalanced three-phase radial systems, the SDP relaxation is a superior model, however it is much less tractable for large problems than a SOCP relaxation.

The SOCP relaxation is achieved by further relaxing constraints (3.10d). This relaxation technique was first proposed for the BIM in [34]. Any convex SDP can be relaxed to an SOCP by relaxing some of the PSD constraints, as shown in [141, p. 23]. One necessary condition for a PSD matrix is that all the principal minors[1] of the matrix are non-negative. The SOCP power flow model relaxes this constraint only requiring one-by-one and two-by-two principal minors to be non-negative instead of all principal minors to be non-negative. Replacing equations (3.10d) with the following two equations we obtain the SOCP relaxed OPF:

$$\mathbf{W}_{nm}\mathbf{W}_{nm}^{*} \leq \text{diag}(\mathbf{W})_n \text{diag}(\mathbf{W})_m, \forall l = (n,m) \in L_n, \tag{3.11a}$$

$$\text{diag}(\mathbf{W}) \geq 0. \tag{3.11b}$$

Note here that the main diagonal of the matrix $\mathbf{W}$ is the squared voltage magnitude of the corresponding node n. With the SOCP relaxation, it can be noted that the voltage angles are removed. This can be verified by examining the two sides of constraint (3.11a). The left side is real-valued and thus the voltage angles are not relevant, and the diagonals of the matrix $\mathbf{W}$ on the right hand side will also always be real-valued. Therefore, the SOCP relaxation is also an angle-relaxation of the QCP OPF. In [36], an SOCP with an angle approximation is introduced which is relevant for SOCP power flow models in meshed networks. However, this is then not a convex relaxation anymore but an approximation, albeit a very precise one.

[1] A minor is the determinant of a sub-matrix. A principal minor is the determinant if the diagonal of the sub-matrix coincides with the main diagonal of the full matrix.

3.3.1 Branch flow models of QCP and SOCP models

In the previous section, the power flow model is centered around nodal power injections and nodal voltages, and thus called the BIM as discussed in Section 3.1. One can reformulate the QCP model (3.1) to be expressed in terms of squared current magnitude and squared voltage magnitude which is termed the BFM.

The voltage angles are not important in radial networks as discussed earlier, since flows are only able to move through one path between any two nodes. Therefore, the BFM model for radial networks relaxes the voltages to remove angles to achieve a simpler notation. The angle relaxed BFM was first described in [152] and called the DistFlow equations. This simplifies notation for radial distribution systems because it is a real-valued set of equations with fewer variables due to the discarding of the angles. For radial networks, the angle relaxed QCP that is described by DistFlow is equivalent to the full QCP and is also non-convex due to a quadratic equality constraint.

In (3.12) the angle relaxed BFM is presented.

$$\min_{\Xi} \quad f(\Xi) \tag{3.12a}$$

$$\text{s.t.} \quad p_l^2 + q_l^2 = \varphi_l |v_n|^2, \qquad \forall l = (n,m) \in \mathcal{L}, \tag{3.12b}$$

$$p_l + p_{l'} = R_l \varphi_l, \qquad \forall l = (n,m) \in \mathcal{L}, \tag{3.12c}$$

$$q_l + q_{l'} = X_l \varphi_l, \qquad \forall l = (n,m) \in \mathcal{L}, \tag{3.12d}$$

$$|v_m|^2 = |v_n|^2 - 2(R_l p_l + X_l q_l) + (R_l^2 + X_l^2)\varphi_l, \qquad \forall l = (n,m) \in \mathcal{L}, \tag{3.12e}$$

$$\text{Equations (3.1b) - (3.1h).} \tag{3.12f}$$

Here φ_l is the squared current magnitude in line $l = (n,m)$. The notation $p_{l'}$ is the power flow in the opposing direction of $l = (n,m)$, i.e. $l' = (m,n)$. Equation (3.12b) is the apparent power flow that is linked to current magnitude and voltage magnitude. In (3.12c) and (3.12d), the active and reactive power losses are defined, respectively. The voltage magnitude is linked to active and reactive line flows in (3.12d).

Convexification of branch flow model

In order to show that (3.12) is actually an angle relaxation of (3.1) we here show how to derive (3.12e). Using Ohm's law in complex notation with complex current I_l and line impedance z_l the voltage drop from node n to m is given as:

$$v_m = v_n - I_l z_l, \tag{3.13}$$

where $I_l \in \mathbb{Z}$ is the complex current in line l. To convexify we take the squared magnitude of both sides which renders the voltage angles obsolete:

$$\begin{aligned} |v_m|^2 &= |v_n - I_l z_l|^2 \\ &= |v_n|^2 - 2\mathrm{Re}[v_n^* I_l z_l] + |I_l|^2 |z_l|^2 \\ &= |v_n|^2 - 2(R_l p_l + X_l q_l) + (R_l^2 + X_l^2)\varphi_l. \end{aligned} \tag{3.14}$$

This shows that (3.12) is an angle relaxation of (3.1). Therefore, (3.12) is a model that is real valued and uses the line flows as variables which is a BFM. This model has been used in literature for distribution systems because it is exact for radial networks. However, it is still a non-convex model due to (3.1b).

The SOCP branch flow relaxation can be easily derived since the only non-convexity of (3.12), is equation (3.12b) and (3.1e). Equation (3.12b) is therefore relaxed to a convex version by replacing $=$ with $\geq$. The branch flow SOCP can be used with good results in radial networks, such as distribution networks, where the exactness almost always holds. The SOCP branch flow model was first presented in [60] and [153] (a two part article). Only in radial systems with a lot of reverse power flow due to large DER power injections the SOCP relaxation might not be exact. Sufficient conditions in order to guarantee the exactness of the solution in radial distribution networks were investigated in recent years (see [55], [59], [153], [154]), though they often shrink the feasible space of the solutions such that the outcomes achieve worse objectives. Alternatively, feasibility recovery of an inexact SOCP relaxation is proposed in [36]. The convex relaxation of (3.12b) is thus:

$$p_{nm}^2 + q_{nm}^2 \leq \varphi_{nm}|v_n|^2. \tag{3.15}$$

In order to maintain convexity we introduce a new variable $u_n = |v_n|^2$ to present squared voltage magnitude. The full SOCP branch flow constraints can now be collected as:

$$\begin{aligned}
\min_{\Xi} \quad & f(\Xi) && && (3.16a)\\
\text{s.t.} \quad & p_l^2 + q_l^2 \leq \varphi_l u_n, && \forall l = (n,m) \in \mathcal{L}, && (3.16b)\\
& p_l + p_{l'} = R_l \varphi_l, && \forall l = (n,m) \in \mathcal{L}, && (3.16c)\\
& q_l + q_{l'} = X_l \varphi_l, && \forall l = (n,m) \in \mathcal{L}, && (3.16d)\\
& u_m = u_n - 2(R_l p_l + X_l q_l) + (R_l^2 + X_l^2)\varphi_l, && \forall l = (n,m) \in \mathcal{L}, && (3.16e)\\
& \underline{V_n}^2 \leq u_n \leq \overline{V_n}^2, && \forall l = (n,m) \in \mathcal{L}, && (3.16f)\\
& \text{Equations (3.1c) to (3.1g) (Flow Limits).} && && (3.16g)
\end{aligned}$$

The constraint in (3.16b) is an SOCP constraint in *hyperbolic* form. It can easily be rewritten into standard SOCP form. An SOCP constraint is also called Lorentz Cone or ice cream cone is a convex constraint. The standard SOCP constraint form is as follows:

$$||A_i x_i + b_i||_2 \leq c_i^{\mathrm{T}} x_i + d_i,$$

where $A_i \in \mathbb{R}^{n \times m}$ and $x_i \in \mathbb{R}^n, b_i \in \mathbb{R}^m, c_i \in \mathbb{R}^n, d_i \in \mathbb{R}$. Here $|| \cdot ||_2$ denotes the 2-norm.

To show that (3.16b) is actually an SOCP we choose the following values for the parameters [141]:

$$A = \begin{bmatrix} 2 & 0 & 0 & 0 \\ 0 & 2 & 0 & 0 \\ 0 & 0 & 1 & -1 \end{bmatrix}, \quad b = [0], \quad c = \begin{bmatrix} 0 \\ 0 \\ 1 \\ 1 \end{bmatrix}, \quad d = [0].$$

With this choice of parameters we can now write the standard SOCP equation where $u_n = |v_n|^2$ is the squared voltage magnitude:

$$\left\| \begin{bmatrix} 2 & 0 & 0 & 0 \\ 0 & 2 & 0 & 0 \\ 0 & 0 & 1 & -1 \end{bmatrix} \begin{bmatrix} p_l \\ q_l \\ \varphi_l \\ u_n \end{bmatrix} \right\|_2 = \left\| \begin{bmatrix} 2p_l \\ 2q_l \\ \varphi_l - u_n \end{bmatrix} \right\|_2 \leq \begin{bmatrix} 0 \\ 0 \\ 1 \\ 1 \end{bmatrix}^T \begin{bmatrix} p_l \\ q_l \\ \varphi_l \\ u_n \end{bmatrix}. \tag{3.17}$$

Now it can be easily seen that (3.17) is equivalent to (3.16b).

CHAPTER 4

A local DSO-level market

In Chapter 3 we collected the background material for Optimal Power Flow (OPF) modeling in power systems. This chapter is leveraging these techniques and uses the asymmetric block offers introduced in [58] to present a novel congestion management tool for the Distribution System Operator (DSO). This chapter is based on the contributions of [**Paper A**]. The asymmetric block offers introduce binary variables which complicate the dispatch problem. Therefore, the impact of three different power flow models is analyzed in depth, which highlights each of their implications to the outcomes of the dispatched asymmetric block offers. The benefit of using asymmetric block offers for congestion management, is that the rebound effect is inherently taken into account in a market clearing mechanism that can be solved in one shot. Previous works have used dynamic programming techniques in order to represent the effect of Thermostatically Controlled Load (TCL)-based Demand Response (DR) rebound which is difficult to align with classical market clearing mechanisms.

Structure of the chapter: The rest of this chapter is structured as following: Section 4.1 presents the background for the proposed DSO level flexibility market. Section 4.2 describes the implementation of asymmetric block offers, and explains the congestion management mechanism. Section 4.3 proposes the congestion management method using three different OPF models. Section 4.4 provides results for two case studies; the first case study is a toy-example and the second case study is using the IEEE 37-node test feeder.

4.1 Congestion management through asymmetric block offers

If the Transmission System Operator (TSO) and DSO each have their own area to control and can access flexibility only from their local domains, as discussed in the *Shared Balancing Responsibility* coordination scheme in Chapter 2, the DSO may choose to re-dispatch local generators and DR units in order to meet grid constraints and avoid

overloading the thermal line limits. Therefore, the market clearing outcomes from the Day-Ahead (DA) market are input parameters to the DSO re-dispatch problem represented in this chapter. A significant part of the flexibility of distribution network connected Distributed Energy Resources (DERs) is expected to be in the form of DR. The emergence of Information and Communications Technology (ICT), smart meters and the internet-of-things have the potential to enable control of small scale DERs and may bring great opportunities to the DSO in the future [9]. If enough DERs are available to take part in an economic dispatch, the DSO can use them for ancillary services such as congestion management. This way, peak-load hours on distribution feeders can be mitigated by peak-shaving and valley filling, thereby flattening out the daily load profile.

In this chapter we assume a separate market for flexibility on the DSO level, which is operating ex-post (meaning after clearing) of the day-ahead market. This way, current market structures are not necessarily changed, as all communication is uni-directional. This means that the information is going from the market clearing agent down to TSO and DSO, and the DSO does not need to share any information with either. In other works it has been proposed that the DSO can share feasibility maps of injection regions at the Point of Common Coupling (PCC) with either the TSO or market clearing agent, in order for them to access flexibility that is located at the DSO level [49], [50].

As discussed in Chapter 2, the rebound effect is caused by the underlying physical properties of the DR unit (see also [18], [19]) in question. Modeling this has before been done by dynamic programming [57]. This however requires iterative solution techniques, that iterate between OPF models and dynamic models to describe DR behaviour, and is therefore not compatible with any market clearing methods in operation today.

Therefore, other alternatives are needed to model rebound effects within market frameworks, e.g., new offering formats for DR units [37]. One appealing market-compatible concept is asymmetric block offers [58], which include two parts, response and rebound. Each part models either load increase or decrease. One can view the combination of these two parts as a load shifting offer in time, but without a time gap between response and rebound time periods. We use the concept of asymmetric block offers, because it allows us to model rebound *a priori* in our market model without the need for an iterative clearing process.

The asymmetric block offers[1] are binary constructs, meaning that they cannot be accepted partially. Therefore, the binary variables that determine their activation increase the computational complexity into being a combinatorial problem that is in general NP-hard to solve. With modern branch-and-bound or similar algorithms there have been great improvements in solving discrete problems in recent years however there exist no proofs of convergence in polynomial time. For an overview of recent

[1] Adding block offers is common place in European zonal electricity markets, as conventional generators are allowed to submit different types of block offers to ensure their internal unit commitment constraints [110].

advances in combinatorial branch and bound algorithms we refer to [155]. As a way to analyse the complexity of the presented combinatorial problems, we examine in this chapter how the changing of the power flow models affect the outcomes and computational burden and precision of the achieved results. This is done with the intent of offering a quantitative assessment of different clearing methods to DSOs that wish to employ asymmetric block offers.

In any DSO-level mechanism involving DR units, it is of importance to model rebound effect, otherwise it may cause another unforeseen congestion. Also in any mechanism without modeling rebound effects, DR units may not be optimally scheduled to exploit their maximum potential flexibility. In the existing literature on congestion management[2] no work has yet addressed the rebound effect of DR units. The rebound effect of DR units was modeled for a balancing market without grid representation in [58], where the concept of asymmetric block offers was introduced.

The following points highlight the contributions of the work presented in this chapter based on **[Paper A]**:

1. We develop a re-dispatch mechanism for a DSO as an ex-post congestion management action, while a-priori accounting for rebound effects of DR units using asymmetric block offers.

2. We provide a comprehensive analysis to explore how different grid representations change the re-dispatch outcomes and the computational burden.

3. We develop the following three distribution optimal power flow (OPF) models in connection to the asymmetric block offers:

   - Mixed-integer Linear Program (MILP) model with voltage approximation (lossless) (similar do LinDistFlow in literature [147], [152])
   - MILP model with voltage approximation and nodal distribution of losses (iterative solving of OPF model required), [148]–[150]
   - Mixed-integer Second-Order Cone Program (SOCP) model which is a conic relaxation of the exact Quadratically Constrained Program (QCP) OPF formulation [31], [32], [59], [60], [153]. The solutions can be analyzed for exactness and in such case are AC-feasible [33]. If not, the AC-feasibility recovery methods have to be employed [36].

4. We analyze the effect of sufficient conditions that guarantee the exactness of the MI-SOCP solution as presented in [55], [154].

In the results section, it is demonstrated that the MILP models have superior computational performance when compared to the SOCP models, but at the cost of reduced precision. Particularly in table 4.4 the results are summarized. The voltage calculation of the MILP models lack precision when compared to the SOCP model

[2]See [56] for a systematic overview on congestion management in distribution networks.

and when validated with an ex-post power flow method based on forward-backward sweep. However, the MILP model with loss approximation gives a reasonably good approximation of the losses in the lines.

4.2 Congestion management using asymmetric block offers

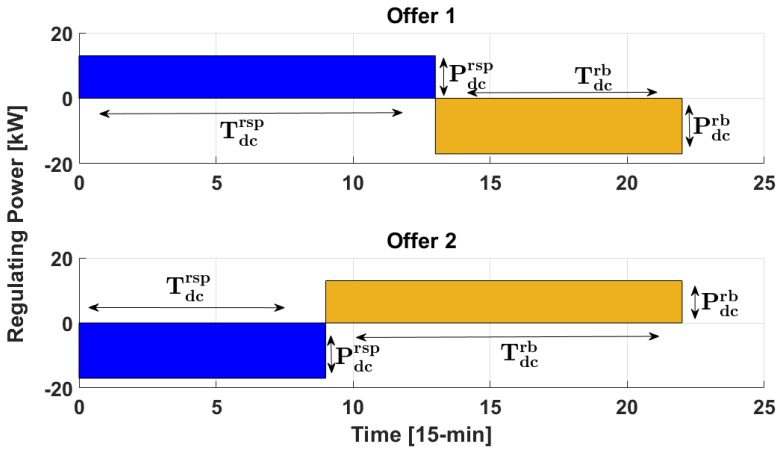

Figure 4.1: Two examples of possible asymmetric block offers for a DR unit. Positive/negative regulating power corresponds to up/down-regulation, respectively. In offer 1 (upper plot), the response part (in blue) provides up-regulation, i.e., a decrease in load power consumption. Its rebound (in yellow) corresponds to a subsequent load increase, i.e. down regulation. Further, offer 2 (lower plot) includes down- and up-regulation in response and rebound parts, respectively. Figure is from [**Paper A**].

In this section we briefly discuss the details of asymmetric block offers. For a more in depth explanation see section II of [**Paper A**].

4.2.1 Asymmetric block offers

Many works have proposed using TCL as DR units [21], [26], [92]. This is possible because the thermal inertia of buildings, fridges and water heaters to some degree decouples the use of electric power from the actual utility. This means that the temperature and the utility to the end-user of the underlying device is not dependent on continuous power usage and can be dynamically scheduled. With the emergence

of smart meters and modern ICT technology it is expected that these units can be aggregated and offered in various electricity markets to exploit their inherent flexibility.

The asymmetric block offers simply mimic the underlying physical properties of the underlying load and are transparent and easy to understand to the market clearing entity. We visualize two asymmetric block offers in figure 4.1, where two examples are plotted with different order of up- and down-regulation directions. By asymmetric, it means that they can have different power consumption levels and duration for response and rebound parts. The asymmetric block offers are indeed the market offers of DR units or flexibility aggregators in general. Since this chapter looks at the problem from a DSO perspective, the asymmetric block offers are exogenous, and their synthesis are out of the scope of this work[3].

4.2.2 Pricing the asymmetric block offers

Similar to unit commitment problems used in US-style markets [157], the use of mixed-integer programming for market clearing poses problems with regards to pricing the traded products. In general, in market clearing problems that need a single equilibrium price at which all trades are paid, the prices are the first-order derivatives of the energy balance constraints. However, first order derivatives are not defined for the discontinuities introduced by binary variables. Therefore, the derivatives are most usually found by fixing the binary variables and solving the resulting continuous problem. In the case of a generator (in our case DR unit) being the marginal producer, which is subject to an integer variable, the found prices will not support the costs of the marginal producer. This problem has been known for a long time in US markets, which use mixed-integer methods for unit commitment problems. In the case of a marginal producer that is activated by a binary variable a method to pay this generator in order not to be paid below the marginal offer needs to be found. One viable way to guarantee cost recovery is uplift payments [158], which is a framework that makes sure that all producers are paid at least their offering price. In [159] the differences of pricing methods for discontinuous problems are discussed, especially the focus is on *convex hull pricing*. We do not go more into depth about the pricing mechanisms in this thesis, but the reader and possible users of asymmetric block offers need to be aware of the pitfalls of different pricing schemes when non-convexities are present in the market clearing problem.

4.2.3 Congestion management: framework and assumptions

The market clearing agent for the day-ahead market does not take into concern any nodal topology and line flow and therefore the outcomes may cause congestion at DSO level. If congestion has to be mitigated by active control, the DSO may be

[3]We refer the interested readers to [156] for offering strategy problem of DR units and flexibility aggregators using asymmetric block offers.

considering market based methods which use economic incentives to local units to correct any scheduled congestion. The line congestion may be caused both by thermal line limits (i.e. the transmitted apparent power) or voltage violations (both over- and under-voltages can cause congestion). Increasing demand for electrical power is going to drive congestion issues and the expansion costs are expected to rise above the costs of using Active Distribution Network Management (ADNM). The use of DR for congestion management has been identified as a prime mover for ADNM [14]. We here propose an ex-post local day-ahead market for the DSO which is to be cleared *right after* the whole-sale energy market. Since a large volume of the DR units with rebound characteristics are expected to be located in radial distribution feeders, it is logical to use their load-shifting potential to resolve local issues.

In this chapter we consider both regular dispatchable generators and DR units that offer asymmetric block offers. However, we leave out battery storage systems, which however could be an extension of this work. The PCC is also considered as a regular generator as the imbalance that is caused there will be offset by the TSO. The Balance Responsible Party (BRP) and/or aggregator that is responsible for the units taking part in the local redispatch will have to reimburse the TSO for the imbalance, and they have to take into account this cost in their offers. The particularities of the imbalance caused to the TSO and the resulting trading schemes are outside the scope of this work, but an observation is that the redispatch by a DSO will be small compared to other trades in TSO-level ancillary services markets.

After collecting the submitted offers, the DSO runs the congestion management mechanism, whose objective is to meet local constraints at the minimum re-dispatch cost. The outcomes are accepted offers for up- and down-regulation. Regarding the potential uncertainty sources, e.g., load and renewable power uncertainties, we assume that they have been already considered during the day-ahead market clearing. Therefore, the proposed ex-post re-dispatch mechanism does not need to model again those uncertainties. Moreover, the DSO may be unwilling to collect and manipulate statistical data in order to model future uncertainties, because in current market frameworks this duty falls to the market operator. However, the modeling of uncertainty on the dispatch of local generators in a DSO congestion management market could be an interesting future work.

The DSO-level networks are usually radial and congested lines can only be relieved, if resources on both sides of the congestion are available for re-dispatch[4]. This is because any up-regulation somewhere in the network has to be matched by an equal down-regulation elsewhere (minus line losses). One important observation is that the accepted offers for up- and down-regulation should be located on both sides of the congested line, in order to maintain power balance.

[4]Since the PCC is always upstream, the downstream units are the most important ones (i.e. as far away from the PCC as possible).

4.3 Mathematical model

In this section the mathematical representation of asymmetric block offers is collected, together with the relevant OPF models from Chapter 3 to offer a complete overview of the proposed methods.

4.3.1 Mathematical representation of asymmetric block offers

This section provides a modified version of formulations for asymmetric block offers from [58], yielding a set of mixed-integer linear inequalities. The binary variable o_{dct} governs the activation of every offer d from unit c in time step t. The activation of a block offer means that the full offer must be activated and therefore the binary variables are linked across time-steps, which makes this an inter-temporally linked problem. Therefore, the dispatch problem cannot be trivially decomposed into different time-steps, similar to any problem including ramping constraints or state of charge modeling for batteries.

Asymmetric block offers beginning with up-regulation response, e.g., Offer 1 in figure 4.1, are modeled by equations (4.1), while offers beginning with down-regulation response, e.g., Offer 2 in figure 4.1, are represented by equations (4.2).

These two different kinds of block offers are differentiated by binary parameter A_{dc}. If A_{dc} is set to 1, it indicates that block offer d of unit c begins with up-regulation, or to 0 if it begins with down-regulation. The binary variable o_{dct} is a decision variable to activate a given offer d from DR unit c in time step t.

$$\Big\{ r^{\mathrm{up}}_{dct} \leq P^{\mathrm{rsp}}_{dc} o_{dct}, \qquad \forall d, c, t, \tag{4.1a}$$

$$r^{\mathrm{dn}}_{dct} \leq P^{\mathrm{rb}}_{dc} o_{dct}, \qquad \forall d, c, t, \tag{4.1b}$$

$$\sum_{\tau=t}^{t+T^{\mathrm{rsp}}_{dc}-1} r^{\mathrm{up}}_{dc\tau} \geq T^{\mathrm{rsp}}_{dc} P^{\mathrm{rsp}}_{dc} (o_{dct} - o_{dc,t-1}), \qquad \forall d, c, t, \tag{4.1c}$$

$$\sum_{\tau=t+T^{\mathrm{rsp}}_{dc}}^{t+T^{\mathrm{rsp}}_{dc}+T^{\mathrm{rb}}_{dc}-1} r^{\mathrm{dn}}_{dc\tau} \geq T^{\mathrm{rb}}_{dc} P^{\mathrm{rb}}_{dc} (o_{dct} - o_{dc,t-1}), \qquad \forall d, c, t \leq |T| - T^{\mathrm{rsp}}_{dc}, \tag{4.1d}$$

$$\sum_{\tau=t}^{t+T^{\mathrm{rsp}}_{dc}-1} r^{\mathrm{dn}}_{dc\tau} \leq T^{\mathrm{rb}}_{dc} P^{\mathrm{rb}}_{dc} (1 - (o_{dct} - o_{dc,t-1})), \qquad \forall d, c, t, \tag{4.1e}$$

$$\sum_{\tau=t+T^{\mathrm{rsp}}_{dc}}^{t+T^{\mathrm{rsp}}_{dc}+T^{\mathrm{rb}}_{dc}-1} r^{\mathrm{up}}_{dc\tau} \leq T^{\mathrm{rsp}}_{dc} P^{\mathrm{rsp}}_{dc} (1 - (o_{dct} - o_{dc,t-1})), \quad \forall d, c, t \leq |T| - T^{\mathrm{rsp}}_{dc} \Big\} \text{ if } A_{dc} = 1. \tag{4.1f}$$

The blocks beginning with down-regulation when $A_{dc} = 0$ are given in (4.2).

$$\Big\{ r^{\mathrm{dn}}_{dct} \le P^{\mathrm{rsp}}_{dc} o_{dct}, \qquad \forall d, c, t, \tag{4.2a}$$

$$r^{\mathrm{up}}_{dct} \le P^{\mathrm{rb}}_{dc} o_{dct}, \qquad \forall d, c, t, \tag{4.2b}$$

$$\sum_{\tau=t}^{t+T^{\mathrm{rsp}}_{dc}-1} r^{\mathrm{dn}}_{dc\tau} \ge T^{\mathrm{rsp}}_{dc} P^{\mathrm{rsp}}_{dc} (o_{dct} - o_{dc,t-1}), \qquad \forall d, c, t, \tag{4.2c}$$

$$\sum_{\tau=t+T^{\mathrm{rsp}}_{dc}}^{t+T^{\mathrm{rsp}}_{dc}+T^{\mathrm{rb}}_{dc}-1} r^{\mathrm{up}}_{dc\tau} \ge T^{\mathrm{rb}}_{dc} P^{\mathrm{rb}}_{dc} (o_{dct} - o_{dc,t-1}), \qquad \forall d, c, t \le |T| - T^{\mathrm{rsp}}_{dc}, \tag{4.2d}$$

$$\sum_{\tau=t}^{t+T^{\mathrm{rsp}}_{dc}-1} r^{\mathrm{up}}_{dc\tau} \le T^{\mathrm{rb}}_{dc} P^{\mathrm{rb}}_{dc} (1 - (o_{dct} - o_{dc,t-1})), \qquad \forall d, c, t, \tag{4.2e}$$

$$\sum_{\tau=t+T^{\mathrm{rsp}}_{dc}}^{t+T^{\mathrm{rsp}}_{dc}+T^{\mathrm{rb}}_{dc}-1} r^{\mathrm{dn}}_{dc\tau} \le T^{\mathrm{rsp}}_{dc} P^{\mathrm{rsp}}_{dc} (1 - (o_{dct} - o_{dc,t-1})), \quad \forall d, c, t \le |T| - T^{\mathrm{rsp}}_{dc} \Big\} \text{ if } A_{dc} = 0. \tag{4.2f}$$

Conditions (4.1a) and (4.1b) restrict up- and down-regulation r^{up}_{dct} and r^{dn}_{dct} to the prescribed magnitude of response P^{rsp}_{dc} and rebound P^{rb}_{dc}, respectively. In (4.1c), the length of the response, if offer d is activated, is set to the prescribed response time T^{rsp}_{dc}. Condition (4.1d) is similar to (4.1c), but for the rebound part of the block offer. Note that $|T|$ indicates the cardinality of set T. Condition (4.1e) ensures that variable r^{dn}_{dct} is 0 during up-regulation. Similarly, condition (4.1f) imposes $r^{\mathrm{up}}_{dct} = 0$ during down-regulation. The equations for the block offers beginning with down-regulation are similar to equations (4.1) and are given in equations (4.2).

In addition to (4.1) and (4.2), a minimum recovery period, if exists, needs to be enforced. This condition is enforced by (4.3). Parameter T^{rec}_{dc} corresponds to the recovery time between the two consecutive asymmetric block offers (not between response and rebound parts of a block offer). In other words, it enforces the minimum recovery time between the rebound part of one block and the response part of the next block.

$$\sum_{\tau=t+T^{\mathrm{resp}}_{dc}+T^{\mathrm{reb}}_{dc}}^{t+T^{\mathrm{resp}}_{dc}+T^{\mathrm{reb}}_{dc}+T^{\mathrm{rec}}_{dc}-1} (1 - o_{dc,\tau}) \ge T^{\mathrm{rec}}_{dc} (o_{dct} - o_{dct-1}),$$
$$\forall d, c, t \le |T| - (T^{\mathrm{resp}}_{dc} + T^{\mathrm{reb}}_{dc}) + 1. \tag{4.3}$$

In (4.4), it is ensured that each DR unit is only able to activate at most one block offer in any time step:

$$\sum_{d} o_{dct} \le 1, \quad \forall c, t. \tag{4.4}$$

The block offers need to be fully dispatched within the planning horizon, such that no activated offers spill into the next planning horizon. This is enforced in constraint (4.5).

$$\begin{gathered} 1 - (o_{dc,t+1} - o_{dct}) \leq 2(1 - o_{dc|T|}), \\ \forall d, c, t = |T| - (T_{dc}^{\text{resp}} + T_{dc}^{\text{reb}}). \end{gathered} \tag{4.5}$$

In total, the collection of equations (4.1) through (4.5) are what is necessary to describe the behaviour of the desired asymmetric block offers. When included in an OPF model, these block offers can be dispatched optimally so that any congestion in the network will be relieved. This is shown in the next section.

4.3.2 OPF revisited and relation to block offers

In Chapter 3 we introduced the different OPF approximation models and also convex conic relaxations based on the AC-OPF. To quickly recap, a convex relaxation may provide a lower bound on the cost associated with a non-convex optimization problem. In the case of a convex relaxation, the duality gap is not necessarily 0, which means that the outcomes are not fulfilling the constraints of the non-convex problem they derive from. However, it is usually easy to check whether the outcome of a convex relaxation model is exact. It turns out that for radial networks, the SOCP-based conic relaxation is very often exact and even if not, provides very good lower bounds. The lower bound can be used for feasibility recovery which has been documented in [36]. In contrast, approximations based on linear models can both over- and under-estimate the variables in question. Most notably, the most common linear OPF models are omitting line losses. The voltage approximations delivered by decoupled linear power flow models, can also both over and under estimate the voltages. An in-depth analysis of the voltage estimation of linear models is presented in [160].

We here assume balanced three-phase systems which simplifies modeling. In the case of large phase imbalances the SOCP relaxation may not provide reasonable outcomes and SOCPs are not amenable to modeling three-phase power flows. As a more complex model the Semi-Definite Program (SDP) relaxation (as shown in [161]) can be used to model phase imbalance in a convex model, however SDP is a magnitude more complex to solve than SOCP and mixed-integer SDP solvers are not very well developed at the moment.

We use three OPF models, but all with the same linear objective function given in equation (4.6)[5]. This objective function minimizes the total system cost including

[5]The use of a linear objective function may have issues regarding uniqueness of the achieved solution, which has been discussed in [162]. This means that there can be several equivalent solutions due to the linear cost functions which may cause a divergence in solutions of similar OPF problems of different agents involved in the clearing of the market. The solution to this is usually to use quadratic cost functions which we here omit to keep the models as simple as possible.

load shedding and redispatch costs of regular generators.

$$\begin{aligned}\min_{\Xi} \quad f(\Xi) = \sum_t \Big[& \underbrace{C_t^{\mathrm{p}\uparrow\mathrm{S}} p_t^{\mathrm{up,S}}}_{\text{Cost of } p^{\mathrm{up}} \text{ from TSO}} - \underbrace{C_t^{\mathrm{p}\downarrow\mathrm{S}} p_t^{\mathrm{dn,S}}}_{\text{cost of } p^{\mathrm{dn}} \text{ to TSO}} \\ & + \underbrace{C_t^{\mathrm{q}\uparrow\mathrm{S}} q_t^{\mathrm{up,S}}}_{\text{Cost of } q^{\mathrm{up}} \text{ from TSO}} - \underbrace{C_t^{\mathrm{q}\downarrow\mathrm{S}} q_t^{\mathrm{dn,S}}}_{\text{Cost of } q^{\mathrm{dn}} \text{ to TSO}} \Big] + \sum_{n,t} \Big[\underbrace{C^{\mathrm{Shed}} s_{nt}^{\mathrm{up}}}_{\text{Curtailment cost}} \Big] \\ & + \sum_{i,t} \Big[\underbrace{C_{it}^{\mathrm{p}\uparrow} p_{it}^{\mathrm{up}}}_{\text{Cost of } p^{\mathrm{up}} \text{ from gen.}} - \underbrace{C_{it}^{\mathrm{p}\downarrow} p_{it}^{\mathrm{dn}}}_{\text{Cost of } p^{\mathrm{dn}} \text{ to gen.}} + \underbrace{C_{it}^{\mathrm{q}\uparrow} q_{it}^{\mathrm{up}}}_{\text{Cost of } q^{\mathrm{up}} \text{ from gen.}} \\ & - \underbrace{C_{it}^{\mathrm{q}\downarrow} q_{it}^{\mathrm{dn}}}_{\text{Cost of } q^{\mathrm{dn}} \text{ to gen.}} \Big] + \sum_{d,c,t} \Big[\underbrace{C_{dct}^{\mathrm{DR}\uparrow} r_{dct}^{\mathrm{up}}}_{\text{Cost of } r^{\mathrm{up}} \text{ from DR}} - \underbrace{C_{dct}^{\mathrm{DR}\downarrow} r_{dct}^{\mathrm{dn}}}_{\text{Cost of } r^{\mathrm{dn}} \text{ to DR}} \Big] \end{aligned} \tag{4.6}$$

where Ξ is the set of optimization variables, including free variables $\{p_{nt},\, q_{nt},\, p_{nmt},\, q_{nmt}\}$, non-negative variables $\{p_{it}^{\mathrm{up}},\, p_{it}^{\mathrm{dn}},\, r_{dct}^{\mathrm{up}},\, r_{dct}^{\mathrm{dn}},\, s_{nt}^{\mathrm{up}},\, p_t^{\mathrm{up,S}},\, p_t^{\mathrm{dn,S}},\, q_{it}^{\mathrm{up}},\, q_{it}^{\mathrm{dn}},\, q_t^{\mathrm{up,S}},\, q_t^{\mathrm{dn,S}},\, u_{nt}\}$, and the binary variable $\{o_{dct}\}$.

The common constraints for all three OPF models are given in (4.7). Note that DR_{ct}^{disp}, D_{nt}^{disp}, S_t^{disp} and P_{it}^{disp} are parameters, indicating day-ahead market outcomes.

$$p_{nt} = \sum_{l \in n \sim m} p_{lt}, \qquad \forall n,t, \tag{4.7a}$$

$$q_{nt} = \sum_{l \in n \sim m} q_{lt}, \qquad \forall n,t, \tag{4.7b}$$

$$\begin{aligned} p_{nt} = & \sum_{d,c \in L_n} \left[r_{dct}^{\mathrm{up}} - r_{dct}^{\mathrm{dn}} \right] - \sum_{c \in L_n} DR_{ct}^{\mathrm{disp}} \\ & + \sum_{i \in L_n} \left[p_{it}^{\mathrm{up}} - p_{it}^{\mathrm{dn}} + P_{it}^{\mathrm{disp}} \right] + \left[S_t^{\mathrm{disp}} + p_t^{\mathrm{up,S}} - p_t^{\mathrm{dn,S}} \right]_{n \in PCC} \\ & - D_{nt}^{\mathrm{disp}} + s_{nt}^{\mathrm{up}} - \sum_{l \in n \sim m} \frac{G_l}{2} u_{nt}, \qquad \forall n,t, \end{aligned} \tag{4.7c}$$

$$\begin{aligned} q_{nt} = & \sum_{i \in L_n} \left[q_{it}^{\mathrm{up}} - q_{it}^{\mathrm{dn}} \right] + \left[q_t^{\mathrm{up,S}} - q_t^{\mathrm{dn,S}} \right]_{n \in PCC} \\ & - Q_{nt} + \sum_{l \in n \sim m} \frac{B_l}{2} u_{nt}, \qquad \forall n,t, \end{aligned} \tag{4.7d}$$

$$\sum_d r_{dct}^{\mathrm{up}} \le DR_{ct}^{\mathrm{disp}}, \qquad \forall c,t, \tag{4.7e}$$

$$p_{it}^{\mathrm{dn}} \le P_{it}^{\mathrm{disp}}, \qquad \forall i,t, \tag{4.7f}$$

$$s_{nt}^{\mathrm{up}} + \sum_{d,c \in L_n} \left[r_{dct}^{\mathrm{up}} - r_{dct}^{\mathrm{dn}} \right] \le D_{nt}^{\mathrm{disp}} + \sum_{c \in L_n} DR_{ct}^{\mathrm{disp}}, \qquad \forall n,t, \tag{4.7g}$$

$$p_{it}^{\mathrm{up}} + P_{it}^{disp} \le P_i^{cap}, \qquad \forall i,t, \tag{4.7h}$$

$$\sum_{d} r_{dct}^{\mathrm{dn}} + DR_{ct}^{disp} \leq P_{ct}^{cap}, \qquad \forall c,t, \qquad (4.7\mathrm{i})$$

$$p_{it}^{\mathrm{up}} \leq \overline{P}_{i}^{\mathrm{up}},\ p_{it}^{\mathrm{dn}} \leq \overline{P}_{i}^{\mathrm{dn}}, \qquad \forall i,t, \qquad (4.7\mathrm{j})$$

$$q_{it}^{\mathrm{up}} \leq \overline{Q}_{i}^{\mathrm{up}},\ q_{it}^{\mathrm{dn}} \leq \overline{Q}_{i}^{\mathrm{dn}}, \qquad \forall i,t, \qquad (4.7\mathrm{k})$$

$$p_{t}^{\mathrm{up,S}} \leq \overline{P}^{\mathrm{up,S}},\ p_{t}^{\mathrm{dn,S}} \leq \overline{P}^{\mathrm{dn,S}}, \qquad \forall t, \qquad (4.7\mathrm{l})$$

$$q_{t}^{\mathrm{up,S}} \leq \overline{Q}^{\mathrm{up,S}},\ q_{t}^{\mathrm{dn,S}} \leq \overline{Q}^{\mathrm{dn,S}}, \qquad \forall t, \qquad (4.7\mathrm{m})$$

$$\underline{V}_{n}^{\mathrm{sq}} \leq u_{nt} \leq \overline{V}_{n}^{\mathrm{sq}}, \qquad \forall n,t. \qquad (4.7\mathrm{n})$$

It must be noted that the proposed OPF method with asymmetric block offers should include (4.1) - (4.7). The net active and reactive power injection at node n is linked to corresponding flow in line l from node n to m (written as $l \in n \sim m$) in (4.7a) and (4.7b). The nodal active power balance is enforced by (4.7c). Note that the last term of (4.7c) takes into account the shunt conductance of the lines[6]. The nodal reactive power balance is enforced by (4.7d), which also takes into account the shunt susceptance of the lines connected to node n. The up-regulation (load decrease) provided by DR unit c is limited to its scheduled consumption DR_{ct}^{disp} in (4.7e). The down-regulation (generation decrease) provided by generator i is restricted to its dispatch from the day-ahead market by (4.7f). Constraint (4.7g) limits the curtailed load s_{nt}^{up} according to total scheduled consumption of flexible and inflexible loads from the day-ahead market and provided regulation from DR units. The up-regulation (generation increase) provided by conventional generator i is limited by (4.7h). Similarly, (4.7i) restricts the down-regulation (load increase) provided by DR unit c. Constraints (4.7j) and (4.7k) limit the active and reactive power regulation of conventional generator i to its maximum capability. Similar constraints are applied to the import/export at the PCC from transmission level in (4.7l) and (4.7m). Constraint (4.7n) limits the voltage magnitude to the upper and lower thresholds.

4.3.3 Mixed-integer linear OPF (lossless)

The linear approximation of the AC-OPF which we introduced in Chapter 3, is here coupled with the asymmetric block offers. It is possible by using this OPF method to include the line congestion and voltage issues. Similar to LinDistFlow model in [30], in order to have an approximation of both active and reactive power flow and their effect on the voltage, the decoupled linear power flow is used. For the radial case, the

[6] Half of the shunt losses due to shunt admittance of every line connected to node n is subtracted from that node. In general, shunt conductance of lines is small and can be ignored. However, shunt susceptance can be significant in underground cables.

linearized branch flow OPF boils down to problem (4.8):

$$\min_{\Xi} \quad f(\Xi) \text{ as in (4.6)} \tag{4.8a}$$

$$\text{s.t.} \quad \sum_n p_{nt} = 0, \qquad \forall t, \tag{4.8b}$$

$$\sum_n q_{nt} = 0, \qquad \forall t, \tag{4.8c}$$

$$p_{lt} + p_{l't} = 0, \qquad \forall l \in \mathcal{L}, t, \tag{4.8d}$$

$$q_{lt} + q_{l't} = 0, \qquad \forall l \in \mathcal{L}, t, \tag{4.8e}$$

$$p_{lt} \leq \overline{F}_l, \qquad \forall l, t, \tag{4.8f}$$

$$u_{mt} = u_{nt} - 2\left(R_l p_{lt} + X_l q_{lt}\right), \qquad \forall l, t, \tag{4.8g}$$

$$(4.1) \text{ to } (4.5) \text{ and } (4.7). \tag{4.8h}$$

Constraints (4.8d), (4.8b) and (4.8c) model the lossless linear power flow. To preserve linearity, (4.8f) imposes the line capacity limit in terms of active power flow only. Finally, (4.8g) links the voltage magnitude of two adjacent nodes with impedance and power flows as a linear approximation. Similar to [30], a variable u_{nt} is introduced to present squared voltage magnitude, such that the model remains linear.

4.3.4 Mixed-integer linear OPF with losses

The losses are modeled by an iterative solution of the linear OPF model which is similar to the previous model in (4.8). The model is the same as in Chapter 3, and it is here repeated for the sake of completeness in (4.9). Two new variables are introduced $y_{nt}^{(\nu)}$ (a slack variable to ensure upper boundedness of the problem see [148] for more details) and $p_{nt}^{\text{loss}(\nu)}$ (the nodal distribution of losses).

$$\min_{\Xi, y_{nt}^{(\nu)} \geq 0} \quad f(\Xi)^{(\nu)} - \sum_{nt} C^y y_{nt}^{(\nu)} \tag{4.9a}$$

$$\text{s.t.} \quad \sum_n (p_{nt}^{(\nu)} - p_{nt}^{\text{loss}(\nu)} - y_{nt}^{(\nu)}) = 0, \qquad \forall t, \tag{4.9b}$$

$$p_{nt}^{(\nu)} - p_{nt}^{\text{loss}(\nu)} - y_{nt}^{(\nu)} = \sum_{l \in n \sim m} p_{lt}^{(\nu)}, \qquad \forall n, t, \tag{4.9c}$$

$$p_{nt}^{\text{loss}(\nu)} - \sum_{l \in n \sim m} (R_l \; P_{ltr}^{\text{fix}}) p_{lt}^{(\nu)} \geq -P_{ntr}^{\text{loss,fix}}, \qquad \forall n, t, r = \{1, \ldots, \nu - 1\}, \tag{4.9d}$$

$$p_{nt}^{\text{loss}(\nu)} \geq 0, \qquad \forall n, t, \tag{4.9e}$$

$$(4.1) \text{ to } (4.5), (4.7\text{b}) \text{ to } (4.7\text{n}), (4.8\text{c}) \text{ - } (4.8\text{g}). \tag{4.9f}$$

The parameters that are updated for every iteration are initialized at 0, i.e. $P^{\text{fix}}_{lt,(r=1)} = 0$ and $P^{\text{loss,fix}}_{nt,(r=1)} = 0$. After solving the model (4.9), these parameters are updated. The nodal distribution of losses $P^{\text{loss,fix}}_{ntr}$ is updated with (4.10) and the line flow is set equal to the flow, i.e. $P^{\text{fix}}_{lt,(r=\nu)} = p^{\nu-1}_{lt}$.

$$P^{\text{loss,fix}}_{nt} = \sum_{l \in n \sim m} \left(\frac{R_l \; p^2_{lt}}{2} \right), \qquad \forall n, t. \tag{4.10}$$

The convergence is reached at iteration ν once $\left| \sum_{nt} P^{\text{loss,fix}}_{nt,(r=\nu)} - \sum_{nt} p^{\text{loss},(\nu)}_{nt} \right| \leq \epsilon$, where ϵ is a small tolerance. Note that the optimal value of slack variable $y^{(\nu)}_{nt}$ should be zero.

4.3.5 Mixed-integer SOCP-OPF

The mixed-integer SOCP OPF model for radial distribution systems is presented in (4.11) [141]. It is convex because all inequality constraints are convex and all equality constraints are affine.

$$\min_{\Xi, \varphi_{lt} \geq 0} \quad f(\Xi) \text{ as in (4.6)} \tag{4.11a}$$

$$\text{s.t.} \quad p^2_{lt} + q^2_{lt} \leq \varphi_{lt} u_{nt}, \qquad \forall l \in \mathcal{L}, \; t \tag{4.11b}$$

$$p_{lt} + p_{l't} = R_l \varphi_{lt}, \qquad \forall l \in \mathcal{L}, \; t, \tag{4.11c}$$

$$q_{lt} + q_{l't} = X_l \varphi_{lt}, \qquad \forall l \in \mathcal{L}, \; t, \tag{4.11d}$$

$$u_{mt} = u_{nt} - 2(R_l p_{lt} + X_l q_{lt}) + (R^2_l + X^2_l)\varphi_{lt}, \quad \forall l \in \mathcal{L}, \; t, \tag{4.11e}$$

$$p^2_{lt} + q^2_{lt} \leq \overline{F}^2_l, \qquad \forall l = (n,m) \in \mathcal{L}, \; t, \tag{4.11f}$$

$$\text{(4.1) to (4.5) and (4.7).} \tag{4.11g}$$

Constraint (4.11b) is the convex relaxation and can be rewritten into standard SOCP form, as detailed in Chapter 3. Constraints (4.11c) and (4.11d) are the active and reactive power losses, respectively. Constraint (4.11e) relates the voltage drop to the power flows and currents. In (4.11f) the line flow limit is enforced.

In our numerical studies, the sufficient conditions introduced in [55] are also added to (4.11) to ensure zero duality gap (i.e., exactness) of the relaxation in radial networks[7]. These sufficient conditions are given in equations (4.12).

[7]Without sufficient conditions, the second-order cone constraint (4.11b) might be still binding in specific cases (e.g., in the case studies of this chapter presented in Section 4.4), but there is no exactness guarantee in general. In case of inexactness, an ex-post procedure for feasibility recovery is required. In [36] it is shown how to recover the angles from the SOCP relaxation for a meshed network. This method can be transferred to radial systems without loss of generality.

The additional sufficient conditions to be included in the MI-SOCP OPF model are listed below[8]:

$$\hat{s}_{lt} = s_{nt} + \sum_{l \in n \sim m} \hat{s}_{lt}, \qquad \forall l, t, \tag{4.12a}$$

$$\hat{v}_{nt} - \hat{v}_{mt} = 2\mathrm{Re}(\overline{Z}_l \hat{s}_{lt}), \qquad \forall l, t, \tag{4.12b}$$

$$\mathrm{Re}(\overline{Z}_l \hat{s}_{lt}) \leq 0, \qquad \forall l, t, \tag{4.12c}$$

$$\hat{v}_{nt} \leq \overline{V}_n^{\mathrm{sq}}, \qquad \forall n, t, \tag{4.12d}$$

where $\hat{s}_{lt} = \hat{p}_{lt} + j\hat{q}_{lt}$ is a linear approximation of the complex line flows $s_{lt} = p_{lt} + jq_{lt}$, and $\overline{Z}_l = R_l - jX_l$ is the complex conjugate line impedance. $s_{nt} = p_{nt} + jq_{nt}$ is the complex nodal apparent power injection. Besides, $\hat{v}_{nt}$ is a linear approximation of the squared nodal voltage. These sufficient conditions are quite mild, as long as there is no combined active and reactive reverse power flow on any line. The main condition is (4.12c), which can be interpreted as: The reverse power flow can be either active or reactive but not both[9]. In other words the active and reactive reverse power flow (which is the power flow toward the PCC) can not simultaneously be positive.

4.4 Case studies

We here present the illustrative case study using a small 6 bus radial network, and results from using a 37 bus IEEE network with DR units using asymmetric block offers. All cases are implemented in the GAMS language[10] and solved with CPLEX version 12.8. All the solved optimization problems are mixed-integer problems, which can benefit from some degree of parallelization. The used solver (CPLEX) allows the parallelization on multicore CPUs, where we used 7 cores.

4.4.1 Illustrative example

In figure 4.2 the diagram of the illustrative case study is illustrated, which is used to introduced the congestion management mechanism. This feeder contains three DR units (c_1 to c_3) and two local conventional generators (i_1 and i_2). The line connecting nodes 3 and 4 is likely to be congested due its limited capacity (40 kVA).

All lines have the same physical properties, with a resistance of 0.001 p.u., reactance of of 0.0005 p.u. and shunt conductance and susceptance of 0.1 p.u. The

[8] Note that these conditions guarantee achieving the exactness, but at the cost of shrinking the feasible space, and potentially increasing the system cost and usually the computational burden.

[9] We found that due to numerical issues with the used solver, convergence is achieved much faster if the right-hand side of equation (4.12c) is replaced with a small positive number, i.e. $\mathrm{Re}(\overline{Z}_l \hat{s}_{lt}) \leq \kappa$ where $0 < \kappa << 1$. This will not affect the tightness of the achieved solution in any significant way if κ is sufficiently small.

[10] https://www.gams.com/

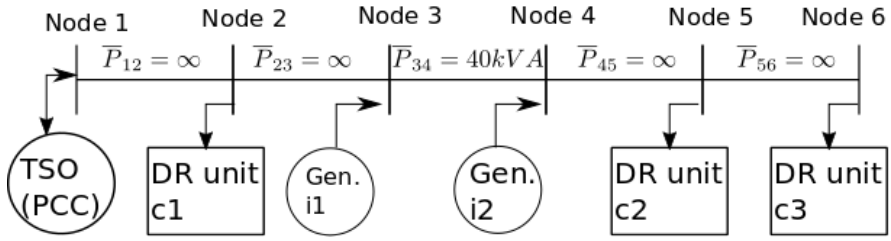

Figure 4.2: Illustrative example: 6-node radial feeder diagram. Taken from [**Paper A**].

Resource*	Up offer price [¢/(kW-30min)]	Down offer price [¢/(kW-30min)]
Regular Generators i	35	10
TSO	21	19
DR units c	25	16

*We assume the same prices for active and reactive regulation offers.
These prices are constant over time.

Table 4.1: The prices for up- and down-regulation offers provided by TSO and local DERs for both the Illustrative example and the Case Study.

day-ahead dispatches are given in in the appendix of [**Paper A**]. The day-ahead dispatch is set such that there will be congestion in the time steps 12 through 26, out of 40 time steps.

Each local generator can provide active power up- and down-regulation up to 80 kW, and reactive power up- and down-regulation up to 30 kVAr. These limits for TSO are 100 kW and 30 kVAr. Each of the three DR units is offering four different asymmetric block offers (d_1 to d_4) as given in table 4.2. The prices that the DR units and regular generators, as well as the TSO offer to the market are given in table 4.1. We assume that DR units are unable to provide reactive power regulation. The upper and lower bounds of the nodal voltage magnitudes are set to 0.9 and 1.1 p.u., respectively. The voltage drop in this test case is very high, such that any differences between the three OPF models will be highlighted.

4.4.2 Results obtained from MILP-OPF (lossless)

Losses are not accounted for and therefore the outcomes are always neutral with respect to the consumed energy (i.e. summing up all re-dispatches always sums to 0). The regulation sources located at the PCC side of the congested line are TSO, DR unit c_1 and local generator i_1 (the so-called upstream sources), while the opposite side contains generator i_2, DR units c_2 and c_3 (downstream sources). The outcomes of the proposed DSO-level congestion management mechanism based on MILP-OPF

DR unit	Offer	P_{dc}^{rsp}	P_{dc}^{rb}	T_{dc}^{rsp}	T_{dc}^{rb}	A_{dc}
c_1	d_1	13	17	13	9	1
	d_2	17	13	9	13	0
	d_3	10	10	20	21	1
	d_4	17	10	9	20	0
c_2	d_1	17	8	9	29	0
	d_2	8	17	29	9	1
	d_3	13	15	13	11	1
	d_4	15	13	11	13	0
c_3	d_1	12	15	15	11	1
	d_2	15	12	11	15	0
	d_3	11	13	18	14	1
	d_4	13	11	14	18	0

Table 4.2: Illustrative Example: The asymmetric block offers provided by DR units.

(lossless) is depicted in figure 4.3a. The total re-dispatch cost of the system, i.e., the value of objective function (4.6), is \$45.35.

4.4.3 Results obtained from iterative MILP-OPF with losses

The iterative problem (4.9) converges in the fourth iteration for the illustrative example. In table 4.3 the data for each iteration of the loss-cut procedure is given, where it can be noted that the first iteration has zero losses and also the same cost as the lossless MILP presented above.

The congestion mechanism outcomes based on this iterative OPF problem is given in figure 4.3b. Compared to figure 4.3a (the MILP-OPF without losses), we observe three main differences: i) a different asymmetric block offer from the down-stream DR unit c_2 is accepted, ii) due to active power losses[11], the total up- and down-regulations at each time step are not equal anymore, iii) the total re-dispatch cost of the system increases by \$48.34 (an increase of 106%).

4.4.4 Results obtained from MI-SOCP OPF

The SOCP problem is given in equations (4.11) and is fundamentally different to the previous two linear approximations. The SOCP model is a convex relaxation, which models both active and reactive power losses.

Here, we provide results obtained from MI-SOCP OPF with and without enforcing the sufficient conditions for exactness in (4.12). The active power re-dispatch results are given in figures 4.3c and 4.3d for cases with and without the sufficient conditions,

[11] The reactive power losses are not modeled, but will be taken into account in MI-SOCP OPF model.

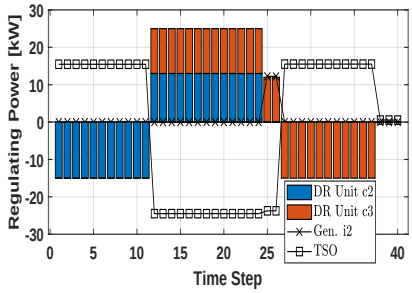

(a) MILP-OPF, lossless (total re-dispatch cost: $45.35)

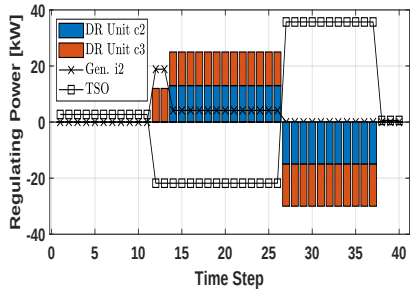

(b) MILP-OPF with losses (total re-dispatch cost: $93.69)

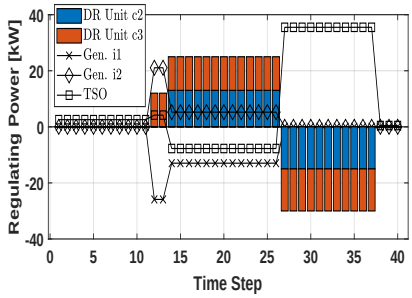

(c) MI-SOCP OPF with sufficient conditions (total re-dispatch cost: $122.59)

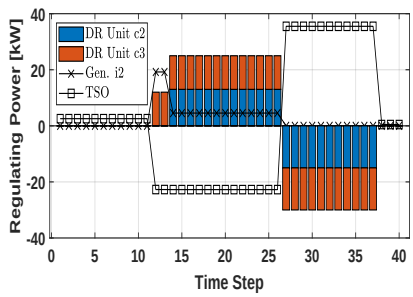

(d) MI-SOCP OPF without sufficient conditions (total re-dispatch cost: $92.24)

Figure 4.3: Illustrative example: Optimal active power regulation obtained from different congestion management mechanisms proposed. From [**Paper A**].

Cut	Cost [$]	$p^{\text{loss,fix}}$	Up Bnd	Low Bnd	Loss	CPU Time [s]
1	45.20	0.46	175.91	0.00	0.000	0.577
2	87.97	0.14	185.64	163.10	0.046	0.686
3	93.37	0.15	188.27	188.24	0.152	0.749
4	93.38	0.15	188.28	188.28	0.152	0.842

Table 4.3: The iteration statistics for the Loss Cut procedure.

respectively. For the same two cases, figure 4.4a depicts the reactive power re-dispatch results. There are three important observations to highlight.

First, the re-dispatch outcomes without sufficient conditions are found to be binding in 4.11b, which means that the convex relaxation is exact, and the solution achieved is AC feasible. The validation results that will be provided in section 4.4.5 also confirm the exactness. However, note that this is case-specific, and in general,

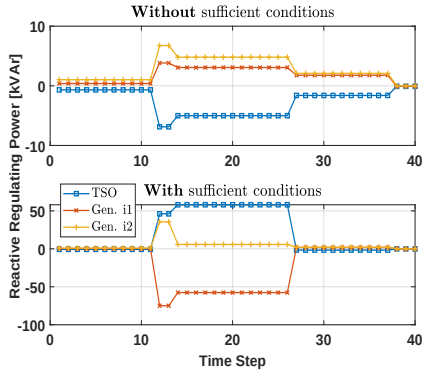

(a) Optimal reactive power regulation obtained from the congestion management mechanism based on MI-SOCP OPF

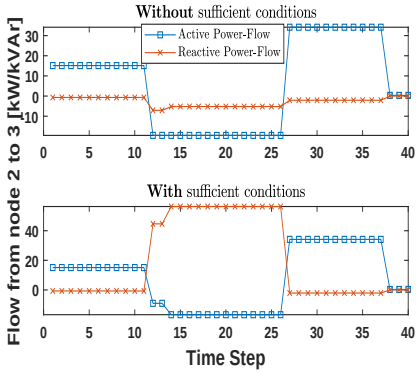

(b) Active and reactive power flow over the line from node n_2 to node n_3

Figure 4.4: Illustrative example: SOCP outcomes with and without sufficient conditions (upper plots: without sufficient conditions; lower plot: with sufficient conditions). From [**Paper A**].

there is no guarantee achieving the exact solution from this relaxed OPF model without enforcing the sufficient conditions.

Second, the active power re-dispatch outcomes and the total re-dispatch cost obtained from MI-SOCP OPF model without sufficient conditions in figure 4.3d are similar to those obtained from the MILP-OPF model with losses in figure 4.3b. However, the voltage profile obtained in the MILP-OPF model with losses is not as accurate as the one in the MI-SOCP OPF model, as it will be demonstrated in section 4.4.5.

Third and last, the system cost when adding the sufficient conditions in this case is \$122.59, which is due to the shrinking of the feasible space by the used sufficient conditions. The main idea of these sufficient conditions is to avoid simultaneous reverse active and reactive power flows, as demonstrated in figure 4.4b for a sample line. In the upper plot of this figure (without sufficient conditions) it can be noticed that there is reverse active and reactive power flow in the time-steps from 12 to 26, which is the period with congestion. In contrast, the lower plot shows the same situation with the sufficient conditions, where there is only reverse active power in the same period. This shrinking of the feasible space requires more expensive generators to be dispatched. Therefore, it is logical to first check the exactness of the results obtained by MI-SOCP OPF model without sufficient conditions, and then to add those conditions if necessary.

4.4.5 Ex-post numerical validation of results from the illustrative case study

We use a forward-backward sweep algorithm to numerically validate the outcomes of the three different OPF methods. This way, we numerically determine the voltage profiles at non-slack nodes (i.e., n_2 to n_6 as PQ nodes), and compare them with those achieved from the OPF models. Figure 4.5 illustrates the voltage profile of node n_6 achieved from each OPF model and forward-backward sweep validation[12]. Based on the validation, as expected, the MI-SOCP OPF model provides the most precise outcomes. The error is 0.0001% for the voltage of the worst node (n_6) when comparing the voltage profile obtained by forward-backward sweep validation method with that obtained from the MI-SOCP OPF model. This error in MILP-OPF models without and with losses is 2.4% and 0.55%, respectively. As another important observation,

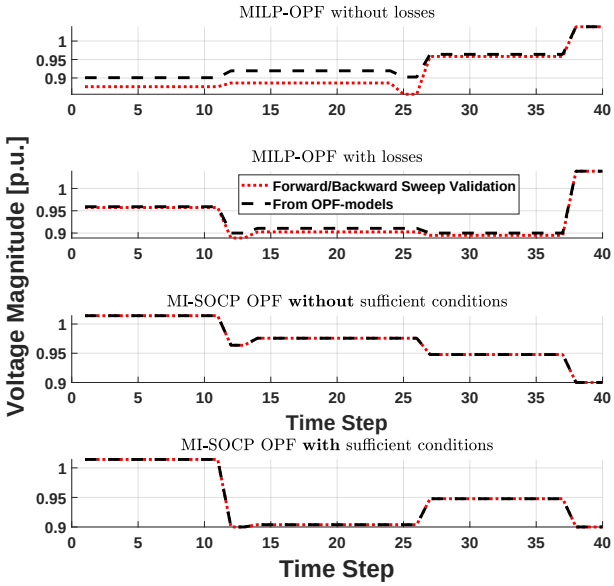

Figure 4.5: Illustrative example: Voltage profile at node n_6 achieved by OPF models and forward-backward sweep validation (first plot: MILP-OPF lossless; second plot: MILP-OPF with losses; third plot: MI-SOCP OPF without sufficient conditions; fourth plot: MI-SOCP OPF with sufficient conditions). From [**Paper A**].

[12]Node n_6 is selected since it is at the end of the feeder and thus is expected to have the most critical voltage profile.

the voltage profiles obtained by the two MILP-OPF models are within the allowable bounds, however when verifying them with forward-backward sweep validation, it becomes apparent that the voltage constraints are violated in some time steps. However, this is not the case for the voltage profiles obtained from MI-SOCP OPF model with and without sufficient conditions, which verifies their solution is AC feasible and exact.

4.4.6 Case study: IEEE 37-node test feeder

In this case study, we use the IEEE 37-node test-feeder [163], with the according diagram given in figure 4.6. All three-phase line impedances and loads are transformed into single phase equivalents, and transformers are removed where necessary. The load data profiles are generated with 30-minute time resolution, yielding a time horizon with 48 time steps. Load curves are given in the online appendix of paper [**Paper A**], which is also available in part II of this thesis. Five conventional generators and four DR units are located at different nodes. The line capacity between nodes 2 and 3 is limited to 1000 kVA, such that it will be congested during the peak load hours.

For computational performance analysis, we consider two cases, namely Cases A and B, with different number of offers per DR unit and thus different number of binary variables in the OPF models. In Case A, each DR unit submits three asymmetric block offers, while it is 8 offers in Case B. In particular, Case A ends up to mixed-integer models with 576 binary variables, while Case B contains 1536 binary variables.

Figure 4.8 presents the voltage profile in Case A for the worst node achieved from the three OPF models and the forward-backward sweep validation. Similar to our results in the illustrative example, MI-SOCP OPF provides more precise outcomes than the other two MILP models. More specific results on the redispatch of generators and DR units are available in the appendix of [**Paper A**] which is attached to this thesis.

We find that the asymmetric block offers dispatched for the DR units are the same for the MILP model with losses and the SOCP model without sufficient conditions. Also the active power losses for these two models are very similar, while the computational time of the iterative MILP model with losses is much lower than for the SOCP model. The total re-dispatch cost, total active and reactive power losses and CPU times[13] among the three OPF models are given in Table 4.4. In particular, note that this table includes the results obtained from the MI-SOCP OPF with and without sufficient conditions. Similar to the illustrative example in the previous section, the MI-SOCP OPF model without sufficient conditions is found to be binding in the second-order cone constraint (4.11b). This implies that the solution of the MI-SOCP OPF model in this specific case study is exact and thus AC feasible. In Case A, compared to the MI-SOCP OPF without sufficient conditions, the MILP-OPF with loss

[13]Hardware used: Huawei XH620 V3 with two Intel Xeon Processors 2650v4 (12 core, 2.20GHz), 256 GB memory, FDR Infiniband, 480 GB-SSD disk

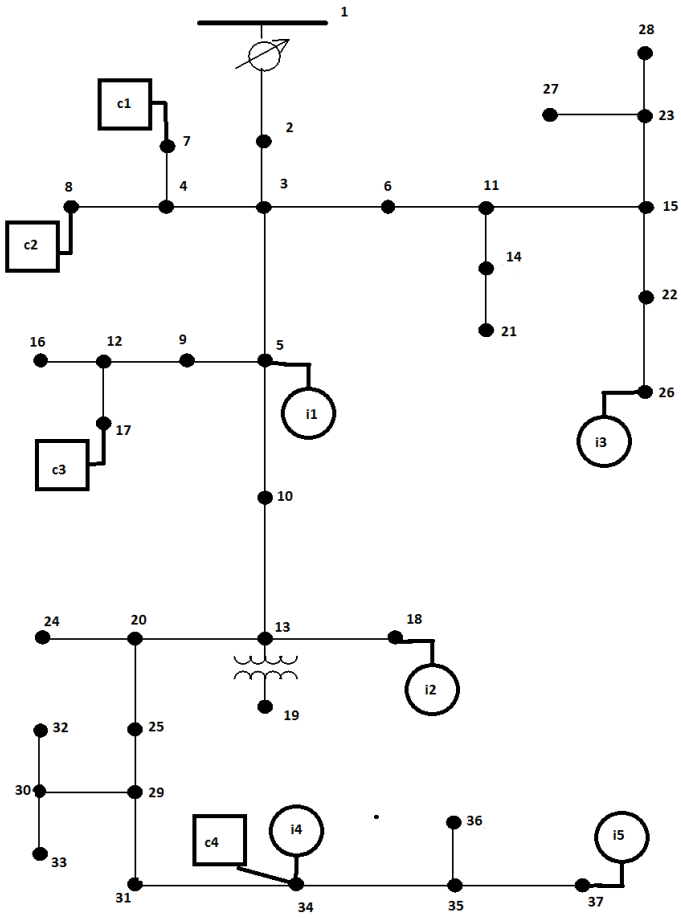

Figure 4.6: The diagram for the IEEE 37-node test feeder with local generators and DR units. Note: The node numbers have been changed compared to the original test case in [163]. From **[Paper A]**.

approximation underestimates the total active power losses and the total re-dispatch cost by 8.7% and 12.3%, respectively. These underestimations in Case B are 8.0% and 13.0%, respectively. When adding sufficient conditions to the MI-SOCP OPF model, the system cost increases significantly. The reason for this cost increase is that the sufficient conditions shrink the feasible space, and consequently, some expensive up-stream generators (closer to the PCC) are re-dispatched. This conic model as the most accurate mechanism among the three models requires more CPU time than the other two MILP mechanisms. The increase in CPU time by increasing the number

Result	Case	No. of binaries	MILP lossless	MILP w. loss	MISOCP w. suff.	MISOCP w/o. suff.
Re-dispatch cost [$]	A	576	1694	2486	5115	2836
Active loss [kWh]			N/A	1454	2819	1593
Reactive loss [kVArh]			N/A	N/A	1913	1379
CPU time [s]			9	72.9	513	288
Re-dispatch cost [$]	B	1536	1594	2371	5007	2725
Active loss [kWh]			N/A	1478	2783	1607
Reactive loss [kVArh]			N/A	N/A	1896	1384
CPU time [s]			34	209	12478	1381

Table 4.4: Case study: Outcomes of the three proposed congestion management mechanisms and their CPU times for Cases A and B.

of binary variables, especially in MI-SOCP OPF model with sufficient conditions, is significant. The CPU time increase is less significant when no sufficient conditions are enforced. In order to get a better insight into the increase in CPU time versus the amount of binary variables in the MI-SOCP OPF model with sufficient conditions, we plot the CPU time as a function of numbers of time steps and asymmetric block offers in figure 4.7.

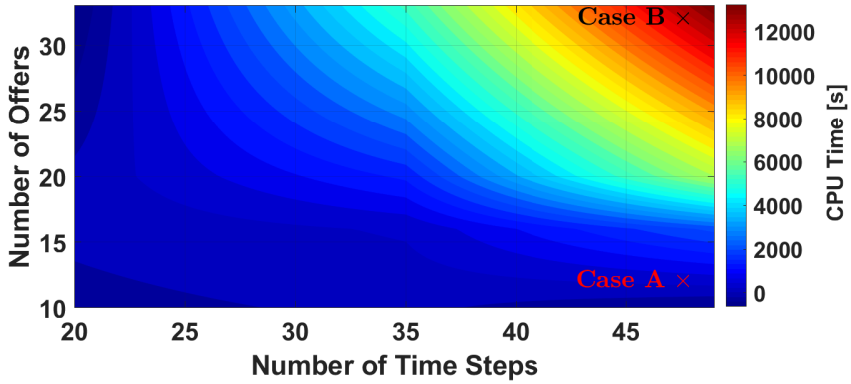

Figure 4.7: Case study: CPU time for the MI-SOCP OPF model with sufficient conditions as function of time steps and total number of block offers. (Note: this is a linear interpolation between at 24, 35 and 48 time steps, and 12, 16, 20 and 32 offers). From [**Paper A**].

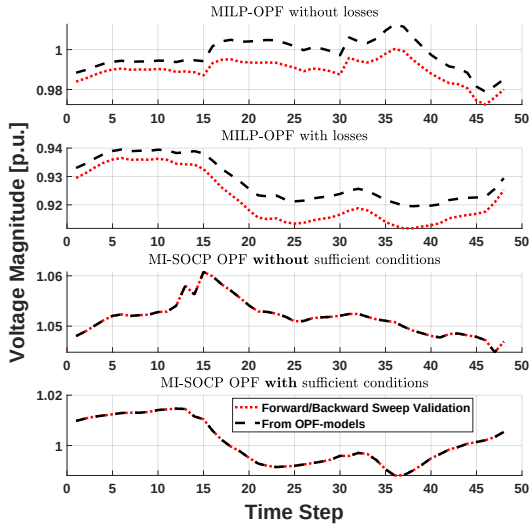

Figure 4.8: Case study (Case A): Voltage profile at node n_{32} achieved by OPF models and forward-backward sweep validation (first plot: MILP-OPF lossless; second plot: MILP-OPF with losses; third plot: MI-SOCP OPF without sufficient conditions; fourth plot: MI-SOCP OPF with sufficient conditions). From [**Paper A**].

CHAPTER 5

TSO-DSO coordination through interface variables

In Chapter 4 a local DSO market for congestion management was proposed. The proposal especially focused on the use of Thermostatically Controlled Load (TCL)-based Distributed Energy Resources (DERs) to participate in a redispatch of the wholesale market outcome. Therefore, the wholesale market outcomes in the previous chapter were input parameters. Now, we propose to analyze the coupling between wholesale and flexibility markets of the TSO and DSO and therefore the Day-Ahead (DA) market outcomes are now variables. The contents of this chapter are based on [**Paper B**] which is attached at the end of this thesis.

The rest of the chapter is structured as follows: Section 5.1 introduces the proposed coordination which is modeled as a hierarchical system due to the hierarchical nature of both the TSO-DSO interactions induced by local markets and the sequential nature of DA market and real-time markets caused by the temporal separation. Section 5.2 provides the required preliminaries, positions the work relative to other works in the literature, and elaborates on the notion behind the proposed coordination method. Section 5.3 explains the structure of the underlying optimization problem. Section 5.4 describes the implementation of Benders' decomposition approach, and provides two benchmark models. In Section 5.5, a case study based on a modified IEEE 24-node network is carried out.

5.1 Introduction to the proposed coordination method

The zonal day-ahead markets in Europe are purely economical dispatch models and do not consider any network constraints or uncertainty of forecasts such as intermittent power generation Renewable Energy Source (RES). The TSO uses ancillary services markets to balance RES production, which is the main concern in systems with high penetration of wind and solar power. In the future small scale units such as DERs

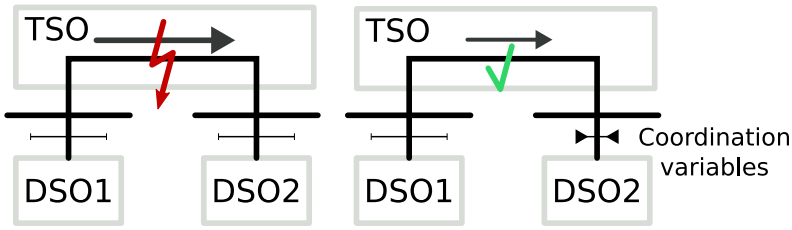

Figure 5.1: Schematic of the proposed method for an example: In the left situation, the day-ahead flow from DSO1 to DSO2 contributes to congestion at the TSO level. In the right situation, restricting the coordination variables for DSO2 prevents congestion at the TSO level, avoiding expensive correction actions. In other potential examples, the congestion may happen in DSO level or both TSO and DSO levels, and then coordination at the interface of DSO1 or at the interface of both DSOs might be needed. From **[Paper B]**.

may participate in the balancing markets. At the same time many proposals are being made such that the DSO can use DERs to mitigate congestion [11], [64], [68].

This leads to the issue of how multiple agents such as TSO and DSOs can share the same resources. The activation of these flexible resources in real-time can be coordinated as proposed by [41], [42], [44], [49], [50] through various different coordination schemes. In Section 2.4.3, we summarize the main notions of the previously proposed coordination schemes. The effect of coordination in the DA stage while also coordinating in real-time has however not been addressed by these works so far. However, TSO-DSO coordination scheme in the day-ahead stage may allow for lower overall cost of system operation. Following this thread, as illustrated in Fig. 5.1, we propose to treat the interface characteristics between TSO and DSOs as *coordination variables* in the day-ahead stage. In this work we identify coordination variables as being prices of interchange in the Point of Common Coupling (PCC)[1] and capacity limits in the interface. The following coordination variables are used:

- $\pi_e^{PCC,DA}$ is the day-ahead price of energy exchange at the PCC of distribution feeder e. The practical interpretation of this exchange variable is subject to the specific design choices of the local forward DSO markets in question. We only assume that the local forward trading markets maximize social welfare and have stochastic information about real-time outcomes. Therefore, practical meaning of $\pi_e^{PCC,DA}$ may be different whether the local market is an energy market or a flexibility capacity only market.

[1] We use interface and PCC interchangeably. It refers to the line (transformer) that connects the DSO domain with the TSO domain.

- $\pi_e^{\uparrow/\downarrow PCC}$ is the expected real-time price of balancing energy at feeder e. These may be interpreted as the prices the DSO has to pay if activating flexibility outside its own domain.

- $\overline{f}_e/\underline{f}_e$ is the upper/lower bound for the allowed apparent power exchange in the PCC in the DA stage. Note, that in real-time the physical capacity has to be respected, while in the DA stage the optimal value is a purely economic construct. They may be interpreted as the maximal amount of hedging the DSO is allowed to trade in forward markets with resources outside of its domain. Again, the physical interpretation of these variables are specific to the practical implementation of local forward markets that are considered, and here are abstract constructs to consider for the DSO.

It is important to note that the creation of local markets will work to separate pricing zones and depending on the arbitrage trading opportunities, there may be a disconnect in the value of energy. The above described coordination variables are exactly the interface prices used for arbitrage trading between the pricing zones and the allowed cross border trading. We introduce a new agent, the "PCC optimizer" who is tasked with the maximization of total system social welfare, i.e. both the TSO network and all DSOs connected to it. The PCC optimizer is finding the optimal value of the above variables, which eventually are treated as exogenous parameters by the corresponding DSO. It is assumed here that the DSO before the clearing of the day-ahead market is clearing a flexibility market of its own. This could be in the form of capacity reservations within DERs connected to its domain, which can be later activated in order to mitigate any congestion that may arise. The specifics of the DSO market are however not influencing the work at hand as we assume efficient markets and ignore any specific design choices that might influence the outcome. Of course, the presented models can be adjusted to accommodate different market designs. In fact, the presented models are meant to be used as proxy models for the implementation of practical coordination in the day-ahead stage, and therefore we also assume that the PCC optimizer can have perfect information. Ultimately we also assume perfect coordination in real-time.

The research contributions of the work in this chapter are the following:

1. We show through hierarchical coordination that a framework built around current European market clearing methods for coordination of local markets with global markets (i.e. wholesale) can improve system social welfare. The hierarchy is cast as a Stackelberg game with the PCC optimizer as leader who is responsible for setting the coordination variables. The PCC optimizer anticipates the optimal response of the DSO and subsequent DA and Real-Time (RT) markets. The coordination is achieved through the day-ahead scheduling of flexibility. In contrast to other works such as [41], [44], [49], [50] which address real-time activation of reserves, we therefore show the benefits of coordination in the day-ahead forward trading markets.

2. We show that the functioning of the proposed PCC optimizer can be implemented as a bi-level optimization problem. Under an assumption of information symmetry between PCC optimizer and DSOs, we are even able to simplify the proposed bi-level structure. We decompose the proposed bi-level problem using a Benders' decomposition algorithm to ease computational burden. The side benefit of this decomposition is that it avoids solving a mixed-integer second-order cone program, and separates it to a mixed-integer linear problem and a set of Second-Order Cone Program (SOCP) (one per scenarion ω).

5.2 Notion behind the proposed coordination method

We assume that local markets are a necessity in the future, as the engagement of end-users and the deployment of DERs rise. The specifics of local markets are out of the scope of this work, as we consider idealized local markets that are designed to be efficient. Also, the ongoing research into these local markets is very diversified and little consensus is currently available due to the missing policy in the area. To mention a few specific recent proposals, there are centralized DSO operated markets such as [48], [64], [65], [68], [119] where the DSO is the market operator. More recently works focused on decentralized local markets are based on peer-to-peer structures or community based mechanisms such as [11], [133] have been published (for a review see [8], [91]). An integral part of this work is that the DERs should be able to participate in local and global markets[2]. If all DERs participating in a local Distribution System Operator (DSO) market also bid in global markets, the DSO market effectively reduces to a *pre-qualification* of bids of the local DERs to global markets[3]. Therefore in the current proposal the DSO is able to reserve capacity in DERs or equivalently to constrain bids of DERs to global markets.

The interface characteristics of local and global markets naturally have an impact on the equilibrium points of the total system, and therefore we opt to use them for TSO-DSO coordination. As discussed earlier these coordination variables are the prices and capacity limits available for trading. The main question is how to design those coordination variables to maximize the system social welfare.

The PCC optimizer is modeled as a Stackelberg game which respects the paradigm of a two-stage market clearing including local DSO markets, i.e. first the DSO clears a market with local resources and then the DA market and a series of RT re-dispatches[4] are made to meet network constraints. The PCC optimizer is the leader, while the DSO-market, DA and RT markets are the Stackelberg followers. The modeling of the PCC optimizer as a bi-level optimization problem has been inspired by recent works such as [96] where the optimal interface limits for trading between zonal day-ahead markets are found through bi-level modeling. Another inspiring work is [130], where the optimal allocation of reserves is analyzed through a bi-level approach.

[2] By global, we refer to day-ahead pool and TSO-level flexibility markets.
[3] Alternatively, this can be seen as reserving flexibility in the DERs by the DSO
[4] This includes any mechanism that changes the day-ahead dispatches.

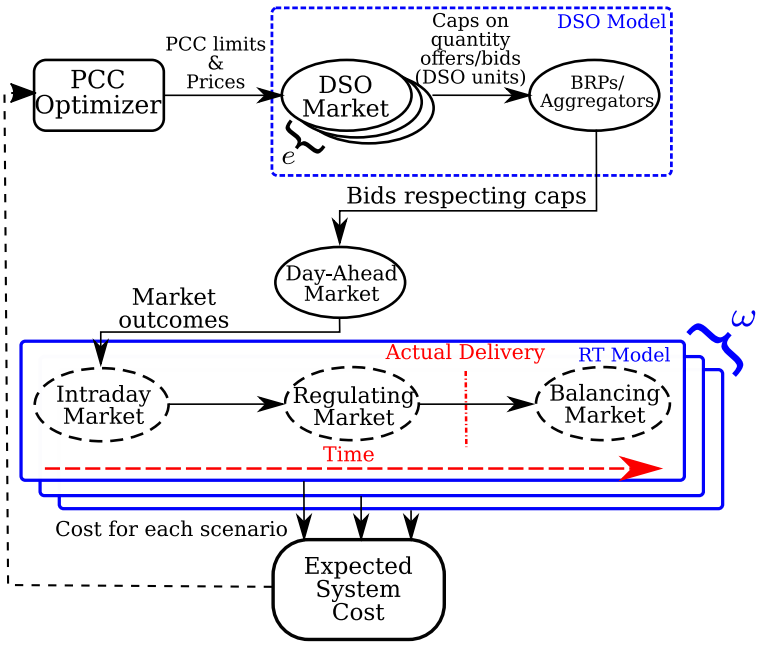

Figure 5.2: Process structure of the proposed coordination scheme involving optimization of coordination variables through the proposed PCC optimizer. The RT model is in reality encompassed by several steps, which are unified into one simplified model. For a relevant survey of RT markets, see [8]. Symbol e is an index for all DSOs connected to the underlying TSO. Symbol ω is an index for all uncertainty scenarios in the DA stage, which realize in the RT stage. From [**Paper B**].

The interactions of agents and markets are schematically illustrated in Fig. 5.2, and explained below by four steps:

1. Before DA market clearing, the PCC optimizer determines the coordination variables at each interface. Its objective is to maximize total system social welfare, including all DSO networks and the TSO network.

2. Given the coordination variables set by the PCC optimizer in step 1 and before DA market-clearing, each DSO (indexed by e) puts a cap on the production/-consumption quantity that each DER located at its domain can offer/bid in the DA market. We refer to this stage as DSO's pre-qualification. Note that DERs can participate in DA market through aggregators/Balance Responsible Partys (BRPs).

3. Given the quantity offers/bids of DER aggregators from step 2, the DA market is cleared.

4. Before RT there may be a series of re-dispatches, which we model as premiums applied to the day-ahead prices. The PCC optimizer and the DSO model the RT stage with uncertainty with the same representative scenarios.

The PCC optimizer in step 1 is the leader which anticipates the moves of the followers. The presented method is minimally invasive if implemented within the current European market architecture and allows for one shot coordination, i.e. non-iterative and unidirectional.

We assume that renewable production is the only source of uncertainty. The production of each RES r is capped by an uncertain parameter $W_{r\omega}^{RT}$ that is dependent on scenario ω (i.e., RES generation can be freely spilled as required). The rest of modeling assumptions are listed in appendix B.1.

5.3 PCC optimizer: Proposed bi-level model

The Stackelberg game can be expressed as a bi-level optimization program as in (5.1) for which a graphical representation is given in figure 5.3a.

$$\max_{\Xi_e^{\text{PCCO}}} \quad \mathcal{SW}^{\text{DA}} - \sum_{\omega} \phi_\omega \Delta\text{Cost}_\omega^{\text{RT}} \tag{5.1a}$$

$$\text{s.t.} \quad \widetilde{p}_g^{\text{DA}}, \widetilde{p}_d^{\text{DA}} \in \mathbf{arg}\left(\text{(B.1)}_e \mid \Xi_e^{\text{PCCO}} \right), \qquad \forall e, \tag{5.1b}$$

$$\mathcal{SW}^{\text{DA}}, \widehat{p}_g^{\text{DA}}, \widehat{p}_d^{\text{DA}} \in \mathbf{arg}\left(\text{(5.3)} \mid \widetilde{p}_g^{\text{DA}}, \widetilde{p}_d^{\text{DA}} \right), \tag{5.1c}$$

$$\Delta\text{Cost}_\omega^{\text{RT}} \in \mathbf{arg}\left(\text{(5.4)}_\omega \mid \widehat{p}_g^{\text{DA}}, \widehat{p}_d^{\text{DA}} \right), \qquad \forall \omega \in \Omega, \tag{5.1d}$$

where $\Xi^{\text{PCCO}} = \{\overline{f}_e, \underline{f}_e, \pi_e^{\text{PCC,DA}}, \pi_e^{\uparrow\text{PCC}}, \pi_e^{\downarrow\text{PCC}}\}$ are the coordination variables of the PCC optimizer. The nomenclature for this chapter is given in the front matter of this thesis.

The upper level objective function in (5.1a) is the leader objective that maximizes the social welfare $\mathcal{SW}^{DA}$ of the day-ahead market minus the expected cost of the real-time re-dispatch which is $\sum_\omega \phi_\omega \Delta\text{Cost}_\omega^{\text{RT}}$. Note that ϕ_ω represents the probability of scenario $\omega \in \Omega$ which is the set of representative scenarios. Here we assume that the scenarios are externally defined and shared by the PCC optimizer and the DSO. The lower level problems in (5.1b), (5.1c) and (5.1d) are respectively the optimization problems of the DSO, the DA and the RT markets. Particularly, the lower-level problem in (5.1b) which is given in (B.1) in appendix B.2 is a stochastic market to be cleared by the DSO, which takes into account uncertainty in real-time. The outcome of the local DSO markets (one for every DSO indexed by e) are the caps $\widetilde{p}_g^{\text{DA}}, \widetilde{p}_d^{\text{DA}}$ which are applied to every DER participating in the DA market.

The problem in (5.1) can be challenging due to especially the lower level problem of the DSO market in (5.1b). This is because the DSO market is modelled as a

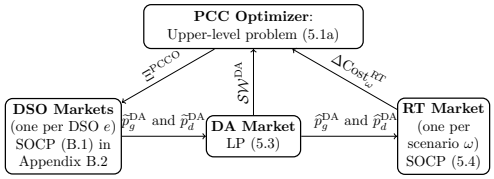

(a) Structure of the original bi-level problem (5.1). Note that LP and SOCP stand for linear problem and second-order cone problem, respectively.

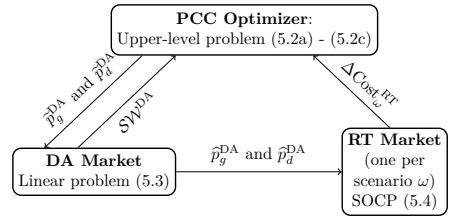

(b) Structure of the reduced bi-level problem (5.2). This problem is equivalent to the original bi-level problem (5.1) illustrated in Fig. 5.3a assuming information symmetry between the PCC optimizer and the DSOs.

Figure 5.3: Structure of two equivalent bi-level problems. From [**Paper B**].

stochastic market with nodal representation of the AC power flow in real time (the convex SOCP relaxation from Chapter 3 is used). Therefore solving the DSO market in this bi-level problem requires solving KKTs of an SOCP. The following proposition allows us to reduce the computational burden.

Proposition 1: Redundancy in the Karush Kuhn Tucker (KKT) conditions of the lower level problem of the DSOs in (5.1b) with respect to the KKTs lower level problem (5.1c) and (5.1d) allow to remove the DSO level market and maintain an equivalent model.

Proof of proposition 1: The KKT conditions can be used to analyze the redundancy. For all three lower level problems the KKTs are presented in appendix B. All the lower level problems are explicitly convex and have non-empty interior. Therefore Slater's condition is fulfilled and strong duality holds and the KKT conditions constitute optimality. Due to redundancy in these first order optimality conditions, the whole DSO market problem can be removed. For a full proof see the appendix B.5 □

Due to proposition 1, the bi-level problem (5.1) with three lower-level problems reduces to an *equivalent* bi-level problem with two lower-level problems as illustrated in Fig. 5.3b. The equivalent model is given by (5.2):

$$\max_{\widetilde{p}_g^{\text{DA}},\widetilde{p}_d^{\text{DA}}} \quad \mathcal{SW}^{\text{DA}} - \sum_{\omega} \phi_\omega \Delta\text{Cost}_{\omega}^{\text{RT}} \tag{5.2a}$$

$$\text{s.t.} \quad 0 \le \widetilde{p}_g^{\text{DA}} \le \overline{P}_g, \qquad \forall e, g \in \mathcal{G}_e^{\text{D}}, \tag{5.2b}$$

$$0 \le \widetilde{p}_d^{\text{DA}} \le \overline{P}_d, \qquad \forall e, d \in \mathcal{D}_e^{\text{D}}, \tag{5.2c}$$

$$\mathcal{SW}^{\text{DA}}, \widehat{p}_g^{\text{DA}}, \widehat{p}_d^{\text{DA}} \in \mathbf{arg}\left(\text{(5.3)} \mid \widetilde{p}_g^{\text{DA}}, \widetilde{p}_d^{\text{DA}} \right), \tag{5.2d}$$

$$\Delta\text{Cost}_{\omega}^{\text{RT}} \in \mathbf{arg}\left(\text{(5.4)}_{\omega} \mid \widehat{p}_g^{\text{DA}}, \widehat{p}_d^{\text{DA}} \right), \qquad \forall \omega \in \Omega. \tag{5.2e}$$

Now, the PCC optimizer directly imposes the caps on quantity bids/offers of local DERs through upper-level constraints (5.2b) and (5.2c). An important observation

with regards to proposition 1 is that the set of representative scenarios must be shared by the PCC optimizer and the DSO, as both are stochastic problems. This assumption is named information symmetry, and can cause complex gaming behaviours if not fulfilled (see for example [164] for a theoretical discussion of this class of problems).

5.3.1 DA market-clearing formulation

The DA market problem is solved as a pool, without modeling the network constraints. We only consider a single pricing zone here, although there may be several pricing zones separated by Available Transfer Capacity (ATC)s as explained in Chapter 2 [96]. The DA market problem is given in (5.3) where the variables from the PCC optimizer $\widetilde{p}_g^{\mathrm{DA}}$ and $\widetilde{p}_d^{\mathrm{DA}}$ are treated as parameters.

$$\max_{\widehat{p}_g^{\mathrm{DA}},\widehat{p}_d^{\mathrm{DA}},s^{\mathrm{DA}},w_r^{\mathrm{DA}}} \mathcal{SW}^{\mathrm{DA}} = \sum_{d\in\mathcal{D}} \pi_d^{\mathrm{DA}}\widehat{p}_d^{\mathrm{DA}} - \sum_{g\in\mathcal{G}} \pi_g^{\mathrm{DA}}\widehat{p}_g^{\mathrm{DA}} - VOLL\ s^{DA} - \pi^R \sum_r w_r^{DA} \tag{5.3a}$$

$$\text{s.t.} \quad \sum_{g\in\mathcal{G}} \widehat{p}_g^{DA} - \sum_{d\in\mathcal{D}} \widehat{p}_d^{DA} + \sum_r w_r^{DA} + s^{DA} = 0, \tag{5.3b}$$

$$\underline{P}_g \le \widehat{p}_g^{DA} \le \widetilde{p}_g^{DA}, \qquad \forall e, g \in \mathcal{G}_e^{\mathrm{D}}, \tag{5.3c}$$

$$\underline{P}_g \le \widehat{p}_g^{DA} \le \overline{P}_g, \qquad \forall g \in \mathcal{G}^{\mathrm{T}}, \tag{5.3d}$$

$$\underline{P}_d \le \widehat{p}_d^{DA} \le \widetilde{p}_d^{DA}, \qquad \forall e, d \in \mathcal{D}_e^{\mathrm{D}}, \tag{5.3e}$$

$$\underline{P}_d \le \widehat{p}_d^{DA} \le \overline{P}_d, \qquad \forall d \in \mathcal{D}^{\mathrm{T}}, \tag{5.3f}$$

$$0 \le w_r^{DA} \le W_r^{DA}, \qquad \forall r \in \mathcal{R}, \tag{5.3g}$$

$$0 \le s^{DA} \le \sum_d \widehat{p}_d^{DA}. \tag{5.3h}$$

The system power balance is ensured by (5.3b) while the dispatched power quantities for demands d, generators g and RES r are enforced by (5.3c) through (5.3h). The load not served s^{DA} is limited by the total load in (5.3h). Note that the caps are only applied to DSO connected units in (5.3c) and (5.3e).

5.3.2 RT re-dispatch formulation

We model the uncertainty in real-time as a redispatch problem in (5.4), which considers a full nodal power flow. For the DSO level lines, a SOCP power flow is used, which models active and reactive line flows as well as losses. It is a convex relaxation as discussed in Chapter 3 and thus constitutes a lower bound. For the transmission network a linear power flow is here deemed sufficient like suggested in [46]. This is an approximation and also called the DC power flow. The problem is solved once for

every scenario ω. The premiums that are applied over the DA market offers are $\pi^{\uparrow/\downarrow}$ in the objective function.

$$
\begin{aligned}
&\min_{\Xi_\omega^{\mathrm{RT}}} \ \Delta\mathrm{Cost}_\omega^{\mathrm{RT}} \\
&\quad = \sum_{g\in\mathcal{G}} \left(\pi_g^{\mathrm{D}A}\left(p_{g\omega}^{\mathrm{RT}} - \widehat{p}_g^{\mathrm{D}A}\right) + \pi_g^{\uparrow} p_{g\omega}^{\uparrow} + \pi_g^{\downarrow} p_{g\omega}^{\downarrow}\right) \\
&\quad + \sum_{d\in\mathcal{D}} \left(\pi_d^{\mathrm{D}A}\left(\widehat{p}_d^{\mathrm{D}A} - p_{d\omega}^{\mathrm{RT}}\right) + \pi_d^{\uparrow} p_{d\omega}^{\uparrow} + \pi_d^{\downarrow} p_{d\omega}^{\downarrow}\right) \\
&\quad + \sum_{r} \left(\pi^{R}\left(w_{r\omega}^{\mathrm{RT}} - w_r^{\mathrm{D}A}\right) + \pi^{\uparrow R} w_{r\omega}^{\uparrow} + \pi^{\downarrow R} w_{r\omega}^{\downarrow}\right) \\
&\quad + VOLL \sum_{n\in\mathcal{N}} s_{n\omega}^{\mathrm{RT}} && && (5.4a)\\
\text{s.t.}\quad & p_{l\omega}^{\mathrm{RT}} = B_l\left(\theta_{n\omega} - \theta_{m\omega}\right), && \forall l \in L^{\mathrm{T}}, && (5.4b)\\
& p_{l\omega}^{\mathrm{RT}} \le S_l, && \forall l \in L^{\mathrm{T}}, && (5.4c)\\
& p_{g\omega}^{\mathrm{RT}} = \widehat{p}_g^{\mathrm{D}A} + p_{g\omega}^{\uparrow} - p_{g\omega}^{\downarrow}, && \forall g \in \mathcal{G}, && (5.4d)\\
& w_{r\omega}^{\mathrm{RT}} = w_r^{\mathrm{D}A} + w_{r\omega}^{\uparrow} - w_{r\omega}^{\downarrow}, && \forall r \in \mathcal{R}, && (5.4e)\\
& p_{d\omega}^{\mathrm{RT}} = \widehat{p}_d^{\mathrm{D}A} - p_{d\omega}^{\uparrow} + p_{d\omega}^{\downarrow}, && \forall d \in \mathcal{D}, && (5.4f)\\
& \sum_{g\in\mathcal{G}_n} p_{g\omega}^{\mathrm{RT}} - \sum_{d\in\mathcal{D}_n} p_{d\omega}^{\mathrm{RT}} + \sum_{r\in\mathcal{R}_n} w_{r\omega}^{\mathrm{RT}} + s_{n\omega}^{\mathrm{RT}} \\
& \qquad = \sum_{l\in n\rightarrow} p_{l\omega}^{\mathrm{RT}} - \sum_{l\in\rightarrow n} p_{l\omega}^{\mathrm{RT}}, && \forall n \in \mathcal{N}, && (5.4g)\\
& \sum_{g\in\mathcal{G}_n} q_{g\omega}^{\mathrm{RT}} - \sum_{d\in\mathcal{D}_n} q_{d\omega}^{\mathrm{RT}} + s_{n\omega}^{\mathrm{q},RT} \\
& \qquad = \sum_{l\in n\rightarrow} q_{l\omega}^{\mathrm{RT}} - \sum_{l\in\rightarrow n} q_{l\omega}^{\mathrm{RT}}, && \forall e, n \in \mathcal{N}_e^{\mathrm{D}}, && (5.4h)\\
& {p_{l\omega}^{\mathrm{RT}}}^2 + {q_{l\omega}^{\mathrm{RT}}}^2 \le \varphi_{l\omega}^{\mathrm{RT}}\ v_{n\omega}^{\mathrm{RT}}, && \forall e, l \in (\mathcal{L}_e^{\mathrm{D}} \cup l_e), && (5.4i)\\
& {p_{l\omega}^{\mathrm{RT}}}^2 + {q_{l\omega}^{\mathrm{RT}}}^2 \le S_l^2, && \forall e, l \in (\mathcal{L}_e^{\mathrm{D}} \cup l_e), && (5.4j)\\
& p_{l\omega}^{\mathrm{RT}} + p_{l'\omega}^{\mathrm{RT}} = R_l\ \varphi_{l\omega}^{\mathrm{RT}}, && \forall e, l \in (\mathcal{L}_e^{\mathrm{D}} \cup l_e), && (5.4k)\\
& q_{l\omega}^{\mathrm{RT}} + q_{l'\omega}^{\mathrm{RT}} = X_l\ \varphi_{l\omega}^{\mathrm{RT}}, && \forall e, l \in (\mathcal{L}_e^{\mathrm{D}} \cup l_e), && (5.4l)\\
& v_{m\omega}^{\mathrm{RT}} = v_{n\omega}^{\mathrm{RT}} - 2(R_l\ p_{l\omega}^{\mathrm{RT}} + X_l\ q_{l\omega}^{\mathrm{RT}}) \\
& \quad + (R_l^2 + X_l^2)\varphi_{l\omega}^{\mathrm{RT}}, && \forall e, l \in (\mathcal{L}_e^{\mathrm{D}} \cup l_e), && (5.4m)\\
& \underline{V}_n^2 \le v_{n\omega}^{\mathrm{RT}} \le \overline{V}_n^2, && \forall e, n \in (\mathcal{N}_e^{\mathrm{D}} \cup n_e^{\mathrm{HV}}), && (5.4n)\\
& 0 \le w_{r\omega}^{\mathrm{RT}} \le W_{r\omega}^{\mathrm{RT}}, && \forall r \in \mathcal{R}, && (5.4o)\\
& \underline{P}_g \le p_{g\omega}^{\mathrm{RT}} \le \overline{P}_g, && \forall g \in \mathcal{G}, && (5.4p)
\end{aligned}
$$

$$\underline{P}_d \leq p^{\mathrm{RT}}_{d\omega} \leq \overline{P}_d, \qquad \forall d \in \mathcal{D}, \tag{5.4q}$$
$$\underline{Q}_g \leq q^{\mathrm{RT}}_{g\omega} \leq \overline{Q}_g, \qquad \forall g \in \mathcal{G}^{\mathrm{D}}_e, \tag{5.4r}$$
$$\underline{Q}_d \leq q^{\mathrm{RT}}_{d\omega} \leq \overline{Q}_d, \qquad \forall d \in \mathcal{D}^{\mathrm{D}}_e, \tag{5.4s}$$
$$0 \leq s^{\mathrm{RT}}_{n\omega} \leq \sum_{d \in \mathcal{D}_n} p^{\mathrm{RT}}_{d\omega}, \qquad \forall n \in \mathcal{N}, \tag{5.4t}$$
$$\left[p^{\uparrow}_{g\omega}, p^{\downarrow}_{g\omega}\right] \geq 0, \qquad \forall g, \tag{5.4u}$$
$$\left[p^{\uparrow}_{d\omega}, p^{\downarrow}_{d\omega}\right] \geq 0, \qquad \forall d, \tag{5.4v}$$
$$\left[w^{\uparrow}_{r\omega}, w^{\downarrow}_{r\omega}\right] \geq 0, \qquad \forall r, \tag{5.4w}$$

where $\Xi^{\mathrm{RT}}_{\omega} = \{p^{\mathrm{RT}}_{g\omega}, p^{\mathrm{RT}}_{d\omega}, w^{\mathrm{RT}}_{r\omega}, p^{\uparrow}_{g\omega}, p^{\downarrow}_{g\omega}, p^{\uparrow}_{d\omega}, p^{\downarrow}_{d\omega}, w^{\uparrow}_{r\omega}, w^{\downarrow}_{r\omega}, s^{\mathrm{RT}}_{n\omega}, s^{\mathrm{q},RT}_{n\omega}, q^{\mathrm{RT}}_{g\omega}, q^{\mathrm{RT}}_{d\omega}, p^{\mathrm{RT}}_{l\omega}, q^{\mathrm{RT}}_{l\omega}, \theta_{n\omega}, \varphi^{\mathrm{RT}}_{l\omega}, v^{\mathrm{RT}}_{n\omega}\}$ is the variable set of (5.4).

Constraint (5.4b) is the DC power flow approximation in the transmission network, while (5.4c) is transmission line power transfer capacity. Constraints (5.4d)-(5.4f) link the day-ahead dispatch and the re-dispatch to the actual power output/consumption of each conventional generator and RES, and final consumption of each demand. The nodal active power balance in both TSO and DSO levels is enforced by (5.4g), while the nodal reactive power balance in the DSO level is imposed by (5.4h). Important to note here is that we do not model reactive power in the transmission system due to the DC power flow approximation.

The SOCP constraint (5.4i) enforces the relation between current and voltage magnitude and apparent power flow and is a convex relaxation of an equality constraint. The SOCP constraint in (5.4j) is enforcing the thermal line rating of the distribution level lines. The SOCP Branch Flow Model (BFM) model used here was discussed in detail in Chapter 3, where its relation to the original non-convex AC model is described.

Active and reactive power losses in distribution network are modeled in (5.4k) and (5.4l), respectively. The nodal voltage magnitudes are related to the apparent power flows by constraint (5.4m). The constraints (5.4n) through (5.4t) are lower and upper bounds for the control variables, while (5.4u) - (5.4w) declare non-negativity conditions for some variables.

The problem of the real-time re-dispatch in (5.4) solves a centralized nodal power flow in both distribution and transmission networks. It is therefore not a practical model because no centralized authority has access to all this information and TSO and DSOs are not likely to share this information. Instead works like [45], [46] have proposed decentralized versions that can be solved without sharing specific network related information in real-time. The implementation of such a model is however outside the scope of the work in this chapter. We justify the use of such a centralized model through the purpose of this work, which is to examine day-ahead coordination while assuming perfect information and perfect real-time coordination.

5.4 Solution strategy and benchmarks

This section explains the solution strategy of the bi-level problem in (5.2). From a modeling perspective the simplest way of solving such a bi-level structure is to replace the lower level problems by the KKTs; this process is however computationally heavy due to the complementarity constraints in the resulting Mathematical Program with Equilibrium Constraints (MPEC). Therefore, the bi-level structure is decomposed per scenario for the lower level problem defined by (5.4).

5.4.1 Benders' decomposition

Here we present the Benders' decomposition approach used to solve the stochastic bi-level problem in 5.2. The implementation of especially (5.2e) is problematic since this is an SOCP that can be hard to solve as KKTs. The decomposition technique is presented in appendix A. The master problem at iteration (i) is (5.5).

$$\max_{\Xi^{\mathrm{MP}^{(i)}}} \quad \mathcal{SW}^{\mathrm{DA}^{(i)}} - \sum_{\omega} \phi_\omega \psi_\omega^{(i)} \tag{5.5a}$$

$$\text{s.t.} \quad (5.2\text{b}) - (5.2\text{c}) \tag{5.5b}$$

$$\mathcal{SW}^{\mathrm{DA}^{(i)}} \in (5.3) \tag{5.5c}$$

$$\psi_\omega^{(i)} \geq \psi^{\min}, \qquad \forall \omega \in \Omega, \tag{5.5d}$$

$$\begin{aligned} \psi_\omega^{(i)} \geq\ & \Delta\mathrm{Cost}_\omega^{\mathrm{RT}^{(m)}} \\ & + \sum_{g \in G} \alpha_{g\omega}^{(m)} \left(\widehat{p}_g^{\mathrm{DA}^{(i)}} - \widehat{p}_g^{\mathrm{DA}^{(m)}} \right) \\ & + \sum_{d \in D} \alpha_{d\omega}^{(m)} \left(\widehat{p}_d^{\mathrm{DA}^{(i)}} - \widehat{p}_g^{\mathrm{DA}^{(m)}} \right) \\ & + \sum_{r \in R} \alpha_{r\omega}^{(m)} \left(w_r^{\mathrm{DA}^{(i)}} - w_r^{\mathrm{DA}^{(m)}} \right), \qquad \forall m \in \{1, \ldots, i-1\}, \omega, \end{aligned} \tag{5.5e}$$

where the variables are $\Xi^{\mathrm{MP}^{(i)}} = \{\widehat{p}_g^{\mathrm{DA}^{(i)}}, \widehat{p}_d^{\mathrm{DA}^{(i)}}, s^{\mathrm{DA}^{(i)}}, w_r^{\mathrm{DA}^{(i)}}, \widehat{p}_g^{\mathrm{DA}^{(i)}}, \widehat{p}_d^{\mathrm{DA}^{(i)}}, \psi_\omega^{(i)}\}$. Due to (5.5c) the master problem (5.5) is also a bi-level problem. The master problem is a proxy problem of the original problem (5.2) that also maximizes the expected social welfare, with the distinction that the real time cost $\Delta\mathrm{Cost}_\omega^{\mathrm{RT}}$ has been replaced by the auxiliary linear benders cut variable $\psi_\omega^{(\mathrm{i})}$. The cuts are given in (5.5e) and are found from the outcomes of the sub-problem that is presented next. The bi-level structure of (5.5c) is replaced by the KKTs of (5.3), which are given in appendix B.3. The complementarity conditions can be resolved using a mixed-integer approach using the Big-M method [165].

After solving the master problem, the DA dispatches are used in the sub-problem which is given in (5.6). Because we incorporate load-shedding as slack variables in

the real-time re-dispatch, the sub-problems are always feasible and we do not need any feasibility cuts in the master problem. There is one sub-problem per scenario.

$$\min_{\Xi_\omega^{\mathrm{RT}^{(i)}}} \quad \Delta\mathrm{Cost}_\omega^{\mathrm{RT}^{(i)}} \tag{5.6a}$$

$$\text{s.t.} \quad \Delta\mathrm{Cost}_\omega^{\mathrm{RT}^{(i)}} \in (5.4)_\omega \tag{5.6b}$$

$$\widehat{p}_g^{\mathrm{DA}^{(i)}} = \widehat{p}_g^{\mathrm{DA,fixed}^{(i)}}, \qquad : \alpha_{g\omega}^{(i)}, \quad \forall g \in G, \tag{5.6c}$$

$$\widehat{p}_d^{\mathrm{DA}^{(i)}} = \widehat{p}_d^{\mathrm{DA,fixed}^{(i)}}, \qquad : \alpha_{d\omega}^{(i)}, \quad \forall d \in D, \tag{5.6d}$$

$$w_r^{\mathrm{DA}^{(i)}} = w_r^{\mathrm{DA,fixed}^{(i)}}, \qquad : \alpha_{r\omega}^{(i)}, \quad \forall r \in R. \tag{5.6e}$$

Note that the equations in (5.6c) through (5.6e) are used to fix the DA dispatches from the master problem and find the according sensitivities α_ω. The sub-problem is also a bi-level problem due to (5.6b). As discussed in appendix A, the subproblem can be made into a single level by observing that the objective function of the lower level problem in (5.6b) is the same as (5.6a). Therefore the subproblem bi-level structure can be omitted and substituted by (5.7c).

$$\min_{\Xi_\omega^{\mathrm{RT}^{(i)}}} \quad \Delta\mathrm{Cost}_\omega^{\mathrm{RT}^{(i)}} \tag{5.7a}$$

$$\text{s.t.} \quad (5.4\mathrm{b})_\omega - (5.4\mathrm{w})_\omega, \tag{5.7b}$$

$$(5.6\mathrm{c}) - (5.6\mathrm{e}). \tag{5.7c}$$

The iterative Benders' decomposition algorithm finds the optimal solution of the bi-level problem (2) with a level of accuracy ϵ if a lower bound $\mathrm{LB}^{(i)} = \mathcal{SW}^{\mathrm{DA}^{(i)}} - \sum_\omega \phi_\omega \psi_\omega^{(i)}$ and an upper bound $\mathrm{UB}^{(i)} = \mathcal{SW}^{\mathrm{DA}^{(i)}} - \sum_\omega \phi_\omega \Delta\mathrm{Cost}_\omega^{\mathrm{RT}^{(i)}}$ converge to within a predefined discrepancy $\epsilon \geq \mathrm{UB}^{(i)} - \mathrm{LB}^{(i)}$ at iteration *(i)*.

5.4.2 Two benchmark models

We use two benchmark models to asses the relative performance of the proposed PCC optimizer scheme. These two models are respectively the uncoordinated sequential case of clearing the day-ahead and real-time markets, and the perfectly coordinated case found through co-optimization.

The perfect coordination given by co-optimization is used as an upper bound on the social welfare as no method can outperform such a scheme. The deterministic clearing of the DA market serves as a lower bound. In (5.8) the model used for the perfect coordination is presented. This is essentially a stochastic dispatch model with

full information of all uncertainties in the DA stage.

$$\max_{\widehat{p}_g^{\mathrm{DA}},\widehat{p}_d^{\mathrm{DA}},s^{\mathrm{DA}},w_r^{\mathrm{DA}},\Xi^{\mathrm{RT}}} \quad \mathcal{SW}^{DA} - \sum_{\omega} \phi_\omega \Delta \mathrm{Cost}_\omega^{\mathrm{RT}} \tag{5.8a}$$

$$\text{s.t.} \quad (5.3\mathrm{b}) - (5.3\mathrm{h}), \tag{5.8b}$$

$$(5.4\mathrm{b})_\omega - (5.4\mathrm{w})_\omega. \tag{5.8c}$$

This perfect (full) coordination is however quite impractical as it requires TSO and DSOs to solve a common single problem, and all information is packed into one optimization problem, which quickly becomes intractable for larger systems.

To obtain the lower bound which is given by the uncoordinated case, we consider a model with no coordination, and solve DA and RT models sequentially. This means that first the DA market (5.3) is cleared without imposing any caps on the quantity bids/offers of DSO-level DERs. Then, the real-time re-dispatch problem (5.4) is solved independently with the DA market outcomes for each scenario separately (i.e. in a deterministic manner). The sum of the achieved surplus from the DA market and the expected cost of real-time re-dispatch is the result of the uncoordinated case.

5.5 Case study

All the models discussed in the previous section are implemented in Matlab with CVX and solved with Mosek 8.0.[5]

The convergence of the Benders decomposition is set to be achieved if the upper and lower bound of the benders decomposition are within a relative gap of 0.1%.

We use a modified IEEE 24-node reliability test system [166] to model the transmission network. This test system is augmented with the addition of five radial distribution feeders that replace loads at nodes 6, 13, 15, 18 and 19. In total, 39.3% of the total system load is now placed in radial distribution feeders, while the remainder is connected to the transmission network. The according network diagram is given in Fig. B.1 in appendix B. We add 7 wind farms to the system, where 3 of them are in the "south" of the network, 4 more in the "north". One of the "northern" wind farms is connected to a DSO feeder (DSO 3). These wind farms are the sole sources of uncertainty in the day-ahead stage, and they are correlated by their physical distances to each other. The calculation of the co-variance matrix is given in appendix B.6. We assume a Gaussian distribution of the uncertainty of the forecast power production. The forecasts and the variances are given in table B.1, while the physical coordinates of the wind farms are given in table B.2 in the appendix. Due to the physical distances all the northern and southern wind farms are weakly correlated, while the they are strongly correlated within the northern and southern area respectively.

[5]Hardware used: Huawei XH620 V3, 2x Intel Xeon Processor 2650v4 (12 core, 2.20GHz), 256 GB memory, 480 GB-SSD disk.

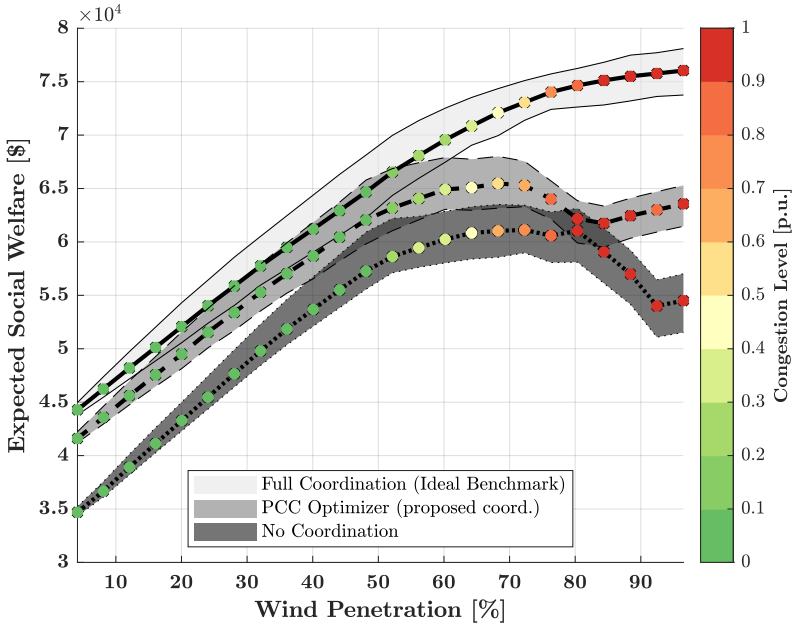

Figure 5.4: The expected social welfare as a function of wind power penetration obtained from the proposed coordination model (PCC optimizer) and the two benchmark models. The 0.2 quantile and 0.8 quantile are also depicted. The colored dots indicate the level of congestion in the transmission network as the probability of at least two lines being congested in RT. The results are from out-of-sample testing with 200 scenarios that are distinct from the 12 in-sample scenarios.

CPU times [s]				
Average subproblem	Average master	Initial master problem	Master in last iteration	Average #Iterations
0.31	0.54	0.67	0.91	29.5

Table 5.1: Computational burden of the Benders multi-cut solution strategy. Note: We average for all solved instances of increasing wind penetration.

The scenarios are found through random sampling of the Gaussian mixture model that is a result of the predefined forecast co-variances and means. We sample 12 in-sample scenarios that are used to find the set-points through the proposed models, while we validate the outcome with 200 new out-of-sample scenarios.

The PCC optimizer problem with the benders decomposition is solved on average within 14 minutes with the 12 in-sample scenarios, when averaging over 24 increasing name-plate capacities of the wind farms. The name-plate capacity of the wind-farms are scaled linearly in order to get insight on the effects of increasing average wind power penetration. The 12 in-sample scenarios are solved in parallel on a multi-core CPU. The average CPU times for master- and sub-problems and the average number of iterations are given in table 5.1.

5.5.1 Coordination under increasing wind power penetration

Due to increasing reliance on RES in the power system, we here examine the relation of the social welfare and increasing the wind penetration under the proposed PCC optimizer and the 2 benchmark models. To achieve this, the nameplate capacity of the 7 wind farms described above is increased step-wise. The wind power penetration is the total wind power forecast in DA divided by the total load bids, i.e., $\sum_r W_r^{DA} / \sum_d \overline{P}_d$.

The results of this study are summarized in figure 5.4, where both mean and inter-quantile range[6] of the 3 models are given. These results are from the out-of-sample validation using 200 samples that are different from the in-sample scenarios. The heat-map that is shown by the dots along the mean of the three curves in figure 5.4 indicate the "congestion level", which we here define as the probability of at least two lines being congested in the TSO network in real-time. This plot highlights the efficiency of the proposed PCC optimizer versus the two benchmark models, and shows the relation of the social welfare to the congestion while increasing wind power penetration.

With increasing wind power penetration it can be seen that there is a strong connection of social welfare and grid congestion. The slope of social welfare increase changes at around 50% for all three models, which is the point where some congestion is to be expected in real-time. The PCC optimizer is in between the perfect coordination and the un-coordinated benchmark. The perfectly coordinated benchmark performs better than the PCC optimizer as it can optimally exploit flexibility of the TSO connected resources as well as DSO connected resources, while the PCC optimizer only improves the coordinated use of DSO connected resources. In the deterministic market dispatch model (the lower benchmark), the social welfare begins to decrease after 70% wind penetration, which is due to the models inability to handle forecast errors. The balancing measures therefore become increasingly costly, as this model will mainly dispatch wind power in the day-ahead stage as it is very cheap, but real-time balancing costs cannot be anticipated. On the other hand, the stochastic dispatch model is able to perfectly handle the anticipated uncertainty, and will not see decreasing social welfare with increasing wind power penetration. The PCC optimizer is able to handle the uncertainty better than the deterministic dispatch model.

[6] 0.2 and 0.8 quantiles are used

5.5.2 Physical capacity of the interface and coordination outcomes

In this section the relation of the actual real-time power flow in the interface (PCC) of the DSOs and the dispatched power in the day-ahead stage is examined. To this end, the power-flow in the PCC of a sample DSO (DSO 3) incurred by the day-ahead dispatch is plotted in figure 5.5a for the three different dispatch models and for increasing wind penetration. The blue shaded bars indicate day-ahead dispatches for the three different models, while the black bars in the center show the expected real-time outcomes after the re-dispatch measures of balancing markets. The uncertainty of the real-time flow is given as inter-quantile ranges with red whisker-plots and the physical limit of the PCC is given by the green line. This plot brings to attention that the PCC optimizer power flow in the day-ahead stage does not necessarily respect the physical capability of the interface. This is possible, as we define the upper-level variable pertaining to the tradable day-ahead quantities of the PCC optimizer $\overline{f}_e/\underline{f}_e$ to be purely economic parameters, which do not get limited by the physical capacity of the interface. This is an important result for practical design policies for TSO-DSO coordination in the day-ahead stage, when defining trading quantities between markets. This should be interpreted as the following: In order to achieve optimal coordination between local markets and global day-ahead markets, the physical capacity of the PCC does not need to be strictly enforced, as the arbitrage trading options to hedge against future uncertainty would be limited and thus reduce total system social welfare.

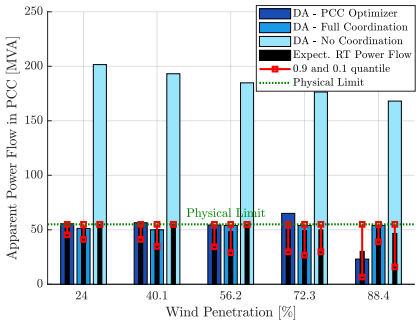

(a) The power flow in the PCC of DSO 3 (connected to n_{19}) incurred by the DA dispatches and the resulting RT power flows. These results are obtained from the proposed coordination method (PCC optimizer) and the two benchmark models.

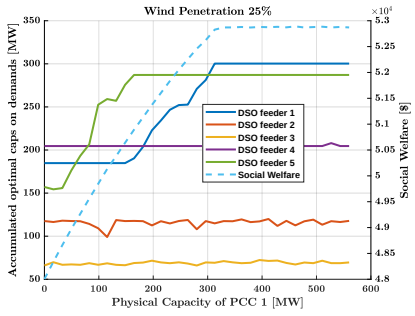

(b) The optimal caps of PCC optimizer on the quantity bid of aggregate flexible loads in different feeders as a function of the physical capacity of PCC of DSO 1 (note: the wind penetration is fixed to 25%).

Figure 5.5: Results pertaining to the capacity of the PCC. It shows the importance of having accurate information about the physical capacity.

Another interesting measure to better understand the coupling of day-ahead coordination and is the sensitivity of the caps versus the physical capacity of the interface. In figure 5.5b we demonstrate the optimal caps on the loads in all the distribution feeders when varying the physical capacity of the interface between DSO 3 and the TSO. This shows the highly non-linear connection of the applied caps and the physical properties of the network. Also, the influence of one DSO's network parameters on the optimal settings of other DSOs is interesting. The interface capacity of DSO 3 not only affects the optimal caps for DSO 3, but also for DSO 1. Moreover, the installation of higher interface capacity does not affect the social welfare after around 300 MW capacity, for this example. In relation to practical coordination schemes, the sensitivity of the underlying network data used to find coordination variables should be analyzed, as this may have a strong effect on the achieved social welfare.

CHAPTER 6

Conclusions and future perspectives

In this thesis, numerous aspects of market-based coordination of Transmission System Operator (TSO)- and Distribution System Operator (DSO)-level networks are addressed, such that the connected resources are used to optimality. Furthermore, it is examined how the flexibility may be shared among system operators through day-ahead scheduling mechanisms. It is expected that the share of Distributed Energy Resource (DER) capacity in power consumption is increasing, and tapping into the resources of these units is promising to deliver large amounts of hidden flexibility. As Information and Communications Technology (ICT) functionality in the power system increases, the controllability of ever smaller units can accelerate the proliferation of DERs. However, the mathematical models that enable their effective use are often complicated and good understanding of DER inter-operability with markets is pertinent to an effective usage of flexibility. The coupling of different market platforms is a promising method of increasing the reach of DER flexibility, however scalability is a major obstacle to system wide coordination. Therefore, the methods applied in this thesis were developed with the computational aspect in mind. Similarly to the computational scalability, the policy shaping of future DER integration will influence the design of market-based methods and the viability of different coordination schemes. An ongoing theme throughout the thesis has therefore been in aligning the proposals with existing policy and foreseeable policy changes. The policy changes are expected to be step-wise incremental so that tasks of system operators, may be expanded gradually to approximate ideal coordination. This approach is aimed to make the system operators overcome difficulties of adapting to new operational paradigms and increase the smart use of flexible resources.

6.1 Discussion and conclusions of scientific contributions

The main scientific contributions of this thesis are within the area of DER flexibility usage, and improve the state of the art of the existing literature in a number

of ways. We applied mathematical modeling methods to reveal the interactions of DERs and system operators through market-based approaches and thus improve the usage of flexibility. The two main research questions have led to novel methods for DSOs to include Thermostatically Controlled Load (TCL)-based demand response in a market-based re-dispatch to mitigate congestion, and the day-ahead coordination of hierarchical market structures imposed by local DSO markets. In the introduction we specified two specific research questions, and we will here conclude the developed methods in regard to these questions.

I. How can complicated demand response behaviour be included by the DSO for congestion management in a precise and effective economic dispatch mechanism?

In [**Paper A**] we model the power flow through three different power flow models, while all of them account for both active and reactive power flow and voltages, only two of them account for losses. This is done in order to optimize the dispatch of asymmetric block offers that accurately model the underlying physical properties of TCL-based demand response. It is expected that large parts of the available DER flexibility is going to be TCL-based, such as heating and refrigeration and thus the backbone of DSO-level flexibility. The asymmetric blocks are currently the most transparent and market compatible way of representing the rebound effect caused by the TCL-based demand response. This rebound effect is due to a payback in a time period after the demand response units change their power consumption behaviour. This payback effect or rebound is needed in order to return to the baseline setting of the underlying load, such as returning to a temperature setting in a heat storage or the like. The main drawback of the asymmetric block offers is that they introduce new binary variables and thus can be difficult to handle within complex power flow models. The resulting combinatorial models are analyzed with respect to computational burden and precision of the outcomes.

The first two of three power flow models we analyzed are mixed-integer linear models, where one of the models approximates active power losses in a sequential linear programming approach while the other model is a lossless approximation. The last model is a mixed-integer Second-Order Cone Program (SOCP) model which is the most precise choice of the three models, that is able to capture losses for both active and reactive power. This model is a convex relaxation by optimizing over the convex hull of the non-convex solution space of the original quadratic optimization problem. The computational burden of the models are increasing quickly with the complexity, and as expected it is found that the mixed-integer SOCP model has the largest computational burden connected to it. The influence of active power losses has a big effect on the outcomes of the dispatched block offers and therefore both the SOCP and sequential Mixed-integer Linear Program (MILP) model with loss approximation achieve similar dispatches of the asymmetric block offers within our various case studies. The voltage approximation in the MILP model with losses

is however less precise and may lead to voltage violations in highly stressed feeders. Further, the MILP model does not incorporate the losses caused by reactive power and thus underestimates the re-dispatch costs slightly. The mixed-integer SOCP model, being a relaxation rather than an approximation, can deliver insightful information on the redispatch outcomes and can be checked for AC feasibility very quickly and easily. The relaxation gap will in many circumstances be zero and therefore precise and AC feasible, as was the case in the applied case studies. Additionally we examine the effect of some sufficient conditions for exactness on the SOCP model and deduce that they both shrink the feasible space and increase computational burden thus limiting their practical usability. The sufficient conditions we use are prohibiting the simultaneous reverse active and reactive power flow and are thus not appropriate if the distribution network is exporting energy to the transmission network or can expect reverse power flows in some of the lines. In general, the sufficient conditions may increase the costs of re-dispatching if reverse power flow is allowed, however they can be useful if the direction of the power flows is only allowed in the forward direction. Presently, many distribution feeders are only able to handle forward power flows due to limitations on safety equipment and voltage regulators, that are not designed to be compatible with reverse power flows.

The proposed re-dispatch mechanism solves the issue of using TCL-based demand response with high rebound effect in a DSO congestion management mechanism. The findings have implications to the used modeling accuracy required by a market-based solution for congestion management. Especially in distribution networks where voltage levels are often an issue for the DSO, the precision of the modeling method is paramount and the more precise dispatch methods via convex relaxation may be needed in order to ensure a feasible dispatch. As a general comment, the modeling of losses should be required in any circumstance to ensure the correct dispatch of asymmetric block offers and an analysis of the bounds of the voltage approximation in the case of linear approximations should be made.

II. How can we coordinate the scheduling of DERs in day-ahead between TSO and DSOs in a practical framework to counter uncertainty of intermittent RES generation?

The modeling approach in [**Paper B**] follows the hierarchical nature of proposed DSO-level markets, where the DSO is able to clear a day-ahead market for flexibility in advance of the wholesale day-ahead market which is cleared on a global level. This hierarchical relationship is modelled as a Stackelberg game, where the DSO markets are interfaced with the remaining markets through interface variables that are controlled by the PCC optimizer. The PCC optimizer is a new virtual agent with the objective to maximize the total social welfare, and we assume in the models that it has access to perfect information about the TSO- and DSO-level networks as well as the market floors and the upcoming bids/offers to them. We study this idealized

situation to show the benefits of this type of coordination and infer recommendations for future day-ahead coordination schemes.

Our findings have implications for designing practical schemes to use this avenue of TSO-DSO coordination, in two ways: The first key finding is that the optimal PCC capacity in the day-ahead stage is related to, but not limited by the physical capacity of the underlying hardware. This means that the capacity limitation in the forward trading market may be viewed as a purely economic construct, that limits the amount of arbitrage trading that the units connected to the DSO-level markets are allowed to trade in the day-ahead stage with outside resources. If this limitation is set too tight, the social welfare may be reduced due to decreased possibilities of local markets to hedge against future uncertainty. Naturally, the physical limit of the PCC has to be taken into account in real-time. Thus, any practical scheme to coordinate local DSO-level markets with global markets should take as guideline the physical PCC capacity but must not be limited by it.

Our second finding is that the optimal caps for one feeder can depend in a non-obvious way on the physical capacity of another feeder or the physical capacity of the transmission network. This is important to highlight as the results of practical coordination schemes should have either access to high quality network data or at least implement a sensitivity analysis of the coordination outcomes with respect to the network data to reveal which areas of the network have high influence on the social welfare.

A third general finding of the PCC optimizer method is that there exists a mathematical equivalence of global and local stochastic markets. Therefore the inclusion of local stochastic markets in a deterministic global trading setup can approach the stochastic ideal dispatch that is used as a benchmark here and in many other works. This is only true if the markets are well coordinated as per the PCC optimizer, and the access to information is sufficient and symmetrical between different agents.

We use optimal real-time coordination to frame the differences in day-ahead dispatch coordination between local and global markets. However, in a practical setup, the real-time coordination may be even harder than practical day-ahead coordination due to the short time horizon between dispatching and activation. Therefore our findings in Chapter 5 are congruent to future real-time coordination methods, because the day-ahead coordinated dispatch may make it easier to achieve feasibility in real-time and reduces the amount of re-dispatch actions that are necessary in real-time. As a general point, the inclusion of day-ahead coordination is complementary to real-time coordination.

The TSO-level network parameters in the case study in Section 5.5 have a large impact on the achieved improvements that are made by coordination in day-ahead. We notice that the congestion in the transmission network in our case study is the factor that works to distinguish the features of different day-ahead coordination schemes. If the transmission system is naturally partitioned in pricing zones which are well sized with respect to the expected network loading, the outcomes of the coordination will show smaller improvements than we document in the current case study. However, highly stressed transmission networks that have large unevenly distributed wind gen-

eration and pricing zones that are not fit well to the expected network loading will more likely benefit from coordination with local markets. This is due to the fact, that the local DSO markets are able to use stochastic information to hedge against future uncertainty.

Any real-time coordination method that increases the system social welfare may overestimate improvements if compared under uncoordinated day-ahead dispatches. Therefore, the presented results also have implications to the future design of real-time coordination schemes. Further, coordination in day-ahead will generally heighten social welfare as premiums are applied closer to real-time; improving coordination in the day-ahead stage will reduce the needed amount of real-time re-dispatching, thus working to reduce prices to end-users.

6.2 Future work and research paths to improve the contributions

In this thesis, through the conducted research, a series of research questions that may be addressed in the future have appeared. As the presented work has involved both electricity markets and system operation with respect to underlying technologies, the questions are ranging over a variety of topics. These are topics related to diverse subjects such as the modeling of systems and technologies, policy on market design and bidding structures, agent representation through game theoretic concepts and mathematical/computational implementations and tractability.

We present the flexibility of TCL-based demand response units through asymmetric block offers that can be traded in a day-ahead market for congestion management. This representation is easy to understand and can by a simple extension of current bidding formats unlock extra flexibility to the DSO or other system operators and agents when trading in forward markets. However, the simplified representation of demand response through these block offers may be somewhat restrictive when the real-time activation of single demand response units has to be analyzed. The flexibility aggregators may be overly conservative in designing these block offers, in order to avoid penalties on balancing markets if the demand response units are not performing according to the block offers. The accurate real-time modeling of TCL-based demand response is most accurately done through partial differential equations or other non-convex modeling approaches as the underlying system is more complex than the asymmetric block offers can capture. However, incorporating this into real-time control leads to both tractability, optimality and pricing issues due to these non-convex models. The more accurate modeling of demand response units could become highly important in real-time when no constraints are allowed to be violated. Especially, if small scale power systems are to be operated in island mode or in micro-grids that rely heavily on demand response this real-time precision could become important. Any practical implementation would have to trade of the optimality and pricing issues with precision and tractability.

In the used models for the distribution networks and the demand response units, we only consider the electricity networks. However, the co-modeling of several energy carrier networks such as the gas and the heating network as well as the electricity network has become an important topic in the literature. Many types of DERs may be at intersections of energy networks, and thus be able to participate not only in electricity markets but also in the trading of heat and/or gas. Congestion management mechanisms with DERs that are at the intersection of energy networks would unlock additional flexibility, if the market clearing was aware of the heat and/or gas markets and adequate coordination schemes should be identified. Naturally, co-optimization is always a challenge just as the case of co-optimizing TSO- and DSO-level networks. Therefore any practical market coordination should happen through the exchange of adequate signals to enable soft coordination. The existing proposals for local energy communities or peer-to-peer energy trading systems in the literature could benefit by being able to trade across different energy carriers while intertwining these markets with flexibility needs of system operators.

The proposed coordination scheme for day-ahead coordination of TSO- and DSO-level networks via interface coordination variables is analyzed with perfect real-time coordination. Naturally, any practical real-time coordination method will perform worse than our model. Therefore, in the future it may be adequate to analyse the interplay between real-time and day-ahead coordination of distribution and transmission networks. The globally optimal coordination of TSO- and DSO-level networks is an unrealistic position, due to separation of responsibilities and knowledge between DSO and TSO. This highlights the need for some afterthought when implementing policies on coordination: Which time stage or which combination of day-ahead and real-time coordination is appropriate? To answer this question, a theoretical analysis of real-time coordination schemes in conjunction with day-ahead coordination should be done. This approach needs to take into account the possibility of gaming between agents and should be modeled via non-cooperative game theory. Also, the expectation of perfectly rational decisions in local markets may be inadequate to model the behaviour of local agents. Thus, the study of bounded rationality of local agents may be needed to increase the effectiveness of real-time coordination and its connection to day-ahead coordination.

In the work presented in Chapter 5 one of the main contributions was the PCC optimizer as an oversight authority that can define the interface prices and tradable quantity that will maximize system wide social welfare. The implemented approach is based on stochastic optimization through scenario representation, a technique that can require large computing power if large numbers of representative scenarios are needed. Therefore, depending on the size of the problem and the uncertainty that is being modelled, this technique can become intractable even when considering advanced scenario reduction techniques. Recently, the trend in power system literature is to model uncertainty through chance-constrained programming. The use of chance-constraints can generalize stochastic programs and has been shown to achieve good results for modeling of uncertainties. A prominent feature of chance-constrained programming is that it can model the underlying uncertainty without using any sce-

narios and may therefore result in a more tractable model. The prerequisite for chance-constraints to be tractable is that an analytical representation of the chance-constraint can be derived; this has been shown to be possible if the uncertainty of the random parameter follows a unimodal distribution and the distribution is known. Usually, the tractable formulations require to model every chance-constraint by itself leading to single chance-constraints (i.e. the violation probability of a constraint can only be verified for single constraints and not jointly). In order to model joint violation probabilities there exist a series of approximations that have been presented in the literature, such as the Bonferroni approximation. Another challenge with chance-constrained programming that has been cited often is that the distribution of the underlying uncertainty is known, and therefore as opposed to scenario based programming the system cannot easily be modelled through data from observations. This topic has been addressed through the use of distributionally robust chance-constraints, where the chance constraints are modelled over a group of probability distributions that are approximating the used data for uncertainty. Here, a popular metric for approximating the probability distributions is the Wasserstein metric (or earth-movers metric) that can be used to fit a series of probability distributions to uncertainty data. As a final remark on this topic, it has been proposed for other types of market coordination schemes that chance-constrained programming approaches to find coordination variables may be more tractable than scenario based optimization, and therefore this would be an interesting avenue of research for TSO-DSO coordination in the future.

The future of local markets are highly uncertain, but the focus toward more decentralization is sparking debate over the nature of these markets. The published works on TSO-DSO coordination make various assumptions on the nature of local DSO-level markets and congestion management mechanisms, and these choices have an impact on the efficacy and design of TSO-DSO coordination schemes. Our approach to modeling day-ahead coordination has been to assume generic DSO-level markets for flexibility procurement with the aim to maximize social welfare. However, recently a series of works have suggested implementation of local energy markets, for example through local energy communities or peer-to-peer markets. The nature of these markets and their ability to maximize social welfare will have an effect on the practical TSO-DSO coordination schemes. Therefore, an in depth analysis of the impact of different local market designs and the ability to coordinate these with global markets would be of future interest to the research community.

Closely related to the notion of local markets and their design, is the availability of information on uncertain parameters. Different agents within local trading areas may have access to different information on sources of uncertainty. This may enable them to make better forecasts, while it is not always in their interest to keep this information private. There have been a series of publications on cooperative game theory, where it is shown that it may be in the interest of some agents to share specific information with other agents. The notion of imperfect information would also alter our proposal for modeling the PCC optimizer, as there may be the option to model information asymmetry between the PCC optimizer and local agents, such as

the DSO. In the future, it may even be conceived that there are markets for trading information on uncertainties, and therefore the pricing of and modeling of *information skewness* should be theoretically analysed. In the end, a proper understanding of the value of information and sharing of such could enable better coordination between trading floors and agents leading to more secure and economic operation of the power system.

As a final remark, the use of ever more data mining and digitization in the energy system, leads to vast amounts of available data. This may be used in the future to achieve better understanding of interactions of small scale systems within the power system and enable local markets to be more efficient. However, classical optimization theory and uncertainty modeling and prediction may be on the edge of computational tractability when trying to incorporate these vast amounts of data. Therefore the use of machine learning and efficient data base generation techniques to make informed, fast and reliable decisions is a promising future research path. These data driven methods may be the gate openers to create efficient operational models to achieve improved coordination between different trading floors and enhance the integration of high shares of renewable energy.

APPENDIX A

Decomposition of bi-level stochastic optimization problems

As mentioned in Chapter 2, the studied problems for coordination in this thesis are of hierarchical nature, and thus can be modelled by Stackelberg games. In this appendix we provide a solution technique for a bi-level problem if the lower level problem is subject to uncertain parameters. This solution technique is based on a stochastic Benders decomposition method. Bi-level optimization consists of nested optimization problems, where the outermost problem (upper level) is describing the leaders actions while taking into consideration reactions of followers in the nested optimization problems (lower levels). The leaders and followers variables are separate, and the follower is subject to the decisions of the leaders variables.

Here we assume a Stackelberg leader with the objective function $f(\Xi^{\text{up}})$ and a Stackelberg follower with the optimization problem in (A.1).

$$\min_{\Xi^{\text{lo}}} \quad g(\Xi^{\text{up}}, \Xi^{\text{lo}}) \tag{A.1a}$$

$$\text{s.t.} \quad l_i(\Xi^{\text{lo}}, \Xi^{\text{up}}) \leq b_i + \xi_i, \forall i = \{1, \ldots, k\} \tag{A.1b}$$

Here, the variable collection in Ξ^{up} is representing the upper level variables of the Stackelberg leader, while Ξ^{lo} represents the lower level variables of the follower. For the follower the leader variables Ξ^{up} are input parameters. The optimization problem is subject to k constraints and parameter b_i is subject to a random disturbance ξ_i, making the follower problem a non-deterministic problem. In general, non-deterministic optimization problems are intractable and have to be rewritten into a deterministic counterpart to be tractable. Here we use a scenario based stochastic optimization procedure.

Therefore, the follower problem is written as a stochastic optimization problem with representative scenarios for the uncertain variables. These stochastic Stackelberg games are most commonly cast as stochastic bi-level optimization problems in the

form of (A.2).

$$\min_{\Xi^{\text{up}}} \quad f(\Xi^{\text{up}} \in X) + \mathbb{E}_\omega \left[g_\omega(\Xi^{\text{up}}, \Xi^{\text{lo}}_\omega) \right] \tag{A.2a}$$

$$\text{s.t.} \quad h(\Xi^{\text{up}}) \leq a \tag{A.2b}$$

$$\left(\Xi^{\text{lo}}_\omega\right) \in \arg\Big\{$$

$$\min_{\Xi^{\text{lo}}} \quad g_\omega(\Xi^{\text{up}}, \Xi^{\text{lo}}_\omega) \tag{A.2c}$$

$$\text{s.t.} \quad l_i(\Xi^{\text{up}}, \Xi^{\text{lo}}_\omega) \leq b_{i\omega}, \forall i \Big\} \quad \forall \omega \tag{A.2d}$$

Here the notation $\mathbb{E}_\omega[\cdot]$ is used to represent the mathematical expectation over the representative scenarios $\omega \in \Omega$ of an uncertainty set and,

$$b_{i\omega} \sim b_i + \xi_i$$

is the set of representative scenarios to the random disturbance ξ_i. The straight forward way to solve this type of bi-level problem is to replace the lower level optimization problem by its Karush Kuhn Tucker (KKT) conditions that yield an equivalent single level problem with complementarity constraints, also called Mathematical Program with Equilibrium Constraints (MPEC). An MPEC is a mathematical optimization problem with an embedded optimization problem represented by the KKT conditions. The KKT conditions are optimality conditions if the problem is strictly convex and strong duality holds [143].

Benders decomposition

A stochastic bi-level problem as the generic example in A.2 can be decomposed by scenario by applying Benders decomposition, and thereby decomposing the problem into one master-problem and several sub-problems (one per scenario). The Benders decomposition approach for stochastic two-stage problems was first introduced in [167] for a problem with fixed recourse, and later used for problems with continuous recourse in [168]. This approach is amenable to bi-level problems as in (A.2) and is presented in e.g. [169].

When fixing the upper level variables that appear in the lower level problems, the sub-problem for scenario ω at iteration (i) becomes

$$\min_{\Xi^{\text{lo}}_\omega} \quad g^{(\text{i})}_\omega(\Xi^{\text{up}}, \Xi^{\text{lo}}_\omega) \tag{A.3a}$$

$$\text{s.t.} \quad \Xi^{\text{up}}_\omega = \Xi^{\text{up},(\text{i})}_\omega \quad : (\alpha^{(\text{i})}_\omega) \tag{A.3b}$$

$$g_\omega(\Xi^{\text{up}}, \Xi^{\text{lo}}_\omega) \in \text{(A.1)}, \tag{A.3c}$$

where $\Xi^{\text{up},(\text{i})}$ are the fixed upper level variables from the master problem. Here the sub-problem in (A.3) is still a bi-level problem due to (A.3c). The constraint

(A.3b) is the fixed upper level variables from the leader and the according sensitivity $\alpha_\omega^{(\mathrm{i})}$. In the special case, where the objective function of (A.3) and (A.1) are the same, the bi-level structure can simply be omitted. This yields the sub-problem in (A.4).

$$\min_{\Xi_\omega^{\mathrm{lo}}} \quad g_\omega^{(\mathrm{i})}(\Xi^{\mathrm{up}}, \Xi_\omega^{\mathrm{lo}}) \tag{A.4a}$$

$$\text{s.t.} \quad \Xi_\omega^{\mathrm{lo}} = \Xi_\omega^{\mathrm{lo},(\mathrm{i})} \quad : (\alpha_\omega^{(\mathrm{i})}) \tag{A.4b}$$

$$l(\Xi^{\mathrm{up}}, \Xi_\omega^{\mathrm{lo}}) \leq b_\omega \tag{A.4c}$$

With the sub-problem as in (A.4), the master problem can be solved with Benders cuts derived from the sensitivities of the sub-problem. The master problem for iteration (i) is given in (A.5).

$$\min_{\Xi^{\mathrm{up},(\mathrm{i})}} \quad f(\Xi^{\mathrm{up}})^{(\mathrm{i})} + \sum_\omega \phi_\omega \psi_\omega^{(\mathrm{i})} \tag{A.5a}$$

$$\text{s.t.} \quad h(\Xi^{\mathrm{up}}) \leq a \tag{A.5b}$$

$$\psi_\omega^{(\mathrm{i})} \geq \psi^{\min}, \quad \forall \omega \in \Omega \tag{A.5c}$$

$$\psi_\omega^{(\mathrm{i})} \geq g_\omega^{(\mathrm{m})}(\Xi^{\mathrm{up}}, \Xi_\omega^{\mathrm{lo}}) + \alpha_\omega^{(\mathrm{m})}(\Xi^{\mathrm{up},(\mathrm{i})} - \Xi^{\mathrm{up},(\mathrm{m})}), \quad \forall m \in \{1, \ldots, i-1\}, \omega \tag{A.5d}$$

Here the constraint in (A.5d) are the Benders optimality cuts. A multicut version is here shown, where several cuts are added per iteration, which is an approach that has been used much with multistage stochastic programs. The objective function now minimizes the expected value of the auxiliary Benders cut variable $\psi_\omega^{(\mathrm{i})}$. This is done by multiplying it with the according probability ϕ_ω, which yields the expected value. In general with Benders decomposition like this, there may arise problems with feasibility in some iterations when the sub-problems become infeasible. There exist several methods such as replacing the optimality cuts in infeasible iterations with feasibility cuts or making the sub-problems always feasible by adding slack variables. The details of these methods will not be discussed further but the interested reader is referred to [170]. In Chapter 5, we apply this Benders decomposition where we have always feasible sub-problems thus omitting the use of feasibility cuts.

The upper bound of the Benders decomposed problems in iteration (i) is found as:

$$UB^{(\mathrm{i})} = f(\Xi^{\mathrm{up}(i)}) - \sum_\omega \phi_\omega g_\omega^{(\mathrm{i})}(\Xi^{\mathrm{up}}, \Xi_\omega^{\mathrm{lo}}) \tag{A.6}$$

The lower bound in iteration (i) is found via:

$$LB^{(\mathrm{i})} = f(\Xi^{\mathrm{up}(i)}) - \sum_\omega \phi_\omega \psi_\omega^{(\mathrm{i})} \tag{A.7}$$

The iterative solution procedure is converged if the upper and lower bound come to within a small predefined residual $\epsilon > UB^{(\mathrm{i})} - LB^{(\mathrm{i})}$.

APPENDIX B

Assumptions and additional models for proposed TSO-DSO coordination

This appendix is an extension of Chapter 5 and contains additional modeling assumptions. Further, the models of the local DSO markets are presented as well as KKT conditions of all models in chapter 5.

B.1 Modeling assumptions for the PCC optimizer

We collect here all modeling assumptions made. We make no specific assumptions to the design of the local DSO markets that are employed. It is merely assumed that these markets are efficient and work to maximize social welfare. Therefore the model in B.1 is a generic market model that we cast as a stochastic optimization problem that maximizes expected social welfare.

Renewable production is the only source of uncertainty. The production of each renewable energy source (RES) r is capped by an uncertain parameter $W_{r\omega}^{\mathrm{R}T}$ that is dependent on scenario ω (i.e., RES can be freely spilled as required). The DA market is deterministic, and the offer of each RES is assumed to be the expected value of its production. The price offer of each RES, i.e., π^{R}, is assumed to be zero in the DA stage.

Although stochastic market-clearing setups depend on the used scenarios and a thorough definition of who generates them is usually pertinent, we here consider them as an external parameter. A scenario generation method, which correlates geographically close renewable sources is used – more information can be found in section B.6 of this appendix.

The RT market is assumed to be any market that changes the DA dispatch. This re-dispatch is assumed to incur an additional cost, due to premiums charged by the market participants. The premiums do not have to be symmetric, such that up- and down-regulation can have different costs.

We take the same view on network modeling as [46], that the meshed HV transmission network is adequately modeled by linear power flow approximations, while the radial LV distribution feeders are best represented by a convex relaxation of the AC power flow equations. Specifically, in this paper a second-order cone program (SOCP) will be used, as explained in more detail in section 5.4.

Ramping constraints, energy storage and other inter-temporal couplings are ignored. Also, binary variables such as the commitment status of conventional generators are ignored, such that both DA and RT market-clearing problems are convex.

In order to be able to calculate the RT re-dispatch cost, topology information of both TSO and DSO networks is necessary. Both TSO and DSOs may be unwilling to share data about their network topology. It is assumed that this information is available to the PCC optimizer, which is a reasonable assumptions as we are examining the best possible outcome. Decentralized optimization such as the proposals in [46] and [45] may in the future make it easier to coordinate in RT without sharing specific network-related proprietary information.

B.2 DSO market lower-level problem

The DSO pre-qualification optimization problem has both constraints from the DA-market and the scenarios for the Real-time realization. Every DSO has its own separate problem such that Cost_e contains one value for every DSO e. The day ahead market is cleared for each distribution network separately, where the day ahead market has no nodal information. The real time realization is a stochastic SOCP problem.

$$
\begin{aligned}
\max_{\Xi^{\mathrm{E}}} \quad & \mathcal{SW}_e = \sum_{d \in D_e^{\mathrm{D}}} \pi_d^{\mathrm{DA}} \widetilde{p}_d^{\mathrm{DA}} - \sum_{g \in G_e^{\mathrm{D}}} \pi_g^{\mathrm{DA}} \widetilde{p}_g^{\mathrm{DA}} \\
& - VOLL_e^{\mathrm{DA}} s_e^{\mathrm{DA}} - \sum_{r \in R_e^{\mathrm{D}}} \pi^R w_r^{\mathrm{DA}} - \pi_e^{\mathrm{PCC,DA}} p_e^{\mathrm{PCC,DA}} \\
& - \sum_{\omega} \phi_\omega \Bigg[\sum_{g \in G_e^{\mathrm{D}}} \Big(\pi_g^{\mathrm{DA}} (p_{g\omega}^{RT} - \widetilde{p}_g^{\mathrm{DA}}) + \pi_g^{\uparrow} p_{g\omega}^{\uparrow} \\
& + \pi_g^{\downarrow} p_{g\omega}^{\downarrow} \Big) + \sum_{d \in D_e^{\mathrm{D}}} \Big(\pi_d^{\mathrm{DA}} (\widetilde{p}_d^{\mathrm{DA}} - p_{d\omega}^{\mathrm{RT}}) \\
& + \pi_d^{\uparrow} p_{d\omega}^{\uparrow} + \pi_d^{\downarrow} p_{d\omega}^{\downarrow} \Big) + \sum_{n \in N_e^{\mathrm{D}}} VOLL_n^{\mathrm{RT}} s_{n\omega}^{\mathrm{RT}} \\
& + \pi_e^{\mathrm{PCC,DA}} (p_{e\omega}^{\mathrm{PCC,RT}} - p_e^{\mathrm{PCC,DA}})
\end{aligned}
\tag{B.1a}
$$

$$+ \pi_e^{\uparrow PCC} p_{e\omega}^{\uparrow PCC} + \pi_e^{\downarrow PCC} p_{e\omega}^{\downarrow PCC}$$
$$+ \sum_{r \in R_e^{\mathrm{D}}} \left(\pi^R (w_{r\omega}^{\mathrm{RT}} - w_r^{\mathrm{DA}}) + \pi^{\uparrow R} w_{r\omega}^{\uparrow} + \pi^{\downarrow R} w_{r\omega}^{\downarrow} \right) \Bigg]$$

subject to:

DA-level constraints:

$$\sum_{g \in G_e} \widetilde{p}_g^{\mathrm{D}A} - \sum_{d \in D_e^{\mathrm{D}}} \widetilde{p}_d^{\mathrm{D}A} + \sum_{r \in R_e^{\mathrm{D}}} w_r^{\mathrm{D}A} + s_e^{\mathrm{D}A} + p_e^{PCC,DA} = 0, \quad : (\lambda_e^{\mathrm{D}A}) \tag{B.1b}$$

$$\underline{P}_g \leq \widetilde{p}_g^{\mathrm{D}A} \leq \overline{P}_g, \quad \forall g \in G_e^{\mathrm{D}} \quad : (\varsigma_g^{\mathrm{D}A-}, \varsigma_g^{DA+}) \tag{B.1c}$$

$$\underline{P}_d \leq \widetilde{p}_d^{\mathrm{D}A} \leq \overline{P}_d, \quad \forall d \in D_e^{\mathrm{D}} \quad : (\varsigma_d^{\mathrm{D}A-}, \varsigma_d^{DA+}) \tag{B.1d}$$

$$0 \leq w_r^{\mathrm{D}A} \leq W_r^{\mathrm{D}A}, \ \forall r \in R_e^{\mathrm{D}} \quad : (\iota_r^-, \iota_r^+) \tag{B.1e}$$

$$\underline{f}_e \leq p_e^{PCC,DA} \leq \overline{f}_e, \quad : (\rho_e^{\mathrm{D}A-}, \rho_e^{\mathrm{D}A+}) \tag{B.1f}$$

$$0 \leq s_e^{\mathrm{D}A} \leq \sum_d p_d^{\mathrm{D}A}, \quad : (\Upsilon_e^{\mathrm{D}A-}, \Upsilon_e^{\mathrm{D}A+}) \tag{B.1g}$$

Real-time constraints:

$$p_{g\omega}^{\mathrm{RT}} = p_g^{\mathrm{D}A} + p_{g\omega}^{\uparrow} - p_{g\omega}^{\downarrow}, \quad \forall \omega, g \in G_e^{\mathrm{D}}, \quad : (\zeta_{g\omega}^p) \tag{B.1h}$$

$$p_{d\omega}^{\mathrm{RT}} = p_d^{\mathrm{D}A} - p_{d\omega}^{\uparrow} + p_{d\omega}^{\downarrow}, \quad \forall \omega, d \in D_e^{\mathrm{D}}, \quad : (\zeta_{d\omega}^p) \tag{B.1i}$$

$$w_{r\omega}^{\mathrm{RT}} = w_r^{\mathrm{D}A} + w_{r\omega}^{\uparrow} - w_{r\omega}^{\downarrow}, \ \forall \omega, r \in R_e^{\mathrm{D}}, : (\zeta_{r\omega}^p) \tag{B.1j}$$

$$\sum_{g \in G_n} p_{g\omega}^{\mathrm{RT}} - \sum_{d \in D_n} p_{d\omega}^{\mathrm{RT}} + \sum_{r \in R_n} w_{r\omega}^{\mathrm{RT}} + p_{e\omega}^{PCC,RT}|_{n=n_e^{\mathrm{L}V}} + s_{n\omega}^{\mathrm{RT}} = \sum_{l \in n\rightarrow} p_{l\omega}^{\mathrm{RT}} - \sum_{l \in \rightarrow n} p_{l\omega}^{\mathrm{RT}}, \ \forall \omega, n \in N_e^{\mathrm{D}} \ : (\lambda_{n\omega}^{\mathrm{p},RT}) \tag{B.1k}$$

$$p_{e\omega}^{PCC,RT} = p_e^{PCC,DA} + p_{e\omega}^{\uparrow PCC} - p_{e\omega}^{\downarrow PCC}, \ \forall \omega, \ : (\zeta_{e\omega}^{\mathrm{PCC}}) \tag{B.1l}$$

$$\sum_{g \in G_n} q_{g\omega}^{\mathrm{RT}} - \sum_{d \in D_n} q_{d\omega}^{\mathrm{RT}} + s_{n\omega}^{\mathrm{q},RT} + q_{e\omega}^{PCC,RT}|_{n=n_e^{\mathrm{L}V}} = \sum_{l \in n\rightarrow} q_{l\omega}^{\mathrm{RT}} - \sum_{l \in \rightarrow n} q_{l\omega}^{\mathrm{RT}}, \ \forall \omega, n \in N_e^{\mathrm{D}} \ : (\lambda_{n\omega}^{\mathrm{q},RT}) \tag{B.1m}$$

$$p_{l\omega}^{(RT)2} + q_{l\omega}^{(RT)2} \leq \varphi_{l\omega}^{\mathrm{RT}} v_{n\omega}^{\mathrm{RT}}, \quad \forall \omega, l \in L_e^{\mathrm{D}} \ : (\gamma_{l\omega}) \tag{B.1n}$$

$$p_{l\omega}^{\mathrm{RT}} + p_{l'\omega}^{\mathrm{RT}} = R_l \varphi_{l\omega}^{\mathrm{RT}}, \quad \forall \omega, l \in L_e^{\mathrm{D}} \ : (\mu_{l\omega}^p) \tag{B.1o}$$

$$q_{l\omega}^{\mathrm{RT}} + q_{l'\omega}^{\mathrm{RT}} = X_l \varphi_{l\omega}^{\mathrm{RT}}, \quad \forall \omega, l \in L_e^{\mathrm{D}} \ : (\mu_{l\omega}^q) \tag{B.1p}$$

$$p_{l\omega}^{(RT)2} + q_{l\omega}^{(RT)2} \leq S_l, \quad \forall \omega, l \in L_e^{\mathrm{D}} \ : (\eta_{l\omega}) \tag{B.1q}$$

$$v_{m\omega}^{\mathrm{RT}} = v_{n\omega}^{\mathrm{RT}} - 2(R_l p_{l\omega}^{\mathrm{RT}} + X_l q_{l\omega}^{\mathrm{RT}}) + (R_l^2 + X_l^2) \varphi_{l\omega}^{\mathrm{RT}}, \quad \forall \omega, l \in L_e^{\mathrm{D}} \quad : (\beta_{l\omega}) \tag{B.1r}$$

$$\underline{V}_n^2 \leq v_{n\omega}^{\mathrm{RT}} \leq \overline{V}_n^2, \quad \forall \omega, n \in N_e^{\mathrm{D}} \quad : (\sigma_{n\omega}^-, \sigma_{n\omega}^+) \tag{B.1s}$$

$$0 \leq w_{r\omega}^{RT} \leq W_{r\omega}^{\mathrm{RT}}, \quad \forall \omega, n \in N_e \quad : (\nu_{n\omega}^-, \nu_{n\omega}^+) \tag{B.1t}$$

$$\underline{P}_g \leq p_{g\omega}^{\mathrm{RT}} \leq \overline{P}_g, \quad \forall \omega, g \in G_e \quad : (\varsigma_{g\omega}^{\mathrm{RT}-}, \varsigma_{g\omega}^{RT+}) \tag{B.1u}$$

$$\underline{P}_d \leq p_{d\omega}^{\mathrm{RT}} \leq \overline{P}_d, \quad \forall \omega, d \in D_e \quad : (\varsigma_{d\omega}^{\mathrm{RT}-}, \varsigma_{d\omega}^{RT+}) \tag{B.1v}$$

$$\underline{Q}_g \leq q_{g\omega}^{\mathrm{RT}} \leq \overline{Q}_g, \quad \forall \omega, g \in G_e \quad : (\kappa_{g\omega}^{RT-}, \kappa_{g\omega}^{\mathrm{RT}+}) \tag{B.1w}$$

$$\underline{Q}_d \leq q_{d\omega}^{\mathrm{RT}} \leq \overline{Q}_d, \quad \forall \omega, d \in D_e \quad : (\kappa_{d\omega}^{\mathrm{RT}-}, \kappa_{d\omega}^{RT+}) \tag{B.1x}$$

$$\underline{f}_e \leq p_{e\omega}^{PCC,RT} \leq \overline{f}_e, \quad \forall \omega \quad : (\rho_{e\omega}^{\mathrm{RT}-}, \rho_{e\omega}^{RT+}) \tag{B.1y}$$

$$p_{g\omega}^{\uparrow} \geq 0, \ \forall \omega, g \ : (\epsilon_{g\omega}^{\mathrm{p}\uparrow}), \quad p_{g\omega}^{\downarrow} \geq 0, \ \forall \omega, g \ : (\epsilon_{g\omega}^{\mathrm{p}\downarrow}) \tag{B.1z}$$

$$p_{d\omega}^{\uparrow} \geq 0, \ \forall d, \omega \ : (\varepsilon_{d\omega}^{\mathrm{p}\uparrow}), \quad p_{d\omega}^{\downarrow} \geq 0, \ \forall d, \omega \ : (\varepsilon_{d\omega}^{\mathrm{p}\downarrow}) \tag{B.1aa}$$

$$p_{e\omega}^{\uparrow PCC} \geq 0, \ \forall \omega, \ : (\epsilon_{e\omega}^{\uparrow PCC}), \ p_{e\omega}^{\downarrow PCC} \geq 0, \ \forall \omega, \ : (\epsilon_{e\omega}^{\downarrow PCC}) \tag{B.1ab}$$

$$0 \leq s_{n\omega}^{\mathrm{RT}} \leq \sum_{d \in D_n} p_{d\omega}^{\mathrm{RT}}, \ \forall \omega, n \in N_e^{\mathrm{D}}, \ : (\Upsilon_{n\omega}^{\mathrm{RT}-}, \Upsilon_{n\omega}^{RT+}) \tag{B.1ac}$$

$$w_{r\omega}^{\uparrow} \geq 0, \ \forall \omega, w \ : (\epsilon_{r\omega}^{\mathrm{p}\uparrow}), \quad w_{r\omega}^{\downarrow} \geq 0, \ \forall \omega, w \ : (\epsilon_{r\omega}^{\mathrm{p}\downarrow}) \tag{B.1ad}$$

Where $\Xi^E = \widetilde{p}_g^{\mathrm{DA}}, \widetilde{p}_d^{\mathrm{DA}}, p_{g\omega}^{\mathrm{RT}}, p_{g\omega}^{\uparrow}, p_{g\omega}^{\downarrow}, p_{d\omega}^{\mathrm{RT}}, p_{d\omega}^{\uparrow}, p_{d\omega}^{\downarrow}, q_{g\omega}^{\mathrm{RT}}, q_{d\omega}^{\mathrm{RT}}, s_{n\omega}^{\mathrm{RT}}, s_e^{DA}, w_{n\omega}^{\mathrm{RT}}, p_{l\omega}^{\mathrm{RT}}, q_{l\omega}^{\mathrm{RT}}, \varphi_{l\omega}^{\mathrm{RT}}$ $, v_{n\omega}^{RT}, w_e^{\mathrm{DA}}, p_e^{PCC,DA}, p_e^{\mathrm{PCC},RT}, p_e^{\uparrow PCC}, p_e^{\downarrow PCC}, s_{n\omega}^{\mathrm{q},RT}$ are the variables of the DSO-level combined day-ahead and real-time market clearing.

The Lagrangian of above problem is:

$$\begin{aligned}
\mathcal{L}_e = & \sum_{d \in D_e^{\mathrm{D}}} \pi_d^{\mathrm{DA}} \widetilde{p}_d^{\mathrm{DA}} - \sum_{g \in G_e^{\mathrm{D}}} \pi_g^{DA} \widetilde{p}_g^{\mathrm{DA}} \\
& - VOLL_e^{\mathrm{DA}} s_e^{DA} - \sum_{r \in R_e^{\mathrm{D}}} \pi^R w_r^{\mathrm{DA}} - \pi_e^{\mathrm{PCC},DA} p_e^{PCC,DA} \\
& - \sum_{\omega} \phi_\omega \Bigg[\sum_{g \in G_e^{\mathrm{D}}} \left(\pi_g^{\mathrm{DA}} (p_{g\omega}^{\mathrm{RT}} - p_g^{\mathrm{DA}}) + \pi_g^{\uparrow} p_{g\omega}^{\uparrow} + \pi_g^{\downarrow} p_{g\omega}^{\downarrow} \right) \\
& + \sum_{d \in D_e^{\mathrm{D}}} \left(\pi_d^{\mathrm{DA}} (p_d^{\mathrm{DA}} - p_{d\omega}^{\mathrm{RT}}) + \pi_d^{\uparrow} p_{d\omega}^{\uparrow} + \pi_d^{\downarrow} p_{d\omega}^{\downarrow} \right) \\
& + \sum_{n \in N_e^{\mathrm{D}}} VOLL_n^{\mathrm{RT}} s_{n\omega}^{RT} \\
& + \sum_{r \in R_e^{\mathrm{D}}} \left(\pi^R (w_{r\omega}^{\mathrm{RT}} - w_r^{\mathrm{DA}}) + \pi^{\uparrow R} w_{r\omega}^{\uparrow} + \pi^{\downarrow R} w_{r\omega}^{\downarrow} \right) \\
& + \pi_e^{\mathrm{PCC},DA} (p_{e\omega}^{PCC,RT} - p_e^{\mathrm{PCC},DA}) \\
& + \pi_e^{\uparrow PCC} p_{e\omega}^{\uparrow PCC} + \pi_e^{\downarrow PCC} p_{e\omega}^{\downarrow PCC} \Bigg]
\end{aligned}$$

$$
\begin{aligned}
&- \lambda_e^{\mathrm{D}A} \Bigg[\sum_{g \in G_e} \widetilde{p}_g^{\,DA} - \sum_{d \in D_e^{\mathrm{D}}} \widetilde{p}_d^{\,DA} + \sum_{r \in R_e^{\mathrm{D}}} w_r^{\mathrm{D}A} \\
&\quad + s_e^{\mathrm{D}A} + p_e^{PCC,DA} \Bigg] \\
&+ \sum_{g \in G_e^{\mathrm{D}}} \left[\varsigma_g^{\mathrm{D}A-} \left(\underline{P}_g - \widetilde{p}_g^{\,DA} \right) + \varsigma_g^{\mathrm{D}A+} \left(\widetilde{p}_g^{\,DA} - \overline{P}_g \right) \right] \\
&- \sum_{r \in R_e^{\mathrm{D}}} \left[\iota_r^- w_r^{\mathrm{D}A} - \iota_r^+ (w_r^{\mathrm{D}A} - W_r^{\mathrm{D}A}) \right] \\
&+ \sum_{d \in D_e^{\mathrm{D}}} \left[\varsigma_d^{\mathrm{D}A-} \left(\underline{P}_d - \widetilde{p}_d^{\,DA} \right) + \varsigma_d^{\mathrm{D}A+} \left(\widetilde{p}_d^{\,DA} - \overline{P}_d \right) \right] \\
&+ \rho_e^{\mathrm{D}A-} (\underline{f}_e - p_e^{PCC,DA}) + \rho_e^{\mathrm{D}A+} (p_e^{PCC,DA} - \overline{f}_e) \\
&- \sum_{g \in G_e^{\mathrm{D}}} \zeta_{g\omega}^{\mathrm{p}} \left(p_{g\omega}^{\mathrm{R}T} - p_g^{\mathrm{D}A} - p_{g\omega}^{\uparrow} + p_{g\omega}^{\downarrow} \right) \\
&- \sum_{d \in D_e^{\mathrm{D}}} \zeta_{d\omega}^{\mathrm{p}} \left(p_{d\omega}^{\mathrm{R}T} - p_d^{\mathrm{D}A} + p_{d\omega}^{\uparrow} - p_{d\omega}^{\downarrow} \right) \\
&- \sum_{r \in R_e^{\mathrm{D}}} \zeta_{r\omega}^{p} \left(w_{r\omega}^{\mathrm{R}T} - w_r^{\mathrm{D}A} - w_{r\omega}^{\uparrow} + w_{r\omega}^{\downarrow} \right) \\
&- \sum_{n \in N_e^{\mathrm{D}}, \omega} \lambda_{n\omega}^{\mathrm{p},RT} \Big(\sum_{g \in G_n} p_{g\omega}^{\mathrm{R}T} - \sum_{d \in D_n} p_{d\omega}^{\mathrm{R}T} + \sum_{r \in R_n} w_{r\omega}^{\mathrm{R}T} \\
&+ s_{n\omega}^{\mathrm{R}T} + p_{e\omega}^{PCC,RT}|_{n=n_e^{\mathrm{L}V}} - \sum_{l \in n\rightarrow} p_{l\omega}^{\mathrm{R}T} + \sum_{l \in \rightarrow n} p_{l\omega}^{\mathrm{R}T} \Big) \\
&- \sum_{\omega} \zeta_{e\omega}^{PCC} \left(p_{e\omega}^{PCC,RT} - p_e^{PCC,DA} - p_{e\omega}^{\uparrow PCC} + p_{e\omega}^{\downarrow PCC} \right) \\
&- \sum_{n \in N_e^{\mathrm{D}}, \omega} \lambda_{n\omega}^{\mathrm{q},RT} \Bigg(\sum_{g \in G_n} q_{g\omega}^{\mathrm{R}T} - \sum_{d \in D_n} q_{d\omega}^{\mathrm{R}T} + s_{n\omega}^{\mathrm{q},RT} \\
&+ q_{e\omega}^{PCC,RT}|_{n=n_e^{\mathrm{L}V}} - \sum_{l \in n\rightarrow} q_{l\omega}^{\mathrm{R}T} + \sum_{l \in \rightarrow n} q_{l\omega}^{\mathrm{R}T} \Bigg) \\
&+ \sum_{l \in L_e^{\mathrm{D}}, \omega} \gamma_{l\omega} \left[p_{l\omega}^{(RT)2} + q_{l\omega}^{(RT)2} - \varphi_{l\omega}^{\mathrm{R}T} v_{n\omega}^{\mathrm{R}T} \right] \\
&- \sum_{l \in L_e^{\mathrm{D}}, \omega} \Big[\mu_{l\omega}^{p} \left(p_{l\omega}^{\mathrm{R}T} + p_{l'\omega}^{\mathrm{R}T} - R_l \varphi_{l\omega}^{\mathrm{R}T} \right) \\
&\quad + \mu_{l\omega}^{q} \left(q_{l\omega}^{\mathrm{R}T} + q_{l'\omega}^{\mathrm{R}T} - X_l \varphi_{l\omega}^{\mathrm{R}T} \right) \Big]
\end{aligned}
$$

$$
\begin{aligned}
&+ \sum_{l\in L_e^{\mathrm{D}},\omega} \left[\eta_{l\omega}\left(p_{l\omega}^{(RT)2} + q_{l\omega}^{(RT)2} - S_l\right)\right] \\
&- \sum_{l\in L_e^{\mathrm{D}},\omega} \Big[\beta_{l\omega}\Big(v_{m\omega}^{\mathrm{R}T} - v_{n\omega}^{\mathrm{R}T} + 2(R_l p_{l\omega}^{\mathrm{R}T} + X_l q_{l\omega}^{\mathrm{R}T}) \\
&\quad - (R_l^2 + X_l^2)\varphi_{l\omega}^{\mathrm{R}T}\Big)\Big] \\
&+ \sum_{n\in N_e^{\mathrm{D}},\omega} \left[\sigma_{n\omega}^{-}\left(\underline{V}_n^2 - v_{n\omega}^{\mathrm{R}T}\right) + \sigma_{n\omega}^{+}\left(v_{n\omega}^{\mathrm{R}T} - \overline{V}_n^2\right)\right] \\
&- \sum_{r\in R_e^{\mathrm{D}},\omega} \left[\nu_{r\omega}^{-} w_{r\omega}^{\mathrm{R}T} - \nu_{r\omega}^{+}\left(w_{r\omega}^{\mathrm{R}T} - W_{r\omega}^{\mathrm{R}T}\right)\right] \\
&+ \sum_{g\in G_e^{\mathrm{D}},\omega} \left[\varsigma_{g\omega}^{\mathrm{R}T-}\left(\underline{P}_g - p_{g\omega}^{\mathrm{R}T}\right) + \varsigma_{g\omega}^{\mathrm{R}T+}\left(p_{g\omega}^{\mathrm{R}T} - \overline{P}_g\right)\right] \\
&+ \sum_{d\in D_e^{\mathrm{D}},\omega} \left[\varsigma_{d\omega}^{\mathrm{R}T-}\left(\underline{P}_d - p_{d\omega}^{\mathrm{R}T}\right) + \varsigma_{d\omega}^{\mathrm{R}T+}\left(p_{d\omega}^{\mathrm{R}T} - \overline{P}_d\right)\right] \\
&+ \sum_{g\in G_e^{\mathrm{D}},\omega} \left[\kappa_{g\omega}^{\mathrm{R}T-}\left(\underline{Q}_g - q_{g\omega}^{\mathrm{R}T}\right) + \kappa_{g\omega}^{\mathrm{R}T+}\left(q_{g\omega}^{\mathrm{R}T} - \overline{Q}_g\right)\right] \\
&+ \sum_{d\in D_e^{\mathrm{D}},\omega} \left[\kappa_{d\omega}^{\mathrm{R}T-}\left(\underline{Q}_d - q_{d\omega}^{\mathrm{R}T}\right) + \kappa_{d\omega}^{\mathrm{R}T+}\left(q_{d\omega}^{\mathrm{R}T} - \overline{Q}_g\right)\right] \\
&+ \sum_{g\in G_e^{\mathrm{D}},\omega} \left[-p_{g\omega}^{\uparrow}\epsilon_{g\omega}^{\mathrm{p}\uparrow} - p_{g\omega}^{\downarrow}\epsilon_{g\omega}^{\mathrm{p}\downarrow}\right] \\
&+ \sum_{r\in R_e^{\mathrm{D}},\omega} \left[-w_{r\omega}^{\uparrow}\epsilon_{r\omega}^{\mathrm{p}\uparrow} - w_{r\omega}^{\downarrow}\epsilon_{r\omega}^{\mathrm{p}\downarrow}\right] \\
&+ \sum_{d\in D_e^{\mathrm{D}},\omega} \left[-p_{d\omega}^{\uparrow}\varepsilon_{d\omega}^{\mathrm{p}\uparrow} - p_{d\omega}^{\downarrow}\varepsilon_{d\omega}^{\mathrm{p}\downarrow}\right] \\
&+ \sum_{\omega} \left[-p_{e\omega}^{\uparrow PCC}\epsilon_{e\omega}^{\uparrow PCC} - p_{e\omega}^{\downarrow PCC}\epsilon_{e\omega}^{\downarrow PCC}\right] \\
&+ \sum_{\omega} \Big[\rho_{e\omega}^{\mathrm{R}T-}\left(\underline{f}_e - \sqrt{p_{e\omega}^{(PCC,RT)2} + q_{e\omega}^{(PCC,RT)2}}\right) \\
&+ \rho_{e\omega}^{\mathrm{R}T+}\left(\sqrt{p_{e\omega}^{(PCC,RT)2} + q_{e\omega}^{(PCC,RT)2}} - \overline{f}_e\right)\Big] \\
&+ \sum_{n\in N_e^{\mathrm{D}},\omega} \left[-\Upsilon_{n\omega}^{\mathrm{R}T-} s_{n\omega}^{\mathrm{R}T} + \Upsilon_{n\omega}^{\mathrm{R}T+}\left(s_{n\omega}^{\mathrm{R}T} - \sum_{d\in D_n} p_{d\omega}^{\mathrm{R}T}\right)\right] \\
&- \Upsilon_e^{\mathrm{D}A-} s_e^{\mathrm{D}A} + \Upsilon_e^{\mathrm{D}A+}\left(s_e^{\mathrm{D}A} - \sum_d p_d^{\mathrm{D}A}\right)
\end{aligned}
\tag{B.2}
$$

The KKT conditions of above problem are (excluding the primal constraints of B.1):

$$(\widetilde{p}_g^{\mathrm{D}A}):\ -\pi_g^{\mathrm{D}A}+\sum_{\omega}\phi_\omega\pi_g^{\mathrm{D}A}-\lambda_e^{\mathrm{D}A}-\varsigma_g^{\mathrm{D}A-}+\varsigma_g^{\mathrm{D}A+}+\sum_{\omega}\zeta_{g\omega}^{p}=0,\quad \forall g\in G_e^{\mathrm{D}} \tag{B.3a}$$

$$(\widetilde{p}_d^{\mathrm{D}A}):\sum_{\omega}\left(\zeta_{d\omega}^{p}-\phi_\omega\pi_d^{\mathrm{D}A}\right)+\pi_d^{\mathrm{D}A}+\lambda_e^{\mathrm{D}A}-\varsigma_d^{\mathrm{D}A-}+\varsigma_d^{\mathrm{D}A+}-\Upsilon_e^{\mathrm{D}A+}=0,\quad \forall d\in D_e^{\mathrm{D}} \tag{B.3b}$$

$$(p_{g\omega}^{\uparrow}):\ -\phi_\omega\pi_g^{\uparrow}+\zeta_{g\omega}^{p}-\epsilon_{g\omega}^{\mathrm{p}\uparrow}=0,\quad \forall\omega,g\in G_e^{\mathrm{D}} \tag{B.3c}$$

$$(p_{g\omega}^{\downarrow}):\ -\phi_\omega\pi_g^{\downarrow}-\zeta_{g\omega}^{p}-\epsilon_{g\omega}^{\mathrm{p}\downarrow}=0,\quad \forall\omega,g\in G_e^{\mathrm{D}} \tag{B.3d}$$

$$(p_{d\omega}^{\uparrow}):\ -\phi_\omega\pi_d^{\uparrow}-\zeta_{d\omega}^{p}-\varepsilon_{i\omega}^{\mathrm{p}\uparrow}=0,\quad \forall\omega,d\in D_e^{\mathrm{D}} \tag{B.3e}$$

$$(p_{d\omega}^{\downarrow}):\ -\phi_\omega\pi_d^{\downarrow}+\zeta_{d\omega}^{p}-\varepsilon_{d\omega}^{\mathrm{p}\downarrow}=0,\quad \forall\omega,d\in D_e^{\mathrm{D}} \tag{B.3f}$$

$$(w_{r\omega}^{\uparrow}):\ -\phi_\omega\pi^{\uparrow R}+\zeta_{r\omega}^{p}-\epsilon_{r\omega}^{\mathrm{p}\uparrow}=0,\quad \forall\omega,r\in R_e^{\mathrm{D}} \tag{B.3g}$$

$$(w_{r\omega}^{\downarrow}):\ -\phi_\omega\pi^{\downarrow R}-\zeta_{r\omega}^{p}-\epsilon_{r\omega}^{\mathrm{p}\downarrow}=0,\quad \forall\omega,r\in R_e^{\mathrm{D}} \tag{B.3h}$$

$$(s_e^{\mathrm{D}A}):-\mathrm{VOLL}_e-\lambda_e^{\mathrm{D}A}-\Upsilon_e^{\mathrm{D}A-}+\Upsilon_e^{\mathrm{D}A+}=0 \tag{B.3i}$$

$$(s_{n\omega}^{\mathrm{R}T}):-\mathrm{VOLL}_n-\lambda_{n\omega}^{\mathrm{p},RT}-\Upsilon_{n\omega}^{\mathrm{R}T-}+\Upsilon_{n\omega}^{\mathrm{R}T+}=0,\ \forall\omega,n\in N_e^{\mathrm{D}} \tag{B.3j}$$

$$(w_{r\omega}^{\mathrm{R}T}):-\phi_\omega\pi^{R}-\zeta_{r\omega}^{p}-\left[\lambda_{n\omega}^{\mathrm{p},RT}\right]_{n_r}+\nu_{r\omega}^{+}-\nu_{r\omega}^{-}=0,\quad \forall\omega,r\in R_e^{\mathrm{D}} \tag{B.3k}$$

$$(w_r^{\mathrm{D}A}):-\pi^{R}+\sum_{\omega}\phi_\omega\pi^{R}-\lambda_e^{\mathrm{D}A}-\iota_r^{-}+\iota_r^{+}+\sum_{\omega}\zeta_{r\omega}^{p}=0,\forall r\in R_e^{\mathrm{D}} \tag{B.3l}$$

$$(p_{g\omega}^{\mathrm{R}T}):-\phi_\omega\pi_g^{\mathrm{D}A}-\zeta_{g\omega}^{p}-\varsigma_{g\omega}^{\mathrm{R}T-}+\varsigma_{g\omega}^{\mathrm{R}T+}-\left[\lambda_{n\omega}^{\mathrm{p},RT}\right]_{n_g}=0,\quad \forall\omega,g\in G_e^{\mathrm{D}} \tag{B.3m}$$

$$(q_{g\omega}^{\mathrm{R}T}):-\kappa_{g\omega}^{\mathrm{R}T-}+\kappa_{g\omega}^{\mathrm{R}T+}-\left[\lambda_{n\omega}^{\mathrm{q},RT}\right]_{n_g}=0,\quad \forall\omega,g\in G_e^{\mathrm{D}} \tag{B.3n}$$

$$(p_{d\omega}^{\mathrm{R}T}):\phi_\omega\pi_d^{\mathrm{D}A}-\zeta_{d\omega}^{p}-\varsigma_{d\omega}^{\mathrm{R}T-}+\varsigma_{d\omega}^{\mathrm{R}T+}+\left[\lambda_{n\omega}^{\mathrm{p},RT}-\Upsilon_{n\omega}^{\mathrm{R}T+}\right]_{n_d}=0,\quad \forall\omega,d\in D_e^{\mathrm{D}} \tag{B.3o}$$

$$(q_{d\omega}^{\mathrm{R}T}):-\kappa_{d\omega}^{\mathrm{R}T-}+\kappa_{d\omega}^{\mathrm{R}T+}+\left[\lambda_{n\omega}^{\mathrm{q},RT}\right]_{n_d}=0,\quad \forall\omega,d\in D_e^{\mathrm{D}} \tag{B.3p}$$

$$(p_{l\omega}^{\mathrm{R}T}):\lambda_{n\omega}^{\mathrm{p},RT}-\lambda_{m\omega}^{\mathrm{p},RT}+2\gamma_{l\omega}p_{l\omega}^{\mathrm{R}T}-\mu_{l\omega}^{p}-\mu_{l'\omega}^{p}+2\eta_{l\omega}p_{l\omega}^{\mathrm{R}T}-2\beta_{l\omega}R_l=0,\quad \forall\omega,l=(n,m)\in L_e^{\mathrm{D}} \tag{B.3q}$$

$$(q_{l\omega}^{\mathrm{RT}}) : \lambda_{n\omega}^{\mathrm{q},RT} - \lambda_{m\omega}^{\mathrm{q},RT} + 2\gamma_{l\omega} q_{l\omega}^{\mathrm{RT}} - \mu_{l\omega}^{q} - \mu_{l'\omega}^{q} + 2\eta_{l\omega} q_{l\omega}^{\mathrm{RT}} - 2\beta_{l\omega} X_l = 0, \quad \forall \omega, l = (n,m) \in L_e^{\mathrm{D}} \tag{B.3r}$$

$$(\varphi_{l\omega}^{\mathrm{RT}}) : -\gamma_{l\omega} v_{n\omega}^{\mathrm{RT}} + \mu_{l\omega}^{p} R_l + \mu_{l\omega}^{q} X_l + \beta_{l\omega}(R_l^2 + X_l^2) = 0, \quad \forall \omega, l = (n,m) \in L_e^{\mathrm{D}} \tag{B.3s}$$

$$(v_{n\omega}^{\mathrm{RT}}) : -\gamma_{l\omega} \varphi_{l\omega}^{\mathrm{RT}} - \beta_{l'\omega} + \beta_{l\omega} - \sigma_{n\omega}^{-} + \sigma_{n\omega}^{+} = 0, \quad \forall \omega, l = (n,m) \in L_e^{\mathrm{D}} \tag{B.3t}$$

$$(p_e^{PCC,DA}) : -\pi_e^{\mathrm{PCC},DA} + \sum_{\omega} \left(\phi_\omega \pi_e^{\mathrm{PCC},DA} + \zeta_{e\omega}^{\mathrm{PCC}}\right) - \lambda_e^{DA} - \rho_e^{\mathrm{DA}-} + \rho_e^{\mathrm{DA}+} = 0 \tag{B.3u}$$

$$(p_{e\omega}^{\mathrm{PCC},RT}) : -\phi_\omega \pi_e^{\mathrm{PCC},DA} - \left[\lambda_{n\omega}^{\mathrm{p},RT}\right]_{n_e^{\mathrm{LV}}} - \zeta_{e\omega}^{\mathrm{PCC}} - \rho_{e\omega}^{\mathrm{RT}-} + \rho_{e\omega}^{\mathrm{RT}+} = 0, \quad \forall \omega \tag{B.3v}$$

$$(q_{e\omega}^{\mathrm{PCC},RT}) : -\left[\lambda_{n\omega}^{\mathrm{q},RT}\right]_{n_e^{\mathrm{LV}}} = 0, \quad \forall \omega \tag{B.3w}$$

$$(p_{e\omega}^{\uparrow PCC}) : -\phi_\omega \pi_e^{\uparrow PCC} + \zeta_{e\omega}^{\mathrm{PCC}} - \epsilon_{e\omega}^{\uparrow PCC} = 0, \quad \forall \omega \tag{B.3x}$$

$$(p_{e\omega}^{\downarrow PCC}) : -\phi_\omega \pi_e^{\downarrow PCC} - \zeta_{e\omega}^{\mathrm{PCC}} - \epsilon_{e\omega}^{\downarrow PCC} = 0, \quad \forall \omega \tag{B.3y}$$

The complimentarity constraints are as follows:

$$0 \le \varsigma_g^{\mathrm{DA}+} \perp \overline{P}_g - \widetilde{p}_g^{\mathrm{DA}} \ge 0, \quad \forall g \in G_e^{\mathrm{D}} \tag{B.4a}$$

$$0 \le \varsigma_g^{\mathrm{DA}-} \perp \widetilde{p}_g^{\mathrm{DA}} - \underline{P}_g \ge 0, \quad \forall g \in G_e^{\mathrm{D}} \tag{B.4b}$$

$$0 \le \varsigma_d^{\mathrm{DA}+} \perp \overline{P}_d - \widetilde{p}_d^{\mathrm{DA}} \ge 0, \quad \forall d \in D_e^{\mathrm{D}} \tag{B.4c}$$

$$0 \le \varsigma_d^{\mathrm{DA}-} \perp \widetilde{p}_d^{\mathrm{DA}} - \underline{P}_d \ge 0, \quad \forall d \in D_e^{\mathrm{D}} \tag{B.4d}$$

$$0 \le \iota_r^{-} \perp w_r^{\mathrm{DA}} \ge 0, \quad \forall r \in R_e^{\mathrm{D}} \tag{B.4e}$$

$$0 \le \iota_r^{+} \perp W_r^{\mathrm{DA}} - w_r^{\mathrm{DA}} \ge 0, \quad \forall r \in R_e^{\mathrm{D}} \tag{B.4f}$$

$$0 \le \rho_e^{\mathrm{DA}-} \perp p_e^{\mathrm{PCC},DA} - \underline{f}_e \ge 0 \tag{B.4g}$$

$$0 \le \rho_e^{\mathrm{DA}+} \perp \overline{f}_e - p_e^{\mathrm{PCC},DA} \ge 0 \tag{B.4h}$$

$$0 \le \gamma_{l\omega} \perp \varphi_{l\omega}^{\mathrm{RT}} v_{n\omega}^{\mathrm{RT}} - (p_{l\omega}^{(RT)2} + q_{l\omega}^{(RT)2}) \ge 0, \ \forall \omega, l \in L_e^{\mathrm{D}} \tag{B.4i}$$

$$0 \le \eta_{l\omega} \perp S_l - p_{l\omega}^{(RT)2} - q_{l\omega}^{(RT)2} \ge 0, \ \forall \omega, l \in L_e^{\mathrm{D}} \tag{B.4j}$$

$$0 \le \sigma_{n\omega}^{-} \perp v_{n\omega}^{\mathrm{RT}} - \underline{V}_n^2 \ge 0, \quad \forall \omega, n \in N_e^{\mathrm{D}} \tag{B.4k}$$

$$0 \le \sigma_{n\omega}^{+} \perp \overline{V}_n^2 - v_{n\omega}^{\mathrm{RT}} \ge 0, \quad \forall \omega, n \in N_e^{\mathrm{D}} \tag{B.4l}$$

$$0 \le \nu_{r\omega}^{-} \perp w_{r\omega}^{\mathrm{RT}} \ge 0, \quad \forall \omega, r \in R_e^{\mathrm{D}} \tag{B.4m}$$

$$0 \le \nu_{r\omega}^{+} \perp W_{r\omega}^{\mathrm{RT}} - w_{r\omega}^{\mathrm{RT}} \ge 0, \quad \forall \omega, r \in R_e^{\mathrm{D}} \tag{B.4n}$$

$$0 \le \varsigma_{g\omega}^{\mathrm{RT}-} \perp p_{g\omega}^{\mathrm{RT}} - \underline{P}_g \ge 0, \quad \forall \omega, g \in G_e^{\mathrm{D}} \tag{B.4o}$$

$$0 \le \varsigma_{g\omega}^{\mathrm{RT}+} \perp \overline{P}_g - p_{g\omega}^{\mathrm{RT}} \ge 0, \quad \forall \omega, g \in G_e^{\mathrm{D}} \tag{B.4p}$$

$$0 \leq \varsigma_{d\omega}^{\mathrm{RT}-} \perp p_{d\omega}^{RT} - \underline{P}_d \geq 0, \quad \forall \omega, d \in D_e^{\mathrm{D}} \tag{B.4q}$$
$$0 \leq \varsigma_{d\omega}^{\mathrm{RT}+} \perp \overline{P}_d - p_{d\omega}^{\mathrm{RT}} \geq 0, \quad \forall \omega, d \in D_e^{\mathrm{D}} \tag{B.4r}$$
$$0 \leq \kappa_{g\omega}^{\mathrm{RT}+} \perp q_{g\omega}^{RT} - \underline{Q}_g \geq 0, \quad \forall \omega, g \in G_e^{\mathrm{D}} \tag{B.4s}$$
$$0 \leq \kappa_{g\omega}^{\mathrm{RT}-} \perp \overline{Q}_g - q_{g\omega}^{\mathrm{RT}} \geq 0, \quad \forall \omega, g \in G_e^{\mathrm{D}} \tag{B.4t}$$
$$0 \leq \kappa_{d\omega}^{\mathrm{RT}+} \perp q_{d\omega}^{\mathrm{RT}} - \underline{Q}_d \geq 0, \quad \forall \omega, d \in D_e^{\mathrm{D}} \tag{B.4u}$$
$$0 \leq \kappa_{d\omega}^{\mathrm{RT}-} \perp \overline{Q}_d - q_{d\omega}^{\mathrm{RT}} \geq 0, \quad \forall \omega, d \in D_e^{\mathrm{D}} \tag{B.4v}$$
$$0 \leq \rho_{e\omega}^{\mathrm{RT}-} \perp p_{e\omega}^{PCC,RT} - \underline{f}_e \geq 0, \quad \forall \omega \tag{B.4w}$$
$$0 \leq \rho_{e\omega}^{\mathrm{RT}+} \perp \overline{f}_e - p_{e\omega}^{PCC,RT} \geq 0, \quad \forall \omega \tag{B.4x}$$
$$0 \leq \epsilon_{g\omega}^{\mathrm{p}\uparrow} \perp p_{g\omega}^{\uparrow} \geq 0, \quad 0 \leq \epsilon_{g\omega}^{\mathrm{p}\downarrow} \perp p_{g\omega}^{\downarrow} \geq 0, \quad \forall \omega, g \in G_e^{\mathrm{D}} \tag{B.4y}$$
$$0 \leq \epsilon_{r\omega}^{\mathrm{p}\uparrow} \perp w_{r\omega}^{\uparrow} \geq 0, \; 0 \leq \epsilon_{r\omega}^{\mathrm{p}\downarrow} \perp w_{r\omega}^{\downarrow} \geq 0, \; \forall \omega, r \in R_e^{\mathrm{D}} \tag{B.4z}$$
$$0 \leq \varepsilon_{d\omega}^{\mathrm{p}\uparrow} \perp p_{d\omega}^{\uparrow} \geq 0, \quad 0 \leq \varepsilon_{d\omega}^{\mathrm{p}\downarrow} \perp p_{d\omega}^{\downarrow} \geq 0, \quad \forall \omega, d \in D_e^{\mathrm{D}} \tag{B.4aa}$$
$$0 \leq \epsilon_{e\omega}^{\uparrow PCC} \perp p_{e\omega}^{\uparrow PCC} \geq 0, \quad 0 \leq \epsilon_{e\omega}^{\downarrow PCC} \perp p_{e\omega}^{\downarrow PCC} \geq 0, \quad \forall \omega \tag{B.4ab}$$
$$0 \leq \Upsilon_{n\omega}^{\mathrm{RT}-} \perp s_{n\omega}^{\mathrm{RT}} \geq 0, \forall n, \omega \tag{B.4ac}$$
$$0 \leq \Upsilon_{n\omega}^{\mathrm{RT}+} \perp \sum_{d \in D_n} p_{d\omega}^{\mathrm{RT}} - s_{n\omega}^{\mathrm{RT}} \geq 0, \; \forall n, \omega \tag{B.4ad}$$
$$0 \leq \Upsilon_{e}^{\mathrm{D}A-} \perp s_{e}^{\mathrm{D}A} \geq 0 \tag{B.4ae}$$
$$0 \leq \Upsilon_{e}^{\mathrm{D}A+} \perp \sum_{d} p_{d}^{\mathrm{D}A} - s_{e}^{\mathrm{D}A} \geq 0 \tag{B.4af}$$

B.3 KKT conditions of day-ahead market

For convenience problem (5.3) is repeated here, with dual varaibles for every constraint added.

$$\max_{\Xi^{\mathrm{D}A}} \mathcal{SW}^{\mathrm{D}A} = \sum_{d \in D} \pi_d^{\mathrm{D}A} \widehat{p}_d^{\mathrm{D}A} - \sum_{g \in G} \pi_g^{\mathrm{D}A} \widehat{p}_g^{\mathrm{D}A} - VOLL^{\mathrm{D}A} s^{\mathrm{D}A} - \pi^R \sum_r w_r^{\mathrm{D}A} \tag{B.5a}$$

subject to:

$$\sum_{g \in G} \widehat{p}_g^{\mathrm{D}A} - \sum_{d \in D} \widehat{p}_d^{\mathrm{D}A} + \sum_r w_r^{\mathrm{D}A} + s^{\mathrm{D}A} = 0, \; : (\lambda^{\mathrm{T},DA}) \tag{B.5b}$$
$$\underline{P}_g \leq \widehat{p}_g^{\mathrm{D}A} \leq \widehat{p}_g^{\mathrm{D}A}, \; \forall g \in G_e^{\mathrm{D}}, \; \forall e \in E \; : (\varsigma_{ge}^{\mathrm{T},DA-}, \varsigma_{ge}^{\mathrm{T},DA+}) \tag{B.5c}$$
$$\underline{P}_g \leq \widehat{p}_g^{\mathrm{D}A} \leq \overline{P}_g, \; \forall g \in G^{\mathrm{T}} \; : (\sigma_g^{\mathrm{T},DA-}, \sigma_g^{\mathrm{T},DA+}) \tag{B.5d}$$
$$\underline{P}_d \leq \widehat{p}_d^{\mathrm{D}A} \leq \widehat{p}_d^{\mathrm{D}A}, \; \forall d \in D_e^{\mathrm{D}}, \; \forall e \in E \; : (\varsigma_{de}^{\mathrm{T},DA-}, \varsigma_{de}^{\mathrm{T},DA+}) \tag{B.5e}$$

$$\underline{P}_d \leq \widehat{p}_d^{\mathrm{D}A} \leq \overline{P}_d,\ \forall d \in D^{\mathrm{T}}\ : (\sigma_d^{\mathrm{T},DA-}, \sigma_d^{\mathrm{T},DA+}) \tag{B.5f}$$

$$0 \leq w_r^{\mathrm{D}A} \leq W_r^{\mathrm{D}A},\ \forall r \in R\ : (\nu_r^{\mathrm{T},DA-}, \nu_r^{\mathrm{T},DA+}) \tag{B.5g}$$

$$0 \leq s^{\mathrm{l},DA} \leq \sum_d \widehat{p}_d^{\mathrm{D}A},\ : (\rho^{\mathrm{T},DA-}, \rho^{\mathrm{T},DA+}) \tag{B.5h}$$

$\widetilde{p}_g^{\mathrm{D}A}$ and $\widetilde{p}_d^{\mathrm{D}A}$ is the day ahead dispatch from problem B.1.

The lagrangian of the TSO day-ahead market problem is as follows:

$$\begin{aligned}
\mathcal{L}^{\mathrm{D}A} &= \sum_{d\in D} \pi_d^{\mathrm{D}A} \widehat{p}_d^{\mathrm{D}A} - \sum_{g\in G} \pi_g^{\mathrm{D}A} \widehat{p}_g^{\mathrm{D}A} \\
&- VOLL^{\mathrm{D}A} s^{\mathrm{D}A} - \pi^R \sum_r w_r^{\mathrm{D}A} \\
&- \lambda^{\mathrm{T},DA} \left[\sum_{g\in G} \widehat{p}_g^{\mathrm{D}A} - \sum_{d\in D} \widehat{p}_d^{\mathrm{D}A} + \sum_{r\in R} w_r^{\mathrm{D}A} + s^{\mathrm{D}A} \right] \\
&+ \sum_{g\in G_e^{\mathrm{D}},e} \left[\varsigma_{ge}^{\mathrm{T},DA-} \left(\underline{P}_g - \widehat{p}_g^{\mathrm{D}A} \right) + \varsigma_{ge}^{\mathrm{T},DA+} \left(\widehat{p}_g^{\mathrm{D}A} - \widetilde{p}_g^{\mathrm{D}A} \right) \right] \\
&+ \sum_{g\in G^{\mathrm{T}}} \left[\sigma_g^{\mathrm{T},DA-} \left(\underline{P}_g - \widehat{p}_g^{\mathrm{D}A} \right) + \sigma_g^{\mathrm{T},DA+} \left(\widehat{p}_g^{\mathrm{D}A} - \overline{P}_g \right) \right] \\
&+ \sum_{d\in D_e^{\mathrm{D}},e} \left[\varsigma_{de}^{\mathrm{T},DA-} \left(\underline{P}_d - \widehat{p}_d^{\mathrm{D}A} \right) + \varsigma_{de}^{\mathrm{T},DA+} \left(\widehat{p}_d^{\mathrm{D}A} - \widetilde{p}_d^{\mathrm{D}A} \right) \right] \\
&+ \sum_{d\in D^{\mathrm{T}}} \left[\sigma_d^{\mathrm{T},DA-} \left(\underline{P}_d - \widehat{p}_d^{\mathrm{D}A} \right) + \sigma_d^{\mathrm{T},DA+} \left(\widehat{p}_d^{\mathrm{D}A} - \overline{P}_d \right) \right] \\
&- \sum_{r\in R} \left[\nu_r^{\mathrm{T},DA-} w_r^{\mathrm{D}A} - \nu_r^{\mathrm{T},DA+} \left(w_r^{\mathrm{D}A} - W_r^{\mathrm{D}A} \right) \right] \\
&- \rho^{\mathrm{T},DA-} s^{\mathrm{D}A} + \rho^{\mathrm{T},DA+} (s^{\mathrm{D}A} - \sum_d \widehat{p}_d^{\mathrm{D}A})
\end{aligned} \tag{B.6}$$

The KKTs of the TSO day-ahead market (excluding primal constraints) are:

$$\begin{aligned}
(\widehat{p}_g^{\mathrm{D}A}): \quad & -\pi_g^{\mathrm{D}A} - \left[\varsigma_{ge}^{\mathrm{T},DA-} - \varsigma_{ge}^{\mathrm{T},DA+} \right]_{g\in G_e^{\mathrm{D}}} \\
& - \left[\sigma_g^{\mathrm{T},DA-} - \sigma_g^{\mathrm{T},DA+} \right]_{g\in G^{\mathrm{T}}} \\
& - \lambda^{\mathrm{T},DA} = 0, \quad \forall g \in G
\end{aligned} \tag{B.7a}$$

$$\begin{aligned}
(\widehat{p}_d^{\mathrm{D}A}): \quad & \pi_d^{\mathrm{D}A} - \left[\varsigma_{de}^{\mathrm{T},DA-} - \varsigma_{de}^{\mathrm{T},DA+} \right]_{d\in D_e^{\mathrm{D}}} \\
& - \left[\sigma_d^{\mathrm{T},DA-} - \sigma_d^{\mathrm{T},DA+} \right]_{d\in D^{\mathrm{T}}} - \rho^{\mathrm{T},DA+} \\
& + \lambda^{\mathrm{T},DA} = 0, \quad \forall d \in D
\end{aligned} \tag{B.7b}$$

$$(s^{\mathrm{l},DA}): \quad -VOLL^{\mathrm{D}A} - \lambda^{\mathrm{T},DA} - \rho^{\mathrm{T},DA-} + \rho^{\mathrm{T},DA+} = 0 \tag{B.7c}$$

$$(w_r^{\mathrm{D}A}): \quad -\pi^R - \lambda^{\mathrm{T},DA} - \left[\nu_r^{\mathrm{T},DA-} - \nu_r^{\mathrm{T},DA+}\right] = 0, \ \forall r \in R \tag{B.7d}$$

The complimentary constraints are:

$$0 \le \varsigma_{ge}^{\mathrm{T},DA-} \perp \widehat{p}_g^{\mathrm{D}A} - \underline{P}_g \ge 0 \quad \forall g, e \tag{B.8a}$$

$$0 \le \varsigma_{ge}^{\mathrm{T},DA+} \perp \widehat{p}_g^{\mathrm{D}A} - \widehat{p}_g^{\mathrm{D}A} \ge 0 \quad \forall g \in G_e^{\mathrm{D}}, e \in E \tag{B.8b}$$

$$0 \le \sigma_g^{\mathrm{T},DA+} \perp \overline{P}_g - \widehat{p}_g^{\mathrm{D}A} \ge 0 \quad \forall g \in G^{\mathrm{T}} \tag{B.8c}$$

$$0 \le \varsigma_{de}^{\mathrm{T},DA-} \perp \widehat{p}_d^{\mathrm{D}A} - \underline{P}_d \ge 0 \quad \forall d, e \tag{B.8d}$$

$$0 \le \varsigma_{de}^{\mathrm{T},DA+} \perp \widehat{p}_d^{\mathrm{D}A} - \widehat{p}_d^{\mathrm{D}A} \ge 0 \quad \forall d \in D_e^{\mathrm{D}}, e \in E \tag{B.8e}$$

$$0 \le \sigma_d^{\mathrm{T},DA+} \perp \overline{P}_d - \widehat{p}_d^{\mathrm{D}A} \ge 0 \quad \forall d \in D^{\mathrm{T}} \tag{B.8f}$$

$$0 \le \nu_r^{\mathrm{T},DA-} \perp w_r^{\mathrm{D}A} \ge 0, \ \forall r \in R \tag{B.8g}$$

$$0 \le \nu_r^{\mathrm{T},DA+} \perp W_r^{\mathrm{D}A} - w_r^{\mathrm{D}A} \ge 0, \ \forall r \in R \tag{B.8h}$$

$$0 \le \rho^{\mathrm{T},DA-} \perp s^{\mathrm{l},DA} \ge 0 \tag{B.8i}$$

$$0 \le \rho^{\mathrm{T},DA+} \perp \sum_d \widehat{p}_d^{\mathrm{D}A} - s^{\mathrm{l},DA} \ge 0 \tag{B.8j}$$

B.4 KKT conditions of real-time market

The KKT conditions of the SOCP problem for the real-time re-dispatch are not actually solved, because the Benders decomposition renders the scenarios solvable as single problems. However, they are used in a proof of equivalence between the DSO market and the global DA-RT combination.

The Real-Time problem from (5.4) is repeated here with dual variables added:

$$\min_{\Xi^{\mathrm{RT}}} \ \phi_\omega(\Delta\mathrm{Cost}_\omega^{\mathrm{RT}}) \tag{B.9a}$$

$$\begin{aligned}
&= \phi_\omega \Big[\sum_{g\in G} (\pi_g^{\mathrm{D}A}(p_{g\omega}^{\mathrm{RT}} - \widehat{p}_g^{\mathrm{D}A}) + \pi_g^{\uparrow} p_{g\omega}^{\uparrow} + \pi_g^{\downarrow} p_{g\omega}^{\downarrow}) \\
&+ \sum_{d\in D} (\pi_d^{\mathrm{D}A}(\widehat{p}_d^{\mathrm{D}A} - p_{d\omega}^{\mathrm{RT}}) + \pi_d^{\uparrow} p_{d\omega}^{\uparrow} + \pi_d^{\downarrow} p_{d\omega}^{\downarrow}) \\
&+ \sum_{n\in N} VOLL_n^{\mathrm{RT}} s_{n\omega}^{\mathrm{RT}} \\
&+ \sum_r \left(\pi^R(w_{r\omega}^{\mathrm{RT}} - w_r^{\mathrm{D}A}) + \pi^{\uparrow R} w_{r\omega}^{\uparrow} + \pi^{\downarrow R} w_{r\omega}^{\downarrow}\right) \Big]
\end{aligned}$$

$$
\begin{aligned}
\text{s.t.}\quad & p^{\mathrm{RT}}_{l\omega} = B_l(\theta_{n\omega} - \theta_{m\omega}), \quad \forall l \in L^{\mathrm{T}},\ : (\gamma^{\mathrm{T}}_{l\omega}) && \text{(B.9b)}\\
& p^{\mathrm{RT}}_{l\omega} \le S_l,\ \forall l \in L^{\mathrm{T}},\ : (\eta^{\mathrm{T}}_{l\omega}) && \text{(B.9c)}\\
& p^{\mathrm{RT}}_{g\omega} = \widehat{p}^{\mathrm{DA}}_{g} + p^{\uparrow}_{g\omega} - p^{\downarrow}_{g\omega}, \quad \forall g \in G,\ : (\zeta^{\mathrm{p},RT}_{g\omega}) && \text{(B.9d)}\\
& p^{\mathrm{RT}}_{d\omega} = \widehat{p}^{\mathrm{DA}}_{d} - p^{\uparrow}_{d\omega} + p^{\downarrow}_{d\omega}, \quad \forall d \in D,\ : (\zeta^{\mathrm{p},RT}_{d\omega}) && \text{(B.9e)}\\
& w^{\mathrm{RT}}_{r\omega} = w^{\mathrm{DA}}_{r} + w^{\uparrow}_{r\omega} - w^{\downarrow}_{r\omega},\ \forall r \in R,,\ : (\zeta^{\mathrm{p},RT}_{r\omega}) && \text{(B.9f)}\\
& \sum_{g\in G_n} p^{\mathrm{RT}}_{g\omega} - \sum_{d\in D_n} p^{\mathrm{RT}}_{d\omega} + \sum_{r\in R_n} w^{\mathrm{RT}}_{r\omega} + s^{\mathrm{RT}}_{n\omega}\\
& \quad = \sum_{l\in n\rightarrow} p^{\mathrm{RT}}_{l\omega} - \sum_{l\in \rightarrow n} p^{\mathrm{RT}}_{l\omega},\ \forall n \in N,\ : (\lambda^{\mathrm{p},RT}_{n\omega}) && \text{(B.9g)}\\
& \sum_{g\in G_n} q^{\mathrm{RT}}_{g\omega} - \sum_{d\in D_n} q^{\mathrm{RT}}_{d\omega} + s^{\mathrm{q},RT}_{n\omega}\\
& \quad = \sum_{l\in n\rightarrow} q^{\mathrm{RT}}_{l\omega} - \sum_{l\in \rightarrow n} q^{\mathrm{RT}}_{l\omega},\ \forall n \in N^{\mathrm{D}}_e,\ : (\lambda^{\mathrm{q},RT}_{n\omega}) && \text{(B.9h)}\\
& p^{(RT)2}_{l\omega} + q^{(RT)2}_{l\omega} \le \varphi^{\mathrm{RT}}_{l\omega} v^{\mathrm{RT}}_{n\omega},\ \forall l \in L^{\mathrm{D}}_e \cup l_e,\ : (\gamma^{\mathrm{D},RT}_{l\omega}) && \text{(B.9i)}\\
& p^{\mathrm{RT}}_{l\omega} + p^{\mathrm{RT}}_{l'\omega} = R_l \varphi^{\mathrm{RT}}_{l\omega},\ \forall l \in L^{\mathrm{D}}_e \cup l_e,\ : (\mu^{\mathrm{p},RT}_{l\omega}) && \text{(B.9j)}\\
& q^{\mathrm{RT}}_{l\omega} + q^{\mathrm{RT}}_{l'\omega} = X_l \varphi^{\mathrm{RT}}_{l\omega},\ \forall l \in L^{\mathrm{D}}_e \cup l_e,\ : (\mu^{\mathrm{q},RT}_{l\omega}) && \text{(B.9k)}\\
& p^{(RT)2}_{l\omega} + q^{(RT)2}_{l\omega} \le S^2_l,\ \forall l \in L^{\mathrm{D}}_e \cup l_e,\ : (\eta^{\mathrm{D}}_{l\omega}) && \text{(B.9l)}\\
& v^{\mathrm{RT}}_{m\omega} = v^{\mathrm{RT}}_{n\omega} - 2(R_l p^{\mathrm{RT}}_{l\omega} + X_l q^{\mathrm{RT}}_{l\omega})\\
& \quad + (R^2_l + X^2_l)\varphi^{\mathrm{RT}}_{l\omega},\ \forall l \in L^{\mathrm{D}}_e \cup l_e,\ : (\beta^{\mathrm{RT}}_{l\omega}) && \text{(B.9m)}\\
& \underline{V}^2_n \le v^{\mathrm{RT}}_{n\omega} \le \overline{V}^2_n, \quad \forall e,n \in N^{\mathrm{D}}_e,\ : (\sigma^{\mathrm{RT}-}_{n\omega}, \sigma^{\mathrm{RT}+}_{n\omega}) && \text{(B.9n)}\\
& 0 \le w^{\mathrm{RT}}_{r\omega} \le W^{\mathrm{RT}}_{r\omega}, \quad \forall r \in R,\ : (\nu^{\mathrm{RT}-}_{r\omega}, \nu^{\mathrm{RT}+}_{r\omega}) && \text{(B.9o)}\\
& \underline{P}_g \le p^{\mathrm{RT}}_{g\omega} \le \overline{P}_g, \quad \forall g \in G,\ : (\varsigma^{\mathrm{RT}-}_{g\omega}, \varsigma^{\mathrm{RT}+}_{g\omega}) && \text{(B.9p)}\\
& \underline{P}_d \le p^{\mathrm{RT}}_{d\omega} \le \overline{P}_d, \quad \forall d \in D,\ : (\varsigma^{\mathrm{RT}-}_{d\omega}, \varsigma^{\mathrm{RT}+}_{d\omega}) && \text{(B.9q)}\\
& \underline{Q}_g \le q^{\mathrm{RT}}_{g\omega} \le \overline{Q}_g, \quad \forall g \in G^{\mathrm{D}}_e,\ : (\kappa^{\mathrm{RT}-}_{g\omega}, \kappa^{\mathrm{RT}+}_{g\omega}) && \text{(B.9r)}\\
& \underline{Q}_d \le q^{\mathrm{RT}}_{d\omega} \le \overline{Q}_d, \quad \forall d \in D^{\mathrm{D}}_e,\ : (\kappa^{\mathrm{RT}-}_{d\omega}, \kappa^{\mathrm{RT}+}_{d\omega}) && \text{(B.9s)}\\
& 0 \le s^{\mathrm{RT}}_{n\omega} \le \sum_{d\in D_n} p^{\mathrm{RT}}_{d\omega},\ \forall n \in N,\ : (\Upsilon^{\mathrm{RT}-}_{n\omega}, \Upsilon^{\mathrm{RT}+}_{n\omega}) && \text{(B.9t)}\\
& p^{\uparrow}_{g\omega} \ge 0,\ , \quad p^{\downarrow}_{g\omega} \ge 0,\ \forall g,\ : (\epsilon^{\uparrow,RT}_{g\omega}, \epsilon^{\downarrow,RT}_{g\omega}) && \text{(B.9u)}\\
& p^{\uparrow}_{d\omega} \ge 0,\ , \quad p^{\downarrow}_{d\omega} \ge 0,\ \forall d,\ : (\epsilon^{\uparrow,RT}_{d\omega}, \epsilon^{\downarrow,RT}_{d\omega}) && \text{(B.9v)}\\
& w^{\uparrow}_{r\omega} \ge 0, \quad w^{\downarrow}_{r\omega} \ge 0, \forall r,\ : (\varepsilon^{\uparrow,RT}_{r\omega}, \varepsilon^{\downarrow,RT}_{r\omega}) && \text{(B.9w)}
\end{aligned}
$$

The Lagrangian of the real-time problem is as follows:

$$
\begin{aligned}
\mathcal{L}^{\mathrm{RT}} = & \sum_{\omega} \phi_{\omega} \Bigg[\sum_{g \in G} \left(\pi_g^{\mathrm{D}A} (p_{g\omega}^{\mathrm{RT}} - p_g^{\mathrm{D}A}) + \pi_g^{\uparrow} p_{g\omega}^{\uparrow} + \pi_g^{\downarrow} p_{g\omega}^{\downarrow} \right) \\
& + \sum_{d \in D} \left(\pi_d^{\mathrm{D}A} (p_d^{\mathrm{D}A} - p_{d\omega}^{\mathrm{RT}}) + \pi_d^{\uparrow} p_{d\omega}^{\uparrow} + \pi_d^{\downarrow} p_{d\omega}^{\downarrow} \right) \\
& + \sum_{n \in N} VOLL_n^{\mathrm{RT}} s_{n\omega}^{\mathrm{RT}} \\
& + \sum_{r \in R} \left(\pi^R (w_{r\omega}^{\mathrm{RT}} - w_r^{\mathrm{D}A}) + \pi^{\uparrow R} w_{r\omega}^{\uparrow} + \pi^{\downarrow R} w_{r\omega}^{\downarrow} \right) \Bigg] \\
& + \sum_{l \in L^{\mathrm{T}}} \gamma_{l\omega}^{\mathrm{T}} \left(p_{l\omega}^{\mathrm{RT}} - B_l (\theta_{n\omega} - \theta_{m\omega}) \right) \\
& + \sum_{l \in L^{\mathrm{T}}} \eta_{l\omega}^{\mathrm{T}} \left(p_{l\omega}^{\mathrm{RT}} - S_l \right) \\
& - \sum_{g \in G} \zeta_{g\omega}^{\mathrm{p}} \left(p_{g\omega}^{\mathrm{RT}} - \widehat{p}_g^{\mathrm{D}A} - p_{g\omega}^{\uparrow} + p_{g\omega}^{\downarrow} \right) \\
& - \sum_{d \in D} \zeta_{d\omega}^{\mathrm{p}} \left(p_{d\omega}^{\mathrm{RT}} - \widehat{p}_d^{\mathrm{D}A} + p_{d\omega}^{\uparrow} - p_{d\omega}^{\downarrow} \right) \\
& - \sum_{r \in R} \zeta_{r\omega}^{p} \left(w_{r\omega}^{\mathrm{RT}} - w_r^{\mathrm{D}A} - w_{r\omega}^{\uparrow} + w_{r\omega}^{\downarrow} \right) \\
& - \sum_{n \in N, \omega} \lambda_{n\omega}^{\mathrm{p},RT} \Big(\sum_{g \in G_n} p_{g\omega}^{\mathrm{RT}} - \sum_{d \in D_n} p_{d\omega}^{\mathrm{RT}} + \sum_{r \in R_n} w_{r\omega}^{\mathrm{RT}} \\
& + s_{n\omega}^{\mathrm{RT}} - \sum_{l \in n\rightarrow} p_{l\omega}^{\mathrm{RT}} + \sum_{l \in \rightarrow n} p_{l\omega}^{\mathrm{RT}} \Big) \\
& - \sum_{n \in N, \omega} \lambda_{n\omega}^{\mathrm{q},RT} \Bigg(\sum_{g \in G_n} q_{g\omega}^{\mathrm{RT}} - \sum_{d \in D_n} q_{d\omega}^{\mathrm{RT}} + s_{n\omega}^{\mathrm{q},RT} \\
& - \sum_{l \in n\rightarrow} q_{l\omega}^{\mathrm{RT}} + \sum_{l \in \rightarrow n} q_{l\omega}^{\mathrm{RT}} \Bigg) \\
& + \sum_{l \in L_e^{\mathrm{D}} \cup l_e, \omega} \gamma_{l\omega} \left[p_{l\omega}^{(RT)2} + q_{l\omega}^{(RT)2} - \varphi_{l\omega}^{\mathrm{RT}} v_{n\omega}^{\mathrm{RT}} \right] \\
& - \sum_{l \in L_e^{\mathrm{D}} \cup l_e, \omega} \Big[\mu_{l\omega}^{p} \left(p_{l\omega}^{\mathrm{RT}} + p_{l'\omega}^{\mathrm{RT}} - R_l \varphi_{l\omega}^{\mathrm{RT}} \right) \\
& \quad + \mu_{l\omega}^{q} \left(q_{l\omega}^{\mathrm{RT}} + q_{l'\omega}^{\mathrm{RT}} - X_l \varphi_{l\omega}^{\mathrm{RT}} \right) \Big] \\
& + \sum_{l \in L_e^{\mathrm{D}} \cup l_e, \omega} \left[\eta_{l\omega} \left(p_{l\omega}^{(RT)2} + q_{l\omega}^{(RT)2} - S_l \right) \right]
\end{aligned}
$$

$$
\begin{aligned}
&- \sum_{l\in L_e^{\mathrm{D}}\cup l_e,\omega} \Big[\beta_{l\omega}\Big(v_{m\omega}^{\mathrm{R}T} - v_{n\omega}^{\mathrm{R}T} + 2(R_l p_{l\omega}^{\mathrm{R}T} + X_l q_{l\omega}^{\mathrm{R}T}) \\
&\quad - (R_l^2 + X_l^2)\varphi_{l\omega}^{\mathrm{R}T}\Big)\Big] \\
&+ \sum_{n\in N_e^{\mathrm{D}}\cup n_e^{HV},\omega} \Big[\sigma_{n\omega}^{-}\Big(\underline{V}_n^2 - v_{n\omega}^{\mathrm{R}T}\Big) + \sigma_{n\omega}^{+}\Big(v_{n\omega}^{\mathrm{R}T} - \overline{V}_n^2\Big)\Big] \\
&- \sum_{r\in R,\omega} \Big[\nu_{r\omega}^{-} w_{r\omega}^{\mathrm{R}T} - \nu_{r\omega}^{+}\left(w_{r\omega}^{\mathrm{R}T} - W_{r\omega}^{\mathrm{R}T}\right)\Big] \\
&+ \sum_{g\in G,\omega} \left[\varsigma_{g\omega}^{\mathrm{R}T-}\left(\underline{P}_g - p_{g\omega}^{\mathrm{R}T}\right) + \varsigma_{g\omega}^{\mathrm{R}T+}\left(p_{g\omega}^{\mathrm{R}T} - \overline{P}_g\right)\right] \\
&+ \sum_{d\in D,\omega} \left[\varsigma_{d\omega}^{\mathrm{R}T-}\left(\underline{P}_d - p_{d\omega}^{\mathrm{R}T}\right) + \varsigma_{d\omega}^{\mathrm{R}T+}\left(p_{d\omega}^{\mathrm{R}T} - \overline{P}_d\right)\right] \\
&+ \sum_{g\in G,\omega} \Big[\kappa_{g\omega}^{\mathrm{R}T-}\Big(\underline{Q}_g - q_{g\omega}^{\mathrm{R}T}\Big) + \kappa_{g\omega}^{\mathrm{R}T+}\left(q_{g\omega}^{\mathrm{R}T} - \overline{Q}_g\right)\Big] \\
&+ \sum_{d\in D_e^{\mathrm{D}},\omega} \Big[\kappa_{d\omega}^{\mathrm{R}T-}\Big(\underline{Q}_d - q_{d\omega}^{\mathrm{R}T}\Big) + \kappa_{d\omega}^{\mathrm{R}T+}\left(q_{d\omega}^{\mathrm{R}T} - \overline{Q}_g\right)\Big] \\
&+ \sum_{g\in G,\omega} \left[-p_{g\omega}^{\uparrow}\epsilon_{g\omega}^{\mathrm{p}\uparrow} - p_{g\omega}^{\downarrow}\epsilon_{g\omega}^{\mathrm{p}\downarrow}\right] \\
&+ \sum_{r\in R,\omega} \left[-w_{r\omega}^{\uparrow}\epsilon_{r\omega}^{\mathrm{p}\uparrow} - w_{r\omega}^{\downarrow}\epsilon_{r\omega}^{\mathrm{p}\downarrow}\right] \\
&+ \sum_{d\in D,\omega} \Big[-p_{d\omega}^{\uparrow}\varepsilon_{d\omega}^{\mathrm{p}\uparrow} - p_{d\omega}^{\downarrow}\varepsilon_{d\omega}^{\mathrm{p}\downarrow}\Big] \\
&+ \sum_{n\in N,\omega} \left[-\Upsilon_{n\omega}^{\mathrm{R}T-} s_{n\omega}^{\mathrm{R}T} + \Upsilon_{n\omega}^{\mathrm{R}T+}\left(s_{n\omega}^{\mathrm{R}T} - \sum_{d\in D_n} p_{d\omega}^{\mathrm{R}T}\right)\right]
\end{aligned}
\tag{B.10}
$$

The KKT conditions of above Lagrangian are (excluding the primal constraints of B.9):

$$(p_{g\omega}^{\uparrow}):\ \phi_\omega \pi_g^{\uparrow} + \zeta_{g\omega}^{p} - \epsilon_{g\omega}^{\mathrm{p}\uparrow} = 0, \quad \forall g \in G_e^{\mathrm{D}} \tag{B.11a}$$

$$(p_{g\omega}^{\downarrow}):\ \phi_\omega \pi_g^{\downarrow} - \zeta_{g\omega}^{p} - \epsilon_{g\omega}^{\mathrm{p}\downarrow} = 0, \quad \forall g \in G_e^{\mathrm{D}} \tag{B.11b}$$

$$(p_{d\omega}^{\uparrow}):\ \phi_\omega \pi_d^{\uparrow} - \zeta_{d\omega}^{p} - \varepsilon_{i\omega}^{\mathrm{p}\uparrow} = 0, \quad \forall d \in D_e^{\mathrm{D}} \tag{B.11c}$$

$$(p_{d\omega}^{\downarrow}):\ \phi_\omega \pi_d^{\downarrow} + \zeta_{d\omega}^{p} - \varepsilon_{d\omega}^{\mathrm{p}\downarrow} = 0, \quad \forall d \in D_e^{\mathrm{D}} \tag{B.11d}$$

$$(w_{r\omega}^{\uparrow}):\ \phi_\omega \pi^{\uparrow R} + \zeta_{r\omega}^{p} - \epsilon_{r\omega}^{\mathrm{p}\uparrow} = 0, \quad \forall r \in R_e^{\mathrm{D}} \tag{B.11e}$$

$$(w_{r\omega}^{\downarrow}):\ \phi_\omega \pi^{\downarrow R} - \zeta_{r\omega}^{p} - \epsilon_{r\omega}^{\mathrm{p}\downarrow} = 0, \quad \forall r \in R_e^{\mathrm{D}} \tag{B.11f}$$

$$(s^{\mathrm{RT}}_{n\omega}) : \phi_\omega \mathrm{VOLL}_n - \lambda^{\mathrm{p},RT}_{n\omega} - \Upsilon^{\mathrm{RT}-}_{n\omega} + \Upsilon^{\mathrm{RT}+}_{n\omega} = 0,\ \forall n \in N \tag{B.11g}$$

$$(w^{\mathrm{RT}}_{r\omega}) : \phi_\omega \pi^R - \zeta^p_{r\omega} - \left[\lambda^{\mathrm{p},RT}_{n\omega}\right]_{n_r} + \nu^+_{r\omega} - \nu^-_{r\omega} = 0, \quad \forall r \in R^{\mathrm{D}}_e \tag{B.11h}$$

$$(p^{\mathrm{RT}}_{g\omega}) : \phi_\omega \pi^{\mathrm{D}A}_g - \zeta^p_{g\omega} - \varsigma^{\mathrm{RT}-}_{g\omega} + \varsigma^{\mathrm{RT}+}_{g\omega} - \left[\lambda^{\mathrm{p},RT}_{n\omega}\right]_{n_g} = 0, \quad \forall g \in G \tag{B.11i}$$

$$(q^{\mathrm{RT}}_{g\omega}) : -\kappa^{\mathrm{RT}-}_{g\omega} + \kappa^{\mathrm{RT}+}_{g\omega} - \left[\lambda^{\mathrm{q},RT}_{n\omega}\right]_{n_g} = 0, \quad \forall g \in G^{\mathrm{D}}_e \tag{B.11j}$$

$$(p^{\mathrm{RT}}_{d\omega}) : -\phi_\omega \pi^{\mathrm{D}A}_d - \zeta^p_{d\omega} - \varsigma^{\mathrm{RT}-}_{d\omega} + \varsigma^{\mathrm{RT}+}_{d\omega} + \left[\lambda^{\mathrm{p},RT}_{n\omega} - \Upsilon^{\mathrm{RT}+}_{n\omega}\right]_{n_d} = 0, \quad \forall d \in D \tag{B.11k}$$

$$(q^{\mathrm{RT}}_{d\omega}) : -\kappa^{\mathrm{RT}-}_{d\omega} + \kappa^{\mathrm{RT}+}_{d\omega} + \left[\lambda^{\mathrm{q},RT}_{n\omega}\right]_{n_d} = 0, \quad \forall d \in D^{\mathrm{D}}_e \tag{B.11l}$$

$$(p^{\mathrm{RT}}_{l\omega}) : \lambda^{\mathrm{p},RT}_{n\omega} - \lambda^{\mathrm{p},RT}_{m\omega} + \Big[2\gamma_{l\omega} p^{\mathrm{RT}}_{l\omega} - \mu^{\mathrm{p}}_{l\omega} - \mu^{\mathrm{p}}_{l'\omega} + 2\eta_{l\omega} p^{\mathrm{RT}}_{l\omega} - 2\beta_{l\omega} R_l\Big]_{l\in L^{\mathrm{D}}_e} + \Big[\gamma^{\mathrm{T}}_{l\omega} + \eta^{\mathrm{T}}_{l\omega}\Big]_{l\in L^{\mathrm{T}}} = 0, \quad \forall l \in L \tag{B.11m}$$

$$(q^{\mathrm{RT}}_{l\omega}) : \lambda^{\mathrm{q},RT}_{n\omega} - \lambda^{\mathrm{q},RT}_{m\omega} + \Big[2\gamma_{l\omega} q^{\mathrm{RT}}_{l\omega} - \mu^{q}_{l\omega} - \mu^{q}_{l'\omega} + 2\eta_{l\omega} q^{\mathrm{RT}}_{l\omega} - 2\beta_{l\omega} X_l\Big]_{l\in L^{\mathrm{D}}_e} = 0, \quad \forall l \in L \tag{B.11n}$$

$$(\varphi^{\mathrm{RT}}_{l\omega}) : -\gamma_{l\omega} v^{\mathrm{RT}}_{n\omega} + \mu^{p}_{l\omega} R_l + \mu^{q}_{l\omega} X_l + \beta_{l\omega}(R_l^2 + X_l^2) = 0, \quad \forall \omega, l = (n,m) \in L^{\mathrm{D}}_e \tag{B.11o}$$

$$(v^{\mathrm{RT}}_{n\omega}) : -\gamma_{l\omega} \varphi^{\mathrm{RT}}_{l\omega} - \beta_{l'\omega} + \beta_{l\omega} - \sigma^-_{n\omega} + \sigma^+_{n\omega} = 0, \quad \forall \omega, l = (n,m) \in L^{\mathrm{D}}_e \tag{B.11p}$$

B.5 Proof of proposition 1

Proposition 1: The first order necessary conditions (KKT conditions) of the day-ahead market and the real-time market combined contain all the KKT conditions of the DSO market in (B.1) and solving (5.2) is equivalent to solving (5.1).

Proof of propositon 1: Problem (5.3) and (5.4) are explicitly convex. Therefore their KKT conditions are also optimality conditions. This is the first part of the proof. The KKT conditions of the DSO market in (B.1) are given in (B.3) and (B.4). The DSO market is also explicitly convex and the KKT conditions define optimality. The KKT conditions of the day-ahead market are presented in (B.7) and (B.8). All equations of (B.3) are contained in either (B.7) or (B.11) with exception of the variables related to the PCC injections in feeder e. The dual constraints with regards to those variables are (B.3u) through (B.3y). The PCC prices $\pi^{PCC,DA}_e, \pi^{\uparrow PCC}_e$, $\pi^{\downarrow PCC}_e$ and

the PCC flow limits $\overline{f}_e, \underline{f}_e$ are variables in the upper level problem (5.1) and therefore constitute slack variables that will not influence the optimality of (B.1). Therefore removing the DSO market lower level problem and solving (5.2) is equivalent to solving (5.1). This ends the proof. □

B.6 Scenario generation

A simple scenario generation method is used for the uncertainties of the wind production. The distance of the wind farms are

$$D_{rw} = \left|\left| \begin{array}{c} x_r - x_w \\ y_r - y_w \end{array} \right|\right|, \quad \forall r \in R, w \in R, r \neq w \tag{B.12}$$

The co-variance matrix is now given in (B.13).

$$\Sigma_{rw} = \frac{\sigma_r^2 + \sigma_w^2}{2} e^{-D_{rw}}, \forall r \in R, w \in R \tag{B.13}$$

The distributions of the wind generators are thus:

$$W \sim \mathcal{N}_r(\mu_r, \Sigma_{rw}) \tag{B.14}$$

Now the scenarios can be drawn by random sampling i.e.

$$W_{r\omega}^{RT} \sim\sim \mathcal{N}_r(\mu_r, \Sigma_{rw}) \tag{B.15}$$

B.7 Modified 24 bus test network

The 24-bus power system – Single area RTS-96 is used here in a modified form. The mean and variance of the wind power plants in the network are given in table B.1. The locations of each wind farm is given in table B.2, which is used to claculate the distance between them as in equation (B.12).

	W_1	W_2	W_3	W_4	W_5	W_6	W_7
Variance σ^2	750	740	760	300	300	300	200
Mean μ	200	200	200	40	40	40	10

Table B.1: The mean of the forecast of the installed RES and variance of the forecast.

B.8 Congestion level

The Congestion level of the colored dots in Fig. 5.4 is here plotted as a line plot in Fig. B.2. The data for the two plots is the same.

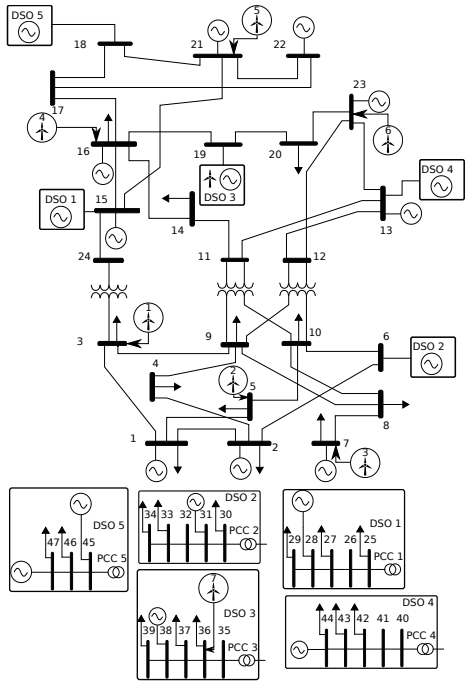

Figure B.1: Diagram of the 24-bus power system – Single area RTS-96. 5 DSO feeders have been added, as well as 7 Wind power plants. The loads from the buses where the DSO feeders are connected have been moved to the DSO feeders.

	W_1	W_2	W_3	W_4	W_5	W_6	W_7
X-coordinate	0	0.25	0.5	6	6.25	6.5	6.75
Y-Coordinate	0	0	0	5	5	5	5.2

Table B.2: Georgraphical location of each wind farm.

B.9 Computational performance

Here we show some results pertaining to the Benders decomposition approach that was presented in section 5.4. In Fig. B.3 we present the convergence of the suggested multicut benders decomposition for a sample point of wind-penetration.

The upper bound of the benders decomposed problems in iteration (i) is found as:

$$UB^{(\mathrm{i})} = \mathcal{SW}^{\mathrm{DA}(i)} - \sum_{\omega} \phi_{\omega} \Delta \mathrm{Cost}_{\omega}^{\mathrm{RT(i)}} \tag{B.16}$$

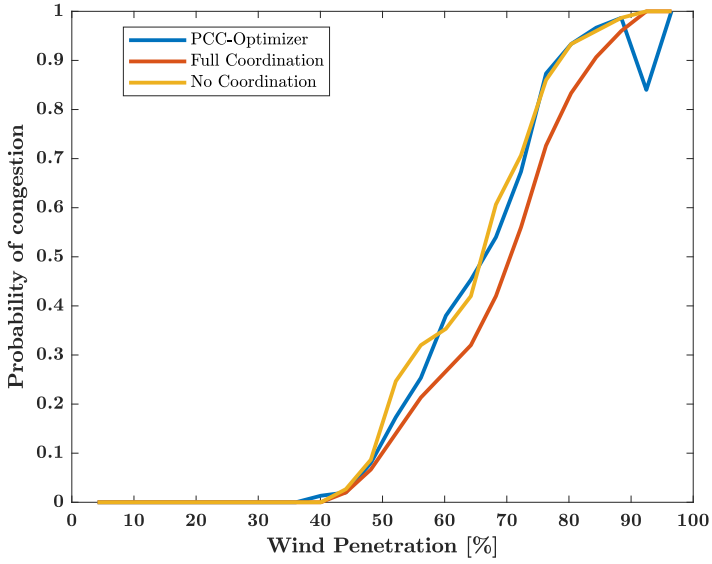

Figure B.2: Probability of at least two transmission lines being congested in RT.

The lower bound in iteration (i) is found via:

$$LB^{(\mathrm{i})} = \mathcal{SW}^{\mathrm{DA}(i)} - \sum_{\omega} \phi_{\omega} \psi_{\omega}^{(\mathrm{i})} \tag{B.17}$$

The computational burden of the decomposed problem is analyzed by logging the time it takes Mosek 8.0 to solve every master-problem and sub-problem for every scenario. The implementation we use in this paper relies on the CVX plugin for Matlab, which yields large overhead due to the time it takes to initialize every master-problem and sub-problem. Therefore the results in table 5.1 only give the time that the solver actually spent, while the full time including the overhead for the initialization is about two to four times this number. In the future we wish to use an implementation that does not rely on CVX which can help solving larger case studies. The data provided in table 5.1 is the average over all the different wind-penetration settings of the RES (i.e. it is the average of 24 different wind penetration settings). Because the sub-problems are independent, and can be solved in parallel, the number of scenarios do not affect the computational time as long as there are enough CPU-cores to solve them in parallel.

The number of binary variables in the master-problem depend on the number of complimentarity constraints in (B.8). Because we choose to solve the complimentarity constraints with the Big-M approach every one of these constraints uses one binary. The number of complimentarity constraints in turn depend mainly on the number

of generators, number of elastic demands and number of RES sources. In the case study for this work the master problem therefore contains 196 binary variables. As a result of the benders decomposition the conic constraints have all been moved to the subproblem, and therefore the master problem is MILP, while the subproblems are continuous SOCP.

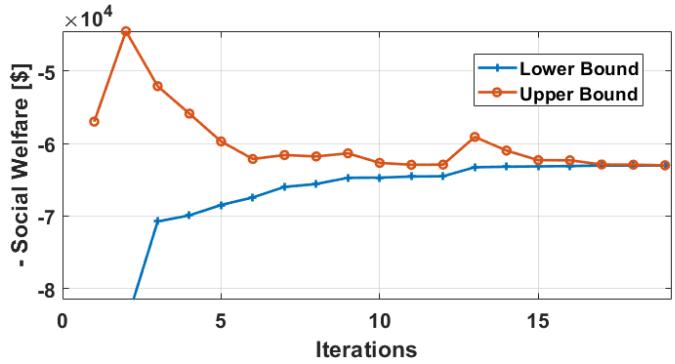

Figure B.3: Convergence of the Benders decomposition upper and lower bound over the iterations. Note, we minimize $-\mathcal{SW}$, which is equivalent to maximizing social welfare.

Bibliography

[1] F. Bouffard and D. S. Kirschen, "Centralised and distributed electricity systems," *Energy Policy*, volume 36, number 12, pages 4504–4508, 2008.

[2] J. M. Morales, A. J. Conejo, H. Madsen, P. Pinson, and M. Zugno, *Integrating renewables in electricity markets - Operational problems*, F. S. Hillier, Ed. Springer, 2014.

[3] Energinet, "Environmental report 2017," Danish TSO, Frederecia, Tech. Rep., 2017. [Online]. Available: `https://en.energinet.dk/About-our-reports/Reports/Environmental-Report-2018`.

[4] C. Eid, P. Codani, Y. Perez, J. Reneses, and R. Hakvoort, "Managing electric flexibility from Distributed Energy Resources: A review of incentives for market design," *Renewable and Sustainable Energy Reviews*, volume 64, pages 237–247, 2016. [Online]. Available: `http://dx.doi.org/10.1016/j.rser.2016.06.008`.

[5] E. Niesten and F. Alkemade, "How is value created and captured in smart grids? A review of the literature and an analysis of pilot projects," *Renewable and Sustainable Energy Reviews*, volume 53, pages 629–638, 2016. [Online]. Available: `http://dx.doi.org/10.1016/j.rser.2015.08.069`.

[6] H. Jiayi, J. Chuanwen, and X. Rong, "A review on distributed energy resources and MicroGrid," *Renewable and Sustainable Energy Reviews*, volume 12, pages 2465–2476, 2008.

[7] M. Behrangrad, "A review of demand side management business models in the electricity market," *Renewable and Sustainable Energy Reviews*, volume 47, pages 270–283, 2015.

[8] J. Villar, R. Bessa, and M. Matos, "Flexibility products and markets: Literature review," *Electric Power Systems Research*, volume 154, pages 329–340, 2018.

[9] N. Good, K. A. Ellis, and P. Mancarella, "Review and classification of barriers and enablers of demand response in the smart grid," *Renewable and Sustainable Energy Reviews*, volume 72, pages 57–72, 2017.

[10] D. Pudjianto, C. K. Gan, V. Stanojevic, M. Aunedi, P. Djapic, and G. Strbac, "Value of integrating distributed energy resources in the UK electricity system," *Power & Energy Society General Meeting (PESGM)*, pages 1–6, 2010.

[11] T. Morstyn, A. Teytelboym, and M. D. Mcculloch, "Designing decentralized markets for distribution system flexibility," *IEEE Transactions on Power Systems*, volume to be publ, pages 1–12, 2018.

[12] Q. Wang, C. Zhang, Y. Ding, G. Xydis, J. Wang, and J. Østergaard, "Review of real-time electricity markets for integrating distributed energy resources and demand response," *Applied Energy*, volume 138, pages 695–706, 2015.

[13] N. O'Connell, P. Pinson, H. Madsen, and M. O'Malley, "Benefits and challenges of electrical demand response : A critical review," *Renewable and Sustainable Energy Reviews*, volume 39, pages 686–699, 2014.

[14] M. Vallés, J. Reneses, R. Cossent, and P. Frías, "Regulatory and market barriers to the realization of demand response in electricity distribution networks : A European perspective," *Electric Power Systems Research*, volume 140, pages 689–698, 2016.

[15] N. O'Connell, "Approaches for Accommodating Demand Response in Operational Problems and Assessing its Value," PhD thesis, Technical University of Denmark, 2016. [Online]. Available: `http://orbit.dtu.dk/files/123041948/phd401%7B%5C_%7DOConnel%7B%5C_%7DN.pdf`.

[16] M. Alizadeh, A. Scaglione, A. Goldsmith, and G. Kesidis, "Capturing aggregate flexibility in demand response," in *53rd Conference on Decision and Control (CDC)*, IEEE, 2014, pages 6439–6445.

[17] N. O'Connell, H. Madsen, P. Pinson, M. O'Malley, and T. Green, "Regulating power from supermarket refrigeration," in *Innovative Smart Grid Technologies Conference (ISGT)*, IEEE, 2015.

[18] L. A. Greening, D. L. Greene, and C. Difiglio, "Energy efficiency and consumption - The rebound effect - A survey," *Energy Policy*, volume 28, pages 389–401, 2000.

[19] S. Sorrell and J. Dimitropoulos, "The rebound effect: Microeconomic definitions, limitations and extensions," *Ecological Economics*, volume 65, number 3, pages 636–649, 2008.

[20] N. O'connell, H. Madsen, P. Delff, P. Pinson, and M. O 'malley, "Model identification for control of display units in supermarket refrigeration systems," Technical University of Denmark, Kgs. Lyngby, Tech. Rep. 2, 2014. [Online]. Available: `http://orbit.dtu.dk/files/108341957/tr14%7B%5C_%7D02%7B%5C_%7DOConnell%7B%5C_%7DN.pdf`.

[21] N. O'Connell, H. Madsen, P. Pinson, and M. O'Malley, "Modelling and assessment of the capabilities of a supermarket refrigeration system for the provision of regulating power," Technical University of Denmark, Kgs. Lyngby, Tech. Rep., 2014, pages 1–35. [Online]. Available: `http://orbit.dtu.dk/en/publications/modelling-and-assessment-of-the-capabilities-of-a-supermarket-refrigeration-system-for-the-provision-of-regulating-power(25f6d19a-7058-4d93-9e60-4a8b2492df31).html`.

[22] S. E. Shafiei, H. Rasmussen, and J. Stoustrup, "Modeling supermarket refrigeration systems for demand-side management," *Energies*, volume 6, number 2, pages 900–920, 2013.

[23] E. Georges, B. Cornélusse, D. Ernst, V. Lemort, and S. Mathieu, "Residential heat pump as flexible load for direct control service with parametrized duration and rebound effect," *Applied Energy*, volume 187, pages 140–153, 2017.

[24] Y. Kim and L. K. Norford, "Optimal use of thermal energy storage resources in commercial buildings through price-based demand response considering distribution network operation," *Applied Energy*, volume 193, pages 308–324, 2017.

[25] R. Halvgaard, N. K. Poulsen, H. Madsen, and J. B. Jorgensen, "Economic model predictive control for building climate control in a smart grid," in *Innovative Smart Grid Technologies Conference (ISGT)*, IEEE, 2012, pages 1–6.

[26] B. Felten and C. Weber, "The value(s) of flexible heat pumps – Assessment of technical and economic conditions," *Applied Energy*, volume 228, pages 1292–1319, 2018.

[27] R. Li, Q. Wu, and S. S. Oren, "Distribution locational marginal pricing for optimal electric vehicle charging management," *IEEE Transactions on Power Systems*, volume 29, number 4, page 1866, 2014.

[28] Z. Liu, Q. Wu, and S. S. Oren, "Distribution locational marginal pricing for optimal electric vehicle charging through chance constrained mixed-integer programming," *IEEE Transactions on Power Systems*, volume 29, number 1, pages 203–211, 2016.

[29] S. Huang, Q. Wu, S. S. Oren, R. Li, and Z. Liu, "Distribution locational marginal pricing through quadratic programming for congestion management in distribution networks," *IEEE Transactions on Power Systems*, volume 30, number 4, pages 2170–2178, 2015.

[30] P. Sulc, S. Backhaus, and M. Chertkov, "Optimal distributed control of reactive power via the alternating direction method of multipliers," *IEEE Transactions on Energy Conversion*, volume 29, number 4, pages 968–977, 2014.

[31] J. Lavaei and S. H. Low, "Zero duality gap in optimal power flow problem," *IEEE Transactions on Power Systems*, volume 27, number 1, pages 92–107, 2012.

[32] S. H. Low, "Convex Relaxation of Optimal Power Flow—Part i: Formulations and Equivalence," *IEEE Transactions on Control of Network Systems*, volume 1, number 1, pages 15–27, 2014.

[33] ——, "Convex relaxation of optimal power flow - Part ii: Exactness," *IEEE Transactions on Control of Network Systems*, volume 1, number 2, pages 177–189, 2014.

[34] R. A. Jabr, "Radial distribution load flow using conic programming," *IEEE Transactions on Power Systems*, volume 21, number 3, pages 1458–1459, 2006.

[35] A. Papavasiliou, "Analysis of distribution locational marginal prices," *IEEE Transactions on Smart Grid*, volume 9, number 5, pages 4872–4882, 2017.

[36] L. Halilbasic, P. Pinson, and S. Chatzivasileiadis, "Convex relaxations and approximations of chance constrained AC-OPF problems," *IEEE Transactions on Power Systems*, volume 34, number 2, pages 1459–1470, 2019.

[37] Y. Liu, J. T. Holzer, and M. C. Ferris, "Extending the bidding format to promote demand response," *Energy Policy*, volume 86, pages 82–92, 2015.

[38] H. Le Cadre, "On the efficiency of local electricity markets," in *International Conference on the European Energy Market (EEM)*, IEEE, 2017.

[39] S. Bose, D. Cai, and A. Wierman, "On the role of a market maker in networked cournot competition," in *53rd Conference on Decision and Control (CDC)*, IEEE, 2014, pages 4479–4484.

[40] Y. Xu, D. Cai, S. Bose, and A. Wierman, "On the efficiency of networked Stackelberg competition," in *51st Annual Conference on Information Sciences and Systems (CISS)*, Baltimore, USA: IEEE, 2017.

[41] I. Mezghani, A. Papavasiliou, and H. Le Cadre, "A generalized nash equilibrium analysis of electric power transmission-distribution coordination," in *e-Energy'18: The Ninth International Conference on Future Energy Systems*, 2018, pages 1–20.

[42] A. Papavasiliou and I. Mezghani, "Coordination schemes for the integration of transmission and distribution system operations," in *20th Power Systems Computation Conference (PSCC)*, IEEE, 2018.

[43] H. Gerard, E. I. Rivero Puente, and D. Six, "Coordination between transmission and distribution system operators in the electricity sector: A conceptual framework," *Utilities Policy*, volume 50, pages 40–48, 2018.

[44] H. Le Cadre, I. Mezghani, and A. Papavasiliou, "A game-theoretic analysis of transmission-distribution system operator coordination," *European Journal of Operational Research*, volume 274, number 1, pages 317–339, 2019.

[45] A. Mohammadi, M. Mehrtash, and A. Kargarian, "Diagonal quadratic approximation for decentralized collaborative TSO+DSO optimal power flow," *IEEE Transactions on Smart Grid*, number to be published, 2018.

[46] M. Caramanis, E. Ntakou, W. W. Hogan, A. Chakrabortty, and J. Schoene, "Co-optimization of power and reserves in dynamic T&D power markets with nondispatchable renewable generation and distributed energy resources," *Proceedings of the IEEE*, volume 104, number 4, pages 807–836, 2016.

[47] A. Saint-Pierre and P. Mancarella, "Active distribution system management : A dual-horizon scheduling framework for DSO/TSO interface under uncertainty," *IEEE Transactions on Smart Grid*, volume 8, number 5, pages 2186–2197, 2016.

[48] A. Vicente Pastor, J. Nieto Martin, D. W. Bunn, and A. Laur, "Evaluation of flexibility markets for Retailer-DSO-TSO coordination," *IEEE Transactions on Power Systems*, 2018.

[49] J. P. Silva, J. A. Sumaili, R. J. Bessa, L. Seca, M. A. Matos, V. Miranda, M. Caujolle, B. Goncer-Maraver, and M. Sebastian-Viana, "Estimating the active and reactive power flexibility area at the TSO-DSO interface," *IEEE Transactions on Power Systems*, volume 33, number 5, pages 4741–4750, 2018.

[50] D. M. Gonzalez, J. Hachenberger, J. Hinker, F. Rewald, C. Rehtanz, and J. Myrzik, "Determination of the time-dependent flexibility of active distribution networks to control their TSO-DSO interconnection power flow," in *20th Power Systems Computation Conference (PSCC)*, IEEE, 2018.

[51] M. Bragin and Y. Dvorkin, "Toward coordinated transmission and distribution operations," in *Power & Energy Society General Meeting (PESGM)*, Portland: IEEE, 2018.

[52] S. Huang, Q. Wu, H. Zhao, and C. Li, "Distributed optimization based dynamic tariff for congestion management in distribution networks," *IEEE Transactions on Smart Grid*, volume 10, number 1, pages 184–192, 2019.

[53] M. R. Sarker, M. A. Ortega-Vazquez, and D. S. Kirschen, "Optimal coordination and scheduling of demand response via monetary incentives," *IEEE Transactions on Smart Grid*, volume 6, number 3, pages 1341–1352, 2015.

[54] H. Zhong, L. Xie, and Q. Xia, "Coupon incentive-based demand response: Theory and case study," *IEEE Transactions on Power Systems*, volume 28, number 2, pages 1266–1276, 2013.

[55] S. Huang, Q. Wu, J. Wang, and H. Zhao, "A sufficient condition on convex relaxation of AC optimal power flow in distribution networks," *IEEE Transactions on Power Systems*, volume 32, number 2, pages 1359–1368, 2017.

[56] R. A. Verzijlbergh, L. J. De Vries, and Z. Lukszo, "Renewable energy sources and responsive demand. Do we need congestion management in the distribution grid?" *IEEE Transactions on Power Systems*, volume 29, number 5, pages 2119–2128, 2014.

[57] F. Sossan, "Indirect control of flexible demand for power system applications," PhD thesis, Technical University of Denmark, 2014. [Online]. Available: `https://core.ac.uk/download/pdf/24847772.pdf`.

[58] N. O'connell, P. Pinson, H. Madsen, and M. O'malley, "Economic Dispatch of Demand Response Balancing Through Asymmetric Block Offers," *IEEE Transactions on Power Systems*, volume 31, number 4, pages 2999–3007, 2016.

[59] L. Gan, N. Li, U. Topcu, and S. H. Low, "Exact convex relaxation of optimal power flow in radial networks," *IEEE Transactions on Automatic Control*, volume 60, number 1, pages 72–87, 2015.

[60] M. Farivar and S. H. Low, "Branch flow model: Relaxations and convexification - part i," *IEEE Transactions on Power Systems*, volume 28, number 3, pages 2554–2564, 2013.

[61] E. J. Coster, J. M. Myrzik, B. Kruimer, and W. L. Kling, "Integration issues of distributed generation in distribution grids," *Proceedings of the IEEE*, volume 99, number 1, pages 28–39, 2011.

[62] J. a. P. Lopes, N. Hatziargyriou, J. Mutale, P. Djapic, and N. Jenkins, "Integrating distributed generation into electric power systems: A review of drivers, challenges and opportunities," *Electric Power Systems Research*, volume 77, pages 1189–1203, 2007.

[63] S. Y. Hadush and L. Meeus, "DSO-TSO cooperation issues and solutions for distribution grid congestion management," *Energy Policy*, volume 120, pages 610–621, 2018.

[64] C. Zhang, Y. Ding, N. C. Nordentoft, P. Pinson, and J. Østergaard, "FLECH: A Danish market solution for DSO congestion management through DER flexibility services," *Journal of Modern Power Systems and Clean Energy*, volume 2, number 2, pages 126–133, 2014.

[65] Y. K. Renani, M. Ehsan, and M. Shahidehpour, "Optimal transactive market operations with distribution system operators," *IEEE Transactions on Smart Grid*, volume 9, number 6, pages 6692–6701, 2018.

[66] S. Huang and Q. Wu, "Real-time congestion management in distribution networks by flexible demand swap," *IEEE Transactions on Smart Grid*, volume 9, number 5, pages 4346–4355, 2018.

[67] N. O'Connell, Q. Wu, J. Østergaard, A. H. Nielsen, S. T. Cha, and Y. Ding, "Day-ahead tariffs for the alleviation of distribution grid congestion from electric vehicles," *Electric Power Systems Research*, volume 92, pages 106–114, 2012.

[68] L. Bai, J. Wang, C. Wang, C. Chen, and F. Li, "Distribution locational marginal pricing (DLMP) for congestion management and voltage support," *IEEE Transactions on Power Systems*, volume 33, number 4, pages 4061–4073, 2018.

[69] M. G. Pollitt, "The role of policy in energy transitions: Lessons from the energy liberalisation era," *Energy Policy*, volume 50, pages 128–137, 2012.

[70] D. M. Newbery, "Privatisation and liberalisation of network utilities," *European Economic Review*, volume 41, number 3-5, pages 357–383, 1997.

[71] D. Kirschen and G. Strbac, *Fundamentals of power system economics*. Hoboken, NJ, USA: Wiley, 2004.

[72] F. C. Schweppe, M. C. Caramanis, R. D. Tabors, and R. E. Bohn, *Spot pricing of electricity*. Springer Science & Business Media, 2013.

[73] P. Kundur, N. J. Balu, and M. G. Lauby, *Power system stability and control*. McGraw-Hill New York, 1994.

[74] M. Rossi, G. Viganò, and D. Moneta, "Hosting capacity of distribution networks: Evaluation of the network congestion risk due to distributed generation," in *International Conference on Clean Electrical Power (ICCEP)*, IEEE, 2015, pages 716–722.

[75] R. Walling, R. Saint, R. C. Dugan, J. Burke, and L. A. Kojovic, "Summary of distributed resources impact on power delivery systems," *IEEE Transactions on Power Delivery*, volume 23, number 3, pages 1636–1644, 2008.

[76] B. Bocker, S. Kippelt, C. Weber, and C. Rehtanz, "Storage valuation in congested grids," *IEEE Transactions on Smart Grid*, volume 9, number 6, pages 6742–6751, 2018.

[77] Federal Energy Regulatory Commission, "Distributed energy resources: Technical considerations for the bulk power system," Federal Energy Regulation Comission, Tech. Rep. February, 2018, pages 0–46. [Online]. Available: `https://www.ferc.gov/CalendarFiles/20180215112833-der-report.pdf`.

[78] E. G. Consortium, *EcoGrid 2.0 website*. [Online]. Available: `http://www.ecogrid.dk/` (visited on April 20, 2018).

[79] E. Comission, *Proposal for a regulation of the european parliament and of the council on the internal market for electricity*, Brussels, 2016. [Online]. Available: `https://eur-lex.europa.eu/resource.html?uri=cellar:d7108c4c-b7b8-11e6-9e3c-01aa75ed71a1.0001.02/DOC%7B%5C_%7D1%7B%5C&%7Dformat=PDF`.

[80] H. Gerard, E. Rivero, and D. Six, "Basic schemes for TSO-DSO coordination and ancillary services provision," Tech. Rep., 2016, page 98.

[81] S. Consortium, *SmartNet project*, 2019. [Online]. Available: `http://smartnet-project.eu/` (visited on January 2, 2019).

[82] W. E. Mabee, J. Mannion, and T. Carpenter, "Comparing the feed-in tariff incentives for renewable electricity in Ontario and Germany," *Energy Policy*, volume 40, number 1, pages 480–489, 2012.

[83] L. Deng, B. F. Hobbs, and P. Renson, "What is the cost of negative bidding by wind? A unit commitment analysis of cost and emissions," *IEEE Transactions on Power Systems*, volume 30, number 4, pages 1805–1814, 2015.

[84] L. Vandezande, L. Meeus, R. Belmans, M. Saguan, and J. M. Glachant, "Well-functioning balancing markets: A prerequisite for wind power integration," *Energy Policy*, volume 38, number 7, pages 3146–3154, 2010.

[85] L. Hirth and I. Ziegenhagen, "Balancing power and variable renewables: Three links," *Renewable and Sustainable Energy Reviews*, volume 50, pages 1035–1051, 2015.

[86] P. Van Den Oosterkamp, P. Koutstaal, A. Van Der Welle, J. De Joode, J. Lenstra, K. Van Hussen, and R. Haffner, "The role of DSOs in a Smart Grid environment," European Comission, Amsterdam/Rotterdam, Tech. Rep., 2014. [Online]. Available: `https://ec.europa.eu/energy/sites/ener/files/documents/20140423%7B%5C_%7Ddso%7B%5C_%7Dsmartgrid.pdf`.

[87] L. Martini and A. Iliceto, "Renewable Integration: An Opinion from the European Perspective 'In My View'," *IEEE Power and Energy Magazine*, volume 16, number 6, pages 112–110, 2018.

[88] B. Biegel, L. H. Hansen, J. Stoustrup, P. Andersen, and S. Harbo, "Value of flexible consumption in the electricity markets," *Energy*, volume 66, pages 354–362, 2014.

[89] A. Mnatsakanyan and S. W. Kennedy, "A novel demand response model with an application for a virtual power plant," *IEEE Transactions on Smart Grid*, volume 6, number 1, pages 230–237, 2015.

[90] F. Lezama, J. Soares, P. Hernandez-Leal, M. Kaisers, T. Pinto, and Z. M. Almeida do Vale, "Local energy markets: Paving the path towards fully transactive energy systems," *IEEE Transactions on Power Systems*, pages 1–8, 2018.

[91] T. Sousa, T. Soares, P. Pinson, F. Moret, T. Baroche, and E. Sorin, "Peer-to-peer and community-based markets: A comprehensive review," *Renewable and Sustainable Energy Reviews*, volume 104, pages 367–378, 2019.

[92] B. Felten, J. Raasch, and C. Weber, "Photovoltaics and heat pumps - Limitations of local pricing mechanisms," *Energy Economics*, volume 71, pages 383–402, 2018.

[93] D. Consortium, *DREM project website*, 2019. [Online]. Available: `https://drem.dk/` (visited on January 2, 2019).

[94] *Nordpool website*, 2019. [Online]. Available: `https://www.nordpoolgroup.com/` (visited on March 1, 2019).

[95] H.-p. Chao and H. G. Huntington, *Designing competetive electricity markets*, 13th edition. Springer Science & Business Media, 2013.

[96] T. V. Jensen, J. Kazempour, and P. Pinson, "Cost-optimal ATCs in zonal electricity markets," *IEEE Transactions on Power Systems*, volume 33, number 4, pages 3624–3633, 2018.

[97] S. Nykamp, T. Rott, N. Dettke, and S. Kueppers, "The project 'ElChe' Wettringen: storage as an alternative to grid reinforcements - Experiences, benefits and challenges from a DSO point of view," in *International ETG Congress*, Bonn: VDE Verlag, 2015, pages 521–526.

[98] S. Ropenus, H. K. Jacobsen, and S. T. Schröder, "Network regulation and support schemes - How policy interactions affect the integration of distributed generation," *Renewable Energy*, volume 36, number 7, pages 1949–1956, 2011.

[99] V. Grimm, A. Martin, M. Weibelzahl, and G. Zöttl, "On the long run effects of market splitting: Why more price zones might decrease welfare," *Energy Policy*, volume 94, pages 453–467, 2016.

[100] J. P. Chaves-Ávila and C. Fernandes, "The Spanish intraday market design: A successful solution to balance renewable generation?" *Renewable Energy*, volume 74, pages 422–432, 2015.

[101] C. Weber, "Adequate intraday market design to enable the integration of wind energy into the European power systems," *Energy Policy*, volume 38, number 7, pages 3155–3163, 2010.

[102] ENTSO-E, *ENTSO-E website*, 2019. [Online]. Available: `https://www.entsoe.eu/about/inside-entsoe/objectives/`.

[103] F. Ocker, S. Braun, and C. Will, "Design of European balancing power markets," in *International Conference on the European Energy Market (EEM)*, volume 2016-July, IEEE, 2016, pages 1–6.

[104] Energinet, *Agreement on future Nordic balancing*, 2018. [Online]. Available: `https://en.energinet.dk/About-our-news/News/2018/03/09/Agreement-on-future-Nordic-balancing`.

[105] Réseau de transport d'électricité SA (Rte), "French capacity market - report accompanying the draft rules," RTE, Tech. Rep., 2014. [Online]. Available: `https://www.rte-france.com/sites/default/files/2014%7B%5C_%7D04%7B%5C_%7D09%7B%5C_%7Dfrench%7B%5C_%7Dcapacity%7B%5C_%7Dmarket.pdf`.

[106] D. Newbery, "Missing money and missing markets: Reliability, capacity auctions and interconnectors," *Energy Policy*, volume 94, pages 401–410, 2016.

[107] P. L. Joskow, "Capacity payments in imperfect electricity markets: Need and design," *Utilities Policy*, volume 16, number 3, pages 159–170, 2008.

[108] P. Cramton and A. Ockenfels, "Economics and design of capacity markets for the power sector," *Zeitschrift für Energiewirtschaft*, volume 36, number 2, pages 113–134, 2011.

[109] C. Ordoudis, "Market-based approaches for the coordinated operation of electricity and natural gas systems," PhD thesis, Technical University of Denmark, 2018.

[110] G. A. Dourbois, P. N. Biskas, and D. I. Chatzigiannis, "Novel approaches for the clearing of the european day-ahead electricity market," *IEEE Transactions on Power Systems*, volume 33, number 6, pages 5820–5831, 2018.

[111] A. J. Conejo, M. Carrión, and J. M. Morales, *Decision making under uncertainty in electricity markets*. Springer, 2010.

[112] J. Kazempour, P. Pinson, and B. F. Hobbs, "A stochastic market design with revenue adequacy and cost recovery by scenario: Benefits and costs," *IEEE Transactions on Power Systems*, volume 33, number 4, pages 3531–3545, 2018.

[113] S. Zhou and M. A. Brown, "Smart meter deployment in Europe: A comparative case study on the impacts of national policy schemes," *Journal of Cleaner Production*, volume 144, number 2017, pages 22–32, 2017.

[114] M. Broman Toft, G. Schuitema, and J. Thøgersen, "The importance of framing for consumer acceptance of the smart grid: A comparative study of Denmark, Norway and Switzerland," *Energy Research and Social Science*, volume 3, pages 113–123, 2014.

[115] AF-Mercados, "Study on tariff design for distribution systems," European Comission, Tech. Rep., 2015, pages 1–650. [Online]. Available: `https://ec.europa.eu/energy/sites/ener/files/documents/20150313%20Tariff%20report%20fina%7B%5C_%7DrevREF-E.PDF`.

[116] S. Huang, Q. Wu, M. Shahidehpour, and Z. Liu, "Dynamic power tariff for congestion management in distribution networks," *IEEE Transactions on Smart Grid*, volume 10, number 2, pages 2148–2157, 2019.

[117] S. Huang and Q. Wu, "Dynamic subsidy method for congestion management in distribution networks," *IEEE Transactions on Smart Grid*, volume 9, number 3, pages 2140–2151, 2016.

[118] S. Weckx, R. D'Hulst, B. Claessens, and J. Driesensam, "Multiagent charging of electric vehicles respecting distribution transformer loading and voltage limits," *IEEE Transactions on Smart Grid*, volume 5, number 6, pages 2857–2867, 2014.

[119] K. Heussen, D. E. M. Bondy, J. Hu, O. Gehrke, and L. H. Hansen, "A clearinghouse concept for distribution-level flexibility services," in *Innovative Smart Grid Technologies Conference Europe (ISGT)*, IEEE, 2013, pages 1–5.

[120] Z. Liu, Q. Wu, S. Huang, and H. Zhao, "Transactive energy: A review of state of the art and implementation," in *PowerTech Conference*, Manchester: IEEE, 2017, pages 1–6.

[121] A. Papavasiliou, H. Hindi, and D. Greene, "Market-based control mechanisms for electric power demand response," in *49th Conference on Decision and Control (CDC)*, IEEE, 2010, pages 1891–1898.

[122] B. Moradzadeh and K. Tomsovic, "Two-stage residential energy management considering network operational constraints," *IEEE Transactions on Smart Grid*, volume 4, number 4, pages 2339–2346, 2013.

[123] N. Good, E. Karangelos, A. Navarro-Espinosa, and P. Mancarella, "Optimization under uncertainty of thermal storage-based flexible demand response with quantification of residential users' discomfort," *IEEE Transactions on Smart Grid*, volume 6, number 5, pages 2333–2342, 2015.

[124] J. Medina, N. Muller, I. Roytelman, and S. Member, "Demand Response and Distribution Grid Operations : Opportunities and Challenges," *IEEE Transactions on Smart Grid*, volume 1, number 2, pages 193–198, 2010.

[125] S. Delikaraoglou, J. M. Morales, and P. Pinson, "Impact of inter- and intra-regional coordination in markets with a large renewable component," *IEEE Transactions on Power Systems*, volume 31, number 6, pages 5061–5070, 2016.

[126] X. Han, K. Heussen, O. Gehrke, H. W. Bindner, and B. Kroposki, "Taxonomy for Evaluation of Distributed Control Strategies for Distributed Energy Resources," *IEEE Transactions on Smart Grid*, volume 9, number 5, pages 5185–5195, 2018.

[127] S. Dempe and J. Dutta, "Is bilevel programming a special case of a mathematical program with complementarity constraints?" *Mathematical Programming*, volume 131, number 1-2, pages 37–48, 2012.

[128] V. V. Kalashnikov, S. Dempe, G. A. Pérez-Valdés, N. I. Kalashnykova, and J. F. Camacho-Vallejo, "Bilevel programming and applications," *Mathematical Problems in Engineering*, volume 2015, pages 1–17, 2015.

[129] G. Anandalingam and T. Friesz, "Hierarchical optimization: An introduction," *Annals of Operations Research*, volume 34, number 1, pages 1–11, 1992.

[130] V. Dvorkin, S. Delikaraoglou, and J. M. Morales, "Setting reserve requirements to approximate the efficiency of the stochastic dispatch," *IEEE Transactions on Power Systems*, volume 34, number 2, pages 1524–1536, 2019.

[131] H. Hoschle, H. Le Cadre, Y. Smeers, A. Papavasiliou, and R. Belmans, "An ADMM-based Method for Computing Risk-Averse Equilibrium in Capacity Markets," *IEEE Transactions on Power Systems*, volume 33, number 5, pages 4819–4830, 2018.

[132] H. Le Cadre and J. S. Bedo, "Dealing with uncertainty in the smart grid: A learning game approach," *Computer Networks*, volume 103, pages 15–32, 2016.

[133] E. Sorin, L. Bobo, and P. Pinson, "Consensus-based approach to peer-to-peer electricity markets with product differentiation," *IEEE Transactions on Power Systems*, volume 34, number 2, pages 994–1004, 2018.

[134] F. Facchinei and C. Kanzow, "Generalized nash equilibrium problems," *Annals of Operations Research*, volume 175, number 1, pages 177–211, 2010.

[135] Y. Smeers, "Market incompleteness in regional electricity transmission," *Networks and Spatial Economics*, volume 3, number 2, pages 151–174, 2003.

[136] K. Förderer and H. Schmeck, "Demo abstract : A building energy management system in the context of the smart grid traffic light concept," *Computer Science - Research and Development*, volume 33, number 1, pages 269–270, 2018.

[137] E. Rivero, P. Mallet, E. France, M. Sebastian-viana, J. Stromsather, and M. Baron, "EVOLVDSO: Assesment of the future roles of DSOs, future Market Architechtures and Regulatory Frameworks for Network Integration of DRES," in *23rd International Conference on Electricity Distribution*, CIRED, 2015, pages 1–5.

[138] Smart Grid Task Force, "Regulatory recommendations for the deployment of flexibility - EG3 report," European Regional Development Fund, Brussels, Tech. Rep. January, 2015, pages 1–94.

[139] Z. Yuan and M. R. Hesamzadeh, "Hierarchical coordination of TSO-DSO economic dispatch considering large-scale integration of distributed energy resources," *Applied Energy*, volume 195, pages 600–615, 2017.

[140] H. Le Cadre, "On the efficiency of local electricity markets under decentralized and centralized designs: a multi-leader Stackelberg game analysis," *Central European Journal of Operations Research*, pages 1–32, 2018.

[141] J. A. Taylor, *Convex optimization of power systems*. Cambridge University Press, 2015.

[142] B. Subhonmesh, S. H. Low, and K. M. Chandy, "Equivalence of branch flow and bus injection models," in *Allerton Conference on Communication, Control, and Computing*, Allerton: IEEE, 2012, pages 1893–1899.

[143] S. Boyd and L. Vandenberghe, *Convex optimization*. Cambridge University Press, 2004.

[144] P. M. Pardalos and S. A. Vavasis, "Quadratic programming with one negative eigenvalue is NP-hard," *Journal of Global Optimization*, volume 1, number 1, pages 15–22, 1991.

[145] K. G. Murty and S. N. Kabadi, "Some NP-Complete problems in quadratic and nonlinear programming," *Mathematical Programming*, volume 39, number 2, pages 117–129, 1987.

[146] R. D. Christie, B. F. Wollenberg, and I. Wangensteen, "Transmission management in the deregulated environment," *Proceedings of the IEEE*, volume 88, number 2, pages 170–195, 2000.

[147] M. Baran and F. Wu, "Optimal capacitor placement on radial distribution systems," *IEEE Transactions on Power Delivery*, volume 4, number 1, pages 725–734, 1989.

[148] A. Helseth, "A linear optimal power flow model considering nodal distribution of losses," in *9th International Conference on the European Energy Market (EEM)*, Florence, Italy: IEEE, 2012, pages 1–8.

[149] T. dos Santos and A. L. Diniz, "A dynamic piecewise linear model for DC transmission losses in optimal scheduling problems," *IEEE Transactions on Power Systems*, volume 26, number 2, pages 508–519, 2011.

[150] B. Eldridge, R. O'Neill, and A. Castillo, "An Improved Method for the DCOPF with Losses," *IEEE Transactions on Power Systems*, volume 33, number 4, pages 3779–3788, 2018.

[151] X. Bai, H. Wei, K. Fujisawa, and Y. Wang, "Semidefinite programming for optimal power flow problems," *Journal of Electrical Power & Energy Systems*, volume 30, number 6-7, pages 383–392, 2008.

[152] M. E. Baran and F. F. Wu, "Optimal sizing of capacitors placed on a radial distribution system.," *IEEE Transactions on Power Delivery*, volume 4, number 1, pages 735–743, 1989.

[153] M. Farivar and S. H. Low, "Branch flow model: Relaxations and convexification - part ii," *IEEE Transactions on Power Systems*, volume 28, number 3, pages 2567–2572, 2013.

[154] M. Nick, R. Cherkaoui, J. Y. LeBoudec, and M. Paolone, "An exact convex formulation of the optimal power flow in radial distribution networks including transverse components," *IEEE Transactions on Automatic Control*, volume 63, number 3, pages 682–697, 2017.

[155] D. R. Morrison, S. H. Jacobson, J. J. Sauppe, and E. C. Sewell, "Branch-and-bound algorithms: A survey of recent advances in searching, branching, and pruning," *Discrete Optimization*, volume 19, pages 79–102, 2016.

[156] L. Bobo, S. Delikaraoglou, N. Vespermann, J. Kazempour, and P. Pinson, "Offering strategy of a flexibility aggregator in a balancing market using asymmetric block offers," in *20th Power Systems Computation Conference (PSCC)*, IEEE, 2018.

[157] Z. Li and M. Shahidehpour, "Security-constrained unit commitment for simultaneous clearing of energy and ancillary services markets," *IEEE Transactions on Power Systems*, volume 20, number 2, pages 1079–1088, 2005.

[158] G. Thompson, C. Li, M. Zhang, and K. W. Hedman, "The effects of extended locational marginal pricing in wholesale electricity markets," in *45th North American Power Symposium (NAPS)*, IEEE, 2013, pages 1–6.

[159] D. A. Schiro, T. Zheng, F. Zhao, and E. Litvinov, "Convex hull pricing in electricity markets: Formulation, analysis, and implementation challenges," *IEEE Transactions on Power Systems*, volume 31, number 5, pages 4068–4075, 2016.

[160] S. Bolognani and S. Zampieri, "On the existence and linear approximation of the power flow solution in power distribution networks," *IEEE Transactions on Power Systems*, volume 31, number 1, pages 163–172, 2016.

[161] E. Dall'Anese, H. Zhu, and G. B. Giannakis, "Distributed optimal power flow for smart microgrids," *IEEE Transactions on Smart Grid*, volume 4, number 3, pages 1464–1475, 2013.

[162] W. Liu and F. Wen, "Discussion on 'Distribution locational marginal pricing for optimal electric vehicle charging management'," *IEEE Transactions on Power Systems*, volume 29, number 4, pages 1867–1867, 2014.

[163] D. Subcommittee, *37-bus Feeder*, 2000. [Online]. Available: `http://sites.ieee.org/pes-testfeeders/resources/` (visited on April 17, 2018).

[164] V. Dvorkin, J. Kazempour, and P. Pinson, "Electricity Market Equilibrium under Information Asymmetry," 2019, [Online]. Available: `http://pierrepinson.com/docs/Dvorkinetal2019.pdf`.

[165] J. Fortuny-Amat and B. McCarl, "A representation and economic interpretation of a two-level programming problem," *Journal of the Operational Research Society*, 1981.

[166] C. Ordoudis, P. Pinson, J. M. Morales-González, and M. Zugno, "An updated version of the IEEE RTS 24-bus system for electricity market and power system operation studies," Technical University of Denmark, Tech. Rep., 2016. [Online]. Available: `http://orbit.dtu.dk/files/120568114/An%7B%5C_%7DUpdated%7B%5C_%7DVersion%7B%5C_%7Dof%7B%5C_%7Dthe%7B%5C_%7DIEEE%7B%5C_%7DRTS%7B%5C_%7D24Bus%7B%5C_%7DSystem%7B%5C_%7Dfor%7B%5C_%7DElectricty%7B%5C_%7DMarket%7B%5C_%7Dan....pdf`.

[167] J. R. Birge and F. V. Louveaux, "A multicut algorithm for two-stage stochastic linear programs," *European Journal of Operational Research*, volume 34, pages 384–392, 1988.

[168] F. You and I. E. Grossmann, "Multicut benders decomposition algorithm for process supply chain planning under uncertainty," *Annals of Operations Research*, volume 210, number 1, pages 191–211, 2013.

[169] G. K. Saharidis and M. G. Ierapetritou, "Resolution method for mixed integer bi-level linear problems based on decomposition technique," *Journal of Global Optimization*, volume 44, number 1, pages 29–51, 2009.

[170] A. Conejo, E. Castillo, R. Minguez, and R. Garcia-Bertrand, *Decomposition techniques in mathematical programming: engineering and science applications*. Springer Science & Business Media, 2006.

Collection of relevant publications

[**Paper A**] Congestion Management in Distribution Networks With Asymmetric Block Offers.

[**Paper B**] TSO-DSO Coordination Via Optimized Interface Capacity Limits

(Paper A) Congestion Management in Distribution Networks With Asymmetric Block Offers.

Authors:
Alexander Hermann, Jalal Kazempour, Shaojun Huang and Jacob Østergaard
Published as:
Submitted to IEEE Transactions on Power Systems, Submitted August 7th 2018, Revised Janurary 30th 2019
Note:
The appendix which is published as an electronic companion on GitHub is attached after the main body of the manuscript. It contains some additional formulae and additional results.

Congestion Management in Distribution Networks With Asymmetric Block Offers

Alexander Hermann, *Student Member, IEEE,* Jalal Kazempour, *Senior Member, IEEE,* Shaojun Huang, *Senior Member, IEEE,* and Jacob Østergaard, *Senior Member, IEEE*

***Abstract*—In current practice, the day-ahead market-clearing outcomes are not necessarily feasible for distribution networks, i.e, the network constraints might not be satisfied. Hence, the distribution system operator may consider an ex-post re-dispatch mechanism, exploiting potential flexibility of local distributed energy resources (DERs) including demand response (DR) units. Many DR units have an inherent "rebound effect", meaning a decrease in power demand (response) must be followed by an increase (rebound) or vice-versa, due to their underlying physical properties. A naive re-dispatch mechanism relying on DR units with non-negligible rebound effect may fail, since those units may cause another congestion in the rebound period. We propose a mechanism, which models the rebound effect of DR units using asymmetric block offers — this way, those units offer their flexibility using two subsequent blocks (response and rebound), each one representing the load decrease/increase in a time period. We demonstrate that though linear approximations of optimal power flow (OPF) models as potential re-dispatch mechanisms are more computationally efficient, they can result in a different dispatch of the asymmetric blocks than an exact convex relaxation of an AC-OPF model, and therefore, must be used with caution.**

***Index Terms*—Congestion management, demand response, rebound effect, asymmetric block offers, convex relaxation.**

NOMENCLATURE

Sets and indices

C	Set of demand response units c
D	Set of offers d of each demand response unit
I	Set of distribution-level conventional generators i
L_n	Set of all facilities located at node n
N	Set of nodes n and j
PCC	Point of common coupling, i.e., the node connecting the distribution and transmission levels
T	Set of time steps t and τ
Φ_n	Set of all nodes connected to node n

Free Variables

p_{nt}/q_{nt}	Net active/reactive power injection at node n and time step t (positive for power injection) [kW/kVAr]
p_{njt}/q_{njt}	Active/reactive power flow from node n to j at time step t [kW/kVAr]

Non-negative Variables

$p_t^{\mathrm{up/dn,S}}$	Active power up/down-regulation provided by the transmission grid at time step t [kW]
$p_{it}^{\mathrm{up/dn}}$	Active power up/down-regulation provided by generator i at time step t [kW]
$q_t^{\mathrm{up/dn,S}}$	Reactive power up/down-regulation provided by the transmission grid at time step t [kVAr]
$q_{it}^{\mathrm{up/dn}}$	Reactive power up/down-regulation by generator i at time step t [kVAr]
$r_{dct}^{\mathrm{up/dn}}$	Active power up/down-regulation provided by demand response offer d of unit c at time step t [kW]
s_{tn}^{up}	Load curtailment at node n and time step t [kW]
v_{nt}	Squared voltage magnitude at node n and time step t [p.u.]
φ_{njt}	Squared current magnitude in line connecting node n to j [p.u.]

Binary Variables

o_{dct}	Activation of block d of demand response unit c at time step t

Parameters

A_{dc}	Orientation of offer d of demand response unit c. Equal to 1 if begins with up-regulation, equal to 0 otherwise
B_{nj}	Shunt susceptance of line connecting node n to j [p.u.]
$C_t^{\mathrm{p/q,\uparrow/\downarrow S}}$	Active/reactive up/down-regulation price provided from transmission level at the PCC at time step t [¢/kWh or ¢/kVArh]
$C_{dct}^{\mathrm{DR\uparrow/\downarrow}}$	Active power up/down-regulation offer price of demand response unit c, offer d, time t [¢/kWh]
C^{Shed}	Cost of load shedding [¢/kWh]
$C_{it}^{\mathrm{p/q,\uparrow/\downarrow}}$	Active/reactive up/down-regulation offer price of conventional generator i at time step t [¢/kWh or ¢/kVArh]
D_{nt}^{disp}	Scheduled active power consumption of all inflexible loads at node n and time step t from the day-ahead market [kW]
DR_{ct}^{disp}	Scheduled active power consumption of demand response unit c at time step t from the day-ahead market [kW]
G_{nj}	Shunt conductance of line connecting node n to j [p.u.]
$\overline{F}_{nj}$	Capacity of line connecting node n to j [kVA]
$\overline{P}_i^{\mathrm{up/dn}}$	Maximum active power up/down-regulation capability of generator i [kW]
$\overline{P}^{\mathrm{up/dn,S}}$	Maximum active power up/down-regulation that can be provided by transmission level [kW]
$P_{dc}^{\mathrm{rsp/rb}}$	Response/rebound power of offer d of demand response unit c [kW]
P_{it}^{disp}	Dispatched active power production of generator i at time step t from the day-ahead market [kW]
P_{ct}^{cap}	Maximum active power consumption of demand response unit c at time step t [kW]
P_i^{cap}	Active power capacity of generator i [kW]
$\overline{Q}^{\mathrm{up/dn,S}}$	Maximum reactive power up/down-regulation that can be provided by transmission level [kVAr]
$\overline{Q}_i^{\mathrm{up/dn}}$	Maximum reactive power up/down-regulation capability of generator i [kVAr]
Q_{nt}	Total reactive power consumption at node n and time step t [kVAr]
R_{nj}	Resistance of line connecting node n to j [p.u.]
S_t^{disp}	Dispatched import/export of active power from the transmission system at time t from the day-ahead market [kW]
$T_{dc}^{\mathrm{rsp/rb/rec}}$	Response/rebound/recovery duration of demand response offer d of unit c [time step]
$\overline{V}_n^{\mathrm{sq}}$, $\underline{V}_n^{\mathrm{sq}}$	Upper and lower limits for voltage magnitude squared at node n [p.u.]
X_{nj}	Reactance of line connecting node n to j [p.u.]

A. Hermann, J. Kazempour and J. Østergaard are with the Technical University of Denmark, Kgs. Lyngby 2800, Denmark (email: alherm@elektro.dtu.dk; seykaz@elektro.dtu.dk; joe@elektro.dtu.dk).

S. Huang is with the University of Southern Denmark, Odense 5230, Denmark (email: shahu@mmmi.sdu.dk).

I. INTRODUCTION

IN current zonal electricity markets in Europe, the day-ahead market does not explicitly take into account the network constraints within zones. Therefore, the market-clearing outcomes are not necessarily feasible in terms of grid constraints. This brings challenges for both transmission and

distribution system operators (TSO and DSO), who are responsible for the secure and safe operation of their underlying systems. To resolve this issue, both TSO and DSO require flexible resources for congestion management and other uses, such as balancing and frequency control [1]. A significant part of such flexible resources is expected to be spread in distribution systems, in the form of distributed energy resources (DERs). These resources are able to provide flexibility to both TSO and DSO, and are also allowed to participate in the day-ahead market through new market players, such as aggregators and balancing responsible parties. Key is that the TSO and DSO need to coordinate how to use the DERs, ensuring both have access to flexible resources while operating their underlying system in a secure manner [2].

Different schemes have been recently proposed for TSO-DSO coordination [3]–[6], including suggestions for having either a common flexibility market for TSO and DSO, or separated markets. In some of those schemes, a bi-directional but non-iterative communication between DSO and TSO is required, in which the DSO shares its feasible region with the TSO [7]. Some other schemes suggest maintaining the current uni-directional communication in which the TSO is not coordinated with the DSO, but the DSO needs ex-post actions. Ex-post here means that the DSO re-dispatches local DERs using a bid-based auction with day-ahead dispatches as inputs. This mechanism uses local flexible resources for congestion management and resolving nodal voltage issues [8]. The focus of this paper is an ex-post method.

Demand response (DR) units are expected to provide a large share of the DER penetration in distribution grids. Many DR units, especially thermostatically controlled loads, exhibit an inherent *rebound (kick-back) effect* because of their underlying physical properties [9]. It means that any load decrease/increase in a specific time period (response) may be followed by a load increase/decrease in the subsequent time period (rebound) [10]. This effect complicates any problem including DR units, since it makes the future load profile *decision-dependent* (i.e. not exogenous anymore). One natural approach to model rebound effect is dynamic programming, such that the dispatch of DR unit at time step k affects load level at time steps $t > k$ [11]. However, dynamic programming with iterative solution techniques is not compatible with existing market-clearing frameworks[1]. Therefore, other alternatives are needed to model rebound effects within market frameworks, e.g., new offering formats for DR units [12]. One appealing market-compatible concept are *asymmetric block offers* [13], which include two parts, response and rebound. Each part models either load increase or decrease. One can view the combination of these two parts as a load shifting offer in time, but without a time gap between response and rebound time periods. We use the concept of asymmetric block offers, because it allows us to model rebound *a priori* in our market model without the need for an iterative clearing process. However, these block offers may bring computational challenges due to additional binary variables required for modeling the blocks[2]. Detailed description of these offers will be provided in the following section.

There is an extensive literature on congestion management in distribution networks using DR units - see [8] for a relevant survey. The two main strategies to reward those units are: i) the price-based methods [15]–[17], where DR units participate in any mechanism as individual profit-maximizing players, and ii) the incentive-based methods, where DR units are paid based on pre-defined incentive rates [18]–[20]. The key point is that all these papers ignore the potential rebound effect of DR units, while this may incur another congestion in the coming time steps, or overestimate the capability of DR units to effectively help the DSO with congestion management.

In this paper, the main technical question is: how should an appropriate DSO-level congestion management mechanism be implemented, while accurately accounting for rebound effects of local DR units? This underlying mechanism is to be solved by the DSO once the day-ahead market is cleared. Therefore, the day-ahead dispatch of local resources is given, and goal of the proposed mechanism is to optimally adjust those resources for meeting local distribution network constraints at the minimum re-dispatch cost. The important constraints to be fulfilled in the re-dispatch mechanism include nodal voltage and line flow limits in the distribution network. In addition, it is of importance to consider power losses in the distribution grid. This raises another technical question: To what extent should the distribution grid constraints and losses be taken into account in the re-dispatch mechanism, and how sensitive are the re-dispatch results to those considerations?

Our first contribution is to develop a re-dispatch mechanism for a DSO as an ex-post congestion management action, while accounting for rebound effects of DR units a priori using asymmetric block offers. To the best of our knowledge, [13] is the only paper in existing literature incorporating the rebound effects in a compatible way into a balancing market framework. However, it ignores network representation, which is essential in any distribution-level mechanism, including the congestion management mechanism in our study. The full grid representation of a distribution system is a non-convex problem with optimality and computational challenges. This becomes worse when adding binary variables due to the representation of blocks. Our second contribution is to provide a comprehensive analysis to explore how different grid representations change the re-dispatch outcomes and the computational burden. In particular, to investigate how distribution network simplifications, as is common in practice, influence the re-dispatch results, we develop three distribution optimal power flow (OPF) models. Each model has increasing accuracy. The more accurate model is indeed the more complex one, which is computationally more expensive. Accounting for the rebound effects, two models are mixed-integer linear programming (MILP) problems (one without and one with loss approximations), while the last one is a mixed-integer second order cone problem (MI-SOCP). The latter model is a convex conic relaxation of the original AC-OPF model, which performs

[1]The current markets prefer non-iterative clearing mechanisms with straightforward, easy-to-implement and transparent clearing mechanisms.

[2]Adding block offers is common place in European zonal electricity markets, as conventional generators are allowed to submit different types of block offers to ensure their internal unit commitment constraints [14].

well in radial networks [21], [22]. To ensure exactness of the convex relaxation we also present some sufficient conditions for exactness and show some of the implications of using those conditions [21], [23]. Our study shows that the MILP models are computationally faster, which makes them suitable to be used in practice. However, they do not necessarily obtain identical re-dispatch results to those in the MI-SOCP model, which solves the problem in our study around 4 to 7 times slower without sufficient conditions for exactness, and 7 to 60 times slower if those conditions are added. Therefore, MILP versions of this re-dispatch mechanism are practical but must be used with caution.

The rest of the paper is structured as following: Section II describes the implementation of asymmetric block offers, and explains the congestion management mechanism. Section III proposes the congestion management method using three different OPF models. Section IV provides results for two case studies. Concluding remarks are given in Section V.

II. Congestion Management using Asymmetric Block Offers

This section describes the details of asymmetric block offers, and the framework of the proposed congestion management mechanism.

A. Asymmetric Block Offers

Examples of some potential flexible loads that exhibit a rebound effect are refrigeration units, water heaters and heat pumps with storage for building temperature control. They can be used as DR units, by deviating from a base-line temperature setting and approaching either an upper or a lower allowable temperature threshold. When the temperature threshold is reached, DR units have to increase (or decrease) their power consumption for a period, in order to return to the base-line setting [9], [10]. The time to reach the upper or lower temperature thresholds can be found by thermal modeling of the underlying system. The time period from DR activation until reaching the temperature threshold is referred to as *response* period, while the subsequent time period until returning to the base-line setting is referred to as *rebound* period [13]. An asymmetric block offer models the response and rebound parts of the DR unit. This type of offer allows exploiting demand-side flexibility by directly modeling temporal load shifting in the dispatch mechanism. These block offers can be designed as shown in Fig. 1, where two examples are plotted with different order of up- and down-regulation directions. By asymmetric, it means that they can have different power consumption levels and duration for response and rebound parts. The asymmetric block offers are indeed the market offers of DR units or flexibility aggregators in general. It is up to the flexibility aggregators to ensure that the block offers are technically feasible. Since this paper looks at the problem from a DSO perspective, the asymmetric block offers are exogenous, and their synthesis are out of the scope of this paper[3]. However, in general, these offers can be derived by approximation models (e.g. ARMAX model [25]) using measurement data from thermal test units.

[3]We refer the interested readers to [24] for offering strategy problem of DR units and flexibility aggregators using asymmetric block offers.

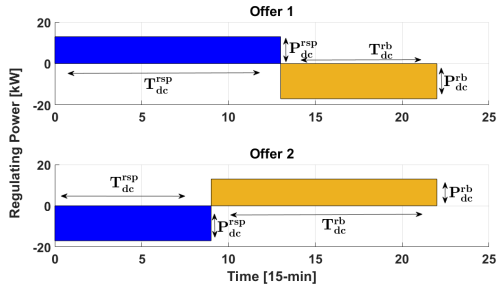

Fig. 1. Two examples of possible asymmetric block offers for a demand response unit. A positive/negative regulating power corresponds to up/down-regulation, respectively. In Offer 1 (upper plot), the response part (in blue) provides up-regulation, i.e., a decrease in load power consumption. Its rebound (in yellow) corresponds to a subsequent load increase, i.e. down regulation. Further, Offer 2 (lower plot) includes down- and up-regulation in response and rebound parts, respectively.

B. Congestion Management: Framework and Assumptions

The outcome of the day-ahead market does not necessarily respect the DSO-level network constraints. When the day-ahead market dispatch does not respect the constraints in the distribution network, the most cost-efficient way is to resolve these violations locally. Distribution network congestion will be one of the prime issues in the future, due to increased line loading, with the expected large scale deployment of distributed photovoltaic power and battery storage. Often congestion will be coupled with voltage limit violations, therefore it is also important to model that aspect of the grid. This paper proposes an ex-post mechanism to be run *right after* the day-ahead market, which is performed locally by the DSO. The DSO uses a market-based solution to determine the optimal re-dispatch actions, while obtaining the minimum total re-dispatch cost. According to the market-clearing outcomes, the DSO pays the DERs. Since the largest volume of the DR units with rebound characteristics are generally located in radial distribution feeders, it is logical to use their load-shifting potential to resolve local issues.

Any DSO-level congestion management mechanism should take as *input* the results of the day-ahead market clearing, as this comprises the power settings of the flexible loads and distributed generation. The DSO uses these values to determine whether there are any issues with congestion and/or voltage limit violations within the distribution network. If any issues are detected, the DSO requests offers for down- and up-regulation from the individual DR units, local conventional generators and flexibility aggregators. These offers can be in the form of conventional offers by local dispatchable generators or of asymmetric block offers by local DR units. Also, the TSO is viewed as a flexibility provider through TSO-level flexible resources but potentially at a higher cost. However,

note that the change of the import/export at the PCC[4] is limited by lower and upper bounds ($\overline{P}^{\mathrm{dn,S}}$ and $\overline{P}^{\mathrm{up,S}}$). Indeed, the TSO provides this limited flexibility by activation of reserve capacity from TSO-level flexible resources without need for changing the day-ahead market outcomes [5].

After collecting the submitted offers, the DSO runs the congestion management mechanism, whose objective is to meet local constraints at the minimum re-dispatch cost. In addition, the outcomes are accepted offers for up- and down-regulation. Regarding the potential uncertainty sources, e.g., load and renewable power uncertainties, we assume that they have been already considered during the day-ahead market clearing. Therefore, the proposed ex-post re-dispatch mechanism does not need to model again those uncertainties. Moreover, the DSO may be unwilling to collect and manipulate statistical data in order to model future uncertainties, because in current market frameworks this duty falls to the market operator.

Since the DSO-level network is usually radial, a congested line can only be relieved, if any resources on both sides of that line are available for re-dispatch. This is because any up-regulation somewhere in the network has to be matched by an equal down-regulation elsewhere (minus line losses). One important observation is that the accepted offers for up- and down-regulation should be located on both sides of the congested line, in order to maintain power balance. The DR units furthest away from the PCC are the ones that are most likely to be scheduled, when congestion occurs.

III. Mathematical Model

Section III-A provides the mathematical representation of asymmetric block offers. Afterwards, Section III-B includes asymmetric block offers within three proposed OPF models as alternative congestion management mechanisms with different levels of complexity.

A. Mathematical Representation of Asymmetric Block Offers

This section provides a modified version of formulations for asymmetric block offers from [13], yielding a set of mixed-integer linear inequalities. These conditions will be included in Section III-B as constraints of OPF models. Asymmetric block offers beginning with up-regulation response, e.g., Offer 1 in Fig. 1, are modeled by equations (1), while offers beginning with down-regulation response, e.g., Offer 2 in Fig. 1, are represented by equations (11) in the online appendix [26]. These two different kinds of block offers are differentiated by binary parameter A_{dc}. If A_{dc} is set to 1, it indicates that block offer d of unit c begins with up-regulation, or to 0 if it begins with down-regulation. The binary variable o_{dct} is a decision variable to activate a given offer d from DR unit c in time step t.

$$\left\{ r^{\mathrm{up}}_{dct} \le P^{\mathrm{rsp}}_{dc} o_{dct}, \quad \forall d,c,t \right. \tag{1a}$$

$$r^{\mathrm{dn}}_{dct} \le P^{\mathrm{rb}}_{dc} o_{dct}, \quad \forall d,c,t \tag{1b}$$

$$\sum_{\tau=t}^{t+T^{\mathrm{rsp}}_{dc}-1} r^{\mathrm{up}}_{dc\tau} \ge T^{\mathrm{rsp}}_{dc} P^{\mathrm{rsp}}_{dc}(o_{dct} - o_{dc,t-1}), \quad \forall d,c,t \tag{1c}$$

$$\sum_{\tau=t+T^{\mathrm{rsp}}_{dc}}^{t+T^{\mathrm{rsp}}_{dc}+T^{\mathrm{rb}}_{dc}-1} r^{\mathrm{dn}}_{dc\tau} \ge T^{\mathrm{rb}}_{dc} P^{\mathrm{rb}}_{dc}(o_{dct} - o_{dc,t-1}), \quad \forall d,c,t \le |T| - T^{\mathrm{rsp}}_{dc} \tag{1d}$$

$$\sum_{\tau=t}^{t+T^{\mathrm{rsp}}_{dc}-1} r^{\mathrm{dn}}_{dc\tau} \le T^{\mathrm{rb}}_{dc} P^{\mathrm{rb}}_{dc}(1-(o_{dct} - o_{dc,t-1})), \forall d,c,t \tag{1e}$$

$$\sum_{\tau=t+T^{\mathrm{rsp}}_{dc}}^{t+T^{\mathrm{rsp}}_{dc}+T^{\mathrm{rb}}_{dc}-1} r^{\mathrm{up}}_{dc\tau} \le T^{\mathrm{rsp}}_{dc} P^{\mathrm{rsp}}_{dc}(1-(o_{dct} - o_{dc,t-1})) \tag{1f}$$

$$\left. , \forall d,c,t \le |T| - T^{\mathrm{rsp}}_{dc} \right\} \text{ if } A_{dc} = 1.$$

Conditions (1a) and (1b) restrict up- and down-regulation r^{up}_{dct} and r^{dn}_{dct} to the prescribed magnitude of response P^{rsp}_{dc} and rebound P^{rb}_{dc}, respectively. In (1c), the length of the response, if offer d is activated, is set to the prescribed response time T^{rsp}_{dc}. Condition (1d) is similar to (1c), but for the rebound part of the block offer. Note that $|T|$ indicates the cardinality of set T. Condition (1e) ensures that variable r^{dn}_{dct} is 0 during up-regulation. Similarly, condition (1f) imposes $r^{\mathrm{up}}_{dct} = 0$ during down-regulation.

In addition to (1) and (11), a minimum recovery period, if exists, needs to be enforced. This condition is enforced by (2). Parameter T^{rec}_{dc} corresponds to the recovery time between the two consecutive asymmetric block offers (not between response and rebound parts of a block offer). In other words, it enforces the minimum recovery time between the rebound part of one block and the response part of the next block.

$$\sum_{\tau=t+T^{\mathrm{resp}}_{dc}+T^{\mathrm{reb}}_{dc}}^{t+T^{\mathrm{resp}}_{dc}+T^{\mathrm{reb}}_{dc}+T^{\mathrm{rec}}_{dc}-1} (1-o_{dc,\tau}) \ge T^{\mathrm{rec}}_{dc}(o_{dct} - o_{dct-1}) \\ , \forall d,c,t \le |T| - (T^{\mathrm{resp}}_{dc} + T^{\mathrm{reb}}_{dc}) + 1. \tag{2}$$

In (3), it is ensured that each DR unit is only able to activate at most one block offer in any time step:

$$\sum_{d} o_{dct} \le 1, \quad \forall c,t. \tag{3}$$

The asymmetric block offers also need to be finished before the end of the planning horizon, such that the whole block offer is realized before the planning horizon. Condition (4) ensures that the entire asymmetric block offer is dispatched within the time horizon considered, e.g., 24 hours. For example, this constraint makes sure that there is no case in which the response part is dispatched in the upcoming 24 hours, while its rebound part is allocated in the beginning hours of the subsequent day.

$$1 - (o_{dc,t+1} - o_{dct}) \le 2(1 - o_{dc|T|}) \\ , \forall d,c,t = |T| - (T^{\mathrm{resp}}_{dc} + T^{\mathrm{reb}}_{dc}). \tag{4}$$

B. Congestion Management Mechanism: OPF Models

Accounting for rebound effect of DR units, this subsection provides three different alternatives for DSO-level congestion management, with increasing levels of accuracy and therefore complexity. The first model is the simplest one, which is a linear DC-OPF problem for radial distributions systems,

[4]The point of common coupling, i.e. the transformer substation which connects the distribution and transmission networks.

ignoring losses while decoupling active and reactive power flows. The second one improves the first model by adding a loss approximation for active power flows via cuts, but at the cost of using an iterative process [27], [28]. As the most accurate alternative among the three OPF models used in this paper, the third one is an SOCP, which takes into account losses for both active and reactive power flows[5] [29]. All these three models will be mixed-integer programs due to binary variables in (1)-(4) and (11).

The objective function of all three OPF models used in this paper is the same as given in (5). It minimizes the total re-dispatch cost, which is a linear combination of the costs for up- and down-regulation[6] of active and reactive power from different sources, i.e. TSO, local conventional generators i, DR units c and involuntary curtailment of loads.

$$\begin{aligned}\min_{\Xi} \quad f(\Xi) = \sum_t \Big[& \underbrace{C_t^{\mathrm{p}\uparrow\mathrm{S}} p_t^{\mathrm{up,S}}}_{\text{Cost of } p^{\mathrm{up}} \text{ from TSO}} - \underbrace{C_t^{\mathrm{p}\downarrow\mathrm{S}} p_t^{\mathrm{dn,S}}}_{\text{cost of } p^{\mathrm{dn}} \text{ to TSO}} \\ & + \underbrace{C_t^{\mathrm{q}\uparrow\mathrm{S}} q_t^{\mathrm{up,S}}}_{\text{Cost of } q^{\mathrm{up}} \text{ from TSO}} - \underbrace{C_t^{\mathrm{q}\downarrow\mathrm{S}} q_t^{\mathrm{dn,S}}}_{\text{Cost of } q^{\mathrm{dn}} \text{ to TSO}} \Big] + \sum_{n,t} \Big[\underbrace{C^{\mathrm{Shed}} s_{nt}^{\mathrm{up}}}_{\text{Curtailment cost}} \Big] \\ & + \sum_{i,t} \Big[\underbrace{C_{it}^{\mathrm{p}\uparrow} p_{it}^{\mathrm{up}}}_{\text{Cost of } p^{\mathrm{up}} \text{ from gen.}} - \underbrace{C_{it}^{\mathrm{p}\downarrow} p_{it}^{\mathrm{dn}}}_{\text{Cost of } p^{\mathrm{dn}} \text{ to gen.}} + \underbrace{C_{it}^{\mathrm{q}\uparrow} q_{it}^{\mathrm{up}}}_{\text{Cost of } q^{\mathrm{up}} \text{ from gen.}} \\ & - \underbrace{C_{it}^{\mathrm{q}\downarrow} q_{it}^{\mathrm{dn}}}_{\text{Cost of } q^{\mathrm{dn}} \text{ to gen.}} \Big] + \sum_{d,c,t} \Big[\underbrace{C_{dct}^{\mathrm{DR}\uparrow} r_{dct}^{\mathrm{up}}}_{\text{Cost of } r^{\mathrm{up}} \text{ from DR}} - \underbrace{C_{dct}^{\mathrm{DR}\downarrow} r_{dct}^{\mathrm{dn}}}_{\text{Cost of } r^{\mathrm{dn}} \text{ to DR}} \Big] \end{aligned} \tag{5}$$

where Ξ is the set of optimization variables, including free variables p_{nt}, q_{nt}, p_{njt}, q_{njt}, non-negative variables p_{it}^{up}, p_{it}^{dn}, r_{dct}^{up}, r_{dct}^{dn}, s_{nt}^{up}, $p_t^{\mathrm{up,S}}$, $p_t^{\mathrm{dn,S}}$, q_{it}^{up}, q_{it}^{dn}, $q_t^{\mathrm{up,S}}$, $q_t^{\mathrm{dn,S}}$, v_{nt}, and binary variables o_{dct}.

The common constraints for all three OPF models are given in (6). Note that DR_{ct}^{disp}, D_{nt}^{disp}, S_t^{disp} and P_{it}^{disp} are parameters, indicating day-ahead market outcomes.

$$p_{nt} = \sum_{j \in \Phi_n} p_{njt}, \quad \forall n,t \tag{6a}$$

$$q_{nt} = \sum_{j \in \Phi_n} q_{njt}, \quad \forall n,t \tag{6b}$$

$$\begin{aligned} p_{nt} = & \sum_{d,c \in L_n} [r_{dct}^{\mathrm{up}} - r_{dct}^{\mathrm{dn}}] - \sum_{c \in L_n} DR_{ct}^{\mathrm{disp}} \\ & + \sum_{i \in L_n} \left[p_{it}^{\mathrm{up}} - p_{it}^{\mathrm{dn}} + P_{it}^{\mathrm{disp}} \right] \\ & + \left[S_t^{\mathrm{disp}} + p_t^{\mathrm{up,S}} - p_t^{\mathrm{dn,S}} \right]_{n \in PCC} \\ & - D_{nt}^{\mathrm{disp}} + s_{nt}^{\mathrm{up}} - \sum_{j \in \Phi_n} \frac{G_{nj}}{2} v_{nt}, \quad \forall n,t \end{aligned} \tag{6c}$$

$$\begin{aligned} q_{nt} = & \sum_{i \in L_n} \left[q_{it}^{\mathrm{up}} - q_{it}^{\mathrm{dn}} \right] + \left[q_t^{\mathrm{up,S}} - q_t^{\mathrm{dn,S}} \right]_{n \in PCC} \\ & - Q_{nt} + \sum_{j \in \Phi_n} \frac{B_{nj}}{2} v_{nt}, \ \forall n,t \end{aligned} \tag{6d}$$

$$\sum_d r_{dct}^{\mathrm{up}} \le DR_{ct}^{\mathrm{disp}}, \quad \forall c,t \tag{6e}$$

$$p_{it}^{\mathrm{dn}} \le P_{it}^{\mathrm{disp}}, \quad \forall i,t \tag{6f}$$

$$s_{nt}^{\mathrm{up}} + \sum_{d,c \in L_n} \left[r_{dct}^{\mathrm{up}} - r_{dct}^{\mathrm{dn}} \right] \le D_{nt}^{\mathrm{disp}} + \sum_{c \in L_n} DR_{ct}^{\mathrm{disp}}, \forall n,t \tag{6g}$$

$$p_{it}^{\mathrm{up}} + P_{it}^{\mathrm{disp}} \le P_i^{\mathrm{cap}}, \quad \forall i,t \tag{6h}$$

$$\sum_d r_{dct}^{\mathrm{dn}} + DR_{ct}^{\mathrm{disp}} \le P_{ct}^{\mathrm{cap}}, \quad \forall c,t \tag{6i}$$

$$p_{it}^{\mathrm{up}} \le \overline{P}_i^{\mathrm{up}}, \ p_{it}^{\mathrm{dn}} \le \overline{P}_i^{\mathrm{dn}}, \ \forall i,t \tag{6j}$$

$$q_{it}^{\mathrm{up}} \le \overline{Q}_i^{\mathrm{up}}, \ q_{it}^{\mathrm{dn}} \le \overline{Q}_i^{\mathrm{dn}}, \quad \forall i,t \tag{6k}$$

$$p_t^{\mathrm{up,S}} \le \overline{P}^{\mathrm{up,S}}, \ p_t^{\mathrm{dn,S}} \le \overline{P}^{\mathrm{dn,S}}, \ \forall t \tag{6l}$$

$$q_t^{\mathrm{up,S}} \le \overline{Q}^{\mathrm{up,S}}, \ q_t^{\mathrm{dn,S}} \le \overline{Q}^{\mathrm{dn,S}}, \ \forall t \tag{6m}$$

$$\underline{V}_n^{\mathrm{sq}} \le v_{nt} \le \overline{V}_n^{\mathrm{sq}}, \quad \forall n,t. \tag{6n}$$

The net active and reactive power injection at node n is linked to corresponding flow from node n to j in (6a) and (6b). The nodal active power balance is enforced by (6c). Note that the last term of (6c) takes into account the shunt conductance of the lines[7]. The nodal reactive power balance is enforced by (6d), which also takes into account the shunt susceptance of the lines connected to node n. The up-regulation (load decrease) provided by DR unit c is limited to its scheduled consumption DR_{ct}^{disp} in (6e). The down-regulation (generation decrease) provided by generator i is restricted to its dispatch from the day-ahead market by (6f). Constraint (6g) limits the curtailed load s_{nt}^{up} according to total scheduled consumption of flexible and inflexible loads from the day-ahead market and provided regulation from DR units. The up-regulation (generation increase) provided by conventional generator i is limited by (6h). Similarly, (6i) restricts the down-regulation (load increase) provided by DR unit c. Constraints (6j) and (6k) limit the active and reactive power regulation of conventional generator i to its maximum capability. Similar constraints are applied to the import/export at the PCC from transmission level in (6l) and (6m). Constraint (6n) limits the voltage magnitude to the upper and lower thresholds.

1) Mixed-Integer Linear OPF (Lossless): The lossless mixed-integer linear OPF is the simplest approximation of the power flow for radial distribution systems used in this paper. It is possible by using this OPF method to include the line congestion and voltage issues. Similar to LinDistFlow model in [30], in order to have an approximation of both active and reactive power flow and their effect on the voltage, a decoupled linear power flow is used. The advantage of this approach is that it is computationally simple and well known. For the radial case, the linearized branch flow OPF boils down to problem (7):

$$\min_{\Xi} \ f(\Xi) \text{ as in (5)} \tag{7a}$$

subject to:

[5]The original AC-OPF model is a non-convex quadratically constrained program [29], which can be convexified by relaxing it to either an SOCP or a semi-definite program. We use the former in this paper.

[6]The DSO pays for up-regulation, while it is paid by sources providing down-regulation.

[7]Half of the shunt losses due to shunt admittance of every line connected to node n is subtracted from that node. In general, shunt conductance of lines is small and can be ignored. However, shunt susceptance can be significant in underground cables.

$$p_{njt} = -p_{jnt},\ q_{njt} = -q_{jnt},\ \forall n, j \in \Phi_n, t \tag{7b}$$
$$\sum_n p_{nt} = 0, \quad \forall t \tag{7c}$$
$$\sum_n q_{nt} = 0, \quad \forall t \tag{7d}$$
$$p_{njt} \le \overline{F}_{nj}, \qquad \forall n, j \in \Phi_n, t \tag{7e}$$
$$v_{jt} = v_{nt} - 2\left(R_{nj}p_{njt} + X_{nj}q_{njt}\right), \forall n, j \in \Phi_n, t \tag{7f}$$
$$(1) \text{ to } (4), (6) \text{ and } (11). \tag{7g}$$

Constraints (7b), (7c) and (7d) model the lossless linear power flow. To preserve linearity, (7e) imposes the line capacity limit in terms of active power flow only. Finally, (7f) links the voltage magnitude of two adjacent nodes with impedance and power flows as a linear approximation. Similar to [30], a variable v_{nt} is introduced to present squared voltage magnitude, such that the model remains linear.

2) Mixed-Integer Linear OPF With Losses: The mixed-integer linear OPF model (7) does not take into account losses. In order to improve the accuracy of the congestion management method, it is desirable to model losses, especially for low-voltage radial systems with relatively large losses. An approximation of active power losses is slightly more complex, since losses generally are quadratic to the flow in a line. In order to keep the model linear, an iterative approach as in [27] and [28] can be used. For every iteration of solving the OPF problem a new *loss-cut* is generated, which approximates the losses successively. This approach usually converges after very few iterations. The loss in a line that can be assigned to a node is approximated by (8) [27]:

$$P_{nt}^{\text{loss,fix}} = \sum_{j\in\Phi_n}\left(\frac{R_{nj}\ p_{njt}^2}{2}\right),\ \forall n, t. \tag{8}$$

Here the losses are a quadratic function of the line flows. The procedure used in [27] is then to add half of the losses to the consumption of every node connected to the ends of the line. In order for the losses to be at the lower bound of the loss-cut at iteration ν, an auxiliary slack variable $y_{nt}^{(\nu)}$ is added to the objective function, but at a negligible small profit C^y. The mixed-integer linear OPF problem at iteration ν including the loss-cuts is given in optimization problem (9):

$$\min_{\Xi, y_{nt}^{(\nu)}\ge 0, p_{nt}^{\text{loss}(\nu)}\ge 0} \quad f(\Xi)^{(\nu)} - \sum_{nt} C^y y_{nt}^{(\nu)} \tag{9a}$$

subject to:

$$\sum_n (p_{nt}^{(\nu)} - p_{nt}^{\text{loss}(\nu)} - y_{nt}^{(\nu)}) = 0,\ \forall t \tag{9b}$$
$$p_{nt}^{(\nu)} - p_{nt}^{\text{loss}(\nu)} - y_{nt}^{(\nu)} = \sum_{j\in\Phi_n} p_{njt}^{(\nu)},\ \forall n, t \tag{9c}$$
$$p_{nt}^{\text{loss}(\nu)} - \sum_{j\in\Phi_n}(R_{nj}\ P_{njtr}^{\text{fix}})p_{njt}^{(\nu)} \ge -P_{ntr}^{\text{loss,fix}}, \forall n, t, r = \{1, \dots, \nu - 1\} \tag{9d}$$
$$(1) \text{ to } (4), (6b) \text{ to } (6n), (7b), (7d), (7e), (7f) \text{ and } (11) \tag{9e}$$

where r is the index of loss-cuts, and parameter $P_{ntr}^{\text{loss,fix}}$ is the fixed loss obtained from the line flow of the previous iterations by solving (8). Furthermore, parameter P_{njtr}^{fix} is the flow in the line connecting nodes n and j from the previous iterations. The problem (9) has to be solved iteratively, adding one cut per iteration in (9d). The convergence is reached at iteration ν once $\left|\sum_{nt} P_{nt,(r=\nu)}^{\text{loss,fix}} - \sum_{nt} p_{nt}^{\text{loss},(\nu)}\right| \le \epsilon$, where ϵ is a small tolerance. Note that the optimal value of slack variable $y_{nt}^{(\nu)}$ should be zero.

3) Mixed-Integer SOCP-OPF: The mixed-integer SOCP OPF model for radial distribution systems is presented in (10) [29]:

$$\min_{\Xi, \varphi_{njt}\ge 0} \ f(\Xi) \text{ as in } (5) \tag{10a}$$

subject to:

$$p_{njt}^2 + q_{njt}^2 \le \varphi_{njt} v_{nt},\ \forall n, j \in \Phi_n,\ t \tag{10b}$$
$$p_{njt} + p_{jnt} = R_{nj}\varphi_{njt},\ \forall n, j \in \Phi_n,\ t \tag{10c}$$
$$q_{njt} + q_{jnt} = X_{nj}\varphi_{njt},\ \forall n, j \in \Phi_n,\ t \tag{10d}$$
$$v_{jt} = v_{nt} - 2(R_{nj}p_{njt} + X_{nj}q_{njt}) + (R_{nj}^2 + X_{nj}^2)\varphi_{njt}, \forall n, j \in \Phi_n,\ t \tag{10e}$$
$$p_{njt}^2 + q_{njt}^2 \le \overline{F}_{nj}^2,\ \forall n, j \in \Phi_n,\ t \tag{10f}$$
$$(1) \text{ to } (4), (6) \text{ and } (11). \tag{10g}$$

Constraint (10b) is a convex relaxation of a quadratic equality constraint from the original non-convex AC-OPF problem. This relaxation is necessary to include the interior space of the quadratic cone described by this equation to ensure convexity. Constraints (10c) and (10d) are the active and reactive power losses, respectively. Constraint (10e) relates the voltage drop to the power flows and currents. In (10f) the line flow limit is enforced. In our numerical studies, the sufficient conditions introduced in [21] are also added to (10) to ensure zero duality gap (i.e., exactness) of the relaxation in radial networks[8]. These sufficient conditions are given in the online appendix [26]. Note that these conditions guarantee achieving the exactness, but at the cost of shrinking the feasible space, and potentially increasing the system cost and usually the computational burden.

IV. Case Studies

An illustrative example and a larger case study using the IEEE 37-node test feeder are provided. All cases are implemented in GAMS and solved using CPLEX version 12.8.

A. Illustrative Example

A radial 6-node system is used to introduce the congestion management mechanism with different OPF models. The diagram of this feeder is illustrated in Fig. 2. This feeder contains three DR units (c_1 to c_3) and two local conventional generators (i_1 and i_2). The line connecting nodes 3 and 4 is likely to be congested due its limited capacity (40 kVA). All line resistances are set to 0.001 p.u. and reactances are fixed to 0.0005 p.u. In addition, the shunt conductance and susceptance of all lines are set to be 0.1 p.u. As input

[8]Without sufficient conditions, the second-order cone constraint (10b) might be still binding in specific cases (e.g., in the case studies of this paper presented in Section IV), but there is no exactness guarantee in general. In case of inexactness, an ex-post procedure for feasibility recovery is required [31].

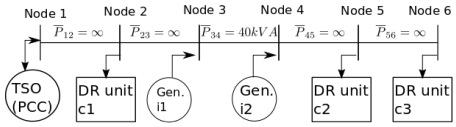

Fig. 2. Illustrative example: 6-node radial feeder.

parameters, the global day-ahead market outcomes are given in the online appendix [26] (particularly, see Fig. 9 in that appendix). This figure includes 40 time steps, with resolution of 15 minutes. These inputs from the day-ahead dispatches makes the line connecting nodes 3 and 4 overloaded by 23 kVA throughout the time periods 12 to 26, and the DSO needs to run the proposed congestion management mechanism to relieve congestion using local flexible resources (two generators and three DR units) as well as changing the import/export from/to the TSO. Each local generator can provide active power up- and down-regulation up to 80 kW, and reactive power up- and down-regulation up to 30 kVAr. These limits for TSO are 100 kW and 30 kVAr. Each of the three DR units is offering four different asymmetric block offers (d_1 to d_4) as given in the online appendix [26] (in particular, see Table II in that appendix). We assume that DR units are unable to provide reactive power regulation. The regulation offer prices of all resources are given in the online appendix C [26]. For simplicity, we assume zero reactive loads in the illustrative example, though the large case study includes reactive loads. The upper and lower bounds of the nodal voltage magnitudes are set to 0.9 and 1.1 p.u., respectively. The voltage drop in this test case is very high, such that any differences between the three OPF models will be highlighted.

1) Results obtained from MILP-OPF (lossless): Since losses are not accounted for, the regulation sources on the two sides of the congested line between nodes 3 and 4 are *symmetrically*[9] re-dispatched, in such a way that the congestion is relieved. The regulation sources located at the PCC side of the congested line are TSO, DR unit c_1 and local generator i_1 (the so-called upstream sources), while the opposite side contains generator i_2, DR units c_2 and c_3 (downstream sources). The outcomes of the proposed DSO-level congestion management mechanism based on MILP-OPF (lossless) is depicted in Fig. 3a. Accordingly, in the time period with congestion (i.e., from time step 12 to 26), the downstream sources c_2 , c_3 and i_2 provide up-regulation while the upstream source with the best offer, i.e., TSO, provides down-regulation. In this time period, DR unit c_2 provides up-regulation through its rebound block, preceded with a response (down-regulation) before the congestion period. In contrast, DR unit c_3 provides up-regulation as its response block in the time period during congestion, and rebounds with down-regulation after the congestion. The total re-dispatch cost of the system, i.e., the value of objective function (5), is \$45.35.

2) Results obtained from iterative MILP-OPF with losses: We solve the iterative problem (9), which converges in the fourth iteration for this illustrative example. The congestion mechanism outcomes based on this iterative OPF problem is

[9]At any time step, the total up-regulation is equal to total down-regulation.

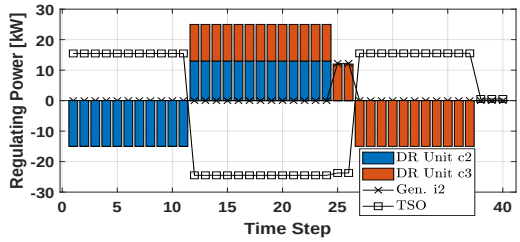

(a) MILP-OPF, lossless (total re-dispatch cost: \$45.35)

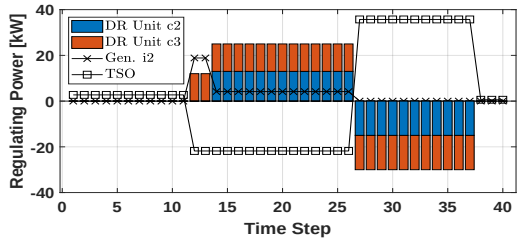

(b) MILP-OPF with losses (total re-dispatch cost: \$93.69)

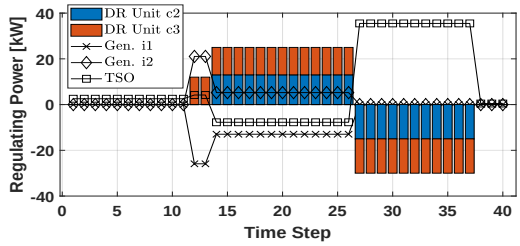

(c) MI-SOCP OPF with sufficient conditions (total re-dispatch cost: \$122.59)

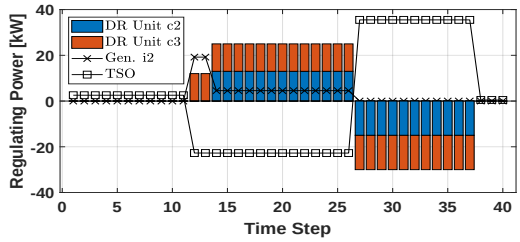

(d) MI-SOCP OPF without sufficient conditions (total re-dispatch cost: \$92.24)

Fig. 3. Illustrative example: Optimal active power regulation obtained from different congestion management mechanisms proposed.

given in Fig. 3b. Compared to Fig. 3a (the MILP-OPF without losses), we observe three main differences: i) a different asymmetric block offer from the down-stream DR unit c_2 is accepted, ii) due to active power losses[10], the total up- and down-regulations at each time step are not equal anymore, iii) the total re-dispatch cost of the system increases by \$48.34 (an increase of 106%).

[10]The reactive power losses are not modeled, but will be taken into account in MI-SOCP OPF model.

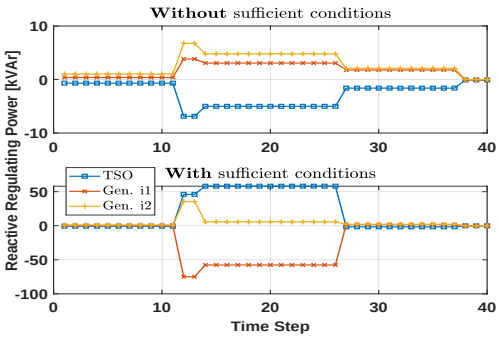

Fig. 4. Illustrative example: Optimal reactive power regulation obtained from the congestion management mechanism based on MI-SOCP OPF (upper plot: without sufficient conditions; lower plot: with sufficient conditions).

3) Results obtained from MI-SOCP OPF: This OPF model formulated in (10) is more precise than the two previous OPF models, as it considers both active and reactive power losses. Besides, voltages are modeled more precisely due to current magnitude modeling. Here, we provide results obtained from MI-SOCP OPF with and without enforcing the sufficient conditions for exactness. The active power re-dispatch results are given in Figs. 3c and 3d for cases with and without the sufficient conditions, respectively. For the same two cases, Fig. 4 depicts the reactive power re-dispatch results. There are three important observations to highlight.

First, the re-dispatch outcomes without sufficient conditions are found to be binding in (10b), which means that the convex relaxation is exact, and the solution achieved is AC feasible. The validation results that will be provided in Section IV.A.4 also confirm the exactness. However, note that this is case-specific, and in general, there is no guarantee achieving the exact solution from this relaxed OPF model without enforcing the sufficient conditions.

Second, the active power re-dispatch outcomes and the total re-dispatch cost obtained from MI-SOCP OPF model without sufficient conditions in Fig. 3d are similar to those obtained from the MILP-OPF model with losses in Fig. 3b. However, the voltage profile obtained in the MILP-OPF model with losses is not as accurate as the one in the MI-SOCP OPF model, as it will be demonstrated in Section IV.A.4.

Third, the total re-dispatch cost obtained from the MI-SOCP OPF model increases from $92.24 to $122.59 when adding the sufficient conditions. The reason for this cost increase is that the sufficient conditions shrink the feasible space. In other words, the MI-SOCP OPF model with sufficient conditions determines the exact optimal solution for the AC-OPF problem with the reduced feasible space. For example, these conditions avoid having simultaneous reverse active and reactive power flows, as demonstrated in Fig. 5 for a sample line. In the upper plot of this figure (without sufficient conditions), there are simultaneous reverse active and reactive power flows over the line from time step 12 to 26 (i.e., peak time period), while it never happens in the lower plot when adding sufficient conditions. For the same reason, the expensive generator i_1 is re-dispatched when enforcing sufficient conditions (Fig. 3c),

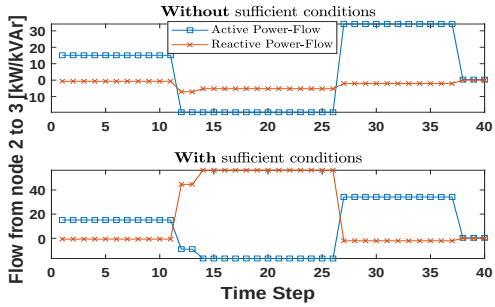

Fig. 5. Active and reactive power flow over the line from node n_2 to node n_3 (upper plot: without sufficient conditions; lower plot: with sufficient conditions).

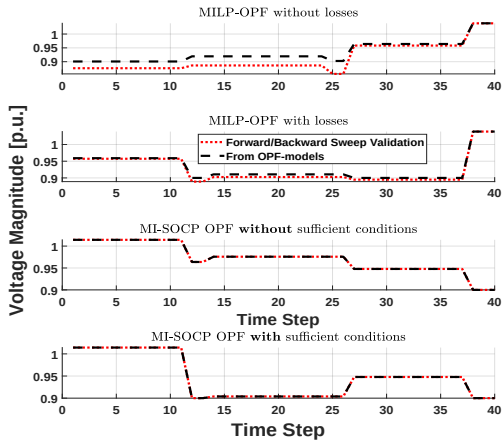

Fig. 6. Illustrative example: Voltage profile at node n_6 achieved by OPF models and forward-backward sweep validation (first plot: MILP-OPF lossless; second plot: MILP-OPF with losses; third plot: MI-SOCP OPF without sufficient conditions; fourth plot: MI-SOCP OPF with sufficient conditions).

while the production of that generator is unchanged in the case without sufficient conditions, and the TSO provides the regulation service instead (Fig. 3d). Therefore, it is logical to first check the exactness of the results obtained by MI-SOCP OPF model without sufficient conditions, and then to add those conditions if necessary.

4) Ex-post numerical validation: For given active and reactive regulation outcomes of flexible resources within the three different OPF models, we solve a power flow problem based on a forward-backward sweep method for validation purposes. This way, we numerically determine the voltage profiles at non-slack nodes (i.e., n_2 to n_6 as PQ nodes), and compare them with those achieved from the OPF models. Fig. 6 illustrates the voltage profile of node n_6 achieved from each OPF model and forward-backward sweep validation[11]. Based on the validation, as expected, the MI-SOCP OPF model provides the most precise outcomes. The error

[11]Node n_6 is selected since it is at the end of the feeder and thus is expected to have the most critical voltage profile.

is 0.0001% for the voltage of the worst node (n_6) when comparing the voltage profile obtained by forward-backward sweep validation method with that obtained from the MI-SOCP OPF model. This error in MILP-OPF models without and with losses is 2.4% and 0.55%, respectively. As another important observation, the voltage profiles obtained by the two MILP-OPF models are within the allowable bounds, however when verifying them with forward-backward sweep validation, it becomes apparent that the voltage constraints are violated in some time steps. However, this is not the case for the voltage profiles obtained from MI-SOCP OPF model with and without sufficient conditions, which verifies their solution is AC feasible and exact.

B. Case Study: IEEE 37-Node Test Feeder

For the case study, we use the IEEE 37-node test-feeder [32], whose diagram is given in the online appendix D [26]. All three-phase line impedances and loads are transformed into single phase equivalents, and transformers are removed where necessary. The load data profiles are generated with 30-minute time resolution, yielding a time horizon with 48 time steps. The spot loads of the original test case are considered as the peak load magnitudes, and then the 24-hour load profiles are normalized based on data for a summer week-day in 2017 for eastern Denmark sector of the Nordpool market. Load curves are given in the online appendix D [26]. Five conventional generators and four DR units are located at different nodes. The line capacity between nodes 2 and 3 is limited to 1000 kVA, such that it will be congested during the peak load hours.

For computational performance analysis, we consider two cases, namely Cases A and B, with different number of offers per DR unit and thus different number of binary variables in the OPF models. In Case A, each DR unit submits three asymmetric block offers, while it is 8 offers in Case B. In particular, Case A ends up to mixed-integer models with 576 binary variables, while Case B contains 1536 binary variables.

Fig. 7 presents the voltage profile in Case A for the worst node achieved from the three OPF models and the forward-backward sweep validation. Similar to our results in the illustrative example, MI-SOCP OPF provides more precise outcomes than the other two MILP models. Some extra results are available in the online appendix [26].

The total re-dispatch cost, total active and reactive power losses and CPU times[12] among the three OPF models are given in Table I. In particular, note that this table includes the results obtained from the MI-SOCP OPF with and without sufficient conditions. Similar to the illustrative example in the previous section, the MI-SOCP OPF model without sufficient conditions is found to be binding in the second-order cone constraint (10b). This implies that the solution of the MI-SOCP OPF model in this specific case study is exact and thus AC feasible. In Case A, compared to the MI-SOCP OPF without sufficient conditions, the MILP-OPF with loss approximation underestimates the total active power losses and the total re-dispatch cost by 8.7% and 12.3%, respectively.

[12]Hardware used: Huawei XH620 V3 with two Intel Xeon Processors 2650v4 (12 core, 2.20GHz), 256 GB memory, FDR Infiniband, 480 GB-SSD disk

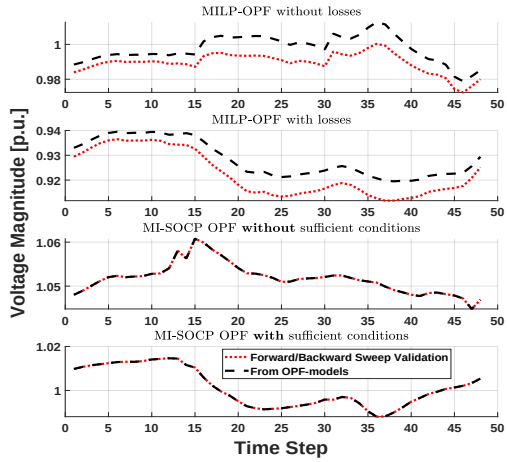

Fig. 7. Case study (Case A): Voltage profile at node n_{32} achieved by OPF models and forward-backward sweep validation (first plot: MILP-OPF lossless; second plot: MILP-OPF with losses; third plot: MI-SOCP OPF without sufficient conditions; fourth plot: MI-SOCP OPF with sufficient conditions).

TABLE I
CASE STUDY: OUTCOMES OF THE THREE PROPOSED CONGESTION MANAGEMENT MECHANISMS AND THEIR CPU TIMES FOR CASES A AND B

Result	Case	MILP lossless	MILP w. loss	MISOCP w. suff.	MISOCP w/o. suff.
Re-dispatch cost [$]	A	1694	2486	5115	2836
Active loss [kWh]		N/A	1454	2819	1593
Reactive loss [kVArh]		N/A	N/A	1913	1379
CPU time [s]		9	72.9	513	288
Re-dispatch cost [$]	B	1594	2371	5007	2725
Active loss [kWh]		N/A	1478	2783	1607
Reactive loss [kVArh]		N/A	N/A	1896	1384
CPU time [s]		34	209	12478	1381

These underestimations in Case B are 8.0% and 13.0%, respectively. When adding sufficient conditions to the MI-SOCP OPF model, the system cost increases significantly. The reason for this cost increase is that the sufficient conditions shrink the feasible space, and consequently, some expensive up-stream generators (closer to the PCC) are re-dispatched. This conic model as the most accurate mechanism among the three models requires more CPU time than the other two MILP mechanisms. The increase in CPU time by increasing the number of binary variables, especially in MI-SOCP OPF model with sufficient conditions, is significant. The CPU time increase is less significant when no sufficient conditions are enforced. In order to get a better insight into the increase in CPU time versus the amount of binary variables in the MI-SOCP OPF model with sufficient conditions, we plot the CPU time as a function of numbers of time steps and asymmetric block offers in Fig. 8.

V. CONCLUSION

This paper proposed a congestion management mechanism for distributions grids, accounting for potential rebound effect of demand response units. To this purpose, we incorporated

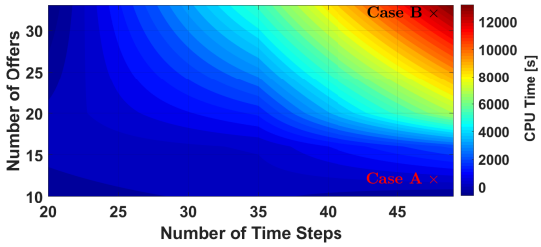

Fig. 8. Case study: CPU time for the MI-SOCP OPF model with sufficient conditions as function of time steps and total number of block offers. (Note: this is a linear interpolation between at 24, 35 and 48 time steps, and 12, 16, 20 and 32 offers.)

asymmetric block offers into the proposed mechanism at the cost of introducing a set of binary variables, which leads to increasing computational burden. For this mechanism, we checked three different OPF models: i) MILP-OPF (lossless) as the most simplified one, ii) MILP-OPF with loss approximations, and iii) MI-SOCP OPF as the most accurate one. We also analyze the performance of MI-SOCP OPF model with and without including sufficient conditions that guarantee an exact relaxation (i.e. AC feasible solution). We show that the outcomes of the proposed mechanism, especially asymmetric blocks dispatched, are sensitive to the OPF model used, i.e., the level of network simplifications considered. Among the three models, the MI-SOCP OPF has the best technical performance, but at the cost of high computational burden, especially when adding sufficient conditions for exactness. It is of our future interest to explore the alternatives to reduce the computational burden, e.g., using decomposition techniques.

REFERENCES

[1] J. Villar, R. Bessa, and M. Matos, "Flexibility products and markets: Literature review," *Electr. Power Syst. Res.*, vol. 154, pp. 329–340, 2018.

[2] S. Y. Hadush and L. Meeus, "DSO-TSO cooperation issues and solutions for distribution grid congestion management," *Energy Policy*, vol. 120, pp. 610–621, 2018.

[3] F. Capitanescu, "TSO–DSO interaction: Active distribution network power chart for TSO ancillary services provision," *Elect. Power Syst. Res.*, vol. 163, pp. 226–230, 2018.

[4] M. Caramanis, E. Ntakou, W. W. Hogan, A. Chakrabortty, and C. Schoene, "Co-optimization of power and reserves in dynamic T&D power markets with nondispatchable renewable generation and distributed energy resources," *Proceedings of the IEEE*, vol. 104, no. 4, pp. 807–836, 2016.

[5] A. Papavasiliou and I. Mezghani, "Coordination schemes for the integration of transmission and distribution system operations," in *Power Syst. Comput. Conf. (PSCC)*, (Dublin, Ireland), Jun. 2018.

[6] A. Vicente-Pastor, J. Nieto-Martin, D. W. Bunn, and A. Laur, "Evaluation of flexibility markets for retailer-DSO-TSO coordination," *IEEE Trans. Power Syst.*, 2018, to be published.

[7] J. P. Silva, J. A. Sumaili, R. J. Bessa, L. Seca, M. A. Matos, V. Miranda, M. Caujolle, B. Goncer-Maraver, and M. Sebastian-Viana, "Estimating the active and reactive power flexibility area at the TSO-DSO interface," *IEEE Trans. Power Syst.*, vol. 33, no. 5, pp. 4741–4750, 2018.

[8] R. A. Verzijlbergh, L. J. De Vries, and Z. Lukszo, "Renewable energy sources and responsive demand. Do we need congestion management in the distribution grid?" *IEEE Trans. Power Syst.*, vol. 29, no. 5, pp. 2119–2128, 2014.

[9] L. A. Greening, D. L. Greene, and C. Difiglio, "Energy efficiency and consumption—the rebound effect—a survey," *Energy Policy*, vol. 28, pp. 389–401, 2000.

[10] S. Sorrell and J. Dimitropoulos, "The rebound effect: Microeconomic definitions, limitations and extensions," *Ecological Economics*, vol. 65, pp. 636–649, 2008.

[11] F. Sossan, *Indirect control of flexible demand for power system applications*. (Ph.D. thesis), Technical University of Denmark, 2014. [Online]. Available: http://orbit.dtu.dk/files/100219481/sossan_thesis.pdf.

[12] Y. Liu, J. T. Holzer, and M. C. Ferris, "Extending the bidding format to promote demand response," *Energy Policy*, vol. 86, pp. 82–92, 2015.

[13] N. O'Connell, P. Pinson, H. Madsen, and M. O'Malley, "Economic dispatch of demand response balancing through asymmetric block offers," *IEEE Trans. Power Syst.*, vol. 31, no. 4, pp. 2999–3007, 2016.

[14] G. A. Dourbois, P. Biskas, and D. I. Chatzigiannis, "Novel approaches for the clearing of the European day-ahead electricity market," *IEEE Trans. Power Syst.*, vol. 33, no. 6, pp. 5820–5831, 2018.

[15] N. O'Connell, Q. Wu, J. Østergaard, A. H. Nielsen, S. T. Cha, and Y. Ding, "Day-ahead tariffs for the alleviation of distribution grid congestion from electric vehicles," *Electr. Power Syst. Res.*, vol. 92, pp. 106–114, 2012.

[16] S. Huang, Q. Wu, S. S. Oren, R. Li, and Z. Liu, "Distribution locational marginal pricing through quadratic programming for congestion management in distribution networks," *IEEE Trans. Power Syst.*, vol. 30, pp. 2170–2178, 2015.

[17] R. Li, Q. Wu, and S. S. Oren, "Distribution locational marginal pricing for optimal electric vehicle charging management," *IEEE Trans. Power Syst.*, vol. 29, no. 1, pp. 203–211, 2014.

[18] H. Zhong, L. Xie, and Q. Xia, "Coupon incentive-based demand response: Theory and case study," *IEEE Trans. Power Syst.*, vol. 28, no. 2, pp. 1266–1276, 2013.

[19] M. R. Sarker, M. A. Ortega-Vazquez, and D. S. Kirschen, "Optimal coordination and scheduling of demand response via monetary incentives," *IEEE Trans. Smart Grid*, vol. 6, no. 3, pp. 1341–1352, 2015.

[20] S. Huang and Q. Wu, "Real-time congestion management in distribution networks by flexible demand swap," *IEEE Trans. Smart Grid*, vol. 9, no. 5, pp. 4346–4355, 2018.

[21] S. Huang, Q. Wu, J. Wang, and H. Zhao, "A sufficient condition on convex relaxation of AC optimal power flow in distribution networks," *IEEE Trans. Power Syst.*, vol. 32, no. 2, pp. 1359–1368, 2017.

[22] S. H. Low, "Convex relaxation of optimal power flow—Part I: Formulations and equivalence," *IEEE Trans. Control Netw. Syst.*, vol. 1, no. 1, pp. 15–27, 2014.

[23] M. Nick, R. Cherkaoui, J.-Y. Le Boudec, and M. Paolone, "An exact convex formulation of the optimal power flow in radial distribution networks including transverse components," *IEEE Trans. Autom. Control*, vol. 63, pp. 682–697, 2018.

[24] L. Bobo, S. Delikaraoglou, N. Vespermann, J. Kazempour, and P. Pinson, "Offering strategy of a flexibility aggregator in a balancing market using asymmetric block offers," in *Power Syst. Comput. Conf. (PSCC)*, (Dublin, Ireland), Jun. 2018.

[25] N. O'Connell, H. Madsen, P. Pinson, M. O'Malley, and T. Green, "Regulating power from supermarket refrigeration," in *Innovative Smart Grid Technologies Conference Europe (ISGT-Europe)*, (Istanbul, Turkey), IEEE, 2014, pp. 1–6.

[26] *Online appendix*. [Online]. Available: https://github.com/alherm/asymmetric_block_offers (visited on 07/30/2018).

[27] A. Helseth, "A linear optimal power flow model considering nodal distribution of losses," in *Conf. on the European Energy Market (EEM)*, (Florence), 2012.

[28] B. Eldridge, R. O'Neill, and A. Castillo, "An improved method for the DCOPF with losses," *IEEE Trans. Power Syst.*, vol. 33, no. 4, pp. 3779–3788, 2018.

[29] J. A. Taylor, *Convex Optimization of Power Systems*. Cambridge University Press, 2015.

[30] P. Sulc, S. Backhaus, and M. Chertkov, "Optimal distributed control of reactive power via the alternating direction method of multipliers," *IEEE Trans. Energy Convers.*, vol. 29, no. 4, pp. 968–977, 2014.

[31] L. Halilbasic, P. Pinson, and S. Chatzivasileiadis, "Convex relaxations and approximations of chance-constrained AC-OPF problems," *IEEE Trans. Power Syst.*, 2018, to be published.

[32] *37-bus feeder*, IEEE, 2000. [Online]. Available: http://sites.ieee.org/pes-testfeeders/resources/ (visited on 04/17/2018).

This appendix is available online at https://github.com/alherm/asymmetric_block_offers.

APPENDIX A
MATHEMATICAL REPRESENTATION OF ASYMMETRIC BLOCK OFFERS

This appendix provides the mathematical expression of the asymmetric block offers beginning with down-regulation, which is similar to equations (1) but with $A_{dc} = 0$:

$$\begin{cases} r^{\mathrm{dn}}_{dct} \le P^{\mathrm{rsp}}_{dc} o_{dct}, \quad \forall d,c,t & \text{(11a)} \\ r^{\mathrm{up}}_{dct} \le P^{\mathrm{rb}}_{dc} o_{dct}, \quad \forall d,c,t & \text{(11b)} \\ \sum_{\tau=t}^{t+T^{\mathrm{rsp}}_{dc}-1} r^{\mathrm{dn}}_{dc\tau} \ge T^{\mathrm{rsp}}_{dc} P^{\mathrm{rsp}}_{dc}(o_{dct} - o_{dc,t-1}), \quad \forall d,c,t & \text{(11c)} \\ \sum_{\tau=t+T^{\mathrm{rsp}}_{dc}}^{t+T^{\mathrm{rsp}}_{dc}+T^{\mathrm{rb}}_{dc}-1} r^{\mathrm{up}}_{dc\tau} \ge T^{\mathrm{rb}}_{dc} P^{\mathrm{rb}}_{dc}(o_{dct} - o_{dc,t-1}), \\ \qquad \forall d,c,t \le |T| - T^{\mathrm{rsp}}_{dc} & \text{(11d)} \\ \sum_{\tau=t}^{t+T^{\mathrm{rsp}}_{dc}-1} r^{\mathrm{up}}_{dc\tau} \le T^{\mathrm{rb}}_{dc} P^{\mathrm{rb}}_{dc}(1 - (o_{dct} - o_{dc,t-1})), \forall d,c,t & \text{(11e)} \\ \sum_{\tau=t+T^{\mathrm{rsp}}_{dc}}^{t+T^{\mathrm{rsp}}_{dc}+T^{\mathrm{rb}}_{dc}-1} r^{\mathrm{dn}}_{dc\tau} \le T^{\mathrm{rsp}}_{dc} P^{\mathrm{rsp}}_{dc}(1 - (o_{dct} - o_{dc,t-1})) & \text{(11f)} \\ \qquad , \forall d,c,t \le |T| - T^{\mathrm{rsp}}_{dc} \end{cases} \text{ if } A_{dc} = 0.$$

APPENDIX B
SUFFICIENT CONDITIONS

The additional sufficient conditions to be included in the MI-SOCP OPF model are listed below:

$$\hat{s}_{njt} = s_{nt} + \sum_{h:h\to n} \hat{s}_{hnt}, \quad \forall n > j \in \Phi_n, t \tag{12a}$$

$$\hat{v}_{nt} - \hat{v}_{jt} = 2\mathrm{Re}(\overline{Z}_{nj}\hat{s}_{njt}), \quad \forall n > j \in \Phi_n, t \tag{12b}$$

$$\mathrm{Re}(\overline{Z}_{nj}\hat{s}_{njt}) \le 0, \quad \forall n > j \in \Phi_n, t \tag{12c}$$

$$\hat{v}_{nt} \le \overline{V}^{\mathrm{sq}}_{n}, \quad \forall n, t, \tag{12d}$$

where $\hat{s}_{njt} = \hat{p}_{njt} + j\hat{q}_{njt}$ is a linear approximation of the complex line flows $s_{njt} = p_{njt} + jq_{njt}$, and $\overline{Z}_{nj} = R_{nj} - jX_{nj}$ is the complex conjugate line impedance. $s_{nt} = p_{nt} + jq_{nt}$ is the complex nodal apparent power injection. Besides, $\hat{v}_{nt}$ is a linear approximation of the squared nodal voltage. The notation $\sum_{h:h\to n}$ means the sum of all lines originating in node n. These sufficient conditions are quite mild, as long as there is no combined active and reactive reverse power flow on any line. The reverse power flow can be either active or reactive but not both[13].

[13]We found out that due to numerical issues with the used solver, convergence is achieved much faster if the right-hand side of equation (12c) is replaced with a small positive number. This will not affect the tightness of the achieved solution in any significant way.

APPENDIX C
INPUT DATA FOR ILLUSTRATIVE EXAMPLE

This appendix presents the input data for the illustrative example (6-node network). As the day-ahead market outcomes, Fig. 9 illustrates the production schedules of local conventional generators and the consumption level of DR units. The day-ahead market outcomes have a peak in power consumption between hours 12 and 26. The line between nodes 3 and 4 is congested during peak hours. The asymmetric block offers provided by the three DR units are given in Table II, where each DR unit offers 4 different blocks to the DSO. The offer prices for these blocks are constant through time and given together with the other applicable prices in Table III.

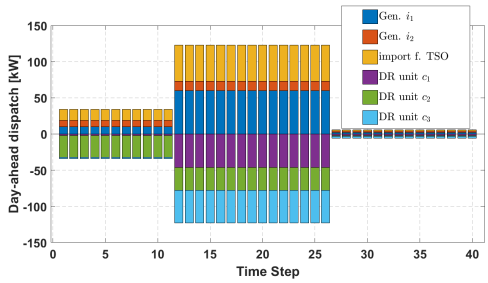

Fig. 9. Illustrative example: The input data, consisting of the day-ahead market outcomes in terms of active power. This market does not consider reactive power trading.

TABLE II
ILLUSTRATIVE EXAMPLE: THE ASYMMETRIC BLOCK OFFERS PROVIDED BY DR UNITS

DR unit	Offer	P^{rsp}_{dc}	P^{rb}_{dc}	T^{rsp}_{dc}	T^{rb}_{dc}	A_{dc}
c_1	d_1	13	17	13	9	1
	d_2	17	13	9	13	0
	d_3	10	10	20	21	1
	d_4	17	10	9	20	0
c_2	d_1	17	8	9	29	0
	d_2	8	17	29	9	1
	d_3	13	15	13	11	1
	d_4	15	13	11	13	0
c_3	d_1	12	15	15	11	1
	d_2	15	12	11	15	0
	d_3	11	13	18	14	1
	d_4	13	11	14	18	0

TABLE III
THE PRICES FOR UP- AND DOWN-REGULATION OFFERS PROVIDED BY TSO AND LOCAL DERS FOR BOTH THE ILLUSTRATIVE EXAMPLE AND THE CASE STUDY.

Resource*	Up offer price [¢/(kW-30min)]	Down offer price [¢/(kW-30min)]
Gen. i_1 and i_2	35	10
TSO	21	19
DR units c_1 to c_3	25	16

*We assume the same prices for active and reactive regulation offers. These prices are constant over time.

TABLE IV
IEEE 37-NODE TEST CASE: THE ASYMMETRIC BLOCK OFFERS PROVIDED BY DR UNITS

DR unit	Offer	P_{dc}^{rsp}	P_{dc}^{rb}	T_{dc}^{rsp}	T_{dc}^{rb}	A_{dc}
c_1	d_1	85	75	12	18	1
	d_2	72	65	13	17	0
	d_3	62	53	14	16	1
	d_4	52	43	15	15	0
	d_5	44	35	16	14	1
	d_6	32	23	17	13	0
	d_7	25	16	18	12	1
	d_8	14	5.8	19	11	0
c_2	d_1	91	11.5	18	11	0
	d_2	84	24.5	17	12	1
	d_3	76	33.5	16	13	0
	d_4	66	43.5	15	14	1
	d_5	56	53.5	14	15	0
	d_6	46	63.5	13	16	1
	d_7	36	73.5	12	17	0
	d_8	20	83.5	11	18	1
c_3	d_1	83	25.5	12	17	1
	d_2	75	34.5	13	16	0
	d_3	63	43.3	14	15	1
	d_4	53	53.3	15	14	0
	d_5	43	63.3	16	13	1
	d_6	33	73.35	17	12	0
	d_7	23	83.35	18	11	1
	d_8	13	93.35	19	10	0
c_4	d_1	102	1.55	18	10	0
	d_2	92	24.5	17	11	1
	d_3	82	33.5	16	12	0
	d_4	75	43.5	15	13	1
	d_5	65	53.5	14	14	0
	d_6	52	63.5	13	15	1
	d_7	45	73.5	12	16	0
	d_8	35	83.5	11	17	1

APPENDIX D
DATA FOR CASE STUDY: THE IEEE 37-NODE SYSTEM

This appendix gives all the input data for the 37-node case study of section IV. The offer prices from all DR units, local conventional generators and TSO are provided in Table III. All asymmetric block offers by the four DR units are listed in Table IV. For Case A, the first three offers of each unit are used, while in Case B all 8 offers for each unit are considered. Fig. 11a depicts the active power loads at each node of the system. Fig. 11b shows the reactive power loads at each node. The dispatch of the local generators and the import from the TSO at the PCC is given in Fig. 11c.

APPENDIX E
EXTRA RESULTS FOR THE IEEE 37-NODE SYSTEM

In this appendix, some extra results of the congestion management mechanism obtained from the IEEE 37-node case study in section IV-B are presented. These results are the re-dispatch of the local conventional generators, re-dispatch of import/export from the TSO and the dispatch of the asymmetric blocks.

The results obtained for Case A for all three OPF models are presented in Fig. 12. Likewise, the optimal results achieved in Case B for the three OPF models are presented in Fig. 13, with Fig. 13a showing the re-dispatch outcome for the linear lossless model, and Fig. 13b showig the re-dispatch for the linear model with loss approximation, and 13c showing the

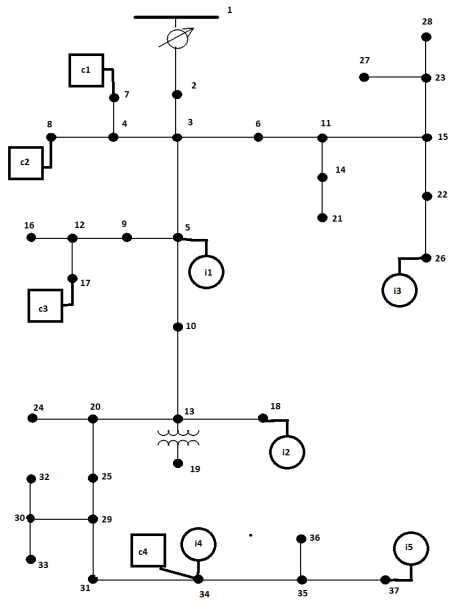

Fig. 10. The diagram for the IEEE 37-node test feeder with local generators and DR units. Note: The node numbers have been changed compared to the original test case in [32].

re-dispatch for the SOCP model. Comparing the dispatch of asymmetric blocks from the lossless MILP-OPF model and the one with loss approximation, it is observed that the same blocks are dispatched for both Cases A and B. There are minor differences in the re-dispatch of conventional generators and the import/export at the PCC due to the active power losses.

The re-dispatch results of the congestion management mechanism using the MI-SOCP OPF model are given in Fig. 12c and 13c. It is worth noticing that the asymmetric blocks dispatched in this model are quite different compared to those in MILP models.

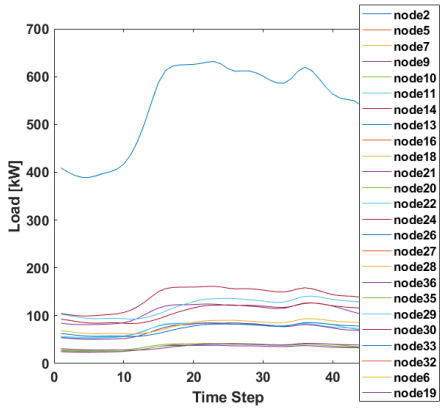

(a) Active power loads

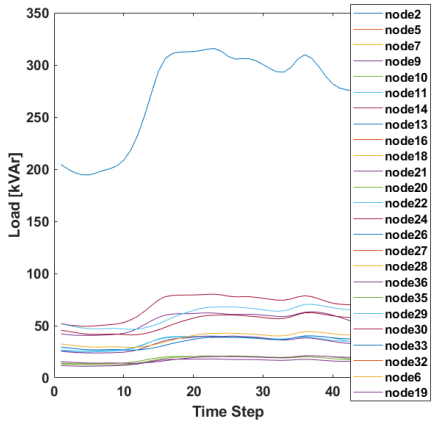

(b) Reactive power loads.

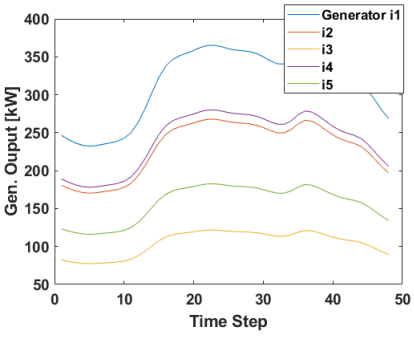

(c) Day-ahead schedule of the five conventional generators.

Fig. 11. IEEE 37-node case study input data.

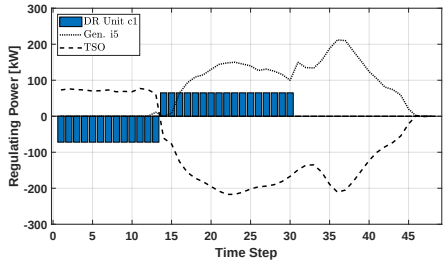

(a) MILP-OPF (lossless)

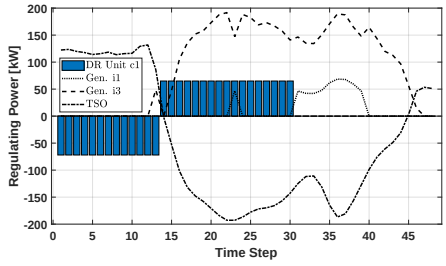

(b) MILP-OPF with loss approximation

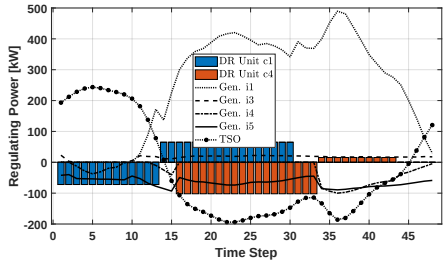

(c) MI-SOCP OPF with sufficient conditions.

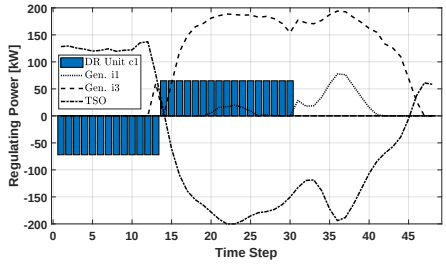

(d) MI-SOCP OPF without sufficient conditions.

Fig. 12. IEEE 37-node test case: Re-dispatch outcomes obtained from Case A with the three different OPF models.

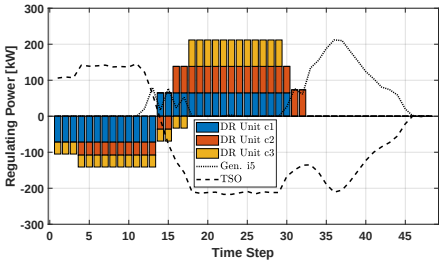

(a) MILP-OPF (lossless)

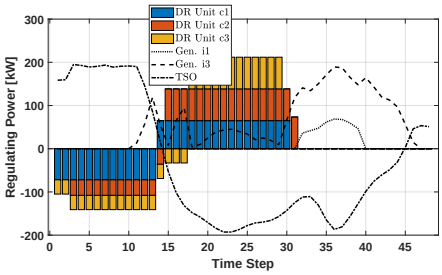

(b) MILP-OPF with loss approximation

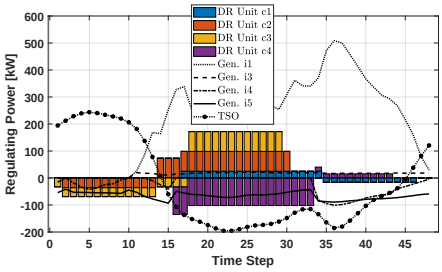

(c) MI-SOCP OPF with sufficient conditions

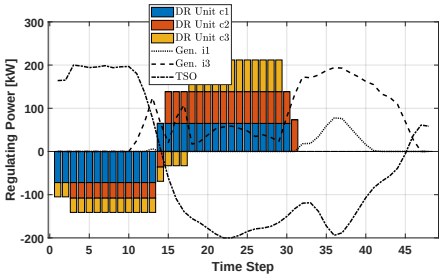

(d) MI-SOCP OPF without sufficient conditions.

Fig. 13. IEEE 37-node test case: Re-dispatch outcomes obtained from Case B with the three different OPF models.

(Paper B) TSO-DSO Coordination Via Optimized Interface Capacity Limits.

Authors:
Alexander Hermann, Tue Vissing Jensen, Jalal Kazempour and Jacob Østergaard
Published as:
Submitted to IEEE Transactions on Power Systems, Submitted March 15th 2019
Note:
The appendix which is published as an electronic companion on GitHub is attached after the main body of the manuscript. It contains some additional formulae and additional results. The Matlab code developed for this paper is published on GitHub.

TSO-DSO Coordination Via Optimized Interface Capacity Limits

Alexander Hermann, *Student Member, IEEE,* Tue Vissing Jensen, *Member, IEEE,*
Jalal Kazempour, *Senior Member, IEEE,* and Jacob Østergaard, *Senior Member, IEEE*

***Abstract*—Proposals for flexibility procurement are envisioning markets where the transmission system operator (TSO) can access flexibility of distribution system operator (DSO)-level units and vice versa, but the coordination between the two is still a matter of active research. In this paper, we examine day-ahead coordination through markets. While allowing the DSO to pre-qualify the participation of distributed energy resources (DERs) in wholesale markets, we treat prices and import/export limits at the interface of TSO and DSO as coordination variables in the day-ahead stage. For given values of these variables, the DSO's pre-qualification is done by imposing caps on the quantity bids of DERs in the wholesale markets. We quantify the potential benefit of this pre-qualification on the social welfare of the overall system. The resulting model is a bi-level optimization problem, which is decomposed to separate the conic modeling of real-time power flows from the mixed-integer linear formulation of the day-ahead market problem.**

***Index Terms*—TSO-DSO coordination, DSO market, congestion management, convex relaxation, Stackelberg Game.**

I. Introduction

DUE to organizational and policy driven issues, network constraint modeling is today left out of European zonal day-ahead electricity markets. The transmission system operator (TSO) is responsible for the safe operation of the whole system in transmission level, and interacts with markets only for flexibility procurement and exchange limits. The balancing of uncertain production of renewables in real-time is one of the main issues for the TSO for which distributed energy resources (DERs) can provide flexibility services [1]. However, DERs will often be located on low-voltage feeders of the distribution systems. In contrast, the distribution system operators (DSOs) currently safeguard their networks by over-dimensioning components and using uncoordinated local control. There are several proposals to liberalize the flexibility procurement, such that the DSO will operate its own local flexibility market to support network constraints [2]–[4]. In parallel, several proposals have been made for how TSO and DSOs can coordinate their real-time dispatch [5]–[7]. Common to these proposals is that the TSO and DSOs do not coordinate their flexibility procurement in the *day-ahead* stage, i.e. they coordinate only in real-time only, or are not congruent with current European electricity market regulations.

However, TSO-DSO coordination scheme in the day-ahead stage may allow for lower overall cost of system operation. Following this thread, as illustrated in Fig. 1, we propose to treat the interface characteristics between TSO and DSOs as 'coordination variables' in the day-ahead stage. These variables are (i) prices at the point of common coupling (PCC)[1] and (ii) the flow capacity limits at the PCC. These variables enable TSO and DSOs to coordinate on the day-ahead dispatch of DERs, because they influence the access of a DER in the DSO's domain to the TSO's flexibility markets, and vice versa. In practice, to coordinate on these variables, there must be an entity which defines the coordinating variables. We here examine the potential for coordination under this scheme, and introduce a new agent to fulfill this function, called the "PCC optimizer".

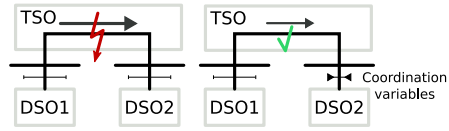

Fig. 1. Schematic of the proposed method for an example: In the left situation, the day-ahead flow from DSO1 to DSO2 creates congestion at the TSO level. In the right situation, restricting the coordination variables for DSO2 prevents congestion at the TSO level, avoiding expensive correction actions. In other potential examples, the congestion may happen in DSO level or both TSO and DSO levels, and then coordination at the interface of DSO1 or at the interface of both DSOs might be needed.

The PCC optimizer seeks to maximize the expected social welfare of the entire system (including both transmission and distribution levels, and in both day-ahead and real-time stages) and optimizes the coordination variables at the interface before day-ahead market clearing. The optimized coordination variables at each interface are eventually treated as exogenous parameters to the corresponding DSO. While in a practical implementation the PCC optimizer would not have full access to all information, e.g., market offers, we examine the idealized situation of perfect information access and assume an optimal coordination in real-time.

The research contributions of this paper are two-fold: (i) We propose a PCC optimizer who determines a set of interface prices and power flow capacity limits, leading the DSO to independently impose caps on quantity bids of DERs connected to its domain before day-ahead market clearing. This optimally restricts the participation of DERs in day-ahead markets, and effectively enables TSO-DSO coordination ex-ante (i.e., before day-ahead market clearing). It is also in line with the proposed market designs for DSO flexibility procurement. In contrast to other works such as [5]–[8], we design coordination in the day-ahead stage. (ii) We show that the functioning of the proposed PCC optimizer can be implemented as a bi-level problem, and under an assumption of information symmetry between PCC optimizer and DSOs, we are even able to simplify the proposed bi-level structure. We decompose the proposed bi-level problem using a Benders' decomposition algorithm to ease computational burden. A benefit of this decomposition is that it avoids solving a mixed-integer second-order cone

[1] 'PCC' here refers to the node connecting a distribution and transmission network. We use interface and PCC interchangeably. While prices at the DSO level are not a feature of current regulation, they are a necessary consequence, implicit or explicit, of any DSO-level market.

program, and separates it to a mixed-integer linear problem and a set of second-order cone problems (SOCP).

The paper is structured as follows: Section II provides the required preliminaries, positions our work relative to other works in the literature, and elaborates on the notion of the proposed coordination method. Section III explains the PCC optimizer and the structure of the underlying optimization problem. Section IV describes the Benders' decomposition approach, and defines two benchmark models. In section V, a case study based on a modified IEEE 24-node network is carried out. Section VI summarizes the findings and discusses their influence on potential practical coordination schemes.

II. Background and proposed Method

A. On the need for TSO-DSO coordination

The large-scale integration of DERs, which is expected in the future, will increase the power being transferred through low-voltage networks and therefore a coordinated use of flexibility is pertinent [1], [9]. Through aggregators and balancing responsible parties (BRPs), DERs will be able to participate in day-ahead and ancillary services markets[2] to smooth out system imbalances for the TSO or to support network constraints by the DSO or the TSO. The inconsistencies between day-ahead dispatching and flexibility procurement on both TSO and DSO sides will pose major challenges. Coordination methods are one way of optimizing the concurrent use of flexible resources.

The low-voltage (LV) distribution network is itself a system of massive scale such that co-optimization of high-voltage (HV) and LV resources is likely to be computationally intractable. One reason for this is that including LV networks introduces a series of issues that are complicated to model. For example, in addition to congestion, LV networks are prone to over and under-voltage issues which are more prominent than in HV transmission networks. Besides, the active and reactive power losses play a more prominent role in LV distribution systems due to a higher R/X ratio of cables. Further, the TSO-DSO role separation is, in a European context, often strictly enforced, such that each entity has limited information about the others' network, further restricting co-optimization.

The creation of local DSO-level flexibility markets is meant to address these issues, though their coordination with day-ahead and TSO-level flexibility markets is an open question.

B. Existing proposals for the TSO-DSO coordination

Previous works have focused on the TSO-DSO coordination in the real-time activation stage only [5], [6], [8], [10], [11]. However, in most countries the bulk of electricity is traded in the day-ahead market, and therefore, this paper aims at quantifying the possible cost-savings through TSO-DSO coordination based on day-ahead market bids. Any coordination that is included in the day-ahead stage is expected to increase the social welfare of the whole system, as a premium on energy is usually applied when moving closer to real-time. In [9], an integrated method for dispatching both active and reactive power and reserves is presented. However, this method is not compatible with current European zonal markets since it relies on co-optimization of energy and reserve as well as a nodal pricing approach.

Another recent proposal is that the DSO constrains the quantity bids of local DERs (or their aggregations) to other markets in order to meet local grid constraints. For example, [10] proposes a DSO-level ancillary services market. This is a framework where the DSO constrains the participation of local DERs in the day-ahead pool and the TSO-level flexibility market. Also, the European SmartNet project [12] and the Danish DREM project [13] have proposed several methods where the DSO constrains bids of DERs.

Another potential coordination method proposed in [9] and [14] is to co-optimize TSO and DSO operation, but using distributed optimization techniques. However, this leads to an iterative market-clearing process and does not comply with current market regulations. If such a co-optimization has to be avoided, an exchange of messages between TSO and DSO needs to happen. One possible method is for the DSO to forecast the grid loading and to share the feasible injection region at the interface with the TSO, as in [5], [6], [11]. This method requires the market-clearing agent to incorporate the feasible region of every DSO, which it may be unwilling to do due to the large scale of the market-clearing problem. Sharing the feasible space, also requires bi-directional exchanges of messages because first the DSO must receive information about prices at the interface, and subsequently communicate the feasible space to the TSO (or the market-clearing responsible).

C. Notion behind the proposed coordination method

The DSO-level congestion management can be achieved by establishing a local DSO market, such that the DSO can include the local grid constraints directly in this market [2]. However, DERs or DER aggregators are expected to participate in both local and global[3] markets. If a DER participates in a local DSO market only, it will reduce its ability for revenue, reducing social welfare of the overall system [7]. If all DERs participating in a local DSO market also bid in global markets, the DSO market effectively reduces to a *pre-qualification* of bids of the local DERs to global market. We thus propose to employ a TSO-DSO coordination method where the DSO can systematically constrain the quantity bids of DERs, and more generally aggregators taking part in the day-ahead markets.

In this setup with local DSO markets, the PCC characteristics (i.e., the prices and capacity limits at each PCC) naturally have an impact on the corresponding DSO market outcomes. This leads to the following question: how to determine the optimal values for these PCC characteristics that maximize the social welfare of the whole system? This motivates us to consider the PCC characteristics as coordination variables. In effect, optimizing these variables will lead to better coordination between the TSO and DSOs in the day-ahead stage. For this, the PCC optimizer which determines the optimal values of coordination variables in the interfaces, is introduced.

[2]We use ancillary services markets and flexibility markets interchangeably. The ancillary services markets operated by TSO exist today, but it is still an area of active research for DSOs. See [1] for a comprehensive review.

[3]By global, we refer to day-ahead pool and TSO-level flexibility markets.

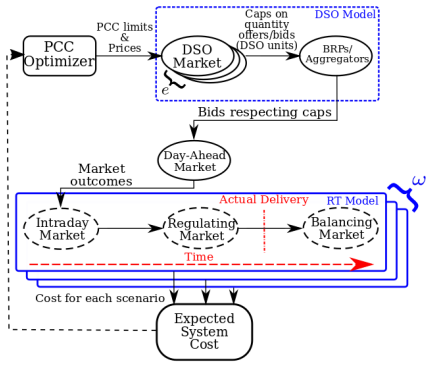

Fig. 2. The conceptual passing of information between different markets and agents involved in the coordination via the proposed PCC optimizer. The RT model is in reality encompassed by several steps, which are unified into one simplified model. For a relevant survey of RT markets, see [1]. Symbol e is an index for all DSOs connected to the underlying TSO. Symbol ω is the index for uncertainty scenarios in the DA stage, which realize in RT.

The PCC optimizer is modeled as a Stackelberg game, which respects the paradigm of a two-stage market clearing, i.e. the day-ahead (DA) market and a series of real-time (RT) re-dispatches[4] to meet network constraints. The PCC optimizer is the leader, while the DA and RT markets are the Stackelberg followers. The modeling of the PCC optimizer as a bi-level optimization problem has been inspired by recent works such as [15], where the optimal interface limits for trading between zonal day-ahead markets are found through bi-level modeling, and [16], where the optimal allocation of reserves is analyzed through a bi-level approach.

The interactions of agents and markets are schematically illustrated in Fig. 2, and explained below by four steps:

1) Before DA market-clearing, the PCC optimizer determines the coordination variables at each PCC, i.e., prices and flow capacity limits. Its objective is to minimize the total expected cost (or maximize the total expected social welfare) of the whole system, containing TSO and all DSOs' domains, and including both DA and RT stages.
2) Given the prices and power flow limits at interfaces set by the PCC optimizer (step 1) and still before DA market-clearing, each DSO (indexed by e) puts a cap on the production/consumption quantity that each DER located at its domain can offer/bid in the DA market. We refer to this stage as DSO's pre-qualification. Note that DERs can participate in DA market through aggregators and BRPs.
3) Given the quantity offers/bids of DER aggregators (step 2), the DA market is cleared.
4) Following the DA market in step 3, there are a series of RT or near RT corrections, both by the TSO and DSOs. We unify the modeling of all of these RT markets into a stochastic model, where premiums are applied to changing the DA dispatches.

Note that step 1 is the action of leader while anticipating the reactions of sequential followers in steps 2-4. The proposed method is uni-directional in message exchanges because the PCC optimizer needs only to send the interface characteristics to the DSO. There is no requirement that the DSO needs to send any cost curves or feasibility regions to the DA market-clearing agent.

We assume that renewable production is the only source of uncertainty. The production of each renewable energy source (RES) r is capped by an uncertain parameter $W^{\mathrm{RT}}_{r\omega}$ that is dependent on scenario ω (i.e., RES can be freely spilled as required). A full list of modeling assumptions is given in online Appendix A [17].

[4]This includes any mechanism that changes the day-ahead dispatches.

III. PCC Optimizer: Proposed Bi-level Model

A diagram of the proposed bi-level structure is shown in Fig. 3a, and its mathematical model is given by (1):

$$\max_{\Xi^{\mathrm{PCCO}}_e} \quad \mathcal{SW}^{\mathrm{DA}} - \sum_{\omega} \phi_\omega \Delta\mathrm{Cost}^{\mathrm{RT}}_\omega \tag{1a}$$

$$\text{s.t.} \quad \widetilde{p}^{\mathrm{DA}}_g, \widetilde{p}^{\mathrm{DA}}_d \in \mathbf{arg}\left((9)_e \mid \Xi^{\mathrm{PCCO}}_e \right), \forall e \tag{1b}$$

$$\mathcal{SW}^{\mathrm{DA}}, \widehat{p}^{\mathrm{DA}}_g, \widehat{p}^{\mathrm{DA}}_d \in \mathbf{arg}\left((3) \mid \widetilde{p}^{\mathrm{DA}}_g, \widetilde{p}^{\mathrm{DA}}_d \right) \tag{1c}$$

$$\Delta\mathrm{Cost}^{\mathrm{RT}}_\omega \in \mathbf{arg}\left((4)_\omega \mid \widehat{p}^{\mathrm{DA}}_g, \widehat{p}^{\mathrm{DA}}_d \right), \forall \omega \in \Omega, \tag{1d}$$

where $\Xi^{\mathrm{PCCO}}_e = \{\overline{f}_e, \underline{f}_e, \pi^{\mathrm{PCC,DA}}_e, \pi^{\uparrow\mathrm{PCC}}_e, \pi^{\downarrow\mathrm{PCC}}_e\}$ is the variable set of the PCC optimizer, which are indeed the coordination variables. A nomenclature is available in Table I.

The upper-level objective function (1a) maximizes the DA social welfare $\mathcal{SW}^{\mathrm{DA}}$ minus the expected RT cost. The incurred re-dispatch cost in RT under each scenario ω is $\Delta\mathrm{Cost}^{\mathrm{RT}}_\omega$, while ϕ_ω is the corresponding probability of that scenario. This objective function is constrained by three lower-level problems (1b), (1c) and (1d). For given values for coordination variables (i.e, the upper-level variables in Ξ^{PCCO}), constraint (1b) provides a pre-qualification, i.e., it clears the local market for each DSO e and obtains the dispatch of each local generator $\widetilde{p}^{\mathrm{DA}}_g$ and each load demand $\widetilde{p}^{\mathrm{DA}}_d$. The conditional symbol '$\mid$' indicates that the DSO market outcomes depend on coordination variables. Each DSO market in (1b) is a stochastic market, accounting for potential realizations of uncertain parameters in real time. The full mathematical model for each DSO market is given by (9) in the online appendix [17]. The optimal dispatch of each local load and generator in DSO markets (i.e., $\widetilde{p}^{\mathrm{DA}}_g$ and $\widetilde{p}^{\mathrm{DA}}_d$) are then treated as caps on quantity bids of these local DERs in the day-ahead market. Given these caps, lower-level problem (1c) clears the DA market, whose formulation is given in (3). Eventually, for given DA dispatches (i.e., $\widehat{p}^{\mathrm{DA}}_g$ and $\widehat{p}^{\mathrm{DA}}_d$), the lower-level problem (1c) clears the RT market under each scenario. The corresponding clearing problem is given in (4).

Solving bi-level problem (1) is difficult, especially because we model the DSO markets in the lower-level constraint (1b) using a SOCP. The following proposition allows to reduce this bi-level problem.

Proposition 1: The collection of the first order optimality conditions associated with the DA market-clearing problem (1c) and the RT market-clearing problem (1d) contains all optimality conditions of the local DSO markets (1b). Therefore, solving the reduced bi-level problem (2) is *equivalent* to solving the original bi-level model (1).

TABLE I
NOMENCLATURE

Indices and sets:	
$d \in D$	Index for demands
$e \in E$	Index for distribution feeders
$g \in G$	Index for conventional generators
$n, m \in N$	Indices for nodes in both DSO and TSO networks
$l \in L$	Index for lines; $l = (n, m)$
$r \in R$	Index for renewable energy sources (RES)
$\omega \in \Omega$	Index for renewable power scenarios
Subsets and special labels:	
D_n, G_n, R_n	Set of assets located at node n
$D_e^{\mathrm{D}} \subset D$	Set of demands connected to distribution feeder e
$D^{\mathrm{T}} \subset D$	Set of demands connected to the transmission grid
$G_e^{\mathrm{D}} \subset G$	Set of generators connected to distribution feeder e
$G^{\mathrm{T}} \subset G$	Set of generators connected to the transmission grid
$L_e^{\mathrm{D}} \subset L$	Set of lines in distribution feeder e
$L^{\mathrm{T}} \subset L$	Set of lines in transmission grid
$N_e^{\mathrm{D}} \subset N$	Set of nodes in distribution feeder e
$N^{\mathrm{T}} \subset N$	Set of nodes in transmission grid
$\rightarrow n$	Set of lines ending at node n
$n \rightarrow$	Set of lines originating at node n
$n_e^{\mathrm{HV}} \in N^{\mathrm{T}}$	Node at HV-side of the PCC of feeder e
$n_e^{\mathrm{LV}} \in N_e^{\mathrm{D}}$	Node at LV-side of the PCC of feeder e
l_e	PCC of feeder e connecting HV- and LV-side nodes
$l' = (m, n)$	Line in the opposing direction of line l
Variables of the PCC optimizer:	
$\overline{f}_e / \underline{f}_e$	Upper/lower limit on import/export of apparent power at the PCC of feeder e [MVA]
$\pi_e^{\mathrm{PCC,DA}}$	Day-ahead price at the PCC of feeder e [$/MWh]
$\pi_e^{\uparrow/\downarrow \mathrm{PCC}}$	Regulating offer markup for up/down-regulation at the PCC of feeder e in real time [$/MWh]
Variables at the day-ahead stage:	
$\widetilde{p}_{g/d}^{\mathrm{DA}}$	Active power dispatch of DSO-level generator g / demand d in the local DSO market. This value is treated as a cap on the quantity bid to the DA market [MW]
$\widehat{p}_{g/d}^{\mathrm{DA}}$	Active power dispatch of generator g / demand d in the DA market [MW]
s^{DA}	Total active power load curtailed [MW]
w_r^{DA}	Active power dispatch of RES r [MW]
Variables at the real-time stage under scenario ω:	
$p_{g\omega}^{\uparrow/\downarrow}$	Active power up/down-regulation of generator g [MW]
$p_{d\omega}^{\uparrow/\downarrow}$	Active power up/down-regulation of demand d [MW]
$p_{g\omega}^{\mathrm{RT}} / q_{g\omega}^{\mathrm{RT}}$	Final active/reactive production of generator g, i.e, its dispatch in DA plus the regulation in RT [MW/MVAr]
$p_{l\omega}^{\mathrm{RT}} / q_{l\omega}^{\mathrm{RT}}$	Final active/reactive power flow across line l, i.e, the flow dispatched in DA plus the regulation in RT [MW/MVAr]
$s_{n\omega}^{\mathrm{RT}}$	Total active power load curtailed at node n [MW]
$s_{n\omega}^{\mathrm{q,RT}}$	Total reactive power load curtailed at node n [MVAr]
$\theta_{n\omega}^{\mathrm{RT}}$	Voltage angle at TSO-level node n [rad]
$w_{r\omega}^{\uparrow/\downarrow}$	Active power up/down-regulation of RES r [MW]
$w_{r\omega}^{\mathrm{RT}}$	Final active power production of RES r [MW]
$v_{n\omega}^{\mathrm{RT}}$	Squared voltage magnitude at DSO-level node n [p.u.]
$\varphi_{l\omega}^{\mathrm{RT}}$	Squared current magnitude flow in DSO-level line l [p.u.]
Parameters:	
$\overline{P}_{g/d}, \underline{P}_{g/d}$	Upper/lower active power limit for output of generator g and consumption of demand d [MW]
$\overline{Q}_{g/d}, \underline{Q}_{g/d}$	Upper/lower reactive power limit for output of generator g and consumption of demand d [MVAr]
$R_l / X_l / S_l$	Resistance/reactance/flow limit of line l [p.u.]/[MVA]
$\overline{V}_n, \underline{V}_n$	Upper/lower limit for voltage magnitude of node n [p.u.]
$VOLL$	Value of lost load [$/MWh]
W_r^{DA}	Power forecast of RES r in the DA stage [MW]
$W_{r\omega}^{\mathrm{RT}}$	Power generation of RES r in RT under scenario ω[MW]
$\pi_{g/d}^{\mathrm{DA}}$	Marginal offer/bid price of generator g / demand d in the DA stage [$/MWh]
π^{R}	Offer price of RES (assumed to be zero) [$/MWh]
$\pi_{g/d}^{\uparrow/\downarrow}$	Regulating offer markup in RT for up/down-regulation of generator g / demand d [$/MWh]
$\pi^{\uparrow/\downarrow \mathrm{R}}$	Up/down-regulation offer of RES in RT [$/MWh]

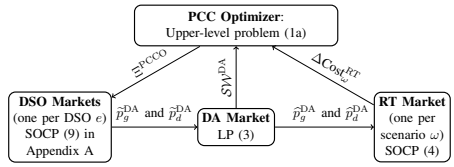

(a) Structure of the original bi-level problem (1). Note that LP and SOCP stand for linear problem and second-order cone problem, respectively.

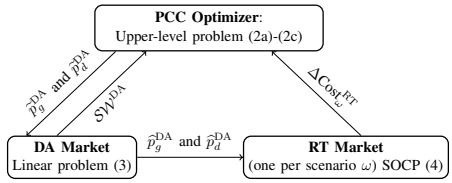

(b) Structure of the reduced bi-level problem (2). This problem is equivalent to the original bi-level problem (1) illustrated in Fig. 3a assuming information symmetry between the PCC optimizer and the DSOs.

Fig. 3. Structure of two equivalent bi-level problems

Proof of proposition 1: See online appendix E [17]. □

Therefore, the original bi-level problem (1) with three lower-level problems reduces to an *equivalent* bi-level problem with two lower-level problems as illustrated in Fig. 3b. The equivalent model is given by (2):

$$\max_{\widetilde{p}_g^{\mathrm{DA}}, \widetilde{p}_d^{\mathrm{DA}}} \quad \mathcal{SW}^{\mathrm{DA}} - \sum_{\omega} \phi_{\omega} \Delta\mathrm{Cost}_{\omega}^{\mathrm{RT}} \tag{2a}$$

$$\text{s.t.} \quad 0 \leq \widetilde{p}_g^{\mathrm{DA}} \leq \overline{P}_g \quad \forall e, g \in G_e^{\mathrm{D}} \tag{2b}$$

$$0 \leq \widetilde{p}_d^{\mathrm{DA}} \leq \overline{P}_d \quad \forall e, d \in D_e^{\mathrm{D}} \tag{2c}$$

$$\mathcal{SW}^{\mathrm{DA}}, \widehat{p}_g^{\mathrm{DA}}, \widehat{p}_d^{\mathrm{DA}} \in \mathbf{arg}\left((3) \mid \widehat{p}_g^{\mathrm{DA}}, \widetilde{p}_d^{\mathrm{DA}} \right) \tag{2d}$$

$$\Delta\mathrm{Cost}_{\omega}^{\mathrm{RT}} \in \mathbf{arg}\left((4)_{\omega} \mid \widehat{p}_g^{\mathrm{DA}}, \widehat{p}_d^{\mathrm{DA}} \right), \forall \omega. \tag{2e}$$

Now, the PCC optimizer directly imposes the caps on quantity bids/offers of local DERs through upper-level constraints (2b) and (2c). Note that the simplification achieved by using proposition 1 is only possible if the PCC optimizer and the local DSO markets have information symmetry. This means that they must hold the same beliefs about the distribution of uncertain variables and use the same set of representative scenarios. The next two subsections present the DA and RT market-clearing problems.

A. DA market-clearing formulation

The linear problem (3) clears the DA market, whose objective function is the social welfare maximization. Following the European zonal DA markets, this market is a pool, including bids and offers of all agents in TSO and DSO levels, without modeling network constraints. However, the network constraints will be considered later in the RT stage. Note that the caps on quantity bids of DSO-level generators and demands, i.e., $\widetilde{p}_g^{\mathrm{DA}}$ and $\widetilde{p}_d^{\mathrm{DA}}$, are treated as parameters in (3), while they are decision variables for the PCC optimizer in (2).

$$\max_{\widehat{p}_g^{\mathrm{DA}}, \widehat{p}_d^{\mathrm{DA}}, s^{\mathrm{DA}}, w_r^{\mathrm{DA}}} \mathcal{SW}^{\mathrm{DA}} = \sum_{d \in D} \pi_d^{\mathrm{DA}} \widehat{p}_d^{\mathrm{DA}} - \sum_{g \in G} \pi_g^{\mathrm{DA}} \widehat{p}_g^{\mathrm{DA}}$$

$$- VOLL\ s^{\mathrm{DA}} - \pi^R \sum_r w_r^{\mathrm{DA}} \tag{3a}$$

$$\text{s.t.} \quad \sum_{g\in G} \widehat{p}_g^{\mathrm{DA}} - \sum_{d\in D} \widehat{p}_d^{\mathrm{DA}} + \sum_r w_r^{\mathrm{DA}} + s^{\mathrm{DA}} = 0 \tag{3b}$$

$$\underline{P}_g \le \widehat{p}_g^{\mathrm{DA}} \le \widetilde{p}_g^{\mathrm{DA}},\ \forall e, g \in G_e^{\mathrm{D}} \tag{3c}$$

$$\underline{P}_g \le \widehat{p}_g^{\mathrm{DA}} \le \overline{P}_g, \quad \forall g \in G^{\mathrm{T}} \tag{3d}$$

$$\underline{P}_d \le \widehat{p}_d^{\mathrm{DA}} \le \widetilde{p}_d^{\mathrm{DA}},\ \forall e, d \in D_e^{\mathrm{D}} \tag{3e}$$

$$\underline{P}_d \le \widehat{p}_d^{\mathrm{DA}} \le \overline{P}_d, \quad \forall d \in D^{\mathrm{T}} \tag{3f}$$

$$0 \le w_r^{\mathrm{DA}} \le W_r^{\mathrm{DA}},\ \forall r \in R \tag{3g}$$

$$0 \le s^{\mathrm{DA}} \le \sum_d \widehat{p}_d^{\mathrm{DA}}. \tag{3h}$$

Constraint (3b) enforces the global power balance, considering all generators and demands in both TSO and DSO levels. Constraints (3c) through (3h) are bounds on the power quantities dispatched. The caps $\widetilde{p}_g^{\mathrm{DA}}$ and $\widetilde{p}_d^{\mathrm{DA}}$ are only enforced for DSO-level generators and demands in (3c) and (3e). In contrast, the dispatch of TSO-level generators and demands is restricted by their real capacity in (3d) and (3f).

B. RT re-dispatch formulation

For each potential scenario ω in RT, problem (4) re-dispatches the generators and demands in both TSO and DSO levels considering the full nodal power flow. For the distribution networks, a convex relaxation of AC power flow is employed, ending up to a SOCP. This model allows for taking into account the reactive power flows over lines, active and reactive power losses and nodal voltage magnitudes in the distribution networks. In contrast, for the transmission network, a linearized approximate power flow model is used, discarding the reactive power flows, active and reactive power losses and nodal voltage magnitudes. The objective function formulates the re-dispatch cost under the underlying scenario, where a premium on up- and down-regulation costs is being minimized.

$$\begin{aligned}\min_{\Xi_\omega^{\mathrm{RT}}}\ \Delta\mathrm{Cost}_\omega^{\mathrm{RT}} &= VOLL \sum_{n\in N} s_{n\omega}^{\mathrm{RT}} \\ &+ \sum_{g\in G} \left(\pi_g^{\mathrm{DA}} \left(p_{g\omega}^{\mathrm{RT}} - \widehat{p}_g^{\mathrm{DA}}\right) + \pi_g^{\uparrow} p_{g\omega}^{\uparrow} + \pi_g^{\downarrow} p_{g\omega}^{\downarrow}\right) \\ &+ \sum_{d\in D} \left(\pi_d^{\mathrm{DA}} \left(\widehat{p}_d^{\mathrm{DA}} - p_{d\omega}^{\mathrm{RT}}\right) + \pi_d^{\uparrow} p_{d\omega}^{\uparrow} + \pi_d^{\downarrow} p_{d\omega}^{\downarrow}\right) \\ &+ \sum_r \left(\pi^R \left(w_{r\omega}^{\mathrm{RT}} - w_r^{\mathrm{DA}}\right) + \pi^{\uparrow \mathrm{R}} w_{r\omega}^{\uparrow} + \pi^{\downarrow \mathrm{R}} w_{r\omega}^{\downarrow}\right)\end{aligned} \tag{4a}$$

$$\text{s.t.} \quad p_{l\omega}^{\mathrm{RT}} = B_l \left(\theta_{n\omega} - \theta_{m\omega}\right), \quad \forall l \in L^{\mathrm{T}} \tag{4b}$$

$$p_{l\omega}^{\mathrm{RT}} \le S_l,\ \forall l \in L^{\mathrm{T}} \tag{4c}$$

$$p_{g\omega}^{\mathrm{RT}} = \widehat{p}_g^{\mathrm{DA}} + p_{g\omega}^{\uparrow} - p_{g\omega}^{\downarrow}, \quad \forall g \in G \tag{4d}$$

$$w_{r\omega}^{\mathrm{RT}} = w_r^{\mathrm{DA}} + w_{r\omega}^{\uparrow} - w_{r\omega}^{\downarrow},\ \forall r \in R \tag{4e}$$

$$p_{d\omega}^{\mathrm{RT}} = \widehat{p}_d^{\mathrm{DA}} - p_{d\omega}^{\uparrow} + p_{d\omega}^{\downarrow}, \quad \forall d \in D \tag{4f}$$

$$\begin{aligned}\sum_{g\in G_n} p_{g\omega}^{\mathrm{RT}} - \sum_{d\in D_n} p_{d\omega}^{\mathrm{RT}} + \sum_{r\in R_n} w_{r\omega}^{\mathrm{RT}} + s_{n\omega}^{\mathrm{RT}} \\ = \sum_{l\in n\rightarrow} p_{l\omega}^{\mathrm{RT}} - \sum_{l\in \rightarrow n} p_{l\omega}^{\mathrm{RT}},\ \forall n \in N\end{aligned} \tag{4g}$$

$$\begin{aligned}\sum_{g\in G_n} q_{g\omega}^{\mathrm{RT}} - \sum_{d\in D_n} q_{d\omega}^{\mathrm{RT}} + s_{n\omega}^{\mathrm{q,RT}} \\ = \sum_{l\in n\rightarrow} q_{l\omega}^{\mathrm{RT}} - \sum_{l\in \rightarrow n} q_{l\omega}^{\mathrm{RT}},\ \forall e, n \in N_e^{\mathrm{D}}\end{aligned} \tag{4h}$$

$$p_{l\omega}^{\mathrm{RT}^2} + q_{l\omega}^{\mathrm{RT}^2} \le \varphi_{l\omega}^{\mathrm{RT}}\ v_{n\omega}^{\mathrm{RT}},\ \forall e, l \in (L_e^{\mathrm{D}} \cup l_e) \tag{4i}$$

$$p_{l\omega}^{\mathrm{RT}^2} + q_{l\omega}^{\mathrm{RT}^2} \le S_l^2,\ \forall e, l \in (L_e^{\mathrm{D}} \cup l_e) \tag{4j}$$

$$p_{l\omega}^{\mathrm{RT}} + p_{l'\omega}^{\mathrm{RT}} = R_l\ \varphi_{l\omega}^{\mathrm{RT}},\ \forall e, l \in (L_e^{\mathrm{D}} \cup l_e) \tag{4k}$$

$$q_{l\omega}^{\mathrm{RT}} + q_{l'\omega}^{\mathrm{RT}} = X_l\ \varphi_{l\omega}^{\mathrm{RT}},\ \forall e, l \in (L_e^{\mathrm{D}} \cup l_e) \tag{4l}$$

$$\begin{aligned}v_{m\omega}^{\mathrm{RT}} = v_{n\omega}^{\mathrm{RT}} - 2(R_l\ p_{l\omega}^{\mathrm{RT}} + X_l\ q_{l\omega}^{\mathrm{RT}}) \\ + (R_l^2 + X_l^2)\varphi_{l\omega}^{\mathrm{RT}},\ \forall e, l \in (L_e^{\mathrm{D}} \cup l_e)\end{aligned} \tag{4m}$$

$$\underline{V}_n^2 \le v_{n\omega}^{\mathrm{RT}} \le \overline{V}_n^2, \quad \forall e, n \in (N_e^{\mathrm{D}} \cup n_e^{\mathrm{HV}}) \tag{4n}$$

$$0 \le w_{r\omega}^{\mathrm{RT}} \le W_{r\omega}^{\mathrm{RT}}, \quad \forall r \in R \tag{4o}$$

$$\underline{P}_g \le p_{g\omega}^{\mathrm{RT}} \le \overline{P}_g, \quad \forall g \in G \tag{4p}$$

$$\underline{P}_d \le p_{d\omega}^{\mathrm{RT}} \le \overline{P}_d, \quad \forall d \in D \tag{4q}$$

$$\underline{Q}_g \le q_{g\omega}^{\mathrm{RT}} \le \overline{Q}_g, \quad \forall g \in G_e^{\mathrm{D}} \tag{4r}$$

$$\underline{Q}_d \le q_{d\omega}^{\mathrm{RT}} \le \overline{Q}_d, \quad \forall d \in D_e^{\mathrm{D}} \tag{4s}$$

$$0 \le s_{n\omega}^{\mathrm{RT}} \le \sum_{d\in D_n} p_{d\omega}^{\mathrm{RT}},\ \forall n \in N \tag{4t}$$

$$p_{g\omega}^{\uparrow} \ge 0,\ \forall g, \quad p_{g\omega}^{\downarrow} \ge 0,\ \forall g \tag{4u}$$

$$p_{d\omega}^{\uparrow} \ge 0,\ \forall d, \quad p_{d\omega}^{\downarrow} \ge 0,\ \forall d \tag{4v}$$

$$w_{r\omega}^{\uparrow} \ge 0,\ \forall r, \quad w_{r\omega}^{\downarrow} \ge 0,\ \forall r, \tag{4w}$$

where $\Xi_\omega^{\mathrm{RT}} = \{p_{g\omega}^{\mathrm{RT}}, p_{d\omega}^{\mathrm{RT}}, w_{r\omega}^{\mathrm{RT}}, p_{g\omega}^{\uparrow}, p_{g\omega}^{\downarrow}, p_{d\omega}^{\uparrow}, p_{d\omega}^{\downarrow}, w_{r\omega}^{\uparrow}, w_{r\omega}^{\downarrow}, s_{n\omega}^{\mathrm{RT}}, s_{n\omega}^{\mathrm{q,RT}}, q_{g\omega}^{\mathrm{RT}}, q_{d\omega}^{\mathrm{RT}}, p_{l\omega}^{\mathrm{RT}}, q_{l\omega}^{\mathrm{RT}}, \theta_{n\omega}, \varphi_{l\omega}^{\mathrm{RT}}, v_{n\omega}^{\mathrm{RT}}\}$ is the variable set of (4). Constraint (4b) uses the lossless linear representation of power flow to determine the active power flow across lines in the TSO level, while (4c) imposes the transmission line capacity limits. Constraints (4d)-(4f) determine the final active power production (i.e., DA dispatch plus the RT regulation) of each conventional generator and RES, and final consumption of each demand. The nodal active power balance in both TSO and DSO levels is enforced by (4g), while the nodal reactive power balance in the DSO level is imposed by (4h). The second-order cone constraints (4i) and (4j) enforce the capacity of distribution lines. Note that (4i) is an equality constraint in the original AC power flow model, but it is relaxed here to achieve convexity. An exact conic relaxation in radial systems can be ensured by adding sufficient conditions, but at the cost of potential sub-optimality and increased computational burden [18] – it is outside the scope of this work. Active and reactive power losses in distribution network are modeled in (4k) and (4l), whereas nodal voltage magnitudes are calculated by (4m). Constraints (4n) through (4t) impose lower and upper bounds for different variables, while (4u)-(4w) declare non-negativity conditions.

Because (4) solves a centralized optimal power flow problem with all nodes in both transmission and distribution networks, it is not practical to implement this problem in reality. Several other works have shown how this problem can be decomposed into separate problems, which are more manageable for large cases [9], [14]. The implementation and discussion of such a distributed problem is however considered outside the scope of this paper.

IV. Solution Strategy and Benchmarks

A. Benders' decomposition

The most common way to solve bi-level problem (2) is to replace lower-level problems (2d) and (2e) by their KKT optimality conditions, which is computationally expensive especially for large case studies. Also, since (4) in lower-level problem (2e) is a SOCP, it is a challenge to deal with complementarity conditions in such a problem. Therefore, we use a decomposition technique to decompose (2) to a set of smaller problems, also avoiding to solve KKTs of a SOCP. We use a multi-cut Benders' decomposition method by choosing DA dispatch decisions $\widehat{p}_g^{\mathrm{DA}}$, $\widehat{p}_d^{\mathrm{DA}}$ and w_r^{DA} as complicating variables [19]. By fixing these variables, the original bi-level problem (2) decomposes into a master problem for the PCC optimizer and a set of sub-problems for RT re-dispatch under each scenario. The master problem at iteration (i) is presented by (5) below:

$$\max_{\Xi^{\mathrm{MP}^{(i)}}} \quad \mathcal{SW}^{\mathrm{DA}^{(i)}} - \sum_{\omega} \phi_\omega \psi_\omega^{(i)} \tag{5a}$$

$$\text{s.t.} \quad (2\text{b}) - (2\text{c}) \tag{5b}$$

$$\mathcal{SW}^{\mathrm{DA}^{(i)}} \in (3) \tag{5c}$$

$$\psi_\omega^{(i)} \geq \psi^{\min}, \quad \forall \omega \in \Omega \tag{5d}$$

$$\begin{aligned}\psi_\omega^{(i)} \geq \Delta\mathrm{Cost}_\omega^{\mathrm{RT}^{(m)}} &+ \sum_{g\in G} \alpha_{g\omega}^{(m)} \left(\widehat{p}_g^{\mathrm{DA}^{(i)}} - \widehat{p}_g^{\mathrm{DA}^{(m)}}\right) \\ &+ \sum_{d\in D} \alpha_{d\omega}^{(m)} \left(\widehat{p}_d^{\mathrm{DA}^{(i)}} - \widehat{p}_g^{\mathrm{DA}^{(m)}}\right) \\ &+ \sum_{r\in R} \alpha_{r\omega}^{(m)} \left(w_r^{\mathrm{DA}^{(i)}} - w_r^{\mathrm{DA}^{(m)}}\right), \\ &\forall m \in \{1,\dots,i-1\}, \omega,\end{aligned} \tag{5e}$$

where variable set $\Xi^{\mathrm{MP}^{(i)}}$ includes $\widehat{p}_g^{\mathrm{DA}^{(i)}}$, $\widehat{p}_d^{\mathrm{DA}^{(i)}}$, $s^{\mathrm{DA}^{(i)}}$, $w_r^{\mathrm{DA}^{(i)}}$, $\widetilde{p}_g^{\mathrm{DA}^{(i)}}$, $\widetilde{p}_d^{\mathrm{DA}^{(i)}}$ and $\psi_\omega^{(i)}$. Note that (5) is still a bi-level problem, whose lower-level problem is (5c). Similar to objective function of the non-decomposed bi-level problem, i.e., (2a), objective function (5a) maximizes the social welfare in DA minus the expected re-dispatch cost in RT. Here, the latter is represented by auxiliary variable $\psi_\omega^{(i)}$. This variable is constrained by a lower bound in (5d) to avoid unbounded solution in the initial iteration, and by multiple cuts in (5e), one per scenario. Note that (m) is an index for previous iterations, and all symbols with superscript (m) are parameters whose values come from the solution of master and sub-problems in the previous iterations. In particular, $\alpha_{g\omega}^{(m)}$, $\alpha_{d\omega}^{(m)}$ and $\alpha_{r\omega}^{(m)}$ are sensitivities, and their values are obtained from sub-problems in the previous iterations. Note also that this bi-level problem can be solved by replacing the lower-level problem (3) in (5c), which is a linear problem, by its KKT conditions as given in the online appendix [17]. After linearizing the complementarity conditions using a Big-M method [20], master problem (5) boils down to a mixed-integer linear problem.

For given values for complicating variables obtained from master problem (5), each sub-problem (6), one for each scenario, re-dispatches the whole system to offset the renewable power imbalance under the corresponding scenario.

$$\min_{\Xi_\omega^{\mathrm{RT}^{(i)}}} \quad \Delta\mathrm{Cost}_\omega^{\mathrm{RT}^{(i)}} \tag{6a}$$

$$\text{s.t.} \quad \Delta\mathrm{Cost}_\omega^{\mathrm{RT}^{(i)}} \in (4)_\omega \tag{6b}$$

$$\widehat{p}_g^{\mathrm{DA}^{(i)}} = \widehat{p}_g^{\mathrm{DA,fixed}^{(i)}}, \quad : \alpha_{g\omega}^{(i)} \quad \forall g \in G, \tag{6c}$$

$$\widehat{p}_d^{\mathrm{DA}^{(i)}} = \widehat{p}_d^{\mathrm{DA,fixed}^{(i)}}, \quad : \alpha_{d\omega}^{(i)} \quad \forall d \in D, \tag{6d}$$

$$w_r^{\mathrm{DA}^{(i)}} = w_r^{\mathrm{DA,fixed}^{(i)}}, \quad : \alpha_{r\omega}^{(i)} \quad \forall r \in R. \tag{6e}$$

Note that each sub-problem (6) at iteration (i) is also a bi-level problem, whose lower-level is SOCP (4) in (6b). The dual variables $\alpha_{g\omega}^{(i)}$, $\alpha_{d\omega}^{(i)}$ and $\alpha_{r\omega}^{(i)}$ are defined for every conventional generator, demand and RES, which are used to construct cuts (5e) in the master problem. One important observation is that the objective function in (6) is the same as in (4). Therefore, the bi-level structure of (6) can be eliminated, and each sub-problem reduces to a single-stage SOCP as below:

$$\min_{\Xi_\omega^{\mathrm{RT}^{(i)}}} \ \Delta\mathrm{Cost}_\omega^{\mathrm{RT}^{(i)}} \quad \text{s.t.} \quad (4\text{b})_\omega - (4\text{w})_\omega \text{ and } (6\text{c}) - (6\text{e}). \tag{7}$$

The iterative Benders' decomposition algorithm finds the optimal solution of the bi-level problem (2) with a level of accuracy ϵ if a lower bound $\mathrm{LB}^{(i)} = \mathcal{SW}^{\mathrm{DA}^{(i)}} - \sum_\omega \phi_\omega \psi_\omega^{(i)}$ and an upper bound $\mathrm{UB}^{(i)} = \mathcal{SW}^{\mathrm{DA}^{(i)}} - \sum_\omega \phi_\omega \Delta\mathrm{Cost}_\omega^{\mathrm{RT}^{(i)}}$ converge to within a predefined discrepancy $\epsilon \geq \mathrm{UB}^{(i)} - \mathrm{LB}^{(i)}$.

B. Two benchmark models

To assess the performance of the proposed coordination scheme based on optimizing the interface characteristics, we define here two benchmarks, one is an ideal benchmark providing an upper bound for the expected social welfare of the whole system, and the other one provides a lower bound.

For an upper bound (ideal benchmark), we consider a full coordination between TSO and DSOs such that both have full information of RT scenarios in the DA stage. This ideal benchmark is indeed a co-optimization problem formulated as a SOCP in (8).

$$\max_{\widehat{p}_g^{\mathrm{DA}}, \widehat{p}_d^{\mathrm{DA}}, s^{\mathrm{DA}}, w_r^{\mathrm{DA}}, \Xi^{\mathrm{RT}}} \ \mathcal{SW}^{\mathrm{DA}} - \sum_\omega \phi_\omega \Delta\mathrm{Cost}_\omega^{\mathrm{RT}} \tag{8a}$$

$$\text{s.t.} \quad (3\text{b}) - (3\text{h}) \text{ and } (4\text{b})_\omega - (4\text{w})_\omega. \tag{8b}$$

This perfect (full) coordination is however quite impractical as it requires TSO and DSOs to solve a common single problem, and all information is packed into one optimization problem, which quickly becomes intractable for larger systems.

To obtain the lower bound, we consider a model with no coordination, and solve DA and RT models sequentially. This means that we first solve DA market (3) without imposing any cap on the quantity bids/offers of DSO-level DERs. Then, we solve the RT problem (4) for each scenario separately, i.e., in a deterministic manner. We then calculate the resultant total mean social welfare.

V. Case Study

The proposed bi-level problem (2) with a solution strategy relying on multi-cut Benders' decomposition as explained in the previous section is implemented in Matlab using CVX and solved with MOSEK 8.0. The Benders' decomposition is set

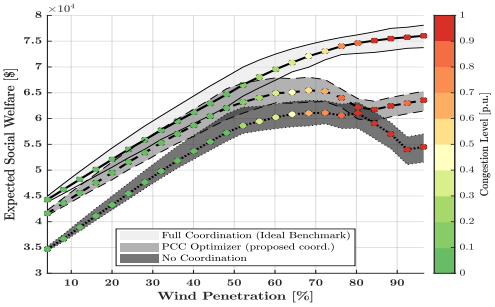

Fig. 4. The expected social welfare as a function of wind power penetration obtained from the proposed coordination model (PCC optimizer) and the two benchmark models. The 0.2 quantile and 0.8 quantile are also depicted. The colored dots indicate the level of congestion in the transmission network as the probability of at least two lines being congested in RT. The results are from out-of-sample testing with 200 scenarios.

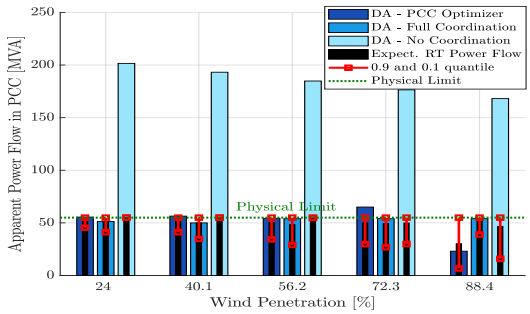

Fig. 5. The power flow in the PCC of DSO 3 (connected to node 19) incurred by the DA dispatches and the resulting RT power flows. These results are obtained from the proposed coordination method (PCC optimizer) and the two benchmark models (i.e., full coordination and no coordination).

to converge if the upper and lower bounds come to within a relative gap of 0.1%. A speed-up is achieved by solving the sub-problems, one per scenario, in parallel[5].

A modified version of the IEEE 24-node reliability test system [21] is used. The network is extended with the addition of five radial distribution feeders, which replace the loads at nodes 6, 13, 15, 18 and 19. In total, 39.3% of the total system load is now placed in radial distribution feeders, while the remainder is connected to the transmission network. A diagram of the total network is given in the online appendix [17]. The system is also equipped with seven additional wind farms, which are the sole source of uncertainty in the system. In order to have some congestion in the network, the capacity of three transmission lines 3-24, 9-11 and 10-12 is reduced to 180 MW, 140 MW and 130 MW, respectively.

The scenarios for the seven wind farms are generated by random sampling from a Gaussian mixture model, where the co-variances are based on the geographical distance of the wind farms to each other. For a more in-depth description of the scenario generation method, we refer to the online appendix [17]. From the scenarios generated, we first pick 12 *in-sample* scenarios to solve the proposed bi-level model, and then use an *out-of-sample* validation using 200 scenarios. For the study in section V-A, the model (2) using decomposition is solved on average within 14 minutes; for more information on computational performance see appendix I in [17].

A. Coordination under increasing wind power penetration

In order to examine the improvement of the social welfare achieved by the proposed TSO-DSO coordination scheme based on PCC optimizer, we simulate the system with increasing wind power penetration. We do this by uniformly scaling the nameplate capacity of each of the seven wind farms, thereby increasing the wind power penetration. We define the wind power penetration as the total forecasted available wind power in DA divided by the total load bids, i.e., $\sum_r W_r^{\mathrm{DA}} / \sum_d \overline{P}_d$.

[5]Hardware used: Huawei XH620 V3, 2x Intel Xeon Processor 2650v4 (12 core, 2.20GHz), 256 GB memory, 480 GB-SSD disk.

As the results of the out-of-sample simulation, Fig. 4 presents the expected (mean) social welfare obtained from the proposed coordination method (PCC optimizer) along with the two benchmark models. The 0.8 quantile and the 0.2 quantile are also given in this figure to show the spread of each curve resulting from the uncertainties. It also includes a heat-map indicating the level of transmission network congestion. We define "congestion level" as the probability of at least two transmission lines being congested in RT. There is a strong connection between the social welfare and wind power penetration. For all three models, the slope of the social welfare changes at around 50% wind penetration, where the congestion in the transmission network also starts to affect the system. Comparing the social welfare obtained in the proposed coordination model (PCC optimizer) versus the two benchmarks, the PCC optimizer improves the social welfare compared to the benchmark with no coordination. Naturally, the PCC optimizer does not perform as well as the ideal benchmark because the ideal benchmark can take advantage of the TSO-level resources in the DA market to meet grid constraints, whereas the PCC-optimizer relies on DSO-level resources only. In the deterministic dispatch model (uncoordinated benchmark), social welfare diminshes after 70% wind penetration due to the system running out of available reserves. This happens because the DA stage clears the market mostly with wind power as it is cheap, however the balancing measures in real-time are costly, reducing overall social welfare. The ideal stochastic dispatch can mitigate this situation by reducing the cleared wind power in the day-ahead stage and the social welfare will not reduce with increasing wind penetration. As evidenced by Fig. 4 the PCC optimizer manages to partially reduce the need for expensive balancing actions.

B. Capacity versus optimal PCC

To get insight into the power flow at the PCC resulting from the proposed coordination model versus the two benchmark models, Fig. 5 depicts the incurred power flow from the DA dispatch in the PCC of one of the DSOs, i.e., DSO 3. The black bars in the center indicate the RT outcome for the power flow in the PCC which must in all scenarios respect the physical limit of the PCC. The 0.9 and 0.1 quantile for the RT scenarios

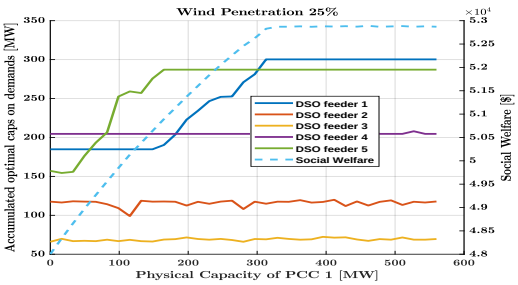

Fig. 6. The optimal caps of PCC optimizer on the quantity bid of aggregate flexible loads in different feeders as a function of the physical capacity of PCC of DSO 1 (note: the wind penetration is fixed to 25%).

are also given. An interesting observation is that the optimal PCC optimizer's outcome does not necessarily respect the physical capacity in the DA stage, which is seen at the 72.3% wind penetration case. This is of interest to anyone wishing to establish a policy that coordinates TSO/DSO network flexibility, because the import/export limits given to a DSO must not necessarily respect the physical limits of the PCC in the DA stage in order to be a good coordination method.

The relation of the optimal caps to the network model is highly non-linear, as demonstrated in Fig. 6. Here, the physical capacity of the PCC of DSO 1 is varied, and the resulting optimal caps are found. This shows that the PCC optimizer is highly reliant on having access to precise network information, and that the decisions of one DSO can affect even other DSOs' optimal dispatch of flexible resources.

VI. Conclusion

The optimal day-ahead schedule for DSO-level flexible resources was modeled through a Stackelberg game, cast as a bi-level problem. The PCC optimizer acting as a leader in the game can provide prices at the interface which lead localized DSO flexibility markets to approximate the stochastic ideal dispatch. Our findings have implications for designing practical schemes to use this avenue of TSO-DSO coordination, in two ways: First, the optimal PCC capacity for coordination is congruent with, but not limited by, the physical capacity of the underlying hardware. Thus, any scheme should take as guideline the physical PCC capacity but must not be limited by it. Second, the optimal caps for one feeder can depend in a non-obvious way on the physical capacity of another feeder or the physical capacity of the transmission network. Therefore, when considering to implement a scheme to coordinate day-ahead dispatches in the manner analyzed here, the sensitivity of the outcomes with respect to the underlying network data should be analyzed.

We find that under strong assumptions, such as symmetry between PCC optimizer and DSO information, a mathematical equivalence exists between local DSO flexibility markets and global (stochastic) markets. This makes for an interesting observation: The implementation of localized DSO markets can lead to an approximation of the stochastic ideal dispatch, given an appropriate coordination mechanism.

This work uses optimal real-time coordination to highlight differences in day-ahead dispatch coordination. However, it is an unrealistic position, due to separation of responsibilities and knowledge between DSO and TSO, as evidenced by the previous works examining methods for real-time coordination. This highlights the need for some afterthought when implementing policies on coordination: Which time stage or which combination of day-ahead and real-time coordination is appropriate? As a general point, the inclusion of day ahead coordination is complementary to real-time coordination. Any real-time coordination method that increases the system social welfare may overestimate improvements if compared under uncoordinated day-ahead dispatches. Further, coordination in day-ahead will generally increase social welfare as premiums are applied closer to real-time; improving coordination in the day-ahead stage will reduce the needed amount of real-time re-dispatching, benefitting end-users.

References

[1] J. Villar, R. Bessa, and M. Matos, "Flexibility products and markets: Literature review," *Electr. Power Syst. Res.*, vol. 154, pp. 329–340, 2018.

[2] C. Zhang, Y. Ding, N. C. Nordentoft, P. Pinson, and J. Østergaard, "FLECH: A Danish market solution for DSO congestion management through DER flexibility services," *J. Mod. Power Syst. Clean Energy*, vol. 2, no. 2, pp. 126–133, 2014.

[3] L. Bai, J. Wang, C. Wang, C. Chen, and F. Li, "Distribution locational marginal pricing (DLMP) for congestion management and voltage support," *IEEE Trans. Power Syst.*, vol. 33, no. 4, pp. 4061–4073, 2018.

[4] T. Morstyn, A. Teytelboym, and M. D. Mcculloch, "Designing decentralized markets for distribution system flexibility," *IEEE Trans. Power Syst.*, 2018, to be published.

[5] J. P. Silva, J. A. Sumaili, R. J. Bessa, L. Seca, M. A. Matos, V. Miranda, M. Caujolle, B. Goncer-Maraver, and M. Sebastian-Viana, "Estimating the active and reactive power flexibility area at the TSO-DSO interface," *IEEE Trans. Power Syst.*, vol. 33, no. 5, pp. 4741–4750, 2018.

[6] D. M. Gonzalez, J. Hachenberger, J. Hinker, F. Rewald, C. Rehtanz, and J. Myrzik, "Determination of the time-dependent flexibility of active distribution networks to control their TSO-DSO interconnection power flow," in *Power Syst. Comput. Conf. (PSCC)*, (Dublin, Ireland), Jun. 2018.

[7] I. Mezghani, A. Papavasiliou, and H. Le Cadre, "A generalized Nash equilibrium analysis of electric power transmission-distribution coordination," in *International Conference on Future Energy Systems*, (Karlsruhe, Germany), Jun. 2018.

[8] H. Le Cadre, I. Mezghani, and A. Papavasiliou, "A game-theoretic analysis of transmission-distribution system operator coordination," *Eur. J. Oper. Res.*, vol. 274, no. 1, pp. 317–339, 2019.

[9] M. Caramanis, E. Ntakou, W. W. Hogan, A. Chakrabortty, and J. Schoene, "Co-optimization of power and reserves in dynamic T&D power markets with nondispatchable renewable generation and distributed energy resources," *Proc. IEEE*, vol. 104, no. 4, pp. 807–836, 2016.

[10] A. Papavasiliou and I. Mezghani, "Coordination schemes for the integration of transmission and distribution system operations," in *Power Syst. Comput. Conf. (PSCC)*, (Dublin, Ireland), Jun. 2018.

[11] Z. Yuan and M. R. Hesamzadeh, "Hierarchical coordination of TSO-DSO economic dispatch considering large-scale integration of distributed energy resources," *Appl. Energy*, vol. 195, pp. 600–615, 2017.

[12] H. Gerard, E. Rivero, and D. Six, "Basic schemes for TSO-DSO coordination and ancillary services provision," *SMARTNET Deliv. D1.3*, 2016.

[13] *DSO's Role in Electricity Market (DREM) Project*. [Online]. Available: https://drem.dk/ (visited on 12/28/2018).

[14] A. Mohammadi, M. Mehrtash, and A. Kargarian, "Diagonal quadratic approximation for decentralized collaborative TSO+DSO optimal power flow," *IEEE Trans. Smart Grid*, 2018, to be published.

[15] T. V. Jensen, J. Kazempour, and P. Pinson, "Cost-optimal ATCs in zonal electricity markets," *IEEE Trans. Power Syst.*, vol. 33, no. 4, pp. 3624–3633, 2018.

[16] V. Dvorkin, S. Delikaraoglou, and J. M. Morales, "Setting reserve requirements to approximate the efficiency of the stochastic dispatch," *IEEE Trans. Power Syst.*, 2018, to be published.

[17] *Online appendix*. [Online]. Available: https://github.com/alherm/TSO-DSO_coordination (visited on 12/01/2019).

[18] M. Farivar and S. H. Low, "Branch flow model: Relaxations and convexification—part I," *IEEE Trans. Power Syst.*, vol. 28, no. 3, pp. 2554–2564, 2013.

[19] A. J. Conejo, E. Castillo, R. Minguez, and R. Garcia-Bertrand, *Decomposition techniques in mathematical programming: engineering and science applications*. Springer Science & Business Media, 2006.

[20] J. Fortuny-Amat and B. McCarl, "A representation and economic interpretation of a two-level programming problem," *J. Oper. Res. Soc.*, 1981.

[21] C. Ordoudis, P. Pinson, J. M. Morales, and M. Zugno, "An updated version of the IEEE RTS 24-bus system for electricity market and power system operation studies," *Technical University of Denmark Report*, 2016.

This appendix is available online at https://github.com/alherm/TSO-DSO_coordination.

APPENDIX A
MODELING ASSUMPTIONS

We collect here all modeling assumptions made. We make no specific assumptions to the design of the local DSO markets that are employed. It is merely assumed that these markets are efficient and work to maximize social welfare. Therefore the model in (9) is a generic market model that we cast as a stochastic optimization problem that maximizes expected social welfare.

Renewable production is the only source of uncertainty. The production of each renewable energy source (RES) r is capped by an uncertain parameter $W_{r\omega}^{\mathrm{RT}}$ that is dependent on scenario ω (i.e., RES can be freely spilled as required). The DA market is deterministic, and the offer of each RES is assumed to be the expected value of its production. The price offer of each RES, i.e., π^{R}, is assumed to be zero in the DA stage.

Although stochastic market-clearing setups depend on the used scenarios and a thorough definition of who generates them is usually pertinent, we here consider them as an external parameter. A scenario generation method, which correlates geographically close renewable sources is used – more information can be found in section F of this appendix.

The RT market is assumed to be any market that changes the DA dispatch. This re-dispatch is assumed to incur an additional cost, due to premiums charged by the market participants. The premiums do not have to be symmetric, such that up- and down-regulation can have different costs.

We take the same view on network modeling as [9], that the meshed HV transmission network is adequately modeled by linear power flow approximations, while the radial LV distribution feeders are best represented by a convex relaxation of the AC power flow equations. Specifically, in this paper a second-order cone program (SOCP) will be used, as explained in more detail in section IV.

Ramping constraints, energy storage and other inter-temporal couplings are ignored. Also, binary variables such as the commitment status of conventional generators are ignored, such that both DA and RT market-clearing problems are convex.

In order to be able to calculate the RT re-dispatch cost, topology information of both TSO and DSO networks is necessary. Both TSO and DSOs may be unwilling to share data about their network topology. It is assumed that this information is available to the PCC optimizer, which is a reasonable assumptions as we are examining the best possible outcome. Decentralized optimization such as the proposals in [9] and [14] may in the future make it easier to coordinate in RT without sharing specific network-related proprietary information.

APPENDIX B
DSO MARKET LOWER LEVEL PROBLEM

The DSO pre-qualification optimization problem has both constraints from the DA-market and the scenarios for the Real-time realization. Every DSO has its own separate problem such that Cost_e contains one value for every DSO e. The day ahead market is cleared for each distribution network separately, where the day ahead market has no nodal information. The real time realization is a stochastic SOCP problem.

$$\begin{aligned}
\max_{\Xi^{\mathrm{E}}} \quad & \mathcal{SW}_e = \sum_{d\in D_e^{\mathrm{D}}} \pi_d^{\mathrm{DA}}\widetilde{p}_d^{\mathrm{DA}} - \sum_{g\in G_e^{\mathrm{D}}} \pi_g^{\mathrm{DA}}\widetilde{p}_g^{\mathrm{DA}} \\
& - VOLL_e^{\mathrm{DA}} s_e^{\mathrm{DA}} - \sum_{r\in R_e^{\mathrm{D}}} \pi^R w_r^{\mathrm{DA}} - \pi_e^{\mathrm{PCC,DA}} p_e^{\mathrm{PCC,DA}} \\
& - \sum_{\omega} \phi_\omega \Bigg[\sum_{g\in G_e^{\mathrm{D}}} \Big(\pi_g^{\mathrm{DA}}(p_{g\omega}^{\mathrm{RT}} - \widetilde{p}_g^{\mathrm{DA}}) + \pi_g^{\uparrow} p_{g\omega}^{\uparrow} \\
& + \pi_g^{\downarrow} p_{g\omega}^{\downarrow} \Big) + \sum_{d\in D_e^{\mathrm{D}}} \Big(\pi_d^{\mathrm{DA}}(\widetilde{p}_d^{\mathrm{DA}} - p_{d\omega}^{\mathrm{RT}}) \\
& + \pi_d^{\uparrow} p_{d\omega}^{\uparrow} + \pi_d^{\downarrow} p_{d\omega}^{\downarrow} \Big) + \sum_{n\in N_e^{\mathrm{D}}} VOLL_n^{\mathrm{RT}} s_{n\omega}^{\mathrm{RT}} \\
& + \pi_e^{\mathrm{PCC,DA}}(p_{e\omega}^{\mathrm{PCC,RT}} - p_e^{\mathrm{PCC,DA}}) \\
& + \pi_e^{\uparrow PCC} p_{e\omega}^{\uparrow PCC} + \pi_e^{\downarrow PCC} p_{e\omega}^{\downarrow PCC} \\
& + \sum_{r\in R_e^{\mathrm{D}}} \left(\pi^R(w_{r\omega}^{\mathrm{RT}} - w_r^{\mathrm{DA}}) + \pi^{\uparrow R} w_{r\omega}^{\uparrow} + \pi^{\downarrow R} w_{r\omega}^{\downarrow} \right) \Bigg]
\end{aligned} \tag{9a}$$

subject to:

DA-level constraints:

$$\begin{aligned}
& \sum_{g\in G_e} \widetilde{p}_g^{\mathrm{DA}} - \sum_{d\in D_e^{\mathrm{D}}} \widetilde{p}_d^{\mathrm{DA}} + \sum_{r\in R_e^{\mathrm{D}}} w_r^{\mathrm{DA}} + s_e^{\mathrm{DA}} \\
& \quad + p_e^{\mathrm{PCC,DA}} = 0, \quad : (\lambda_e^{\mathrm{DA}})
\end{aligned} \tag{9b}$$

$$\underline{P}_g \le \widetilde{p}_g^{\mathrm{DA}} \le \overline{P}_g, \quad \forall g \in G_e^{\mathrm{D}} \quad : (\varsigma_g^{\mathrm{DA}-}, \varsigma_g^{\mathrm{DA}+}) \tag{9c}$$

$$\underline{P}_d \le \widetilde{p}_d^{\mathrm{DA}} \le \overline{P}_d, \quad \forall d \in D_e^{\mathrm{D}} \quad : (\varsigma_d^{\mathrm{DA}-}, \varsigma_d^{\mathrm{DA}+}) \tag{9d}$$

$$0 \le w_r^{\mathrm{DA}} \le W_r^{\mathrm{DA}}, \ \forall r \in R_e^{\mathrm{D}} \quad : (\iota_r^-, \iota_r^+) \tag{9e}$$

$$\underline{f}_e \le p_e^{\mathrm{PCC,DA}} \le \overline{f}_e, \quad : (\rho_e^{\mathrm{DA}-}, \rho_e^{\mathrm{DA}+}) \tag{9f}$$

$$0 \le s_e^{\mathrm{DA}} \le \sum_d p_d^{\mathrm{DA}}, \quad : (\Upsilon_e^{\mathrm{DA}-}, \Upsilon_e^{\mathrm{DA}+}) \tag{9g}$$

Real-time constraints:

$$p_{g\omega}^{\mathrm{RT}} = p_g^{\mathrm{DA}} + p_{g\omega}^{\uparrow} - p_{g\omega}^{\downarrow}, \quad \forall \omega, g \in G_e^{\mathrm{D}}, \quad : (\zeta_{g\omega}^{p}) \tag{9h}$$

$$p_{d\omega}^{\mathrm{RT}} = p_d^{\mathrm{DA}} - p_{d\omega}^{\uparrow} + p_{d\omega}^{\downarrow}, \quad \forall \omega, d \in D_e^{\mathrm{D}}, \quad : (\zeta_{d\omega}^{p}) \tag{9i}$$

$$w_{r\omega}^{\mathrm{RT}} = w_r^{\mathrm{DA}} + w_{r\omega}^{\uparrow} - w_{r\omega}^{\downarrow}, \ \forall \omega, r \in R_e^{\mathrm{D}}, : (\zeta_{r\omega}^{p}) \tag{9j}$$

$$\begin{aligned}
& \sum_{g\in G_n} p_{g\omega}^{\mathrm{RT}} - \sum_{d\in D_n} p_{d\omega}^{\mathrm{RT}} + \sum_{r\in R_n} w_{r\omega}^{\mathrm{RT}} + p_{e\omega}^{\mathrm{PCC,RT}}|_{n=n_e^{\mathrm{LV}}} \\
& + s_{n\omega}^{\mathrm{RT}} = \sum_{l\in n\rightarrow} p_{l\omega}^{\mathrm{RT}} - \sum_{l\in \rightarrow n} p_{l\omega}^{\mathrm{RT}}, \ \forall \omega, n \in N_e^{\mathrm{D}} \ : (\lambda_{n\omega}^{\mathrm{p,RT}})
\end{aligned} \tag{9k}$$

$$p_{e\omega}^{\mathrm{PCC,RT}} = p_e^{\mathrm{PCC,DA}} + p_{e\omega}^{\uparrow PCC} - p_{e\omega}^{\downarrow PCC}, \ \forall \omega, \ : (\zeta_{e\omega}^{\mathrm{PCC}}) \tag{9l}$$

$$\begin{aligned}
& \sum_{g\in G_n} q_{g\omega}^{\mathrm{RT}} - \sum_{d\in D_n} q_{d\omega}^{\mathrm{RT}} + s_{n\omega}^{\mathrm{q,RT}} + q_{e\omega}^{\mathrm{PCC,RT}}|_{n=n_e^{\mathrm{LV}}} \\
& = \sum_{l\in n\rightarrow} q_{l\omega}^{\mathrm{RT}} - \sum_{l\in \rightarrow n} q_{l\omega}^{\mathrm{RT}}, \ \forall \omega, n \in N_e^{\mathrm{D}} \ : (\lambda_{n\omega}^{\mathrm{q,RT}})
\end{aligned} \tag{9m}$$

$$p_{l\omega}^{(RT)2} + q_{l\omega}^{(RT)2} \le \varphi_{l\omega}^{\mathrm{RT}} v_{n\omega}^{\mathrm{RT}}, \quad \forall \omega, l \in L_e^{\mathrm{D}} \ : (\gamma_{l\omega}) \tag{9n}$$

$$p_{l\omega}^{\mathrm{RT}} + p_{l'\omega}^{\mathrm{RT}} = R_l \varphi_{l\omega}^{\mathrm{RT}}, \quad \forall \omega, l \in L_e^{\mathrm{D}} \ : (\mu_{l\omega}^{p}) \tag{9o}$$

$$q_{l\omega}^{\mathrm{RT}} + q_{l'\omega}^{\mathrm{RT}} = X_l \varphi_{l\omega}^{\mathrm{RT}}, \quad \forall \omega, l \in L_e^{\mathrm{D}} \ : (\mu_{l\omega}^{q}) \tag{9p}$$

$$p_{l\omega}^{(RT)2}+q_{l\omega}^{(RT)2}\le S_l,\quad \forall\omega,l\in L_e^{\mathrm{D}}\ :(\eta_{l\omega}) \tag{9q}$$
$$v_{m\omega}^{\mathrm{RT}}=v_{n\omega}^{\mathrm{RT}}-2(R_l p_{l\omega}^{\mathrm{RT}}+X_l q_{l\omega}^{\mathrm{RT}})+(R_l^2+X_l^2)\varphi_{l\omega}^{\mathrm{RT}},\quad \forall\omega,l\in L_e^{\mathrm{D}}\ :(\beta_{l\omega}) \tag{9r}$$
$$\underline{V}_n^2\le v_{n\omega}^{\mathrm{RT}}\le\overline{V}_n^2,\quad \forall\omega,n\in N_e^{\mathrm{D}}\ :(\sigma_{n\omega}^-,\sigma_{n\omega}^+) \tag{9s}$$
$$0\le w_{r\omega}^{\mathrm{RT}}\le W_{r\omega}^{\mathrm{RT}},\quad \forall\omega,n\in N_e\ :(\nu_{n\omega}^-,\nu_{n\omega}^+) \tag{9t}$$
$$\underline{P}_g\le p_{g\omega}^{\mathrm{RT}}\le\overline{P}_g,\quad \forall\omega,g\in G_e\ :(\varsigma_{g\omega}^{\mathrm{RT}-},\varsigma_{g\omega}^{\mathrm{RT}+}) \tag{9u}$$
$$\underline{P}_d\le p_{d\omega}^{\mathrm{RT}}\le\overline{P}_d,\quad \forall\omega,d\in D_e\ :(\varsigma_{d\omega}^{\mathrm{RT}-},\varsigma_{d\omega}^{\mathrm{RT}+}) \tag{9v}$$
$$\underline{Q}_g\le q_{g\omega}^{\mathrm{RT}}\le\overline{Q}_g,\quad \forall\omega,g\in G_e\ :(\kappa_{g\omega}^{\mathrm{RT}-},\kappa_{g\omega}^{\mathrm{RT}+}) \tag{9w}$$
$$\underline{Q}_d\le q_{d\omega}^{\mathrm{RT}}\le\overline{Q}_d,\quad \forall\omega,d\in D_e\ :(\kappa_{d\omega}^{\mathrm{RT}-},\kappa_{d\omega}^{\mathrm{RT}+}) \tag{9x}$$
$$\underline{f}_e\le p_{e\omega}^{\mathrm{PCC,RT}}\le\overline{f}_e,\quad \forall\omega\ :(\rho_{e\omega}^{\mathrm{RT}-},\rho_{e\omega}^{\mathrm{RT}+}) \tag{9y}$$
$$p_{g\omega}^{\uparrow}\ge 0,\ \forall\omega,g\ :(\epsilon_{g\omega}^{\mathrm{p}\uparrow}),\quad p_{g\omega}^{\downarrow}\ge 0,\ \forall\omega,g\ :(\epsilon_{g\omega}^{\mathrm{p}\downarrow}) \tag{9z}$$
$$p_{d\omega}^{\uparrow}\ge 0,\ \forall d,\omega\ :(\varepsilon_{d\omega}^{\mathrm{p}\uparrow}),\quad p_{d\omega}^{\downarrow}\ge 0,\ \forall d,\omega\ :(\varepsilon_{d\omega}^{\mathrm{p}\downarrow}) \tag{9aa}$$
$$p_{e\omega}^{\uparrow PCC}\ge 0,\ \forall\omega,\ :(\epsilon_{e\omega}^{\uparrow PCC}),\ p_{e\omega}^{\downarrow PCC}\ge 0,\ \forall\omega,\ :(\epsilon_{e\omega}^{\downarrow PCC}) \tag{9ab}$$
$$0\le s_{n\omega}^{\mathrm{RT}}\le\sum_{d\in D_n}p_{d\omega}^{\mathrm{RT}},\ \forall\omega,n\in N_e^{\mathrm{D}},\ :(\Upsilon_{n\omega}^{\mathrm{RT}-},\Upsilon_{n\omega}^{\mathrm{RT}+}) \tag{9ac}$$
$$w_{r\omega}^{\uparrow}\ge 0,\ \forall\omega,w\ :(\epsilon_{r\omega}^{\mathrm{p}\uparrow}),\quad w_{r\omega}^{\downarrow}\ge 0,\ \forall\omega,w\ :(\epsilon_{r\omega}^{\mathrm{p}\downarrow}) \tag{9ad}$$

Where $\Xi^E=\widetilde{p}_g^{\mathrm{DA}},\widetilde{p}_d^{\mathrm{DA}},p_{g\omega}^{\mathrm{RT}},p_{g\omega}^{\uparrow},p_{g\omega}^{\downarrow},p_{d\omega}^{\mathrm{RT}},p_{d\omega}^{\uparrow},p_{d\omega}^{\downarrow},q_{g\omega}^{\mathrm{RT}},q_{d\omega}^{\mathrm{RT}},s_{n\omega}^{\mathrm{RT}},s_e^{\mathrm{DA}},w_{n\omega}^{\mathrm{RT}},p_{l\omega}^{\mathrm{RT}},q_{l\omega}^{\mathrm{RT}},\varphi_{l\omega}^{\mathrm{RT}},v_{n\omega}^{\mathrm{RT}},w_e^{\mathrm{DA}},p_e^{\mathrm{PCC,DA}},p_e^{\mathrm{PCC,RT}},p_e^{\uparrow PCC},p_e^{\downarrow PCC},s_{n\omega}^{\mathrm{q,RT}}$ are the variables of the DSO-level combined day-ahead and real-time market clearing.

The Lagrangian of above problem is:

$$\begin{aligned}
\mathcal{L}_e=&\sum_{d\in D_e^{\mathrm{D}}}\pi_d^{\mathrm{DA}}\widetilde{p}_d^{\mathrm{DA}}-\sum_{g\in G_e^{\mathrm{D}}}\pi_g^{\mathrm{DA}}\widetilde{p}_g^{\mathrm{DA}}\\
&-VOLL_e^{\mathrm{DA}}s_e^{\mathrm{DA}}-\sum_{r\in R_e^{\mathrm{D}}}\pi^R w_r^{\mathrm{DA}}-\pi_e^{\mathrm{PCC,DA}}p_e^{\mathrm{PCC,DA}}\\
&-\sum_{\omega}\phi_\omega\Bigg[\sum_{g\in G_e^{\mathrm{D}}}\left(\pi_g^{\mathrm{DA}}(p_{g\omega}^{\mathrm{RT}}-p_g^{\mathrm{DA}})+\pi_g^{\uparrow}p_{g\omega}^{\uparrow}+\pi_g^{\downarrow}p_{g\omega}^{\downarrow}\right)\\
&+\sum_{d\in D_e^{\mathrm{D}}}\left(\pi_d^{\mathrm{DA}}(p_d^{\mathrm{DA}}-p_{d\omega}^{\mathrm{RT}})+\pi_d^{\uparrow}p_{d\omega}^{\uparrow}+\pi_d^{\downarrow}p_{d\omega}^{\downarrow}\right)\\
&+\sum_{n\in N_e^{\mathrm{D}}}VOLL_n^{\mathrm{RT}}s_{n\omega}^{\mathrm{RT}}\\
&+\sum_{r\in R_e^{\mathrm{D}}}\left(\pi^R(w_{r\omega}^{\mathrm{RT}}-w_r^{\mathrm{DA}})+\pi^{\uparrow R}w_{r\omega}^{\uparrow}+\pi^{\downarrow R}w_{r\omega}^{\downarrow}\right)\\
&+\pi_e^{\mathrm{PCC,DA}}(p_{e\omega}^{\mathrm{PCC,RT}}-p_e^{\mathrm{PCC,DA}})\\
&+\pi_e^{\uparrow PCC}p_{e\omega}^{\uparrow PCC}+\pi_e^{\downarrow PCC}p_{e\omega}^{\downarrow PCC}\Bigg]\\
&-\lambda_e^{\mathrm{DA}}\Bigg[\sum_{g\in G_e}\widetilde{p}_g^{\mathrm{DA}}-\sum_{d\in D_e^{\mathrm{D}}}\widetilde{p}_d^{\mathrm{DA}}+\sum_{r\in R_e^{\mathrm{D}}}w_r^{\mathrm{DA}}\\
&\quad+s_e^{\mathrm{DA}}+p_e^{\mathrm{PCC,DA}}\Bigg]\\
&+\sum_{g\in G_e^{\mathrm{D}}}\left[\varsigma_g^{\mathrm{DA}-}\left(\underline{P}_g-\widetilde{p}_g^{\mathrm{DA}}\right)+\varsigma_g^{\mathrm{DA}+}\left(\widetilde{p}_g^{\mathrm{DA}}-\overline{P}_g\right)\right]\\
&-\sum_{r\in R_e^{\mathrm{D}}}\left[\iota_r^-w_r^{\mathrm{DA}}-\iota_r^+(w_r^{\mathrm{DA}}-W_r^{\mathrm{DA}})\right]\\
&+\sum_{d\in D_e^{\mathrm{D}}}\left[\varsigma_d^{\mathrm{DA}-}\left(\underline{P}_d-\widetilde{p}_d^{\mathrm{DA}}\right)+\varsigma_d^{\mathrm{DA}+}\left(\widetilde{p}_d^{\mathrm{DA}}-\overline{P}_d\right)\right]\\
&+\rho_e^{\mathrm{DA}-}(\underline{f}_e-p_e^{\mathrm{PCC,DA}})+\rho_e^{\mathrm{DA}+}(p_e^{\mathrm{PCC,DA}}-\overline{f}_e)\\
&-\sum_{g\in G_e^{\mathrm{D}}}\varsigma_{g\omega}^{\mathrm{p}}\left(p_{g\omega}^{\mathrm{RT}}-p_g^{\mathrm{DA}}-p_{g\omega}^{\uparrow}+p_{g\omega}^{\downarrow}\right)\\
&-\sum_{d\in D_e^{\mathrm{D}}}\varsigma_{d\omega}^{\mathrm{p}}\left(p_{d\omega}^{\mathrm{RT}}-p_d^{\mathrm{DA}}+p_{d\omega}^{\uparrow}-p_{d\omega}^{\downarrow}\right)\\
&-\sum_{r\in R_e^{\mathrm{D}}}\varsigma_{r\omega}^{p}\left(w_{r\omega}^{\mathrm{RT}}-w_r^{\mathrm{DA}}-w_{r\omega}^{\uparrow}+w_{r\omega}^{\downarrow}\right)\\
&-\sum_{n\in N_e^{\mathrm{D}},\omega}\lambda_{n\omega}^{\mathrm{p,RT}}\Bigg(\sum_{g\in G_n}p_{g\omega}^{\mathrm{RT}}-\sum_{d\in D_n}p_{d\omega}^{\mathrm{RT}}+\sum_{r\in R_n}w_{r\omega}^{\mathrm{RT}}\\
&+s_{n\omega}^{\mathrm{RT}}+p_{e\omega}^{\mathrm{PCC,RT}}|_{n=n_e^{\mathrm{LV}}}-\sum_{l\in n\rightarrow}p_{l\omega}^{\mathrm{RT}}+\sum_{l\in\rightarrow n}p_{l\omega}^{\mathrm{RT}}\Bigg)\\
&-\sum_{\omega}\zeta_{e\omega}^{\mathrm{PCC}}\left(p_{e\omega}^{\mathrm{PCC,RT}}-p_e^{\mathrm{PCC,DA}}-p_{e\omega}^{\uparrow PCC}+p_{e\omega}^{\downarrow PCC}\right)\\
&-\sum_{n\in N_e^{\mathrm{D}},\omega}\lambda_{n\omega}^{\mathrm{q,RT}}\Bigg(\sum_{g\in G_n}q_{g\omega}^{\mathrm{RT}}-\sum_{d\in D_n}q_{d\omega}^{\mathrm{RT}}+s_{n\omega}^{\mathrm{q,RT}}\\
&+q_{e\omega}^{\mathrm{PCC,RT}}|_{n=n_e^{\mathrm{LV}}}-\sum_{l\in n\rightarrow}q_{l\omega}^{\mathrm{RT}}+\sum_{l\in\rightarrow n}q_{l\omega}^{\mathrm{RT}}\Bigg)\\
&+\sum_{l\in L_e^{\mathrm{D}},\omega}\gamma_{l\omega}\left[p_{l\omega}^{(RT)2}+q_{l\omega}^{(RT)2}-\varphi_{l\omega}^{\mathrm{RT}}v_{n\omega}^{\mathrm{RT}}\right]\\
&-\sum_{l\in L_e^{\mathrm{D}},\omega}\Big[\mu_{l\omega}^{p}\left(p_{l\omega}^{\mathrm{RT}}+p_{l'\omega}^{\mathrm{RT}}-R_l\varphi_{l\omega}^{\mathrm{RT}}\right)\\
&\quad+\mu_{l\omega}^{q}\left(q_{l\omega}^{\mathrm{RT}}+q_{l'\omega}^{\mathrm{RT}}-X_l\varphi_{l\omega}^{\mathrm{RT}}\right)\Big]\\
&+\sum_{l\in L_e^{\mathrm{D}},\omega}\left[\eta_{l\omega}\left(p_{l\omega}^{(RT)2}+q_{l\omega}^{(RT)2}-S_l\right)\right]\\
&-\sum_{l\in L_e^{\mathrm{D}},\omega}\Big[\beta_{l\omega}\Big(v_{m\omega}^{\mathrm{RT}}-v_{n\omega}^{\mathrm{RT}}+2(R_l p_{l\omega}^{\mathrm{RT}}+X_l q_{l\omega}^{\mathrm{RT}})\\
&\quad-(R_l^2+X_l^2)\varphi_{l\omega}^{\mathrm{RT}}\Big)\Big]\\
&+\sum_{n\in N_e^{\mathrm{D}},\omega}\left[\sigma_{n\omega}^-\left(\underline{V}_n^2-v_{n\omega}^{\mathrm{RT}}\right)+\sigma_{n\omega}^+\left(v_{n\omega}^{\mathrm{RT}}-\overline{V}_n^2\right)\right]\\
&-\sum_{r\in R_e^{\mathrm{D}},\omega}\left[\nu_{r\omega}^-w_{r\omega}^{\mathrm{RT}}-\nu_{r\omega}^+\left(w_{r\omega}^{\mathrm{RT}}-W_{r\omega}^{\mathrm{RT}}\right)\right]\\
&+\sum_{g\in G_e^{\mathrm{D}},\omega}\left[\varsigma_{g\omega}^{\mathrm{RT}-}\left(\underline{P}_g-p_{g\omega}^{\mathrm{RT}}\right)+\varsigma_{g\omega}^{\mathrm{RT}+}\left(p_{g\omega}^{\mathrm{RT}}-\overline{P}_g\right)\right]\\
&+\sum_{d\in D_e^{\mathrm{D}},\omega}\left[\varsigma_{d\omega}^{\mathrm{RT}-}\left(\underline{P}_d-p_{d\omega}^{\mathrm{RT}}\right)+\varsigma_{d\omega}^{\mathrm{RT}+}\left(p_{d\omega}^{\mathrm{RT}}-\overline{P}_d\right)\right]\\
&+\sum_{g\in G_e^{\mathrm{D}},\omega}\left[\kappa_{g\omega}^{\mathrm{RT}-}\left(\underline{Q}_g-q_{g\omega}^{\mathrm{RT}}\right)+\kappa_{g\omega}^{\mathrm{RT}+}\left(q_{g\omega}^{\mathrm{RT}}-\overline{Q}_g\right)\right]\\
&+\sum_{d\in D_e^{\mathrm{D}},\omega}\left[\kappa_{d\omega}^{\mathrm{RT}-}\left(\underline{Q}_d-q_{d\omega}^{\mathrm{RT}}\right)+\kappa_{d\omega}^{\mathrm{RT}+}\left(q_{d\omega}^{\mathrm{RT}}-\overline{Q}_g\right)\right]\\
&+\sum_{g\in G_e^{\mathrm{D}},\omega}\left[-p_{g\omega}^{\uparrow}\epsilon_{g\omega}^{\mathrm{p}\uparrow}-p_{g\omega}^{\downarrow}\epsilon_{g\omega}^{\mathrm{p}\downarrow}\right]
\end{aligned}$$

$$
\begin{aligned}
&+\sum_{r\in R_e^{\mathrm{D}},\omega}\left[-w_{r\omega}^{\uparrow}\epsilon_{r\omega}^{\mathrm{p}\uparrow}-w_{r\omega}^{\downarrow}\epsilon_{r\omega}^{\mathrm{p}\downarrow}\right]\\
&+\sum_{d\in D_e^{\mathrm{D}},\omega}\left[-p_{d\omega}^{\uparrow}\varepsilon_{d\omega}^{\mathrm{p}\uparrow}-p_{d\omega}^{\downarrow}\varepsilon_{d\omega}^{\mathrm{p}\downarrow}\right]\\
&+\sum_{\omega}\left[-p_{e\omega}^{\uparrow PCC}\epsilon_{e\omega}^{\uparrow PCC}-p_{e\omega}^{\downarrow PCC}\epsilon_{e\omega}^{\downarrow PCC}\right]\\
&+\sum_{\omega}\Big[\rho_{e\omega}^{\mathrm{RT}-}\left(\underline{f}_e-\sqrt{p_{e\omega}^{(PCC,RT)2}+q_{e\omega}^{(PCC,RT)2}}\right)\\
&+\rho_{e\omega}^{\mathrm{RT}+}\left(\sqrt{p_{e\omega}^{(PCC,RT)2}+q_{e\omega}^{(PCC,RT)2}}-\overline{f}_e\right)\Big]\\
&+\sum_{n\in N_e^{\mathrm{D}},\omega}\left[-\Upsilon_{n\omega}^{\mathrm{RT}-}s_{n\omega}^{\mathrm{RT}}+\Upsilon_{n\omega}^{\mathrm{RT}+}\left(s_{n\omega}^{\mathrm{RT}}-\sum_{d\in D_n}p_{d\omega}^{\mathrm{RT}}\right)\right]\\
&-\Upsilon_e^{\mathrm{DA}-}s_e^{\mathrm{DA}}+\Upsilon_e^{\mathrm{DA}+}\left(s_e^{\mathrm{DA}}-\sum_d p_d^{\mathrm{DA}}\right) \qquad (10)
\end{aligned}
$$

The KKT conditions of above problem are (excluding the primal constraints of 9):

$$
\begin{aligned}
&(\widetilde{p}_g^{\mathrm{DA}}):\ -\pi_g^{\mathrm{DA}}+\sum_{\omega}\phi_\omega\pi_g^{\mathrm{DA}}-\lambda_e^{\mathrm{DA}}-\varsigma_g^{\mathrm{DA}-}\\
&\quad+\varsigma_g^{\mathrm{DA}+}+\sum_{\omega}\zeta_{g\omega}^{p}=0,\quad \forall g\in G_e^{\mathrm{D}} \qquad (11a)\\
&(\widetilde{p}_d^{\mathrm{DA}}):\sum_{\omega}\left(\zeta_{d\omega}^{p}-\phi_\omega\pi_d^{\mathrm{DA}}\right)+\pi_d^{\mathrm{DA}}+\lambda_e^{\mathrm{DA}}\\
&\quad-\varsigma_d^{\mathrm{DA}-}+\varsigma_d^{\mathrm{DA}+}-\Upsilon_e^{\mathrm{DA}+}=0,\quad \forall d\in D_e^{\mathrm{D}} \qquad (11b)\\
&(p_{g\omega}^{\uparrow}):\ -\phi_\omega\pi_g^{\uparrow}+\zeta_{g\omega}^{p}-\epsilon_{g\omega}^{\mathrm{p}\uparrow}=0,\quad \forall\omega,g\in G_e^{\mathrm{D}} \qquad (11c)\\
&(p_{g\omega}^{\downarrow}):\ -\phi_\omega\pi_g^{\downarrow}-\zeta_{g\omega}^{p}-\epsilon_{g\omega}^{\mathrm{p}\downarrow}=0,\quad \forall\omega,g\in G_e^{\mathrm{D}} \qquad (11d)\\
&(p_{d\omega}^{\uparrow}):\ -\phi_\omega\pi_d^{\uparrow}-\zeta_{d\omega}^{p}-\varepsilon_{i\omega}^{\mathrm{p}\uparrow}=0,\quad \forall\omega,d\in D_e^{\mathrm{D}} \qquad (11e)\\
&(p_{d\omega}^{\downarrow}):\ -\phi_\omega\pi_d^{\downarrow}+\zeta_{d\omega}^{p}-\varepsilon_{d\omega}^{\mathrm{p}\downarrow}=0,\quad \forall\omega,d\in D_e^{\mathrm{D}} \qquad (11f)\\
&(w_{r\omega}^{\uparrow}):\ -\phi_\omega\pi^{\uparrow R}+\zeta_{r\omega}^{p}-\epsilon_{r\omega}^{\mathrm{p}\uparrow}=0,\quad \forall\omega,r\in R_e^{\mathrm{D}} \qquad (11g)\\
&(w_{r\omega}^{\downarrow}):\ -\phi_\omega\pi^{\downarrow R}-\zeta_{r\omega}^{p}-\epsilon_{r\omega}^{\mathrm{p}\downarrow}=0,\quad \forall\omega,r\in R_e^{\mathrm{D}} \qquad (11h)\\
&(s_e^{\mathrm{DA}}):-\mathrm{VOLL}_e-\lambda_e^{\mathrm{DA}}-\Upsilon_e^{\mathrm{DA}-}+\Upsilon_e^{\mathrm{DA}+}=0 \qquad (11i)\\
&(s_{n\omega}^{\mathrm{RT}}):-\mathrm{VOLL}_n-\lambda_{n\omega}^{\mathrm{p,RT}}-\Upsilon_{n\omega}^{\mathrm{RT}-}\\
&\quad+\Upsilon_{n\omega}^{\mathrm{RT}+}=0,\ \forall\omega,n\in N_e^{\mathrm{D}} \qquad (11j)\\
&(w_{r\omega}^{\mathrm{RT}}):-\phi_\omega\pi^{R}-\zeta_{r\omega}^{p}-\left[\lambda_{n\omega}^{\mathrm{p,RT}}\right]_{n_r}+\nu_{r\omega}^{+}\\
&\quad-\nu_{r\omega}^{-}=0,\quad \forall\omega,r\in R_e^{\mathrm{D}} \qquad (11k)\\
&(w_r^{\mathrm{DA}}):-\pi^{R}+\sum_{\omega}\phi_\omega\pi^{R}-\lambda_e^{\mathrm{DA}}-\iota_r^{-}\\
&\quad+\iota_r^{+}+\sum_{\omega}\zeta_{r\omega}^{p}=0,\forall r\in R_e^{\mathrm{D}} \qquad (11l)\\
&(p_{g\omega}^{\mathrm{RT}}):-\phi_\omega\pi_g^{\mathrm{DA}}-\zeta_{g\omega}^{p}-\varsigma_{g\omega}^{\mathrm{RT}-}+\varsigma_{g\omega}^{\mathrm{RT}+}\\
&\quad-\left[\lambda_{n\omega}^{\mathrm{p,RT}}\right]_{n_g}=0,\quad \forall\omega,g\in G_e^{\mathrm{D}} \qquad (11m)\\
&(q_{g\omega}^{\mathrm{RT}}):-\kappa_{g\omega}^{\mathrm{RT}-}+\kappa_{g\omega}^{\mathrm{RT}+}-\left[\lambda_{n\omega}^{\mathrm{q,RT}}\right]_{n_g}=0,\quad \forall\omega,g\in G_e^{\mathrm{D}} \qquad (11n)\\
&(p_{d\omega}^{\mathrm{RT}}):\phi_\omega\pi_d^{\mathrm{DA}}-\zeta_{d\omega}^{p}-\varsigma_{d\omega}^{\mathrm{RT}-}+\varsigma_{d\omega}^{\mathrm{RT}+}\\
&\quad+\left[\lambda_{n\omega}^{\mathrm{p,RT}}-\Upsilon_{n\omega}^{\mathrm{RT}+}\right]_{n_d}=0,\quad \forall\omega,d\in D_e^{\mathrm{D}} \qquad (11o)\\
&(q_{d\omega}^{\mathrm{RT}}):-\kappa_{d\omega}^{\mathrm{RT}-}+\kappa_{d\omega}^{\mathrm{RT}+}+\left[\lambda_{n\omega}^{\mathrm{q,RT}}\right]_{n_d}=0,\quad \forall\omega,d\in D_e^{\mathrm{D}} \qquad (11p)\\
&(p_{l\omega}^{\mathrm{RT}}):\lambda_{n\omega}^{\mathrm{p,RT}}-\lambda_{m\omega}^{\mathrm{p,RT}}+2\gamma_{l\omega}p_{l\omega}^{\mathrm{RT}}-\mu_{l\omega}^{p}-\mu_{l'\omega}^{p}+2\eta_{l\omega}p_{l\omega}^{\mathrm{RT}}\\
&\quad-2\beta_{l\omega}R_l=0,\quad \forall\omega,l=(n,m)\in L_e^{\mathrm{D}} \qquad (11q)\\
&(q_{l\omega}^{\mathrm{RT}}):\lambda_{n\omega}^{\mathrm{q,RT}}-\lambda_{m\omega}^{\mathrm{q,RT}}+2\gamma_{l\omega}q_{l\omega}^{\mathrm{RT}}-\mu_{l\omega}^{q}-\mu_{l'\omega}^{q}+2\eta_{l\omega}q_{l\omega}^{\mathrm{RT}}\\
&\quad-2\beta_{l\omega}X_l=0,\quad \forall\omega,l=(n,m)\in L_e^{\mathrm{D}} \qquad (11r)\\
&(\varphi_{l\omega}^{\mathrm{RT}}):-\gamma_{l\omega}v_{n\omega}^{\mathrm{RT}}+\mu_{l\omega}^{p}R_l+\mu_{l\omega}^{q}X_l+\beta_{l\omega}(R_l^2+X_l^2)\\
&\quad=0,\quad \forall\omega,l=(n,m)\in L_e^{\mathrm{D}} \qquad (11s)\\
&(v_{n\omega}^{\mathrm{RT}}):-\gamma_{l\omega}\varphi_{l\omega}^{\mathrm{RT}}-\beta_{l'\omega}+\beta_{l\omega}-\sigma_{n\omega}^{-}+\sigma_{n\omega}^{+}\\
&\quad=0,\quad \forall\omega,l=(n,m)\in L_e^{\mathrm{D}} \qquad (11t)\\
&(p_e^{\mathrm{PCC,DA}}):-\pi_e^{\mathrm{PCC,DA}}+\sum_{\omega}\left(\phi_\omega\pi_e^{\mathrm{PCC,DA}}+\zeta_{e\omega}^{\mathrm{PCC}}\right)\\
&\quad-\lambda_e^{\mathrm{DA}}-\rho_e^{\mathrm{DA}-}+\rho_e^{\mathrm{DA}+}=0 \qquad (11u)\\
&(p_{e\omega}^{\mathrm{PCC,RT}}):-\phi_\omega\pi_e^{\mathrm{PCC,DA}}-\left[\lambda_{n\omega}^{\mathrm{p,RT}}\right]_{n_e^{\mathrm{LV}}}-\zeta_{e\omega}^{\mathrm{PCC}}\\
&\quad-\rho_{e\omega}^{\mathrm{RT}-}+\rho_{e\omega}^{\mathrm{RT}+}=0,\quad \forall\omega \qquad (11v)\\
&(q_{e\omega}^{\mathrm{PCC,RT}}):-\left[\lambda_{n\omega}^{\mathrm{q,RT}}\right]_{n_e^{\mathrm{LV}}}=0,\quad \forall\omega \qquad (11w)\\
&(p_{e\omega}^{\uparrow PCC}):-\phi_\omega\pi_e^{\uparrow PCC}+\zeta_{e\omega}^{\mathrm{PCC}}-\epsilon_{e\omega}^{\uparrow PCC}=0,\quad \forall\omega \qquad (11x)\\
&(p_{e\omega}^{\downarrow PCC}):-\phi_\omega\pi_e^{\downarrow PCC}-\zeta_{e\omega}^{\mathrm{PCC}}-\epsilon_{e\omega}^{\downarrow PCC}=0,\quad \forall\omega \qquad (11y)
\end{aligned}
$$

The complimentarity constraints are as follows:

$$
\begin{aligned}
&0\le\varsigma_g^{\mathrm{DA}+}\perp\overline{P}_g-\widetilde{p}_g^{\mathrm{DA}}\ge0,\quad \forall g\in G_e^{\mathrm{D}} \qquad (12a)\\
&0\le\varsigma_g^{\mathrm{DA}-}\perp\widetilde{p}_g^{\mathrm{DA}}-\underline{P}_g\ge0,\quad \forall g\in G_e^{\mathrm{D}} \qquad (12b)\\
&0\le\varsigma_d^{\mathrm{DA}+}\perp\overline{P}_d-\widetilde{p}_d^{\mathrm{DA}}\ge0,\quad \forall d\in D_e^{\mathrm{D}} \qquad (12c)\\
&0\le\varsigma_d^{\mathrm{DA}-}\perp\widetilde{p}_d^{\mathrm{DA}}-\underline{P}_d\ge0,\quad \forall d\in D_e^{\mathrm{D}} \qquad (12d)\\
&0\le\iota_r^{-}\perp w_r^{\mathrm{DA}}\ge0,\quad \forall r\in R_e^{\mathrm{D}} \qquad (12e)\\
&0\le\iota_r^{+}\perp W_r^{\mathrm{DA}}-w_r^{\mathrm{DA}}\ge0,\quad \forall r\in R_e^{\mathrm{D}} \qquad (12f)\\
&0\le\rho_e^{\mathrm{DA}-}\perp p_e^{\mathrm{PCC,DA}}-\underline{f}_e\ge0 \qquad (12g)\\
&0\le\rho_e^{\mathrm{DA}+}\perp\overline{f}_e-p_e^{\mathrm{PCC,DA}}\ge0 \qquad (12h)\\
&0\le\gamma_{l\omega}\perp\varphi_{l\omega}^{\mathrm{RT}}v_{n\omega}^{\mathrm{RT}}-(p_{l\omega}^{(RT)2}+q_{l\omega}^{(RT)2})\ge0,\ \forall\omega,l\in L_e^{\mathrm{D}} \qquad (12i)\\
&0\le\eta_{l\omega}\perp S_l-p_{l\omega}^{(RT)2}-q_{l\omega}^{(RT)2}\ge0,\ \forall\omega,l\in L_e^{\mathrm{D}} \qquad (12j)\\
&0\le\sigma_{n\omega}^{-}\perp v_{n\omega}^{\mathrm{RT}}-\underline{V}_n^2\ge0,\quad \forall\omega,n\in N_e^{\mathrm{D}} \qquad (12k)\\
&0\le\sigma_{n\omega}^{+}\perp\overline{V}_n^2-v_{n\omega}^{\mathrm{RT}}\ge0,\quad \forall\omega,n\in N_e^{\mathrm{D}} \qquad (12l)\\
&0\le\nu_{r\omega}^{-}\perp w_{r\omega}^{\mathrm{RT}}\ge0,\quad \forall\omega,r\in R_e^{\mathrm{D}} \qquad (12m)\\
&0\le\nu_{r\omega}^{+}\perp W_{r\omega}^{\mathrm{RT}}-w_{r\omega}^{\mathrm{RT}}\ge0,\quad \forall\omega,r\in R_e^{\mathrm{D}} \qquad (12n)\\
&0\le\varsigma_{g\omega}^{\mathrm{RT}-}\perp p_{g\omega}^{\mathrm{RT}}-\underline{P}_g\ge0,\quad \forall\omega,g\in G_e^{\mathrm{D}} \qquad (12o)\\
&0\le\varsigma_{g\omega}^{\mathrm{RT}+}\perp\overline{P}_g-p_{g\omega}^{\mathrm{RT}}\ge0,\quad \forall\omega,g\in G_e^{\mathrm{D}} \qquad (12p)\\
&0\le\varsigma_{d\omega}^{\mathrm{RT}-}\perp p_{d\omega}^{\mathrm{RT}}-\underline{P}_d\ge0,\quad \forall\omega,d\in D_e^{\mathrm{D}} \qquad (12q)\\
&0\le\varsigma_{d\omega}^{\mathrm{RT}+}\perp\overline{P}_d-p_{d\omega}^{\mathrm{RT}}\ge0,\quad \forall\omega,d\in D_e^{\mathrm{D}} \qquad (12r)\\
&0\le\kappa_{g\omega}^{\mathrm{RT}+}\perp q_{g\omega}^{\mathrm{RT}}-\underline{Q}_g\ge0,\quad \forall\omega,g\in G_e^{\mathrm{D}} \qquad (12s)\\
&0\le\kappa_{g\omega}^{\mathrm{RT}-}\perp\overline{Q}_g-q_{g\omega}^{\mathrm{RT}}\ge0,\quad \forall\omega,g\in G_e^{\mathrm{D}} \qquad (12t)\\
&0\le\kappa_{d\omega}^{\mathrm{RT}+}\perp q_{d\omega}^{\mathrm{RT}}-\underline{Q}_d\ge0,\quad \forall\omega,d\in D_e^{\mathrm{D}} \qquad (12u)\\
&0\le\kappa_{d\omega}^{\mathrm{RT}-}\perp\overline{Q}_d-q_{d\omega}^{\mathrm{RT}}\ge0,\quad \forall\omega,d\in D_e^{\mathrm{D}} \qquad (12v)\\
&0\le\rho_{e\omega}^{\mathrm{RT}-}\perp p_{e\omega}^{\mathrm{PCC,RT}}-\underline{f}_e\ge0,\quad \forall\omega \qquad (12w)\\
&0\le\rho_{e\omega}^{\mathrm{RT}+}\perp\overline{f}_e-p_{e\omega}^{\mathrm{PCC,RT}}\ge0,\quad \forall\omega \qquad (12x)\\
&0\le\epsilon_{g\omega}^{\mathrm{p}\uparrow}\perp p_{g\omega}^{\uparrow}\ge0,\quad 0\le\epsilon_{g\omega}^{\mathrm{p}\downarrow}\perp p_{g\omega}^{\downarrow}\ge0,\quad \forall\omega,g\in G_e^{\mathrm{D}} \qquad (12y)
\end{aligned}
$$

$$0 \le \epsilon^{\mathrm{p}\uparrow}_{r\omega} \perp w^{\uparrow}_{r\omega} \ge 0,\ 0 \le \epsilon^{\mathrm{p}\downarrow}_{r\omega} \perp w^{\downarrow}_{r\omega} \ge 0,\ \forall \omega, r \in R^{\mathrm{D}}_e \tag{12z}$$

$$0 \le \varepsilon^{\mathrm{p}\uparrow}_{d\omega} \perp p^{\uparrow}_{d\omega} \ge 0, \quad 0 \le \varepsilon^{\mathrm{p}\downarrow}_{d\omega} \perp p^{\downarrow}_{d\omega} \ge 0, \quad \forall \omega, d \in D^{\mathrm{D}}_e \tag{12aa}$$

$$0 \le \epsilon^{\uparrow PCC}_{e\omega} \perp p^{\uparrow PCC}_{e\omega} \ge 0, \quad 0 \le \epsilon^{\downarrow PCC}_{e\omega} \perp p^{\downarrow PCC}_{e\omega} \ge 0, \quad \forall \omega \tag{12ab}$$

$$0 \le \Upsilon^{\mathrm{RT}-}_{n\omega} \perp s^{\mathrm{RT}}_{n\omega} \ge 0, \forall n, \omega \tag{12ac}$$

$$0 \le \Upsilon^{\mathrm{RT}+}_{n\omega} \perp \sum_{d \in D_n} p^{\mathrm{RT}}_{d\omega} - s^{\mathrm{RT}}_{n\omega} \ge 0,\ \forall n, \omega \tag{12ad}$$

$$0 \le \Upsilon^{\mathrm{DA}-}_{e} \perp s^{\mathrm{DA}}_{e} \ge 0 \tag{12ae}$$

$$0 \le \Upsilon^{\mathrm{DA}+}_{e} \perp \sum_{d} p^{\mathrm{DA}}_{d} - s^{\mathrm{DA}}_{e} \ge 0 \tag{12af}$$

APPENDIX C
KKTS OF DA MARKET

For convenience problem (3) is repeated here, with dual varaibles for every constraint added.

$$\max_{\Xi^{\mathrm{DA}}} \mathcal{SW}^{\mathrm{DA}} = \sum_{d \in D} \pi^{\mathrm{DA}}_d \widehat{p}^{\mathrm{DA}}_d - \sum_{g \in G} \pi^{\mathrm{DA}}_g \widehat{p}^{\mathrm{DA}}_g - VOLL^{\mathrm{DA}} s^{\mathrm{DA}} - \pi^R \sum_r w^{\mathrm{DA}}_r \tag{13a}$$

subject to:

$$\sum_{g \in G} \widehat{p}^{\mathrm{DA}}_g - \sum_{d \in D} \widehat{p}^{\mathrm{DA}}_d + \sum_r w^{\mathrm{DA}}_r + s^{\mathrm{DA}} = 0,\ : (\lambda^{\mathrm{T,DA}}) \tag{13b}$$

$$\underline{P}_g \le \widehat{p}^{\mathrm{DA}}_g \le \widetilde{p}^{\mathrm{DA}}_g,\ \forall g \in G^{\mathrm{D}}_e,\ \forall e \in E\ : (\varsigma^{\mathrm{T,DA}-}_{ge}, \varsigma^{\mathrm{T,DA}+}_{ge}) \tag{13c}$$

$$\underline{P}_g \le \widehat{p}^{\mathrm{DA}}_g \le \overline{P}_g,\ \forall g \in G^{\mathrm{T}}\ : (\sigma^{\mathrm{T,DA}-}_g, \sigma^{\mathrm{T,DA}+}_g) \tag{13d}$$

$$\underline{P}_d \le \widehat{p}^{\mathrm{DA}}_d \le \widetilde{p}^{\mathrm{DA}}_d,\ \forall d \in D^{\mathrm{D}}_e,\ \forall e \in E\ : (\varsigma^{\mathrm{T,DA}-}_{de}, \varsigma^{\mathrm{T,DA}+}_{de}) \tag{13e}$$

$$\underline{P}_d \le \widehat{p}^{\mathrm{DA}}_d \le \overline{P}_d,\ \forall d \in D^{\mathrm{T}}\ : (\sigma^{\mathrm{T,DA}-}_d, \sigma^{\mathrm{T,DA}+}_d) \tag{13f}$$

$$0 \le w^{\mathrm{DA}}_r \le W^{\mathrm{DA}}_r,\ \forall r \in R\ : (\nu^{\mathrm{T,DA}-}_r, \nu^{\mathrm{T,DA}+}_r) \tag{13g}$$

$$0 \le s^{\mathrm{l,DA}} \le \sum_d \widehat{p}^{\mathrm{DA}}_d,\ : (\rho^{\mathrm{T,DA}-}, \rho^{\mathrm{T,DA}+}) \tag{13h}$$

$\widetilde{p}^{\mathrm{DA}}_g$ and $\widetilde{p}^{\mathrm{DA}}_d$ is the day ahead dispatch from problem 9.

The lagrangian of the TSO day-ahead market problem is as follows:

$$\begin{aligned}
\mathcal{L}^{\mathrm{DA}} &= \sum_{d \in D} \pi^{\mathrm{DA}}_d \widehat{p}^{\mathrm{DA}}_d - \sum_{g \in G} \pi^{\mathrm{DA}}_g \widehat{p}^{\mathrm{DA}}_g \\
&- VOLL^{\mathrm{DA}} s^{\mathrm{DA}} - \pi^R \sum_r w^{\mathrm{DA}}_r \\
&- \lambda^{\mathrm{T,DA}} \left[\sum_{g \in G} \widehat{p}^{\mathrm{DA}}_g - \sum_{d \in D} \widehat{p}^{\mathrm{DA}}_d + \sum_{r \in R} w^{\mathrm{DA}}_r + s^{\mathrm{DA}} \right] \\
&+ \sum_{g \in G^{\mathrm{D}}_e, e} \left[\varsigma^{\mathrm{T,DA}-}_{ge} \left(\underline{P}_g - \widehat{p}^{\mathrm{DA}}_g \right) + \varsigma^{\mathrm{T,DA}+}_{ge} \left(\widehat{p}^{\mathrm{DA}}_g - \widetilde{p}^{\mathrm{DA}}_g \right) \right] \\
&+ \sum_{g \in G^{\mathrm{T}}} \left[\sigma^{\mathrm{T,DA}-}_g \left(\underline{P}_g - \widehat{p}^{\mathrm{DA}}_g \right) + \sigma^{\mathrm{T,DA}+}_g \left(\widehat{p}^{\mathrm{DA}}_g - \overline{P}_g \right) \right] \\
&+ \sum_{d \in D^{\mathrm{D}}_e, e} \left[\varsigma^{\mathrm{T,DA}-}_{de} \left(\underline{P}_d - \widehat{p}^{\mathrm{DA}}_d \right) + \varsigma^{\mathrm{T,DA}+}_{de} \left(\widehat{p}^{\mathrm{DA}}_d - \widetilde{p}^{\mathrm{DA}}_d \right) \right] \\
&+ \sum_{d \in D^{\mathrm{T}}} \left[\sigma^{\mathrm{T,DA}-}_d \left(\underline{P}_d - \widehat{p}^{\mathrm{DA}}_d \right) + \sigma^{\mathrm{T,DA}+}_d \left(\widehat{p}^{\mathrm{DA}}_d - \overline{P}_d \right) \right] \\
&- \sum_{r \in R} \left[\nu^{\mathrm{T,DA}-}_r w^{\mathrm{DA}}_r - \nu^{\mathrm{T,DA}+}_r \left(w^{\mathrm{DA}}_r - W^{\mathrm{DA}}_r \right) \right] \\
&- \rho^{\mathrm{T,DA}-} s^{\mathrm{DA}} + \rho^{\mathrm{T,DA}+} (s^{\mathrm{DA}} - \sum_d \widehat{p}^{\mathrm{DA}}_d)
\end{aligned} \tag{14}$$

The KKTs of the TSO day-ahead market (excluding primal constraints) are:

$$\begin{aligned}
(\widehat{p}^{\mathrm{DA}}_g): \quad & -\pi^{\mathrm{DA}}_g - \left[\varsigma^{\mathrm{T,DA}-}_{ge} - \varsigma^{\mathrm{T,DA}+}_{ge} \right]_{g \in G^{\mathrm{D}}_e} \\
& - \left[\sigma^{\mathrm{T,DA}-}_g - \sigma^{\mathrm{T,DA}+}_g \right]_{g \in G^{\mathrm{T}}} \\
& - \lambda^{\mathrm{T,DA}} = 0, \quad \forall g \in G
\end{aligned} \tag{15a}$$

$$\begin{aligned}
(\widehat{p}^{\mathrm{DA}}_d): \quad & \pi^{\mathrm{DA}}_d - \left[\varsigma^{\mathrm{T,DA}-}_{de} - \varsigma^{\mathrm{T,DA}+}_{de} \right]_{d \in D^{\mathrm{D}}_e} \\
& - \left[\sigma^{\mathrm{T,DA}-}_d - \sigma^{\mathrm{T,DA}+}_d \right]_{d \in D^{\mathrm{T}}} - \rho^{\mathrm{T,DA}+} \\
& + \lambda^{\mathrm{T,DA}} = 0, \quad \forall d \in D
\end{aligned} \tag{15b}$$

$$\begin{aligned}
(s^{\mathrm{l,DA}}): \quad & -VOLL^{\mathrm{DA}} - \lambda^{\mathrm{T,DA}} - \rho^{\mathrm{T,DA}-} \\
& + \rho^{\mathrm{T,DA}+} = 0
\end{aligned} \tag{15c}$$

$$\begin{aligned}
(w^{\mathrm{DA}}_r): \quad & -\pi^R - \lambda^{\mathrm{T,DA}} \\
& - \left[\nu^{\mathrm{T,DA}-}_r - \nu^{\mathrm{T,DA}+}_r \right] = 0,\ \forall r \in R
\end{aligned} \tag{15d}$$

The complimentary constraints are:

$$0 \le \varsigma^{\mathrm{T,DA}-}_{ge} \perp \widehat{p}^{\mathrm{DA}}_g - \underline{P}_g \ge 0 \quad \forall g, e \tag{16a}$$

$$0 \le \varsigma^{\mathrm{T,DA}+}_{ge} \perp \widetilde{p}^{\mathrm{DA}}_g - \widehat{p}^{\mathrm{DA}}_g \ge 0 \quad \forall g \in G^{\mathrm{D}}_e, e \in E \tag{16b}$$

$$0 \le \sigma^{\mathrm{T,DA}+}_g \perp \overline{P}_g - \widehat{p}^{\mathrm{DA}}_g \ge 0 \quad \forall g \in G^{\mathrm{T}} \tag{16c}$$

$$0 \le \varsigma^{\mathrm{T,DA}-}_{de} \perp \widehat{p}^{\mathrm{DA}}_d - \underline{P}_d \ge 0 \quad \forall d, e \tag{16d}$$

$$0 \le \varsigma^{\mathrm{T,DA}+}_{de} \perp \widetilde{p}^{\mathrm{DA}}_d - \widehat{p}^{\mathrm{DA}}_d \ge 0 \quad \forall d \in D^{\mathrm{D}}_e, e \in E \tag{16e}$$

$$0 \le \sigma^{\mathrm{T,DA}+}_d \perp \overline{P}_d - \widehat{p}^{\mathrm{DA}}_d \ge 0 \quad \forall d \in D^{\mathrm{T}} \tag{16f}$$

$$0 \le \nu^{\mathrm{T,DA}-}_r \perp w^{\mathrm{DA}}_r \ge 0,\ \forall r \in R \tag{16g}$$

$$0 \le \nu^{\mathrm{T,DA}+}_r \perp W^{\mathrm{DA}}_r - w^{\mathrm{DA}}_r \ge 0,\ \forall r \in R \tag{16h}$$

$$0 \le \rho^{\mathrm{T,DA}-} \perp s^{\mathrm{l,DA}} \ge 0 \tag{16i}$$

$$0 \le \rho^{\mathrm{T,DA}+} \perp \sum_d \widehat{p}^{\mathrm{DA}}_d - s^{\mathrm{l,DA}} \ge 0 \tag{16j}$$

APPENDIX D
KKT CONDITIONS OF REAL-TIME MARKET

The KKT conditions of the SOCP problem for the real-time re-dispatch are not actually solved, because the Benders decomposition renders the scenarios solvable as single problems. However, they are used in a proof of equivalence between the DSO market and the global DA-RT combination.

The Real-Time problem from (4) is repeated here with dual variables added:

$$\min_{\Xi^{\mathrm{RT}}} \phi_\omega(\Delta \mathrm{Cost}^{\mathrm{RT}}_\omega) \tag{17a}$$

$$= \phi_\omega \Big[\sum_{g \in G} (\pi^{\mathrm{DA}}_g (p^{\mathrm{RT}}_{g\omega} - \widehat{p}^{\mathrm{DA}}_g) + \pi^{\uparrow}_g p^{\uparrow}_{g\omega} + \pi^{\downarrow}_g p^{\downarrow}_{g\omega})$$

$$
\begin{aligned}
&+\sum_{d\in D}(\pi_d^{\mathrm{DA}}(\widehat{p}_d^{\mathrm{DA}}-p_{d\omega}^{\mathrm{RT}})+\pi_d^{\uparrow}p_{d\omega}^{\uparrow}+\pi_d^{\downarrow}p_{d\omega}^{\downarrow})\\
&+\sum_{n\in N}VOLL_n^{\mathrm{RT}}s_{n\omega}^{\mathrm{RT}}\\
&+\sum_{r}\left(\pi^{R}(w_{r\omega}^{\mathrm{RT}}-w_r^{\mathrm{DA}})+\pi^{\uparrow\mathrm{R}}w_{r\omega}^{\uparrow}+\pi^{\downarrow\mathrm{R}}w_{r\omega}^{\downarrow}\right)\Big]
\end{aligned}
$$

$$
\text{s.t.}\quad p_{l\omega}^{\mathrm{RT}}=B_l(\theta_{n\omega}-\theta_{m\omega}),\quad \forall l\in L^{\mathrm{T}},\ :(\gamma_{l\omega}^{\mathrm{T}}) \tag{17b}
$$

$$
p_{l\omega}^{\mathrm{RT}}\le S_l,\ \forall l\in L^{\mathrm{T}},\ :(\eta_{l\omega}^{\mathrm{T}}) \tag{17c}
$$

$$
p_{g\omega}^{\mathrm{RT}}=\widehat{p}_g^{\mathrm{DA}}+p_{g\omega}^{\uparrow}-p_{g\omega}^{\downarrow},\quad \forall g\in G,\ :(\zeta_{g\omega}^{\mathrm{p,RT}}) \tag{17d}
$$

$$
p_{d\omega}^{\mathrm{RT}}=\widehat{p}_d^{\mathrm{DA}}-p_{d\omega}^{\uparrow}+p_{d\omega}^{\downarrow},\quad \forall d\in D,\ :(\zeta_{d\omega}^{\mathrm{p,RT}}) \tag{17e}
$$

$$
w_{r\omega}^{\mathrm{RT}}=w_r^{\mathrm{DA}}+w_{r\omega}^{\uparrow}-w_{r\omega}^{\downarrow},\ \forall r\in R,,\ :(\zeta_{r\omega}^{\mathrm{p,RT}}) \tag{17f}
$$

$$
\begin{aligned}
&\sum_{g\in G_n}p_{g\omega}^{\mathrm{RT}}-\sum_{d\in D_n}p_{d\omega}^{\mathrm{RT}}+\sum_{r\in R_n}w_{r\omega}^{\mathrm{RT}}+s_{n\omega}^{\mathrm{RT}}\\
&\quad=\sum_{l\in n\rightarrow}p_{l\omega}^{\mathrm{RT}}-\sum_{l\in\rightarrow n}p_{l\omega}^{\mathrm{RT}},\ \forall n\in N,\ :(\lambda_{n\omega}^{\mathrm{p,RT}})
\end{aligned} \tag{17g}
$$

$$
\begin{aligned}
&\sum_{g\in G_n}q_{g\omega}^{\mathrm{RT}}-\sum_{d\in D_n}q_{d\omega}^{\mathrm{RT}}+s_{n\omega}^{\mathrm{q,RT}}\\
&\quad=\sum_{l\in n\rightarrow}q_{l\omega}^{\mathrm{RT}}-\sum_{l\in\rightarrow n}q_{l\omega}^{\mathrm{RT}},\ \forall n\in N_e^{\mathrm{D}},\ :(\lambda_{n\omega}^{\mathrm{q,RT}})
\end{aligned} \tag{17h}
$$

$$
p_{l\omega}^{(\mathrm{RT})2}+q_{l\omega}^{(\mathrm{RT})2}\le\varphi_{l\omega}^{\mathrm{RT}}v_{n\omega}^{\mathrm{RT}},\ \forall l\in L_e^{\mathrm{D}}\cup l_e,\ :(\gamma_{l\omega}^{\mathrm{D,RT}}) \tag{17i}
$$

$$
p_{l\omega}^{\mathrm{RT}}+p_{l'\omega}^{\mathrm{RT}}=R_l\varphi_{l\omega}^{\mathrm{RT}},\ \forall l\in L_e^{\mathrm{D}}\cup l_e,\ :(\mu_{l\omega}^{\mathrm{p,RT}}) \tag{17j}
$$

$$
q_{l\omega}^{\mathrm{RT}}+q_{l'\omega}^{\mathrm{RT}}=X_l\varphi_{l\omega}^{\mathrm{RT}},\ \forall l\in L_e^{\mathrm{D}}\cup l_e,\ :(\mu_{l\omega}^{\mathrm{q,RT}}) \tag{17k}
$$

$$
p_{l\omega}^{(\mathrm{RT})2}+q_{l\omega}^{(\mathrm{RT})2}\le S_l^2,\ \forall l\in L_e^{\mathrm{D}}\cup l_e,\ :(\eta_{l\omega}^{\mathrm{D}}) \tag{17l}
$$

$$
\begin{aligned}
&v_{m\omega}^{\mathrm{RT}}=v_{n\omega}^{\mathrm{RT}}-2(R_lp_{l\omega}^{\mathrm{RT}}+X_lq_{l\omega}^{\mathrm{RT}})\\
&\quad+(R_l^2+X_l^2)\varphi_{l\omega}^{\mathrm{RT}},\ \forall l\in L_e^{\mathrm{D}}\cup l_e,\ :(\beta_{l\omega}^{\mathrm{RT}})
\end{aligned} \tag{17m}
$$

$$
\underline{V}_n^2\le v_{n\omega}^{\mathrm{RT}}\le\overline{V}_n^2,\quad \forall e,n\in N_e^{\mathrm{D}},\ :(\sigma_{n\omega}^{\mathrm{RT}-},\sigma_{n\omega}^{\mathrm{RT}+}) \tag{17n}
$$

$$
0\le w_{r\omega}^{\mathrm{RT}}\le W_{r\omega}^{\mathrm{RT}},\quad \forall r\in R,\ :(\nu_{r\omega}^{\mathrm{RT}-},\nu_{r\omega}^{\mathrm{RT}+}) \tag{17o}
$$

$$
\underline{P}_g\le p_{g\omega}^{\mathrm{RT}}\le\overline{P}_g,\quad \forall g\in G,\ :(\varsigma_{g\omega}^{\mathrm{RT}-},\varsigma_{g\omega}^{\mathrm{RT}+}) \tag{17p}
$$

$$
\underline{P}_d\le p_{d\omega}^{\mathrm{RT}}\le\overline{P}_d,\quad \forall d\in D,\ :(\varsigma_{d\omega}^{\mathrm{RT}-},\varsigma_{d\omega}^{\mathrm{RT}+}) \tag{17q}
$$

$$
\underline{Q}_g\le q_{g\omega}^{\mathrm{RT}}\le\overline{Q}_g,\quad \forall g\in G_e^{\mathrm{D}},\ :(\kappa_{g\omega}^{\mathrm{RT}-},\kappa_{g\omega}^{\mathrm{RT}+}) \tag{17r}
$$

$$
\underline{Q}_d\le q_{d\omega}^{\mathrm{RT}}\le\overline{Q}_d,\quad \forall d\in D_e^{\mathrm{D}},\ :(\kappa_{d\omega}^{\mathrm{RT}-},\kappa_{d\omega}^{\mathrm{RT}+}) \tag{17s}
$$

$$
0\le s_{n\omega}^{\mathrm{RT}}\le\sum_{d\in D_n}p_{d\omega}^{\mathrm{RT}},\ \forall n\in N,\ :(\Upsilon_{n\omega}^{\mathrm{RT}-},\Upsilon_{n\omega}^{\mathrm{RT}+}) \tag{17t}
$$

$$
p_{g\omega}^{\uparrow}\ge 0,\ ,\quad p_{g\omega}^{\downarrow}\ge 0,\ \forall g,\ :(\epsilon_{g\omega}^{\uparrow,\mathrm{RT}},\epsilon_{g\omega}^{\downarrow,\mathrm{RT}}) \tag{17u}
$$

$$
p_{d\omega}^{\uparrow}\ge 0,\ ,\quad p_{d\omega}^{\downarrow}\ge 0,\ \forall d,\ :(\epsilon_{d\omega}^{\uparrow,\mathrm{RT}},\epsilon_{d\omega}^{\downarrow,\mathrm{RT}}) \tag{17v}
$$

$$
w_{r\omega}^{\uparrow}\ge 0,\quad w_{r\omega}^{\downarrow}\ge 0,\forall r,\ :(\varepsilon_{r\omega}^{\uparrow,\mathrm{RT}},\varepsilon_{r\omega}^{\downarrow,\mathrm{RT}}) \tag{17w}
$$

The Lagrangian of the real-time problem is as follows:

$$
\begin{aligned}
\mathcal{L}^{\mathrm{RT}}=&\sum_{\omega}\phi_{\omega}\Bigg[\sum_{g\in G}\left(\pi_g^{\mathrm{DA}}(p_{g\omega}^{\mathrm{RT}}-p_g^{\mathrm{DA}})+\pi_g^{\uparrow}p_{g\omega}^{\uparrow}+\pi_g^{\downarrow}p_{g\omega}^{\downarrow}\right)\\
&+\sum_{d\in D}\left(\pi_d^{\mathrm{DA}}(p_d^{\mathrm{DA}}-p_{d\omega}^{\mathrm{RT}})+\pi_d^{\uparrow}p_{d\omega}^{\uparrow}+\pi_d^{\downarrow}p_{d\omega}^{\downarrow}\right)\\
&+\sum_{n\in N}VOLL_n^{\mathrm{RT}}s_{n\omega}^{\mathrm{RT}}\\
&+\sum_{r\in R}\left(\pi^{R}(w_{r\omega}^{\mathrm{RT}}-w_r^{\mathrm{DA}})+\pi^{\uparrow R}w_{r\omega}^{\uparrow}+\pi^{\downarrow R}w_{r\omega}^{\downarrow}\right)\Bigg]\\
&+\sum_{l\in L^{\mathrm{T}}}\gamma_{l\omega}^{\mathrm{T}}\left(p_{l\omega}^{\mathrm{RT}}-B_l(\theta_{n\omega}-\theta_{m\omega})\right)\\
&+\sum_{l\in L^{\mathrm{T}}}\eta_{l\omega}^{\mathrm{T}}\left(p_{l\omega}^{\mathrm{RT}}-S_l\right)\\
&-\sum_{g\in G}\zeta_{g\omega}^{\mathrm{p}}\left(p_{g\omega}^{\mathrm{RT}}-\widehat{p}_g^{\mathrm{DA}}-p_{g\omega}^{\uparrow}+p_{g\omega}^{\downarrow}\right)\\
&-\sum_{d\in D}\zeta_{d\omega}^{\mathrm{p}}\left(p_{d\omega}^{\mathrm{RT}}-\widehat{p}_d^{\mathrm{DA}}+p_{d\omega}^{\uparrow}-p_{d\omega}^{\downarrow}\right)\\
&-\sum_{r\in R}\zeta_{r\omega}^{p}\left(w_{r\omega}^{\mathrm{RT}}-w_r^{\mathrm{DA}}-w_{r\omega}^{\uparrow}+w_{r\omega}^{\downarrow}\right)\\
&-\sum_{n\in N,\omega}\lambda_{n\omega}^{\mathrm{p,RT}}\Big(\sum_{g\in G_n}p_{g\omega}^{\mathrm{RT}}-\sum_{d\in D_n}p_{d\omega}^{\mathrm{RT}}+\sum_{r\in R_n}w_{r\omega}^{\mathrm{RT}}\\
&+s_{n\omega}^{\mathrm{RT}}-\sum_{l\in n\rightarrow}p_{l\omega}^{\mathrm{RT}}+\sum_{l\in\rightarrow n}p_{l\omega}^{\mathrm{RT}}\Big)\\
&-\sum_{n\in N,\omega}\lambda_{n\omega}^{\mathrm{q,RT}}\Bigg(\sum_{g\in G_n}q_{g\omega}^{\mathrm{RT}}-\sum_{d\in D_n}q_{d\omega}^{\mathrm{RT}}+s_{n\omega}^{\mathrm{q,RT}}\\
&-\sum_{l\in n\rightarrow}q_{l\omega}^{\mathrm{RT}}+\sum_{l\in\rightarrow n}q_{l\omega}^{\mathrm{RT}}\Bigg)\\
&+\sum_{l\in L_e^{\mathrm{D}}\cup l_e,\omega}\gamma_{l\omega}\left[p_{l\omega}^{(RT)2}+q_{l\omega}^{(RT)2}-\varphi_{l\omega}^{\mathrm{RT}}v_{n\omega}^{\mathrm{RT}}\right]\\
&-\sum_{l\in L_e^{\mathrm{D}}\cup l_e,\omega}\Big[\mu_{l\omega}^{p}\left(p_{l\omega}^{\mathrm{RT}}+p_{l'\omega}^{\mathrm{RT}}-R_l\varphi_{l\omega}^{\mathrm{RT}}\right)\\
&+\mu_{l\omega}^{q}\left(q_{l\omega}^{\mathrm{RT}}+q_{l'\omega}^{\mathrm{RT}}-X_l\varphi_{l\omega}^{\mathrm{RT}}\right)\Big]\\
&+\sum_{l\in L_e^{\mathrm{D}}\cup l_e,\omega}\left[\eta_{l\omega}\left(p_{l\omega}^{(RT)2}+q_{l\omega}^{(RT)2}-S_l\right)\right]\\
&-\sum_{l\in L_e^{\mathrm{D}}\cup l_e,\omega}\Big[\beta_{l\omega}\Big(v_{m\omega}^{\mathrm{RT}}-v_{n\omega}^{\mathrm{RT}}+2(R_lp_{l\omega}^{\mathrm{RT}}+X_lq_{l\omega}^{\mathrm{RT}})\\
&-(R_l^2+X_l^2)\varphi_{l\omega}^{\mathrm{RT}}\Big)\Big]\\
&+\sum_{n\in N_e^{\mathrm{D}}\cup n_e^{HV},\omega}\left[\sigma_{n\omega}^{-}\left(\underline{V}_n^2-v_{n\omega}^{\mathrm{RT}}\right)+\sigma_{n\omega}^{+}\left(v_{n\omega}^{\mathrm{RT}}-\overline{V}_n^2\right)\right]\\
&-\sum_{r\in R,\omega}\left[\nu_{r\omega}^{-}w_{r\omega}^{\mathrm{RT}}-\nu_{r\omega}^{+}\left(w_{r\omega}^{\mathrm{RT}}-W_{r\omega}^{\mathrm{RT}}\right)\right]\\
&+\sum_{g\in G,\omega}\left[\varsigma_{g\omega}^{\mathrm{RT}-}\left(\underline{P}_g-p_{g\omega}^{\mathrm{RT}}\right)+\varsigma_{g\omega}^{\mathrm{RT}+}\left(p_{g\omega}^{\mathrm{RT}}-\overline{P}_g\right)\right]\\
&+\sum_{d\in D,\omega}\left[\varsigma_{d\omega}^{\mathrm{RT}-}\left(\underline{P}_d-p_{d\omega}^{\mathrm{RT}}\right)+\varsigma_{d\omega}^{\mathrm{RT}+}\left(p_{d\omega}^{\mathrm{RT}}-\overline{P}_d\right)\right]\\
&+\sum_{g\in G,\omega}\left[\kappa_{g\omega}^{\mathrm{RT}-}\left(\underline{Q}_g-q_{g\omega}^{\mathrm{RT}}\right)+\kappa_{g\omega}^{\mathrm{RT}+}\left(q_{g\omega}^{\mathrm{RT}}-\overline{Q}_g\right)\right]\\
&+\sum_{d\in D_e^{\mathrm{D}},\omega}\left[\kappa_{d\omega}^{\mathrm{RT}-}\left(\underline{Q}_d-q_{d\omega}^{\mathrm{RT}}\right)+\kappa_{d\omega}^{\mathrm{RT}+}\left(q_{d\omega}^{\mathrm{RT}}-\overline{Q}_g\right)\right]\\
&+\sum_{g\in G,\omega}\left[-p_{g\omega}^{\uparrow}\epsilon_{g\omega}^{\mathrm{p}\uparrow}-p_{g\omega}^{\downarrow}\epsilon_{g\omega}^{\mathrm{p}\downarrow}\right]
\end{aligned}
$$

$$+\sum_{r\in R,\omega}\left[-w^{\uparrow}_{r\omega}\epsilon^{\mathrm{p}\uparrow}_{r\omega}-w^{\downarrow}_{r\omega}\epsilon^{\mathrm{p}\downarrow}_{r\omega}\right]$$
$$+\sum_{d\in D,\omega}\left[-p^{\uparrow}_{d\omega}\varepsilon^{\mathrm{p}\uparrow}_{d\omega}-p^{\downarrow}_{d\omega}\varepsilon^{\mathrm{p}\downarrow}_{d\omega}\right]$$
$$+\sum_{n\in N,\omega}\left[-\Upsilon^{\mathrm{RT}-}_{n\omega}s^{\mathrm{RT}}_{n\omega}+\Upsilon^{\mathrm{RT}+}_{n\omega}\left(s^{\mathrm{RT}}_{n\omega}-\sum_{d\in D_n}p^{\mathrm{RT}}_{d\omega}\right)\right] \tag{18}$$

The KKT conditions of above Lagrangian are (excluding the primal constraints of 17):

$$(p^{\uparrow}_{g\omega}):\ \phi_\omega\pi^{\uparrow}_g+\zeta^{p}_{g\omega}-\epsilon^{\mathrm{p}\uparrow}_{g\omega}=0,\quad \forall g\in G^{\mathrm{D}}_e \tag{19a}$$
$$(p^{\downarrow}_{g\omega}):\ \phi_\omega\pi^{\downarrow}_g-\zeta^{p}_{g\omega}-\epsilon^{\mathrm{p}\downarrow}_{g\omega}=0,\quad \forall g\in G^{\mathrm{D}}_e \tag{19b}$$
$$(p^{\uparrow}_{d\omega}):\ \phi_\omega\pi^{\uparrow}_d-\zeta^{p}_{d\omega}-\varepsilon^{\mathrm{p}\uparrow}_{i\omega}=0,\quad \forall d\in D^{\mathrm{D}}_e \tag{19c}$$
$$(p^{\downarrow}_{d\omega}):\ \phi_\omega\pi^{\downarrow}_d+\zeta^{p}_{d\omega}-\varepsilon^{\mathrm{p}\downarrow}_{d\omega}=0,\quad \forall d\in D^{\mathrm{D}}_e \tag{19d}$$
$$(w^{\uparrow}_{r\omega}):\ \phi_\omega\pi^{\uparrow R}+\zeta^{p}_{r\omega}-\epsilon^{\mathrm{p}\uparrow}_{r\omega}=0,\quad \forall r\in R^{\mathrm{D}}_e \tag{19e}$$
$$(w^{\downarrow}_{r\omega}):\ \phi_\omega\pi^{\downarrow R}-\zeta^{p}_{r\omega}-\epsilon^{\mathrm{p}\downarrow}_{r\omega}=0,\quad \forall r\in R^{\mathrm{D}}_e \tag{19f}$$
$$(s^{\mathrm{RT}}_{n\omega}):\ \phi_\omega\mathrm{VOLL}_n-\lambda^{\mathrm{p,RT}}_{n\omega}-\Upsilon^{\mathrm{RT}-}_{n\omega}+\Upsilon^{\mathrm{RT}+}_{n\omega}=0,\ \forall n\in N \tag{19g}$$
$$(w^{\mathrm{RT}}_{r\omega}):\ \phi_\omega\pi^{R}-\zeta^{p}_{r\omega}-\left[\lambda^{\mathrm{p,RT}}_{n\omega}\right]_{n_r}+\nu^{+}_{r\omega}-\nu^{-}_{r\omega}=0,\quad \forall r\in R^{\mathrm{D}}_e \tag{19h}$$
$$(p^{\mathrm{RT}}_{g\omega}):\ \phi_\omega\pi^{\mathrm{DA}}_g-\zeta^{p}_{g\omega}-\varsigma^{\mathrm{RT}-}_{g\omega}+\varsigma^{\mathrm{RT}+}_{g\omega}-\left[\lambda^{\mathrm{p,RT}}_{n\omega}\right]_{n_g}=0,\quad \forall g\in G \tag{19i}$$
$$(q^{\mathrm{RT}}_{g\omega}):\ -\kappa^{\mathrm{RT}-}_{g\omega}+\kappa^{\mathrm{RT}+}_{g\omega}-\left[\lambda^{\mathrm{q,RT}}_{n\omega}\right]_{n_g}=0,\quad \forall g\in G^{\mathrm{D}}_e \tag{19j}$$
$$(p^{\mathrm{RT}}_{d\omega}):\ -\phi_\omega\pi^{\mathrm{DA}}_d-\zeta^{p}_{d\omega}-\varsigma^{\mathrm{RT}-}_{d\omega}+\varsigma^{\mathrm{RT}+}_{d\omega}+\left[\lambda^{\mathrm{p,RT}}_{n\omega}-\Upsilon^{\mathrm{RT}+}_{n\omega}\right]_{n_d}=0,\quad \forall d\in D \tag{19k}$$
$$(q^{\mathrm{RT}}_{d\omega}):\ -\kappa^{\mathrm{RT}-}_{d\omega}+\kappa^{\mathrm{RT}+}_{d\omega}+\left[\lambda^{\mathrm{q,RT}}_{n\omega}\right]_{n_d}=0,\quad \forall d\in D^{\mathrm{D}}_e \tag{19l}$$
$$(p^{\mathrm{RT}}_{l\omega}):\ \lambda^{\mathrm{p,RT}}_{n\omega}-\lambda^{\mathrm{p,RT}}_{m\omega}+\left[2\gamma_{l\omega}p^{\mathrm{RT}}_{l\omega}-\mu^{\mathrm{p}}_{l\omega}-\mu^{\mathrm{p}}_{l'\omega}+2\eta_{l\omega}p^{\mathrm{RT}}_{l\omega}-2\beta_{l\omega}R_l\right]_{l\in L^{\mathrm{D}}_e}+\left[\gamma^{\mathrm{T}}_{l\omega}+\eta^{\mathrm{T}}_{l\omega}\right]_{l\in L^{\mathrm{T}}}=0,\quad \forall l\in L \tag{19m}$$
$$(q^{\mathrm{RT}}_{l\omega}):\ \lambda^{\mathrm{q,RT}}_{n\omega}-\lambda^{\mathrm{q,RT}}_{m\omega}+\left[2\gamma_{l\omega}q^{\mathrm{RT}}_{l\omega}-\mu^{q}_{l\omega}-\mu^{q}_{l'\omega}+2\eta_{l\omega}q^{\mathrm{RT}}_{l\omega}-2\beta_{l\omega}X_l\right]_{l\in L^{\mathrm{D}}_e}=0,\quad \forall l\in L \tag{19n}$$
$$(\varphi^{\mathrm{RT}}_{l\omega}):\ -\gamma_{l\omega}v^{\mathrm{RT}}_{n\omega}+\mu^{p}_{l\omega}R_l+\mu^{q}_{l\omega}X_l+\beta_{l\omega}(R^2_l+X^2_l)=0,\quad \forall\omega,l=(n,m)\in L^{\mathrm{D}}_e \tag{19o}$$
$$(v^{\mathrm{RT}}_{n\omega}):\ -\gamma_{l\omega}\varphi^{\mathrm{RT}}_{l\omega}-\beta_{l'\omega}+\beta_{l\omega}-\sigma^{-}_{n\omega}+\sigma^{+}_{n\omega}=0,\quad \forall\omega,l=(n,m)\in L^{\mathrm{D}}_e \tag{19p}$$

APPENDIX E
PROOF OF PROPOSITION 1

Proposition 1: The first order necessary conditions (KKT conditions) of the day-ahead market and the real-time market combined contain all the KKT conditions of the DSO market in (9) and solving (2) is equivalent to solving (1).

Proof of propositon 1: Problem (3) and (4) are explicitly convex. Therefore their KKT conditions are also optimality conditions. This is the first part of the proof. The KKT conditions of the DSO market in (9) are given in (11) and (12). The DSO market is also explicitly convex and the KKT conditions define optimality. The KKT conditions of the day-ahead market are presented in (15) and (16). All equations of (11) are contained in either (15) or (19) with exception of the variables related to the PCC injections in feeder e. The dual constraints with regards to those variables are (11u) through (11y). The PCC prices $\pi^{\mathrm{PCC,DA}}_e, \pi^{\uparrow\mathrm{PCC}}_e, \pi^{\downarrow\mathrm{PCC}}_e$ and the PCC flow limits $\overline{f}_e, \underline{f}_e$ are variables in the upper level problem (1) and therefore constitute slack variables that will not influence the optimality of (9). Therefore removing the DSO market lower level problem and solving (2) is equivalent to solving (1). This ends the proof. □

APPENDIX F
SCENARIO GENERATION

A simple scenario generation method is used for the uncertainties of the wind production. The distance of the wind farms are

$$D_{rw}=\left\|\begin{array}{c}x_r-x_w\\ y_r-y_w\end{array}\right\|,\quad \forall r\in R,w\in R,r\neq w \tag{20}$$

The co-variance matrix is now given in (21).

$$\Sigma_{rw}=\frac{\sigma^2_r+\sigma^2_w}{2}e^{-D_{rw}},\forall r\in R,w\in R \tag{21}$$

The distributions of the wind generators are thus:

$$W\sim\mathcal{N}_r(\mu_r,\Sigma_{rw}) \tag{22}$$

Now the scenarios can be drawn by random sampling i.e.

$$W^{\mathrm{RT}}_{r\omega}\sim\sim\mathcal{N}_r(\mu_r,\Sigma_{rw}) \tag{23}$$

APPENDIX G
MODIFIED 24 BUS TEST NETOWK

The 24-bus power system – Single area RTS-96 is used here in a modified form. The mean and variance of the wind power plants in the network are given in table II. The locations of each wind farm is given in table III, which is used to claculate the distance between them as in equation (20).

TABLE II
THE MEAN OF THE FORECAST OF THE INSTALLED RES AND VARIANCE OF THE FORECAST.

	W_1	W_2	W_3	W_4	W_5	W_6	W_7
Variance σ^2	750	740	760	300	300	300	200
Mean μ	200	200	200	40	40	40	10

APPENDIX H
CONGESTION LEVEL

The Congestion level of the colored dots in Fig. 4 is here plotted as a line plot in Fig. 8. The data for the two plots is the same.

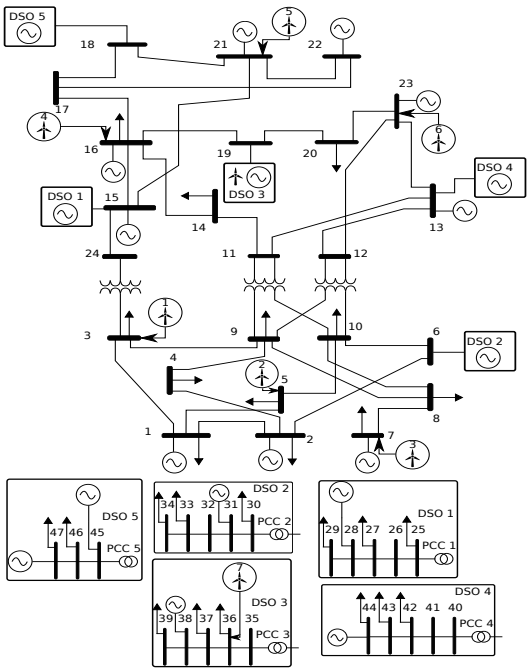

Fig. 7. Diagram of the 24-bus power system – Single area RTS-96. 5 DSO feeders have been added, as well as 7 Wind power plants. The loads from the buses where the DSO feeders are connected have been moved to the DSO feeders.

TABLE III
GEORGRAPHICAL LOCATION OF EACH WIND FARM.

	W_1	W_2	W_3	W_4	W_5	W_6	W_7
X-coordinate	0	0.25	0.5	6	6.25	6.5	6.75
Y-Coordinate	0	0	0	5	5	5	5.2

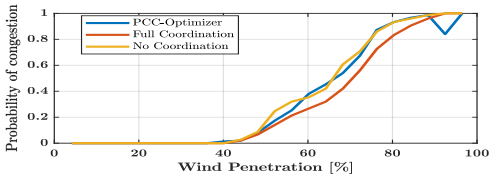

Fig. 8. Probability of at least two transmission lines being congested in RT.

APPENDIX I
COMPUTATIONAL PERFORMANCE

Here we show some results pertaining to the Benders decomposition approach that was presented in section IV. In Fig. 9 we present the convergence of the suggested multicut benders decomposition for a sample point of wind-penetration.

The upper bound of the benders decomposed problems in iteration (i) is found as:

$$UB^{(\mathrm{i})} = \mathcal{SW}^{\mathrm{DA}(i)} - \sum_{\omega} \phi_{\omega} \Delta \mathrm{Cost}_{\omega}^{\mathrm{RT}(\mathrm{i})} \tag{24}$$

The lower bound in iteration (i) is found via:

$$LB^{(\mathrm{i})} = \mathcal{SW}^{\mathrm{DA}(i)} - \sum_{\omega} \phi_{\omega} \psi_{\omega}^{(\mathrm{i})} \tag{25}$$

The computational burden of the decomposed problem is analyzed by logging the time it takes Mosek 8.0 to solve every master-problem and sub-problem for every scenario. The implementation we use in this paper relies on the CVX plugin for Matlab, which yields large overhead due to the time it takes to initialize every master-problem and sub-problem. Therefore the results in table IV only give the time that the solver actually spent, while the full time including the overhead for the initialization is about two to four times this number. In the future we wish to use an implementation that does not rely on CVX which can help solving larger case studies. The data provided in table IV is the average over all the different wind-penetration settings of the RES (i.e. it is the average of 24 different wind penetration settings). Because the sub-problems are independent, and can be solved in parallel, the number of scenarios do not affect the computational time as long as there are enough CPU-cores to solve them in parallel.

The number of binary variables in the master-problem depend on the number of complimentarity constraints in (16). Because we choose to solve the complimentarity constraints with the Big-M approach every one of these constraints uses one binary. The number of complimentarity constraints in turn depend mainly on the number of generators, number of elastic demands and number of RES sources. In the case study for this work the master problem therefore contains 196 binary variables. As a result of the benders decomposition the conic constraints have all been moved to the subproblem, and therefore the master problem is MILP, while the subproblems are continuous SOCP.

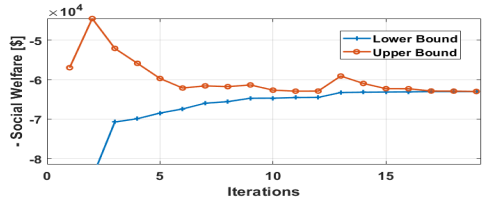

Fig. 9. Convergence of the Benders decomposition upper and lower bound over the iterations. Note, we minimize $-\mathcal{SW}$, which is equivalent to maximizing social welfare.

TABLE IV
COMPUTATIONAL BURDEN OF THE BENDERS MULTI-CUT SOLUTION STRATEGY. NOTE: WE AVERAGE FOR ALL SOLVED INSTANCES OF INCREASING WIND PENETRATION.

CPU times [s]				
Average subproblem	Average master	Initial master problem	Master in last iteration	Average #Iterations
0.31	0.54	0.67	0.91	29.5

{2.7182818284}ϑφερτυθιοπσδφγηξκλ